PHOSPHOLIPID SELECTION AND TRANSPORT BY P4-ATPASES

By

Ryan Douglas Baldridge

Dissertation

Submitted to the Faculty of the

Graduate School of Vanderbilt University

in partial fulfillment of the requirements

for the degree of

DOCTOR OF PHILOSOPHY

in

Biological Sciences

May, 2013

Nashville, Tennessee

Approved:

Professor Katherine L. Friedman

Professor Kathleen L. Gould

Professor Todd R. Graham

Professor Hassane S. Mchaourab

Professor James G. Patton

For Jennifer and Maximilian.

ACKNOWLEDGEMENTS

First, I want to thank Todd for the opportunity he provided me to join his lab. Without his support and enthusiasm, none of this would have been possible. His genuine interest in his students' success is an admirable quality. I've been incredibly lucky to have a mentor who is a stellar scientist and loves science as much as Todd; I aspire to continue with the same excitement throughout my career.

My lab-mates have been excellent during my time at Vanderbilt, thank you for your friendship. In particular, I want to thank Dr. Peng Xu for the countless wonderful discussions we have had. I would also like to thank my thesis committee for providing excellent critiques of my work, challenging me to become a better scientist, and helping in every way they could.

The support our lab has received from the National Institutes of Health has funded all of the work described here (NIH Grant GM62367 (to T.R.G.)) and I am grateful to the Cellular and Molecular Microbiology Training Program for support during my first two years in Todd's lab (T32AI007611-11 (to R.D.B.)). The Gisela Mosig Travel Fund allowed me to travel to meetings across the country to present my results to other scientists.

I cannot thank my family enough and I will be forever indebted to my parents for all of their support through the years. I would like to thank my son Max, for the constant joy he has brought to Jennifer and I. To my wife Jennifer, only you know how much you mean to me.

Finally, I would like to thank Jennifer and Max for reminding me about the best things in life every single day.

TABLE OF CONTENTS

Page

DEDICATION....ii

ACKNOWLEDGEMENTS....iii

LIST OF TABLES....viii

LIST OF FIGURES....ix

ABBREVIATIONS....xiii

CHAPTER I....1

INTRODUCTION....1

P-type ATPases and the mechanism of ion transport....1

P4-ATPases and phospholipid flip....7

P4-ATPases and the Cdc50 family....13

P4-ATPases and vesicular protein transport....16

Concluding remarks....21

CHAPTER II....23

IDENTIFICATION OF RESIDUES DEFINING PHOSPHOLIPID FLIPPASE SUBSTRATE SPECIFICITY OF TYPE-IV P-TYPE ATPASES*....23

ABSTRACT....23

INTRODUCTION....24

RESULTS....26

Drs2 TM segments 3-4 confer NBD-PS uptake activity to Dnf1....26

TM4 is required for PS activity, but not specificity....30

The reciprocal Drs2 F511Y substitution disrupts PS asymmetry....36

The rate of NBD-PL uptake by Dnf1 Y618F is comparable to WT Dnf1....40

PC recognition by Dnf1....41

Function of Dnf1[Drs2] chimeras *in vivo*....42

Lem3 is required for Dnf1[Drs2] chimera ER export....43

Potential P4-ATPase substrate transport pathway 45
DISCUSSION 47
MATERIALS AND METHODS 52
Reagents 52
Strains and culture 52
Edelfosine screen 53
Viability assay 53
Fluorescence microscopy 53
NBD-lipid uptake 54
Flow cytometry 54
Data analysis 54
Modeling 55
Cloning 55
Plasmid shuffling assay 55
Cell extracts and western blotting 56
ACKNOWLEDGEMENTS 56
CHAPTER III 57
A TWO GATE MECHANISM FOR PHOSPHOLIPID SELECTION AND TRANSPORT BY P4-ATPASES* 57
ABSTRACT 57
INTRODUCTION 58
RESULTS 61
TM1-2 residues defining substrate specificity 61
TM3-4 residues defining substrate specificity 64
TM5-6 residues modulate Dnf1 activity 70
The cytosolic and exofacial gates cooperate to restrict PS flip by Dnf1 73
Drs2 uses a similar two-gate mechanism for PS selection and transport 76
DISCUSSION 80
MATERIALS AND METHODS 87
Strains and culture 87
Edelfosine resistance screen 87
Viability assay 88

Fluorescence microscopy 88
Cell extracts and western blotting 88
NBD-lipid uptake 88
Flow cytometry 89
Data analysis 89
Reagents 89
Cloning and mutagenesis 90
Lipid extraction and TLC analysis 91
ACKNOWLEDGEMENTS 91
CHAPTER IV 92
A ROLE FOR PHOSPHATIDYLSERINE FLIP IN VESICLE-MEDIATED PROTEIN TRANSPORT 92
INTRODUCTION 92
RESULTS 94
Dnf1 N550S flips endogenous PS 94
Dnf1 suppressors of Drs2 function 96
Recognition of mono vs. di-acylated phospholipid. 98
PS flip is important for anterograde traffic 101
PS flip is required for retrograde traffic 103
DISCUSSION 107
MATERIALS AND METHODS 111
Cold resistance screen 111
Strains and culture 112
Viability assay 112
α-factor secretion assay 112
Pulse-chase labeling and immunoprecipitation of cargo proteins 112
Serial dilutions 113
Lipid uptake 113
Flow cytometry 114
Calcofluor white staining 114
Fluorescence microscopy 115
Data analysis 115

ACKNOWLEDGEMENTS 115
CHAPTER V 116
PROBING THE MECHANISM FOR HOW P4-ATPASES WITH A PROLINE +4 LEUCINE RECOGNIZE SUBSTRATE 116
INTRODUCTION 116
RESULTS AND DISCUSSION 118
CHAPTER VI 123
TESTING THE BIOCHEMICAL PROPERTIES OF DNF1 123
INTRODUCTION 123
RESULTS AND DISCUSSION 124
Probing the orientation of residues critical for substrate specificity 124
Purification and measurement of ATPase activity with Dnf1 128
MATERIALS AND METHODS 130
Cloning 130
Purification 130
CHAPTER VII 132
DISCUSSION 132
Identification of residues selecting phospholipid suggests a novel transport pathway 132
Phosphatidylserine is important for Drs2 function 137
P4-ATPases use a novel two-gate mechanism 139
Transport along the TM1-4 groove 142
The proline +4 position 146
Conclusion 150
APPENDIX A 152
YEAST STRAINS, PLASMIDS AND PRIMERS 152
REFERENCES 163

LIST OF TABLES

Table Page

1-1. P4-ATPases form α−β heterodimers..... 16

LIST OF FIGURES

Figure		Page
1-1.	Phylogeny of P-type ATPases	2
1-2.	The Na^+/K^+ ATPase Post-Albers cycle	3
1-3.	Structural conservation among distant P-type ATPases	3
1-4.	Conformational changes associated with the catalytic cycle of the Ca^{2+} ATPase	5
1-5.	Ion binding sites for P2-ATPases	6
1-6.	P4-ATPases form α−β heterodimers	8
1-7	Physiological roles of disrupting membrane phospholipid asymmetry	9
1-8	Erythrocyte morphology changes in response to exogenous phospholipid addition	11
1-9	Vesicular mediated protein transport pathways in *S. cerevisiae*	17
2-1.	Transmembrane segments 3–4 from Drs2 are sufficient to confer a PS activity to Dnf1	27
2-2.	Topological diagrams of WT Dnf1, WT Drs2 and most of the chimeras reported in this study	28
2-3.	Drs2 TM3-4 confers PS preference to Dnf1, while TM4 confers a PS activity without affecting the recognition of PC or PE	31
2-4.	Activity and specificity of Dnf1[TM1-4]	32
2-5.	A single amino acid change, Y618F, specifically confers PS uptake activity to Dnf1	33
2-6.	The enhanced uptake for all three substrates noted for Dnf1[YIS→FVT] was also observed for Dnf1[YI→FV]	34
2-7.	Expression levels of Flag-Dnf1, Flag-Dnf1[YIS→FVT] and Flag-Dnf1 Y618F are similar	35
2-8.	The PS uptake observed in Dnf1[Drs2] chimeras is not attributable to Drs2	36

2-9. Drs2 F511Y specifically perturbs plasma membrane PS asymmetry..... 37

2-10. Dnf1 Y618F is unable to suppress the PapB hypersensitivity of the *drs2Δ* strain....38

2-11. Complementation of *dnf1,2,3Δdrs2Δ* by *DNF1[DRS2]* chimeric genes..... 39

2-12. The rate of NBD-PC and NBD-PS uptake mediated by Dnf1 Y618F is comparable, suggesting a similar transport mechanism..... 40

2-13. Phe587 substitutions specifically perturb PC uptake activity by Dnf1.....42

2-14. GFP tagged Dnf1[Drs2] chimeras retain a Lem3 requirement for ER export and flippase activity..... 44

2-15. Model of the Dnf1 structure showing the orientation of Y618 and a proposed pathway for phospholipid translocation..... 46

2-16. Structural conservation of the P-type ATPase TM domain..... 49

3-1. Transmembrane segments 1 and 2 (TM1-2) contribute to phospholipid selection..... 63

3-2. Summary of the Dnf1 mutagenesis edelfosine-resistance screen.....65

3-3. TM3 mutations conferring edelfosine resistance alter Dnf1 substrate specificity.. .66

3-4. LL3-4 and TM4 mutations conferring edelfosine resistance alter Dnf1 substrate specificity..... 68

3-5. Alanine scanning mutagenesis highlights additional residues involved in Dnf1 function and substrate specificity.....69

3-6. Substrate preference of TM5-6 edelfosine-resistant Dnf1 mutants..... 71

3-7. Mutation of conserved TM5 lysine and Dnf1 alleles with multiple TM5-6 mutations reduce activity without changing specificity..... 73

3-8. Specificity determinants on both sides of the membrane cooperate to transport phospholipid..... 74

3-9. NBD-PC and NBD-PS are not modified prior to uptake into *dnf1,2Δ* yeast..... 75

3-10. Key Dnf1 constructs allowing PS flip still require the β subunit, Lem3..... 76

3-11. Control of Drs2 PS recognition by both cytosolic and exofacial residues..... 77

3-12. Drs2 entry and exit gate substitutions act similarly to reciprocal substitutions in Dnf1..... 78

3-13. Residues affecting the phospholipid specificity of P4-ATPases cluster into two gates..... 82

3-14. Phospholipid interaction with Ca^{2+} ATPase in E2 conformation..... 85

4-1. Dnf1 N550S suppresses *drs2Δ* PS asymmetry and cold-sensitive growth.....95

4-2. Identification of additional Dnf1 variants which suppress *drs2Δ* cold-sensitivity and PS asymmetry..... 97

4-3. Di-acyl PS is transported across the plasma membrane by Dnf1 suppressors.....99

4-4. Dnf1,2 mediate uptake of lyso-PS across the plasma membrane..... 100

4-5. The ability to transport endogenous PS allow restoration of Drs2-dependent trafficking pathways..... 101

4-6. Endocytic recycling requires PS flip..... 104

4-7. SNC1 trafficking from the trans-Golgi network does not require PS..... 105

4-8. Dnf1 N550S cannot support recycling from the plasma membrane.....106

4-9. Dnf1 variants do not bypass the requirement for RCY1 cold-resistant growth..... 107

4-10. Phospholipid interaction with Ca^{2+} ATPase in E2 conformation..... 111

5-1. Atp8a1 and Atp8a2 are PS flippases with a P+4 leucine..... 117

5-2. Activity to Drs2 F511L is restores with N445S.....118

5-3. Papuamide A selects against mutants exposing PS in a *drs2Δ*..... 119

5-4. Summary of residues changed in a screen for Drs2 mutants restoring PS asymmetry..... 120

5-5. Coupling between P+4 position and novel substitutions..... 121

5-6. Critical residues in substrate selection by P4-ATPases..... 121

6-1. Diagram for proposed gel shift assays to test the Dnf1 structural model..... 125

6-2. Positioning of TM1-4 residues targeted for cysteine mutagenesis and crosslinking..... 126

6-3. Many introduced cysteines support *dnf1,2,3Δdrs2Δ* growth..... 126

6-4. TAP-Dnf1 gives relatively poor cleavage with TEV protease…… 127

6-5. Detection of Flag3-Dnf1-TEV cleavage…… 128

6-6. Purification and *in vitro* activity of Dnf1……129

7-1. Summary of residues capable of affecting substrate specificity of P4-ATPases…… 141

7-2. The proposed phospholipid transport pathway is unique for Dnf1…… 145

7-3. Exit-gate coupling with the P+4 position……..... 149

ABBREVIATIONS

PS	Phosphatidylserine
PC	Phosphatidylcholine
PE	Phosphatidylethanolamine
PI	Phosphatidylinositol
SM	Sphingomyelin
NBD	7-nitro-2-1,3-benzoxadiazol-4-yl
PapB	Papuamide B
5-FOA	5-fluoroorotic acid
ER	Endoplasmic reticulum
TGN	*trans*-Golgi network
EE	early endosome
LE	late endosome
PM	plasma membrane
HA	hemagglutinin
M6P	mannose-6-phosphate
GGA	Golgi-localized, γ-ear-containing, Arf-binding family of proteins
AP-1	Adaptor protein 1
P4-ATPase	type-IV P-type ATPase

CHAPTER I

INTRODUCTION

P-type ATPases and the mechanism of ion transport

P-type ATPases are a family of integral membrane proteins that catalyze active transport of substrate across membrane bilayers and are phylogenetically grouped into 5 subclasses (Figure 1-1) (Axelsen & Palmgren, 1998). Type-I (P1) are heavy metal pumps, type-II (P2) are cation transporters, type-III (P3) are proton pumps, type-IV (P4) are phospholipid flippases and the type-V (P5) have unknown substrate specificity. The best characterized subclass, the type II P-type ATPases (P2-ATPases) catalyze the energy-dependent movement of cations across lipid bilayers.

Jens Skou first reported an ATPase isolated from shore crab neurons that was stimulated by a combination of Na^+, K^+ and Mg^{2+} (Skou, 1957). Over the decades, the catalytic cycle for the Na^+/K^+ ATPase was meticulously investigated. Eventually, the relationships between phosphorylation, Na^+ export and K^+ import were unraveled, leading to the model of the Post-Albers cycle (Figure 1-2) (Albers, Fahn, & Koval, 1963; Charnock & Post, 1963; Post, Hegyvary, & Kume, 1972; Post & Jolly, 1957; Post & Sen, 1965; Post, Sen, & Rosenthal, 1965). Although the mechanics of the reaction cycle were described by Robert Post and R. Wayne Albers, the discovery of the Na^+/K^+ ATPase resulted in the Nobel Prize in Chemistry awarded to Jens Skou for "the first discovery of an ion-transporting enzyme, Na^+, K^+ -ATPase" (The Nobel Prize in Chemistry, 1997). Decades of work formed an incredible knowledge base for Na^+/K^+ transport (and later Ca^{2+} transport) which culminated in the x-ray crystal structures of the

sarcoplasmic/endoplasmic reticulum Ca^{2+} ATPase (SERCA) from Chikashi Toyoshima's Lab (Toyoshima & Mizutani, 2004; Toyoshima, Nakasako, Nomura, & Ogawa, 2000; Toyoshima & Nomura, 2002; Toyoshima, Nomura, & Tsuda, 2004).

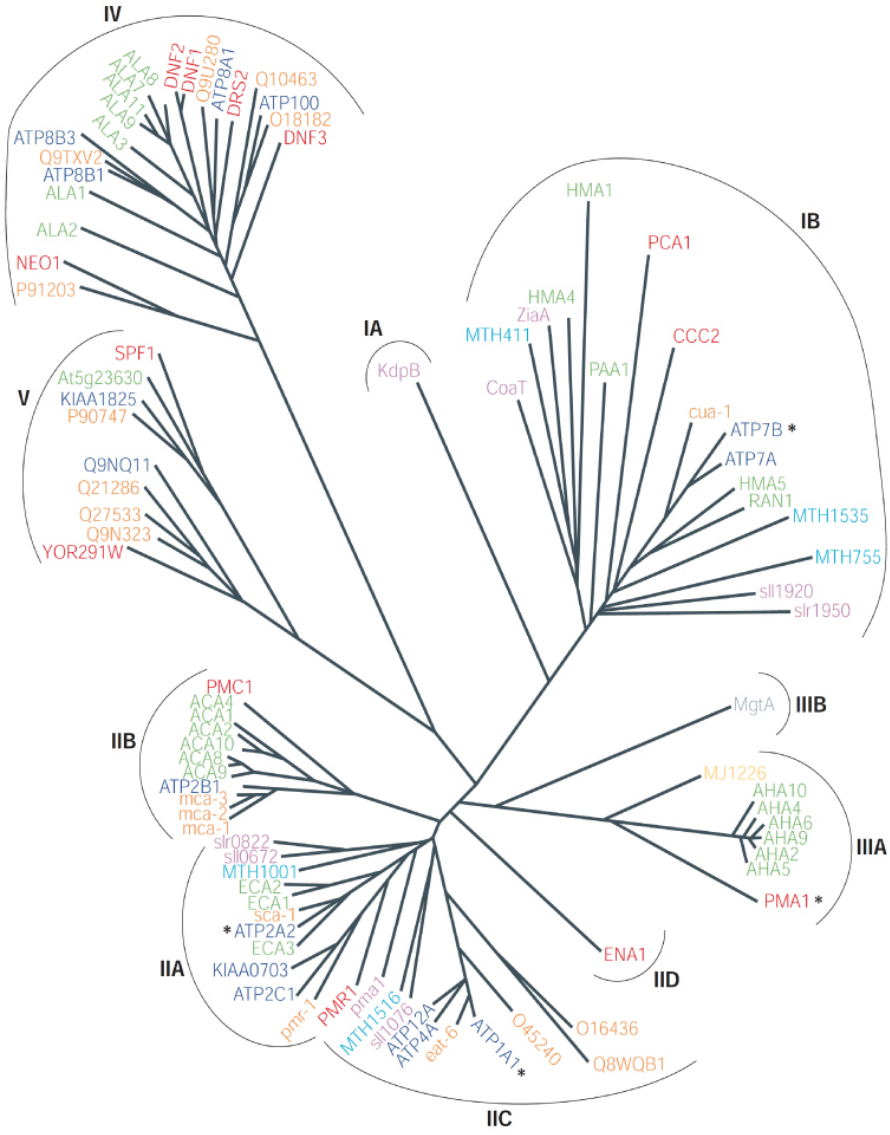

Figure 1-1. Phylogeny of P-type ATPases (image from (Kuhlbrandt, 2004))

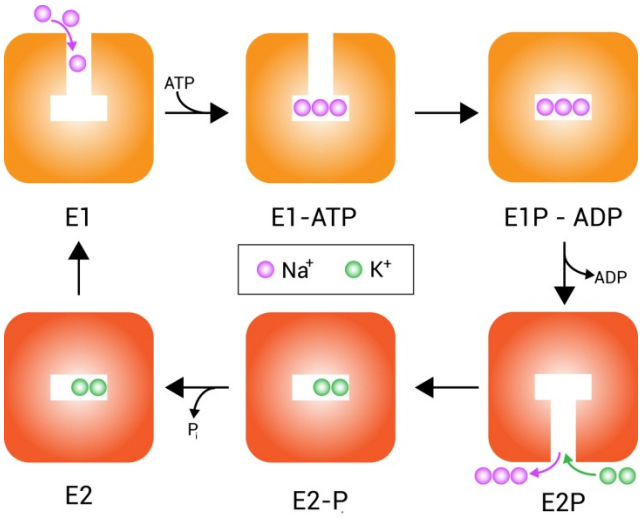

Figure 1-2. The Na^+/K^+ ATPase Post-Albers cycle.

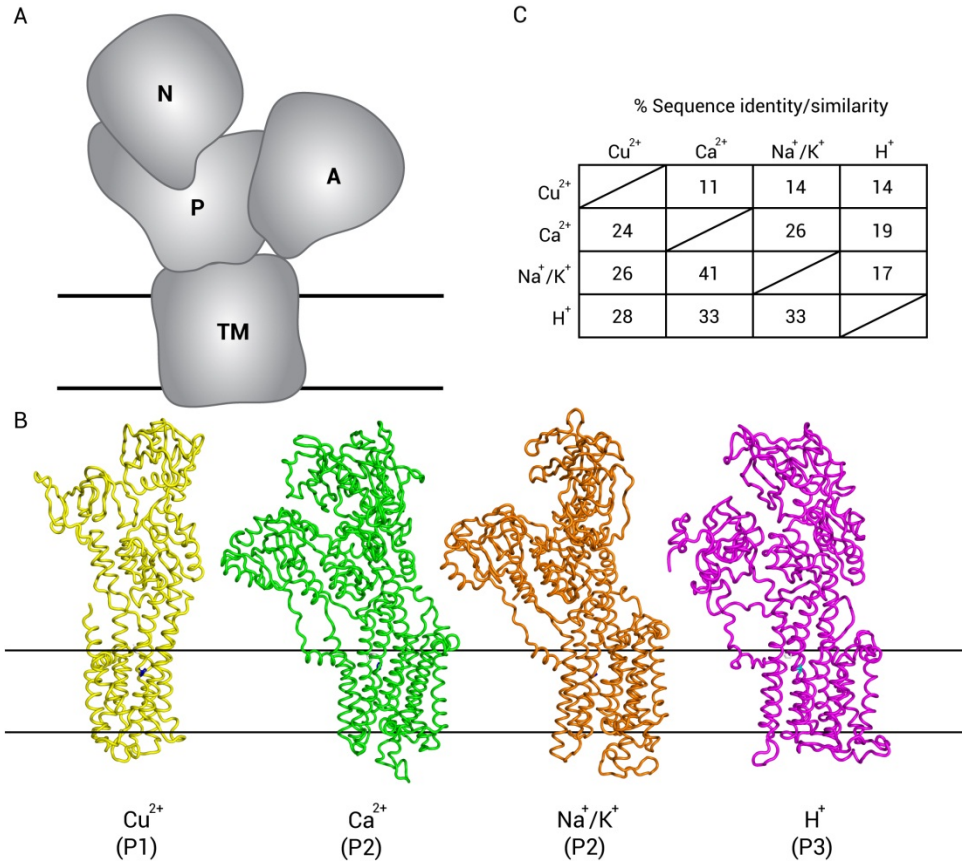

Figure 1-3. Structural conservation among distant P-type ATPases (A) Domain layout for P-type ATPases; A, actuator domain; N, nucleotide-binding domain; P, phosphorylation domain. (B) Sequence identity above the line, sequence similarity below the line. (C) Comparison of the crystalized P1, P2 and P3 ATPases.

The x-ray crystal structures revealed four characteristic domains which serve specific functions: nucleotide-binding (N), phosphorylation (P), actuator (A), and transmembrane (TM)(Figure 1-3A)(Toyoshima, et al., 2000). To date, x-ray crystal structures have been reported for P1 (Gourdon et al., 2011), P2 (Morth et al., 2007; Toyoshima, et al., 2000) and P3 ATPases (Pedersen, Buch-Pedersen, Morth, Palmgren, & Nissen, 2007). Despite the primary sequence divergence, there is a remarkable conservation of the overall structure and individual domains among the P-type ATPases (Figure 1-3B). The Toyoshima lab has reported SERCA structures in different states of the Post-Albers cycle. With these independent structures, the dramatic conformational changes P-type ATPases undergo during the catalytic cycle became apparent (Figure 1-4). ATP hydrolysis drives the Post-Albers cycle in one direction, and the N domain interacts with ATP to position the γ-phosphate in close proximity to the P-domain. The γ-phosphate is transferred to a conserved aspartate residue within the P domain forming a phosphorylated intermediate (hence the name P-type ATPases). As the cycle proceeds, the A domain catalyzes hydrolysis of the γ-phosphate from the conserved aspartate within the P-domain. The conservation of key features in several P-type ATPase classes also suggests there may be common substrate binding sites within the transmembrane domain.

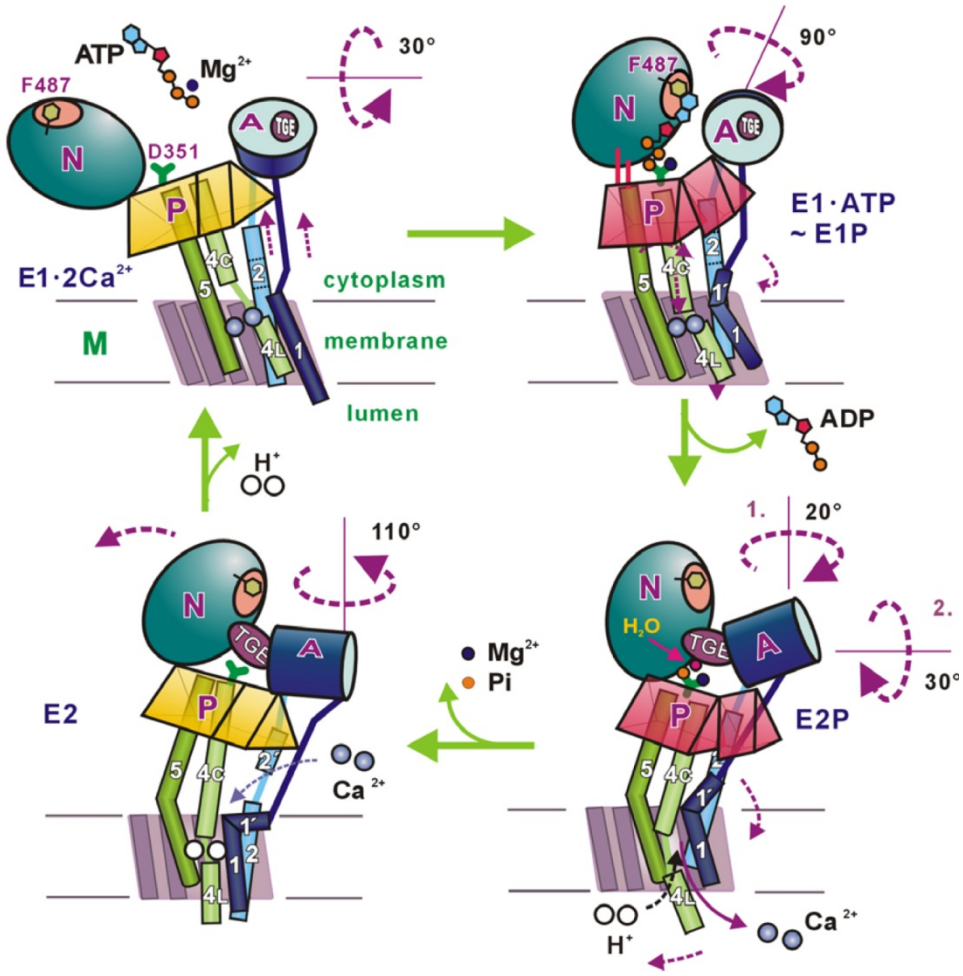

Figure 1-4. Conformational changes associated with the catalytic cycle of the Ca^{2+} ATPase. Image from (Toyoshima, 2008).

The substantial domain movements are directly coupled to gating access of the substrate binding sites within the transmembrane domain. The substrate binding sites of ion transporting P-type ATPases lie within the transmembrane (TM) domain, and involve multiple residues on separate transmembrane segments coordinating the cations in a well-defined binding pocket. Access to the cation binding sites alternates between the cytosolic and exofacial sides of the membrane, and is classically defined by E1-E2 conformational transitions of the Post-Albers transport cycle. For the Na^+/K^+ ATPase, the cycle begins in the E1 state with the

substrate binding sites accessible to the cytosol. Three Na^+ ions enter into the binding site formed by charged residues in TM segments 4, 5, 6, 7 and 9. The N domain interacts with ATP and swings to position the γ-phosphate near to the conserved aspartate (Asp369 in the Na^+/K^+ ATPase). Simultaneously, rotation of the A domain drags TM1 and TM2 towards the cytosolic membrane surface (E1-ATP). The close proximity of ATP to Asp369 allows the subsequent transfer of the γ–phosphate to the conserved aspartate, triggering the occlusion of the substrate binding sites from both sides of the membrane (E1P-ADP). The transition of the pump to E2P involves release of ADP, rotation of the A domain to bring the TGES motif close to the phosphorylated aspartate, and exposure of substrate binding sites to the exofacial side of the membrane. This permits a rapid exchange of three Na^+ ions for two K^+ ions. Hydrolysis of the aspartyl-phosphate by the TGES motif triggers occlusion of the substrate binding sites from both membrane faces until N domain and A domain rotations induce the exposure of the substrate binding sites to cytosol, releasing the two K^+ ions and resetting the pump to the E1 state.

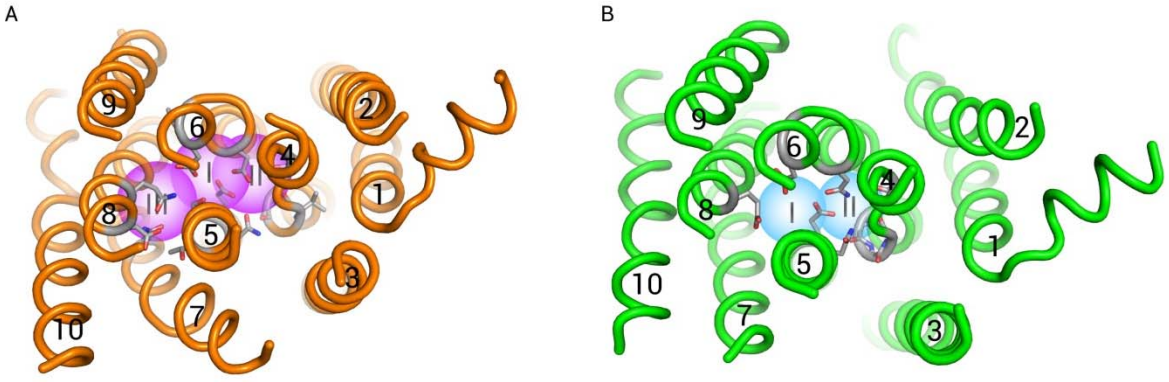

Figure 1-5. Ion binding sites for P2-ATPases. Arabic numeral indicate TM segment and roman numeral indicate the ion binding sites for: (A) Na^+/K^+ ATPase (B) Ca^{2+} ATPase.

The ion-transporting P-type ATPases use a highly-conserved ion binding pocket (6/9 residues identical between Ca^{2+} ATPase and Na^{+}/K^{+} ATPase, indicated by *). The ion coordination site I is formed by TM5, 6, 9 (Asn776*, Glu779*, Thr807*, Asp808*, Gln923), site II by TM4, 6 (two main chain carbonyls, Glu327*, Asp804, Asp808*), and site III by TM5, 7, 9 (Ser775, Thr774, Gln854, Asp926)(Figure 1-5A). The sarcoplasmic-endoplasmic reticulum Ca^{2+} ATPase (SERCA) ion binding pocket is formed by TM segments 4, 5, 6, 8; site I from TM5,6,8 (Asn768*, Glu771*,Thr799*, Asp800*, Glu908 and two water molecules) and site II from TM4 (three main chain carbonyls, Glu309*, Asn796, Asp800*)(Figure 1-5B). The Post-Albers mechanism of the Ca^{2+} ATPase is equivalent to that of the Na^{+}/K^{+} ATPase. In SERCA, two Ca^{2+} are transported in the direction corresponding to Na^{+} movement and one to two protons are counter-transported (in the direction of the K^{+} ions). Mutational studies defining important residues combined with the x-ray crystal structures indicate the Cu^{2+} ATPase (P1) and H^{+} ATPase (P3) are using similar ion binding sites to P2-ATPases (Buch-Pedersen & Palmgren, 2003; Buch-Pedersen, Venema, Serrano, & Palmgren, 2000; González-Guerrero, Eren, Rawat, Stemmler, & Argüello, 2008; Gourdon, et al., 2011; Pedersen, et al., 2007). Importantly, all of these pumps establish both an ion concentration gradient and electrical gradient because of the unbalanced charge (electrochemical gradient). This electrochemical gradient is important for other coupled transport processes, signaling processes and ultimately, cell survival. Whether the mechanism of substrate recognition and transport through the well-defined ion binding site is conserved for all P-type ATPase subclasses is unknown.

P4-ATPases and phospholipid flip

Members of the P4-ATPase subfamily were also originally thought to be Ca^{2+} ATPases based on sequence homology. Based on conservation of key sequence motifs, P4-ATPases have

each of the four characteristic P-type ATPase domains, A, N, P, TM (Figure 1-6A). Like many of the ion-transporters, they have 10 TM segments. However, in contrast to the cation transporters, members of the P4-ATPase subfamily translocate phospholipids across a membrane bilayer, a flippase activity. The P4-ATPase subfamily is conserved among eukaryotes from yeast to humans, but appears to be absent among prokaryotes. *Saccharomyces cerevisiae* has five P4-ATPases, whereas mammals have at least 14. P4-ATPases are essential for viability in yeast (Hua, Fatheddin, & Graham, 2002) and the mammalian proteins are implicated in B cell development (Siggs et al., 2011; Yabas et al., 2011), neuronal growth (Q. Xu et al., 2012), hippocampal-dependent learning (Levano et al., 2011), cell migration (Kato et al., 2012) and spermatogenesis (P. Xu et al., 2009). They also play roles in pathological conditions such as neurodegenerative disease (Zhu et al., 2012), intellectual disability disorder (Emre Onat et al., 2012), obesity and type II diabetes (Dhar et al., 2004), intrahepatic cholestasis (Bull et al., 1998), progressive hearing loss (Stapelbroek et al., 2009) and male infertility (Wang, Beserra, & Garbers, 2004). In addition, this family plays basic biological roles in vesicle-mediated protein trafficking and establishing phospholipid asymmetry of the plasma membrane.

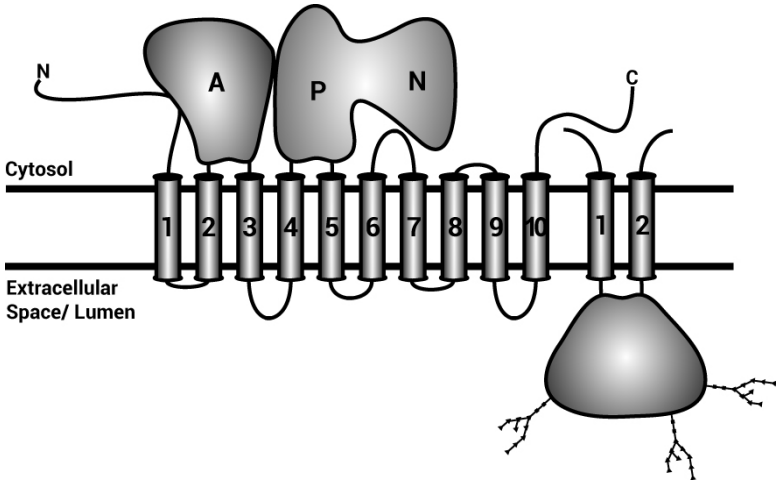

Figure 1-6. P4-ATPases form α−β heterodimers. Topology diagram for P4-ATPases and their β-subunits.

The plasma membrane of living cells is an asymmetric structure with an uneven distribution of specific phospholipids between the inner (cytosolic) and outer (extracellular) leaflets. PS and PE, for example, are confined almost exclusively to the inner leaflet while PC and sphingolipids are enriched in the outer leaflet. This asymmetry creates different chemical environments on opposing membrane faces that are important for integral membrane protein function, interaction of soluble proteins with the membrane surface and cell-cell interactions (van Meer, Voelker, & Feigenson, 2008). Controlled disruption of the plasma membrane asymmetry plays important roles in physiological phenomena including apoptosis, blood coagulation, cytokinesis and some host-pathogen interactions (Figure 1-7)(Emoto et al., 1996; Mercer & Helenius, 2008; Zwaal & Schroit, 1997).

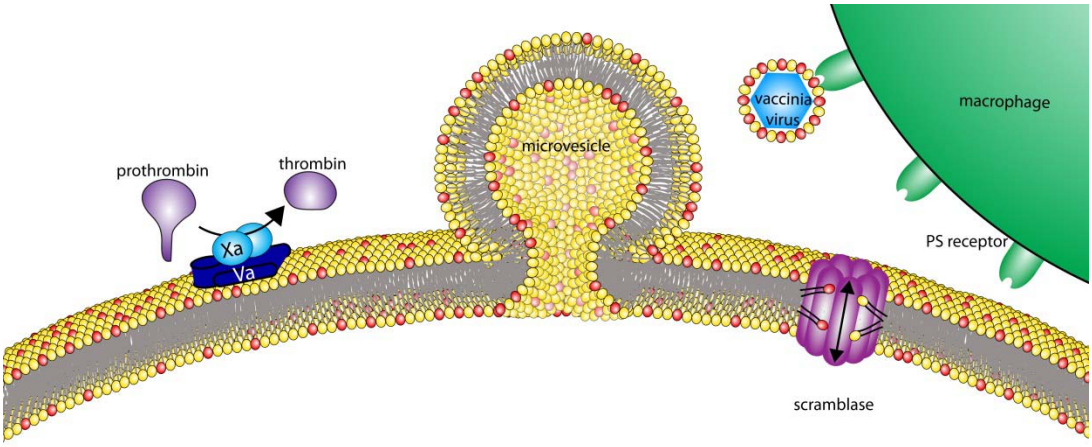

Figure 1-7. Physiological roles of disrupting membrane phospholipid asymmetry. Activation of the scramblase protein allows bi-directional energy-independent movement of lipids. Exposure of phosphatidylserine (red phospholipid) allows assembly of blood clotting factors (left), shedding of pro-coagulatory microvesicles (middle) and recognition by the macrophage (right). Vaccinia virus mimics apoptotic cells by exposing phosphatidylserine on the viral envelope.

In contrast to biological membranes, when bilayers are formed spontaneously from lipids suspended in water, the component phospholipids are evenly distributed between the two faces of the bilayer. The hydrophobic core of the membrane provides an energy barrier that prevents transverse movement of the hydrophilic headgroup, and so spontaneous flip/flop of

component phospholipids like PC, PS or PE is a rare event in artificial membranes (Kornberg & McConnell, 1971). A low intrinsic rate of spontaneous phospholipid flip/flop allows plasma membrane asymmetry to be maintained with minimal energy input, but how is the ordered plasma membrane structure with PS and PE enriched in the cytosolic leaflet initially established?

The discovery of an energy-driven aminophospholipid translocase (APLT) activity in human erythrocytes provided the first mechanistic insight into how cells create an asymmetric plasma membrane structure (Seigneuret & Devaux, 1984). Spin-labeled analogs of PS and PE incorporated into the extracellular leaflet are rapidly transported to the cytosolic leaflet of the erythrocytes, while spin-labeled PC remains in the extracellular leaflet. The selective transport of spin-labeled PS and PE to the cytosolic leaflet by the APLT suggested that this enzyme pumps endogenous PS and PE to establish asymmetry. The energy requirement for flipping the charged lipid headgroup across the hydrophobic membrane core was provided by ATP and vanadate inhibited translocation, providing the first hint that a member of the P-type ATPase family catalyzed this translocase activity. This study provided the first evidence for an APLT activity in human erythrocytes, but reports of an APLT activity in bovine chromaffin granules (Zachowski, Henry, & Devaux, 1989), platelets (Sune, Bette-Bobillo, Bienvenue, Fellmann, & Devaux, 1987) and yeast (Kean, Fuller, & Nichols, 1993; Tang, Halleck, Schlegel, & Williamson, 1996) followed.

The erythrocyte APLT is also able to flip unlabeled PS and PE to the inner leaflet as measured by changes in the shape of the cells (Daleke & Huestis, 1985; Seigneuret & Devaux, 1984). As described by the bilayer couple hypothesis, an unbalanced increase in the lipid number in one face of the membrane creates curvature in the direction of the leaflet with the greater surface area (Sheetz & Singer, 1974). Incorporation of exogenous phospholipid into the extracellular face of the bilayer induces a dramatic outward bending of the membrane, and changes the erythrocyte shape from the normal discocyte shape to an echinocytic shape

resembling a sea urchin (Figure 1-8). When a substrate of the APLT is incorporated into the membrane (PS or PE), erythrocytes rapidly revert from echinocytes (Figure 1-8A) back to discocytes (Figure 1-8B), and then to crenated stomatocytes (Figure 1-8C) as phospholipid is pumped to the inner leaflet. However, if a non-substrate for the aminophospholipid translocase, such as PC, is incorporated into the outer leaflet, the cells retain their echinocyte shape (Daleke & Huestis, 1985; Seigneuret & Devaux, 1984). Importantly, these experiments demonstrated specificity of phospholipid flippases and the potential to induce curvature in biological membranes.

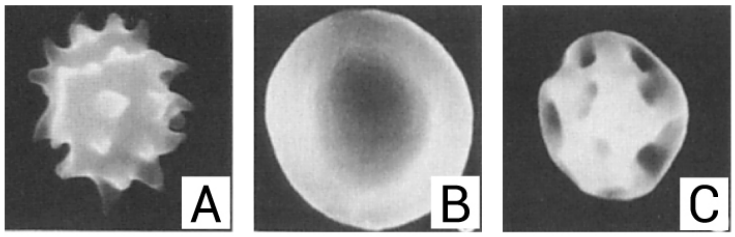

Figure 1-8. Erythrocyte morphology changes in response to exogenous phospholipid addition (A) Echinocyte (B) Discocyte (C) Crenated stomatocyte (Image modified from: (Daleke & Huestis, 1989)).

The identity of the APLT is still uncertain (Daleke, 2007), although ATP8A1 remains the best candidate for the erythrocyte (Soupene & Kuypers, 2006) and bovine chromaffin granule flippase (Zachowski, et al., 1989). This connection derived from the purification of a novel 115 kDa ATPase from bovine chromaffin granules, called ATPase II at the time; the ATPase activity of which is dramatically stimulated by PS (and PE to a minor extent) (Moriyama & Nelson, 1988; Xie, Stone, & Racker, 1989). A similar 110 - 120 kDa Mg^{2+} dependent ATPase purified from human erythrocytes was suspected to be homologous to ATPase II and responsible for the aminophospholipid translocase activity of the erythrocyte plasma membrane (Morrot, Zachowski, & Devaux, 1990). This ATPase was partially purified from human erythrocytes and

reconstituted into proteoliposomes, which displayed a PS translocase activity (Auland, Roufogalis, Devaux, & Zachowski, 1994). However, the protein responsible for the reconstituted APLT activity was not identified.

Validation that ATPase II (ATP8A1) is a P-type ATPase occurred when the gene encoding the bovine chromaffin granule enzyme was cloned, a discovery that nucleated a dramatic expansion of the field as additional homologs were uncovered (Tang, et al., 1996). ATPase II was initially found to be homologous to the yeast protein Drs2, and soon after to ATP8B1 (FIC1)(Bull, et al., 1998). Disruption of *DRS2* (*drs2Δ)* was reported to cause a defect in PS translocation at the plasma membrane of *S. cerevisiae* (Tang, et al., 1996), although later reports suggested that Drs2 had a negligible impact on this activity (Marx et al., 1999; Siegmund et al., 1998). The discovery of protein trafficking defects in *drs2Δ* cells also raised concerns that the influence of Drs2 on the plasma membrane flippase activity was indirect.

However, a number of subsequent genetic studies strongly supported a direct role for P4-ATPases in phospholipid translocation. In *S. cerevisiae*, Dnf1 and Dnf2 are required for the plasma membrane flippase activity towards NBD-labeled PC and PE (Pomorski et al., 2003). Drs2 localizes to the TGN, and purified TGN membranes carrying a temperature-sensitive form of Drs2 contain an NBD-PS flippase activity that is inactivated at the nonpermissive temperature (Natarajan, Wang, Hua, & Graham, 2004). Secretory vesicles exiting the TGN contain a flippase activity that is Drs2 and Dnf3-dependent (Alder-Baerens, Lisman, Luong, Pomorski, & Holthuis, 2006) and all of the *DRS2* and *DNF* genes contribute to the establishment of membrane asymmetry (S. Chen et al., 2006; Pomorski, et al., 2003). The *Arabidopsis* P4-ATPases ALA1, ALA2 and ALA3, and murine Atp8b5 (FetA) can support plasma membrane flippase activity when expressed in yeast P4-ATPase mutants (Poulsen et al., 2008; P. Xu, et al., 2009). In addition, overexpression of ATP8B1 in CHOK1 cells results in increased PS translocation at the plasma

membrane (Coen C. Paulusma et al., 2008; Ujhazy et al., 2001) (although see also (Verhulst et al., 2010)) and Atp8b1 deficiency in mice results in disruption of the membrane asymmetry in bile canalicular membranes (Cai et al., 2009; Coen C. Paulusma et al., 2006).

Only recently has biochemical evidence emerged indicating that the P4-ATPases directly catalyze a phospholipid flippase activity. Working independently, the Graham and Molday groups were able to purify two P4-ATPases to near homogeneity, Drs2 and ATP8A2, respectively, reconstitute the P4-ATPases into proteoliposomes and demonstrate *in vitro* flippase activities (Coleman, Kwok, & Molday, 2009; Zhou & Graham, 2009). Two and a half decades after the report of a protein component responsible, these studies provided the first evidence that a P4-ATPase is sufficient to catalyze an ATP-dependent phospholipid flippase activity.

P4-ATPases and the Cdc50 family

Many P4-ATPases associate with β subunits, which have two TM segments, a large glycosylated ectoplasmic domain, and are potentially analogous to the Na^+/K^+ ATPase β and γ subunits (Figure 1-6A). The P4-ATPase β subunits were independently identified in genetic screens for loss of membrane asymmetry or phospholipid translocase activity. For example, *LEM3/ROS3* (encoding a member of the Cdc50 family (Radji, Kim, Togan, Yoshikawa, & Shirahige, 2001)) was identified in a screen for mutants exhibiting a loss of phosphatidylethanolamine asymmetry in *S. cerevisiae* (Kato et al., 2002), and *lem3Δ* mutants were also found to be deficient in the uptake of edelfosine, a toxic PC analog (Hanson, Malone, Birchmore, & Nichols, 2003). More recently, a forward genetic screen for loss of PS asymmetry in *C. elegans* uncovered mutations in a Cdc50 homolog (CHAT-1) as well as TAT-1 (a Drs2 homolog) (B. Chen et al., 2010). The connection of the Cdc50 family to membrane asymmetry was not immediately clear because it seemed unlikely that these proteins could transport lipid directly as they have only

two transmembrane segments and no ATPase domain. However, the Tanaka group linked a series of observations showing similar phenotypes of P4-ATPase mutants and Cdc50 family mutants to discover the functionally essential interaction between P4-ATPases (α subunits) and the Cdc50 family members (β subunits) (Saito et al., 2004). In sum, these genetic studies clearly demonstrate that the P4-ATPases and their β subunits are necessary for phospholipid flippase activities detected in several different membranes, and for the establishment of plasma membrane asymmetry.

At this point, it is generally accepted that most P4-ATPases associate with a β subunit and this interaction is required for their mutual export from the ER (for a summary see Table 1-1) (Bryde et al., 2010; Coen C. Paulusma, et al., 2008; Poulsen, López-Marqués, McDowell, et al., 2008; Saito, et al., 2004; Takatsu et al., 2011; van der Velden et al., 2010). Whether or not the β-subunit has additional roles in the trafficking, substrate transport, or regulation of flippase activity is still uncertain. In Drs2 proteoliposomes, a sub-stoichiometric amount of the Cdc50 beta subunit was present, and it is unclear if the flippase activity was catalyzed by the heterodimers in the preparation or if Drs2 can translocate substrate in the absence of Cdc50 (Zhou & Graham, 2009). ATP8A2 associates with CDC50A, and the complex was purified by a dual affinity approach using monoclonal antibodies that recognize each subunit. The purified heterodimer retained a robust PS-stimulated ATPase activity and NBD-PS flippase activity in proteoliposomes (Coleman & Molday, 2011). However, the ATP8A2 monomer was not assayed to determine if it is capable of flipping phospholipid in the absence of CDC50A. Recent evidence with *Arabidopsis thaliana* and human P4-ATPase complexes suggest the beta subunit is not responsible for the substrate specificity or localization of the P4-ATPase heterodimer (López-Marqués et al., 2010; van der Velden, et al., 2010). However, with both yeast and human complexes, the β subunit appears to preferentially bind the E2-P form of the P4-ATPases,

suggesting an important role in the catalytic cycle (Bryde, et al., 2010; Lenoir, Williamson, Puts, & Holthuis, 2009). Translocation of phospholipid is proposed to occur at the E2-P to E1 transition based upon biochemical data demonstrating that in a human P4-ATPase, Atp8a1, dephosphorylation is stimulated by addition of phospholipid substrate (Ding et al., 2000). The direction of phospholipid translocation, from exofacial to cytosolic leaflet, is also consistent with the E2-P to E1 transition.

In addition, conditional mutant forms of Cdc50 have been isolated that retain the ability to bind Drs2, but show a loss of function *in vivo* at the nonpermissive temperature. This observation implies an important role for the Cdc50-Drs2 interaction with the TGN-endosomal system (Takahashi, Fujimura-Kamada, Kondo, & Tanaka, 2011). By creating a series of chimeras between CDC50A and CDC50B, Coleman et al. found that the TM segments and ectoplasmic domain of CDC50A are critical for association with ATP8A2, and the N-terminal cytosolic domain had a significant influence on catalytic activity (Coleman & Molday, 2011). It appears that the β-subunit can modulate the activity of the α-subunit, but whether this is a regulatory interaction or an essential component of the pump is an important open question.

Table 1-1 P4-ATPases form α−β heterodimers

P4-ATPase (α)	β	Ref
Drs2	CDC50	(Saito, et al., 2004)
Dnf1	LEM3	(Saito, et al., 2004)
Dnf2	LEM3	(Furuta, Fujimura-Kamada, Saito, Yamamoto, & Tanaka, 2007)
Dnf3	CRF1	(Furuta, et al., 2007)
Neo1	None detected	
TAT-1	CHAT-1	(B. Chen, et al., 2010)
ALA2	ALIS1, ALIS3, ALIS5	(López-Marqués, et al., 2010)
ALA3	ALIS1, ALIS3, ALIS5	(Poulsen, López-Marqués, McDowell, et al., 2008)
ATP8A1	CDC50A (also CDC50B?)	(Bryde, et al., 2010; van der Velden, et al., 2010)
ATP8A2	CDC50A	(van der Velden, et al., 2010)
ATP8B1	CDC50A, CDC50B	(Coen C. Paulusma, et al., 2008)
ATP8B2	CDC50A, CDC50B	(Bryde, et al., 2010; van der Velden, et al., 2010)
ATP8B3		
ATP8B4	CDC50A (also CDC50B?)	(Bryde, et al., 2010; van der Velden, et al., 2010)
ATP9A	independent	(Takatsu, et al., 2011)
ATP9B	independent	(Takatsu, et al., 2011)
ATP10A	CDC50A	(Takatsu, et al., 2011)
ATP10B	CDC50A	(Takatsu, et al., 2011)
ATP10C		
ATP10D	CDC50A	(Takatsu, et al., 2011)
ATP11A	CDC50A	(Takatsu, et al., 2011)
ATP11B	CDC50A	(Takatsu, et al., 2011)
ATP11C	CDC50A	(Takatsu, et al., 2011)
LdMT	LdRos3	(Pérez-Victoria, Sánchez-Cañete, Castanys, & Gamarro, 2006)

P4-ATPases and vesicular protein transport

The Graham lab first identified a connection between P4-ATPases and protein trafficking. Using *S. cerevisiae* the authors searched for genetic interactions with the small G-protein ADP-ribosylation factor 1 (ARF1). GTP-bound Arf1 is involved in recruiting adaptors and coat proteins to Golgi and endosomal membranes. They identified seven genes that were synthetically lethal with *arf1Δ* (*SWA1*-7) (C. Y. Chen & Graham, 1998). While Arf1 is involved in both COPI and clathrin recruitment, this screen turned out to be biased towards proteins involved in clathrin function identifying the clathrin heavy chain (*SWA5*), auxilin (*SWA2*), Drs2

(*SWA3*) and Cdc50 (*SWA4*) (C. Y. Chen, Ingram, Rosal, & Graham, 1999; S. Chen, et al., 2006; Walter E. Gall et al., 2000). Drs2 has been demonstrated to function in several trafficking pathways within the Golgi-endosomal system. Drs2 is primarily localized to the TGN but does cycle to and from the early endosome, where it is involved in retrograde traffic to the TGN.

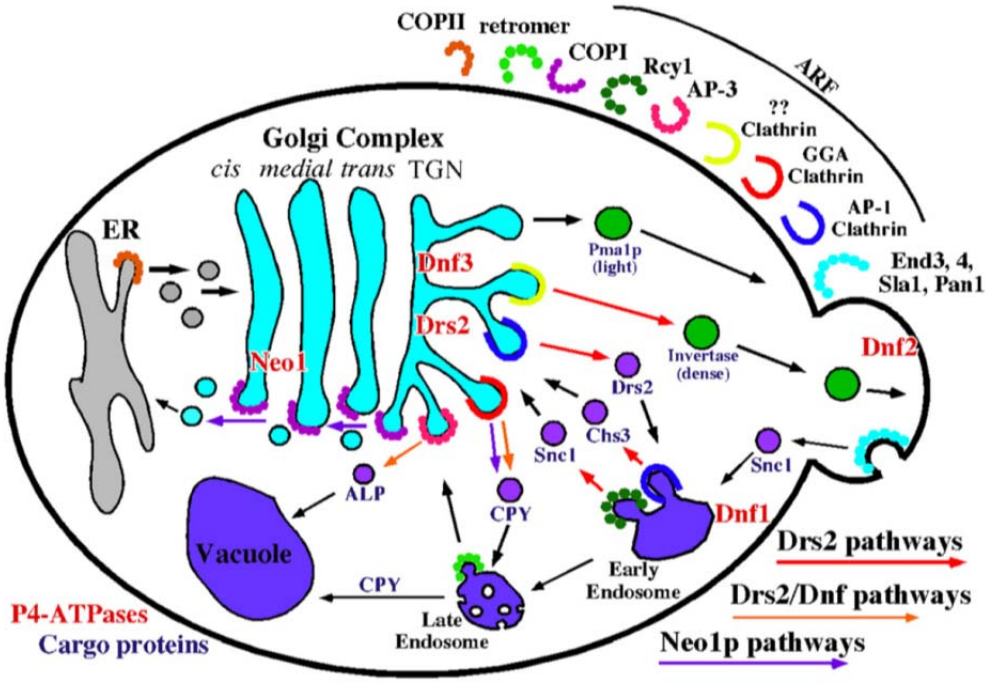

Figure 1-9. Vesicular mediated protein transport pathways in *S. cerevisiae*. Image from: (Muthusamy, Natarajan, Zhou, & Graham, 2009).

From the TGN, Drs2 is involved in trafficking anterograde cargo to at least 4 target organelles. Cargo can be destined to the plasma membrane, in either dense-class or light-class secretory vesicles (Harsay & Bretscher, 1995). In a *drs2Δ* strain, there is no apparent defect in secretion of invertase or α-factor because a defect in one pathway re-routes cargo into the other (C. Y. Chen, et al., 1999; Hua, et al., 2002). However, in *sla2Δ* cells, fusion of the dense vesicles with the plasma membrane is blocked and they accumulate intracellularly. In *drs2Δsla2Δ* cells the dense class vesicles do not accumulate because they fail to form. A *drs2Δ* strain accumulates swollen TGN, caused by a defect in clathrin-coated vesicle budding from the

TGN (C. Y. Chen, et al., 1999; W.E. Gall et al., 2002). This phenotype is exacerbated in a *drsΔ2dnf1Δ* double mutant (Hua, et al., 2002). Dnf1 also plays a partially overlapping role with Drs2 in trafficking of a tryptophan permease, Tat2, from the TGN to plasma membrane (Hachiro, Yamamoto, Nakano, & Tanaka, 2012).

Traffic from the TGN to early endosome is mediated by AP-1/clathrin-coated vesicles that play an important role in retaining Golgi resident proteins and sorting cargos away from the exocytic route. AP-1 clathrin functions in both anterograde and retrograde directions and Drs2 is both a facilitator and cargo for these pathways (K. Liu, Surendhran, Nothwehr, & Graham, 2008). In the absence of Drs2, this pathway seems to stop functioning completely. Chitin synthase 3 (Chs3) is another cargo protein of the AP-1 pathway that can be used to monitor AP-1 trafficking (Shaw et al., 1991). Chs3 is normally retained within the Golgi-endosomal system through AP-1/clathrin-coated vesicle traffic. Yeast with disrupted Drs2/AP-1 trafficking become hypersensitive to the chitin stain (calcofluor white) because of increased cell wall chitin deposition from constitutive mis-sorting of Chs3 to the PM (K. Liu, et al., 2008; Valdivia, Baggott, Chuang, & Schekman, 2002).

Vesicular traffic from the TGN to late endosome is directed by the Golgi-localized, γ-ear-containing, Arf-binding family of proteins (GGA) proteins and clathrin. In mammals, this pathway was originally identified by the Kornfeld lab as the route taken by mannose-6-phosphate (M6P) receptors in trafficking of many lysosomal proteins, but they originally suggested AP-1/clathrin (Duncan & Kornfeld, 1988). The Bonifacino lab later established GGA as the adaptor protein functioning in this specific pathway (Puertollano, Aguilar, Gorshkova, Crouch, & Bonifacino, 2001). Many of these lysosomal proteins acquire M6P in the Golgi, targeting them to M6P receptors, driving transport to the endosomal system, where they release cargo upon exposure to the low pH in late endosomes. For yeast, M6P is not used as a sorting signal, but VPS10

functions in a similar manner, sorting vacuolar residents to the endosomes and, eventually, the vacuole (Marcusson, Horazdovsky, Cereghino, Gharakhanian, & Emr, 1994). Drs2 is important in this pathway, at low temperature *drs2Δ* displays a kinetic defect in trafficking of carboxypeptidase Y (CPY) to the late endosome and ultimately the vacuole. At optimal growth temperatures, the GGA pathway seems to still function in the *drs2Δ* strain, perhaps because of partially overlapping functions of Dnf1. Anterograde traffic to the endosomal system is vital because disrupting both AP-1 and GGA pathways causes a very severe growth defect (Costaguta, Stefan, Bensen, Emr, & Payne, 2001). Similarly, a triple mutant of *gga1Δgga2Δdrs2Δ* also shows a severe growth defect (K. Liu, et al., 2008). However, combining AP-1 and *drs2* deletions doesn't cause a synthetic phenotype indicating they function in the same pathway. The final anterograde pathway is a direct pathway from the TGN to vacuole. This pathway is mediated by AP-3 in a clathrin-independent fashion (Odorizzi, Cowles, & Emr, 1998). Again this pathway is facilitated by Drs2 (and Dnf1), at low temperature a *drs2Δ* strain displays a kinetic defect in trafficking of alkaline phosphatase (ALP) to the vacuole (Hua, et al., 2002).

Anterograde trafficking is clearly crucial for normal function and survival, but retrograde traffic is required to return proteins to the TGN to repeat these processes. AP-1/clathrin actually mediates both anterograde and retrograde traffic between the TGN and early endosomes. Drs2 helps drive this pathway and participates as a cargo, because completely blocking this pathway with deletion of AP-1 subunits results in mis-sorting of Drs2 to the plasma membrane (K. Liu, et al., 2008). However, Drs2 is recycled to the TGN through the endosomes. This suggested a second pathway for early endosome to TGN transport. Drs2 and Cdc50 are also cargoes in a retrograde pathway involving Arf, Gcs1 (an ArfGAP), Ypt31/32 (Rab proteins), and the F-box protein, Rcy1 (Furuta, et al., 2007). This pathway is followed by the v-SNARE protein Snc1 involved in TGN-derived vesicle fusion with the plasma membrane (Lewis, Nichols, Prescianotto-

Baschong, Riezman, & Pelham, 2000). In wild-type cells, SNC1 is present primarily at the plasma membrane because endocytosis is the rate-limiting step in the recycling pathway (PM→endosome→TGN). When one of the aforementioned components of the Rcy1 retrograde pathway are deleted, the SNC1 rate-limiting step becomes the endosome to TGN step and SNC1 accumulates intracellularly (Furuta, et al., 2007; Hua, et al., 2002; Robinson et al., 2006). This retrograde pathway again has some overlap with Dnf1, deletion of either *dnf1,2Δ* or *dnf1,3Δ* (but not *dnf2,3Δ*) causes a partial defect in GFP-SNC1 recycling (Hua, et al., 2002). In addition to the partially overlapping functions with Drs2 in the GGA, AP-3 and Rcy1 pathways, Dnf1 is important for bulk-phase endocytosis (Pomorski, et al., 2003).

The CPY sorting receptor VPS10 uses the GGA pathway to transport cargo to the late endosome. For trafficking of newly synthesized CPY, VPS10 must be recycled back to the TGN from the late endosome (Cooper & Stevens, 1996). VPS10 is transported back to TGN in vesicles formed through the action of the retromer complex (Seaman, Michael McCaffery, & Emr, 1998). In mammals, a few key discoveries for post-Golgi retrograde trafficking pathways have been described. The Johannes lab provided some of the first direct evidence for a trafficking pathway from early endosome to TGN by demonstrating Shiga toxin follows this path (Mallard et al., 1998). Retrograde traffic is essential for formation of insulin responsive vesicles (IRVs) (Bogan & Kandror, 2010). Wntless functions as a sorting receptor of Wnt, directing its secretion (Bänziger et al., 2006). Again, Wntless needs to be endocytosed and returned to the TGN to direct secretion of new Wnt. The retromer complex is required for recycling Wntless to TGN from endosomes (Belenkaya et al., 2008). The final defined post-Golgi retrograde trafficking pathway has no direct analog in *S. cerevisiae* but is defined by the Golgi-resident TGN38 which appears to traffic from the early endosome to recycling endosome to the TGN (Ghosh, Mallet, Soe, McGraw, & Maxfield, 1998).

While many vesicular-mediated protein trafficking pathways involve P4-ATPases, the specific role for P4-ATPases is unclear. Some trafficking components can physically interact with P4-ATPases, but these components can assemble on the membrane even in the absence of Drs2. Our preferred model for the P4-ATPase contribution is based on the Singer-Sheetz bilayer-couple hypothesis (Sheetz & Singer, 1974). By flipping phospholipid unidirectionally the one face of the bilayer is expanded while the other is contracted, driving curvature. Membrane curvature can recruit other proteins involved in recruiting or forming the coat complex facilitating the budding of vesicles. While the P4-ATPases appear to have certain substrate preferences, the contribution of specific phospholipids to these processes remains unclear.

Concluding remarks

The observation of membrane phospholipid asymmetry necessitated the earliest proposal of an aminophospholipid translocase activity. With the identification of the protein component responsible, the flippase activity has been attributed to the P4-ATPase family. Recently, *in vitro* assays have validated P4-ATPases as aminophospholipid translocases, but how these proteins recognize and transport their phospholipid substrates remains an enigma. The mechanism of phospholipid transport by P4-ATPases is undefined and has been described as the "giant substrate problem" because fitting a phospholipid into the structurally conserved, but spatially restrictive, ion binding pockets would be nearly impossible within the confines of the available P-type ATPase crystal structures (Puts & Holthuis, 2009). Moreover, P4-ATPases lack the charged residues that form the cation binding sites in P2-ATPases and no phospholipid binding site has been identified. For P4-ATPases, nothing is known about: (1) the residues in the TM domain that recognize the phospholipid substrate, (2) how different P4-ATPases recognize different phospholipid substrates and (3) the pathway phospholipid follows through the TM

domain from exofacial to cytosolic leaflets. The giant substrate problem is a critical remaining question concerning the function of P4-ATPases.

An overarching goal of the work presented here is to determine how P4-ATPases recognize and transport their phospholipid substrates. We aim to test whether P4-ATPases use the canonical ion-binding site, or a non-canonical mechanism. We started by mapping determinants of phospholipid specificity through creation of Dnf1/Drs2 chimeras, two flippases of differing phospholipid specificity. These experiments led to the discovery that the first four TM segments, and individual residues therein, are involved in substrate specificity for yeast P4-ATPases (Chapter II, published as Baldridge and Graham, 2012). Concurrently, the Molday lab published a second study reporting a residue in the canonical ion-binding site important for activity (Coleman, Vestergaard, Molday, Vilsen, & Peter Andersen, 2012). Next, we used a genetic screening procedure to identify additional residues conferring substrate specificity of P4-ATPases. Our results strongly argued against use of the canonical binding site, and instead identified two “gates” on opposing membrane faces that are individually capable of selecting phospholipid substrate (Chapter III, published as Baldridge and Graham, 2013). Through these studies we identified Dnf1 variants with the ability to flip endogenous phosphatidylserine. Interestingly, Dnf1 mutants capable of flipping PS are able to replace Drs2 in certain trafficking pathways. (Chapter IV). Through the screening procedures we have used, we have identified sets of residues that seem to couple together to define phospholipid selection and may explain some differences in the yeast and mammalian homologs (Chapter V). We have also initiated studies to biochemically characterize Dnf1 and to probe the orientation of critical residues involved in phospholipid selection (Chapter VI). Finally, I summarize my results and propose a model for the mechanism of phospholipid flip and its role in protein traffic (Chapter VII).

CHAPTER II

IDENTIFICATION OF RESIDUES DEFINING PHOSPHOLIPID FLIPPASE SUBSTRATE SPECIFICITY OF TYPE-IV P-TYPE ATPASES*

ABSTRACT

Type IV P-type ATPases (P4-ATPases) catalyze translocation of phospholipid across a membrane to establish an asymmetric bilayer structure with phosphatidylserine (PS) and phosphatidylethanolamine (PE) restricted to the cytosolic leaflet. The mechanism for how P4-ATPases recognize and flip phospholipid is unknown, and is described as the "giant substrate problem" because the canonical substrate binding pockets of homologous cation pumps are too small to accommodate a bulky phospholipid. Here, we identify residues that confer differences in substrate specificity between Drs2 and Dnf1, *S. cerevisiae* P4-ATPases that preferentially flip phosphatidylserine (PS) and phosphatidylcholine (PC), respectively. Transplanting transmembrane segments 3 and 4 (TM3-4) of Drs2 into Dnf1 alters the substrate preference of Dnf1 from PC to PS. Acquisition of the PS substrate maps to a Tyr618Phe substitution in TM4 of Dnf1, representing the loss of a single hydroxyl group. The reciprocal Phe511Tyr substitution in Drs2 specifically abrogates PS recognition by this flippase causing PS exposure on the outer leaflet of the plasma membrane without disrupting PE asymmetry. TM3 and the adjoining lumenal loop contribute residues important for Dnf1 PC preference, including Phe587. Modeling of residues involved in substrate selection suggests a novel P-type ATPase transport pathway at the protein/lipid interface and a potential solution to the giant substrate problem.

* This chapter has been published as Baldridge and Graham (2012) Identification of residues defining phospholipid flippase substrate specificity of type IV P-type ATPases. *Proc Natl Acad Sci U S A* 109: E290-E298.

INTRODUCTION

P-type ATPases are phylogenetically grouped into 5 subclasses of integral membrane pumps that mediate active transport of substrate across membrane bilayers (Axelsen & Palmgren, 1998). This family is defined by the formation of a phosphorylated intermediate (P-type) and four characteristic domains: actuator (A), nucleotide-binding (N), phosphorylation (P) and transmembrane (TM). The best characterized subclass, the type II P-type ATPases (P2-ATPases) catalyze the energy-dependent movement of cations across lipid bilayers to establish an electrochemical gradient. The substrate binding sites of P2-ATPases lie within the transmembrane (TM) domain, and involve multiple residues that coordinate the cations in a well-defined binding pocket formed by charged and polar residues in TM 4, 5, 6 and 8 in the Ca^{2+} ATPase (Toyoshima, 2008) and TM segments 4, 5, 6, 8 and 9 in the Na^{+}/K^{+} ATPase (Shinoda, Ogawa, Cornelius, & Toyoshima, 2009). Access to the cation binding sites alternates between the cytosolic and exofacial sides of the membrane, and is driven by E1-E2 conformational changes associated with ATP binding, transfer of the γ-phosphate from ATP to a conserved aspartate, and subsequent hydrolysis of the aspartyl-phosphate bond (Morth et al., 2011). Whether or not this alternating half-channel mechanism of substrate recognition and transport is conserved for all P-type ATPase subclasses is unknown.

In contrast to the cation transporters, members of the type IV P-type ATPase subfamily (P4-ATPases) translocate phospholipid across a membrane bilayer by flipping their substrate from the exofacial leaflet to the cytosolic leaflet (Coleman, et al., 2009; Zhou & Graham, 2009). The unidirectional flip of specific phospholipid species, such as phosphatidylserine (PS) and phosphatidylethanolamine (PE), creates an asymmetric membrane structure with PS and PE concentrated within the cytosolic leaflet. The P4-ATPase subfamily is conserved among eukaryotes with *Saccharomyces cerevisiae* expressing five members that are essential for

viability (Hua, et al., 2002), whereas mammals have at least 14 members (C.C. Paulusma & Oude Elferink, 2005; P. Xu, et al., 2009). Several of these mammalian flippases are implicated in pathological conditions such as obesity and type II diabetes (Dhar, et al., 2004), intrahepatic cholestasis (Bull, et al., 1998; Siggs, Schnabl, Webb, & Beutler, 2011), progressive hearing loss (Stapelbroek, et al., 2009), male infertility (Wang, et al., 2004) and deficiencies in B cell lymphopoiesis (Siggs, Arnold, et al., 2011; Yabas, et al., 2011). In addition, P4-ATPases play critical roles in vesicle-mediated protein trafficking in the secretory and endocytic pathways (Muthusamy, Natarajan, et al., 2009). Many P4-ATPases associate with Cdc50 family proteins that are potentially analogous to the Na^+/K^+ ATPase β and γ subunits. For example, the yeast P4-ATPase Drs2 interacts with Cdc50 to allow their mutual export from the endoplasmic reticulum (ER) to the Golgi complex (Saito, et al., 2004).

The mechanism of phospholipid transport by P4-ATPases is undefined and has been described as the "giant substrate problem" because fitting a phospholipid into the structurally conserved, but spatially restrictive, substrate binding pockets would be impossible within the confines of the available P-type ATPase crystal structures (Puts & Holthuis, 2009). Moreover, P4-ATPases lack the charged residues that form the cation binding sites in P2-ATPases and no phospholipid binding site has been identified. Translocation of phospholipid is proposed to occur at the E2-P to E1 transition based upon the direction of substrate translocation and the demonstration that phospholipid substrate stimulates dephosphorylation of Atp8a1, a mammalian P4-ATPase (Ding, et al., 2000). Cdc50 preferentially associates with Drs2 in the E2P state, suggesting that Cdc50 might form part of the phospholipid binding pocket (Lenoir, et al., 2009). However, recent evidence from *Arabidopsis thaliana* P4-ATPases indicates the Cdc50 subunit does not affect the substrate specificity of the heterodimer, implying that determinants of substrate specificity primarily reside within the catalytic subunit (López-Marqués, et al.,

2010). For P4-ATPases, nothing is known about: (1) the residues in the TM domain that recognize the phospholipid substrate, (2) how different P4-ATPases recognize different phospholipid substrates and (3) the pathway phospholipid follows through the TM domain from the exofacial to cytosolic leaflet. The giant substrate problem is one of the paramount questions concerning the function of P4-ATPases.

To gain insight into the mechanism of phospholipid flip by P4-ATPases, we sought to identify residues that define phospholipid substrate specificity. Our strategy was to generate chimeras between two P4-ATPases that differ in substrate preference in order to map residues determining this preference. The yeast P4-ATPase Dnf1 prefers phosphatidylcholine (PC) and phosphatidylethanolamine (PE) (Kato, et al., 2002; Pomorski, et al., 2003), whereas Drs2 prefers phosphatidylserine (PS) (Natarajan, et al., 2004; Zhou & Graham, 2009) with a minor activity towards PE (Alder-Baerens, et al., 2006). Here we report the identification of sequences in TM segments 3-4 that help determine phospholipid specificity in Dnf1 and Drs2. From a structural model of Dnf1 and the positions of the key residues impacting phospholipid specificity, we suggest an entirely novel mechanism of transport by a member of the P-type ATPase superfamily.

RESULTS

Drs2 TM segments 3-4 confer NBD-PS uptake activity to Dnf1

P4-ATPases initially select their substrate from the exofacial leaflet of the bilayer; therefore, residues involved in substrate selection must lie within the exofacial loops or within the transmembrane region (Figure 2-1A). We systematically generated chimeras by exchanging pairs of transmembrane segments with intervening lumenal loops from Drs2 into Dnf1 (Figure 2-

2) and tested the Dnf1[Drs2] chimeras for a change in substrate specificity. Advantages of this approach include 1) Dnf1 is expressed on the plasma membrane (Hua, et al., 2002), allowing us to easily assay the chimera translocase activity in living cells. 2) Mutations causing a change in substrate preference, rather than loss, must be compatible with appropriate folding and trafficking of the flippase. 3) The ratio of PS to PC uptake for each chimera provides a measure of substrate specificity that is independent of translocase number at the plasma membrane.

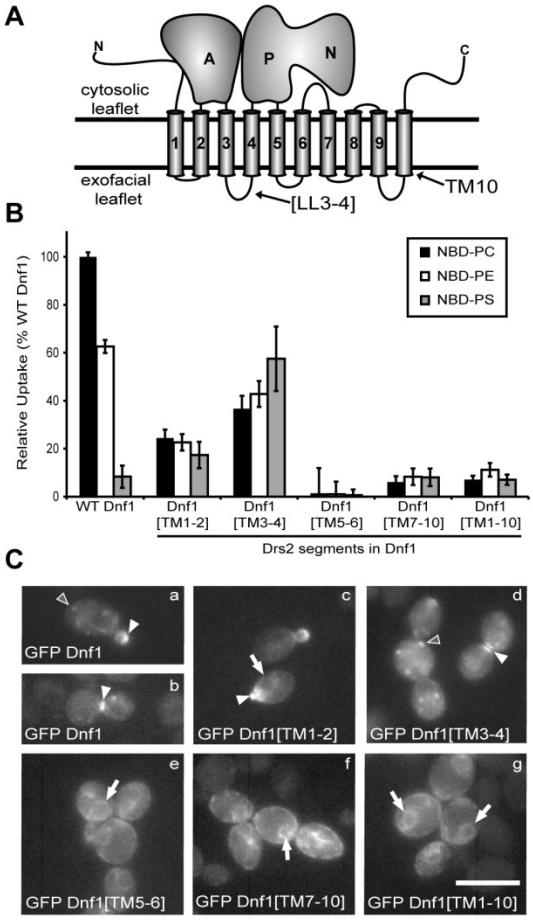

Figure 2-1. Transmembrane segments 3-4 from Drs2 are sufficient to confer a PS activity to Dnf1. (A) Topology diagram of a P4-ATPase; A, actuator domain; N, nucleotide-binding domain; P, phosphorylation domain; LL3-4, lumenal loop between TM3 and TM4; black lines denote the membrane boundaries. (B) NBD-PL uptake across the plasma membrane mediated by Dnf1[Drs2] chimeras. TM3-4 contains important sequence for phospholipid recognition. Results represent averages of at least three independently-isolated transformants from at least three independent experiments (mean ± SEM). (C) Localization of N-terminal GFP fused Dnf1 and Dnf1[Drs2] chimeras in *S. cerevisiae*. GFP-Dnf1 is localized to intracellular punctae in non-budded cells (a,d), to the bud tip in small-budded cells (a,c) and to the bud neck in large-budded

cells (b,d). A subset of GFP Dnf1[Drs2] chimeras mislocalize to the ER (e-g). Arrowheads designate polarized expression patterns (bud tip or bud neck); open arrowheads show punctate localization; arrows indicate perinuclear ER fluorescence. Fluorescence intensities for the images are scaled independently to emphasize localization. The scale bar is 10µm.

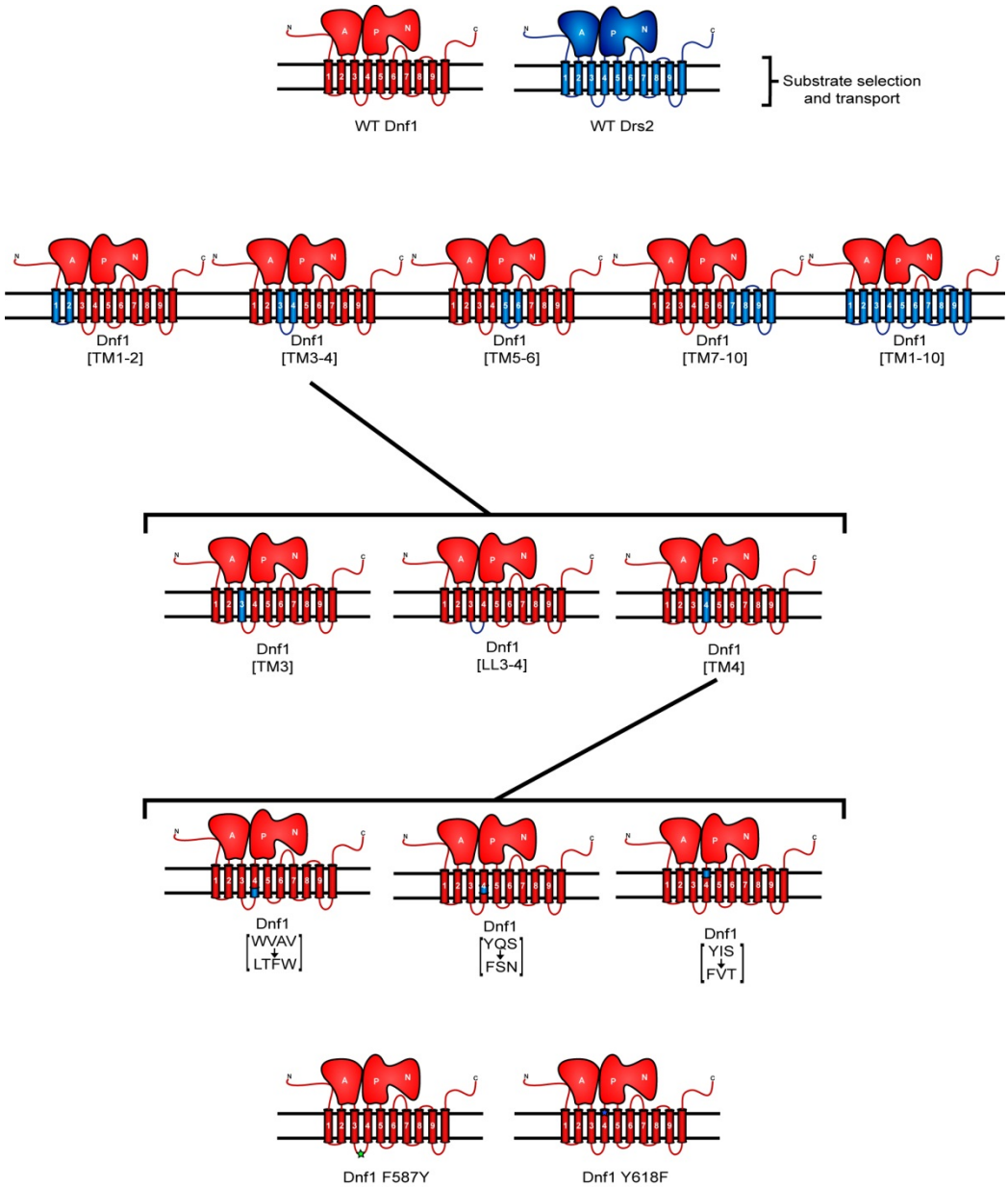

Figure 2-2. Topological diagrams of WT Dnf1 (red), WT Drs2 (blue) and most of the chimeras reported in this study. Black lines are membrane boundaries. A is the actuator domain, N is the nucleotide binding domain and P is the phosphorylation domain.

To assay flippase activity, chimeras were expressed in a *dnf1Δdnf2Δ* strain lacking the major plasma membrane P4-ATPases in yeast (Pomorski, et al., 2003) and we measured uptake of 7-nitro-2–1,3-benzoxadiazol-4-yl phospholipid (NBD-PL) across the plasma membrane by flow cytometry. In each experiment, *dnf1,2Δ* cells bearing an empty vector control were assayed to subtract chimera-independent uptake of each NBD-PL and the uptake of NBD-PC by wild-type (WT) Dnf1 was used to normalize the data. WT Dnf1 is reported to translocate PC and PE, and debatably PS (Pomorski, et al., 2003; Stevens, Malone, & Nichols, 2008). In these experiments, WT Dnf1 mediated robust uptake of PC and PE and had a minor influence on the uptake of PS (n=150+) (Figure 1B). The Dnf1[TM1-2] chimera showed reduced activity for both PC and PE, but no significant change in activity for PS (Figure 2-1B). In contrast, Dnf1[TM3-4] had a reduced activity to PC and PE, but gained an activity towards PS, the preferred substrate of Drs2. Dnf1[TM5-6], Dnf1[TM7-10] and Dnf1[TM1-10] each had little to no activity at the plasma membrane for any of the NBD-PLs tested (Figure 2-1B).

The lack of activity for some of the chimeras could be caused by a failure to traffic through the secretory pathway to the plasma membrane. We tested this possibility by tagging each chimera with GFP for localization studies. WT Dnf1 exhibits a polarized localization that depends on the cell cycle (Hua, et al., 2002; Saito, et al., 2004). GFP-Dnf1 localized to intracellular punctae in non-budded cells, to the bud tip in small-budded cells and to the bud neck in large-budded cells (Figure 2-1C(a-b), arrowheads). GFP-Dnf1[TM1-2] and GFP-Dnf1[TM3-4] retained similar localization patterns to GFP-Dnf1 regardless of cell cycle stage (Figure 1C(c-d)), indicating the decrease in activity by Dnf1[TM1-2] is not caused by an inability to localize to the plasma membrane. GFP-Dnf1[TM5-6], GFP-Dnf1[TM7-10] and GFP-Dnf1[TM1-10] exhibited localization patterns characteristic of the ER, as indicated by the ring of fluorescence surrounding the nucleus (Figure 2-1C(e-g), arrows). ER retention is a common problem for

improperly folded integral membrane proteins (Lodish, 1988), providing a likely explanation for the lack of PM uptake activity for these chimeras.

TM4 is required for PS activity, but not specificity

TM3-4 from Drs2 was sufficient to confer a PS activity to Dnf1, and this Dnf1[TM3-4] chimera also showed a reduced activity for PC and PE (Figure 2-1B and 2-3A). By plotting the ratio of PS to PC uptake, we quantified a nearly 8-fold increase in PS preference for the Dnf1[TM3-4] chimera relative to Dnf1 (Figure 2-3B). Because Dnf1[TM1-2] displayed reduced PC and PE activities, it was possible that TM1-2 from Drs2 contributed to selection against PC and PE. However, exchanging TM1-4 as a unit, to generate Dnf1[TM1-4], yielded a chimera with a similar PC and PE activity to Dnf1[TM3-4], but with a slightly lower PS activity (Figure 2-4). This result suggests TM1-2 does not contribute additional substrate specificity to TM3-4.

We analyzed each section of TM3-4 individually to determine their relative contribution to this change in substrate specificity. Dnf1[TM3] and Dnf1[LL3-4] showed reduced PC, PE and PS activity and so these segments failed to confer PS activity to Dnf1 (Figure 2-3A). Dnf1[TM4] retained WT activity for PC, showed a modest increase in activity for PE, but had a substantial increase in PS activity (Figure 2-3A). Thus, TM4 from Drs2 was sufficient to confer a PS activity to Dnf1, but still allowed for translocation of PC and PE. Relative to WT Dnf1, Dnf1[TM3-4] showed the greatest preference for PS (Figure 2-3B) even though Dnf1[TM4] showed a greater increase in PS activity (Figure 2-3A). The localization pattern of each of these chimeras was similar to WT Dnf1 (Figure 2-3C, fluorescence at the bud tip or bud neck) and was therefore unlikely to be responsible for any difference in activity or substrate preference. These results suggest that TM3 and LL3-4 in Dnf1 contribute to PC and PE selection, and TM4 from Drs2 contributed residues important for PS selection.

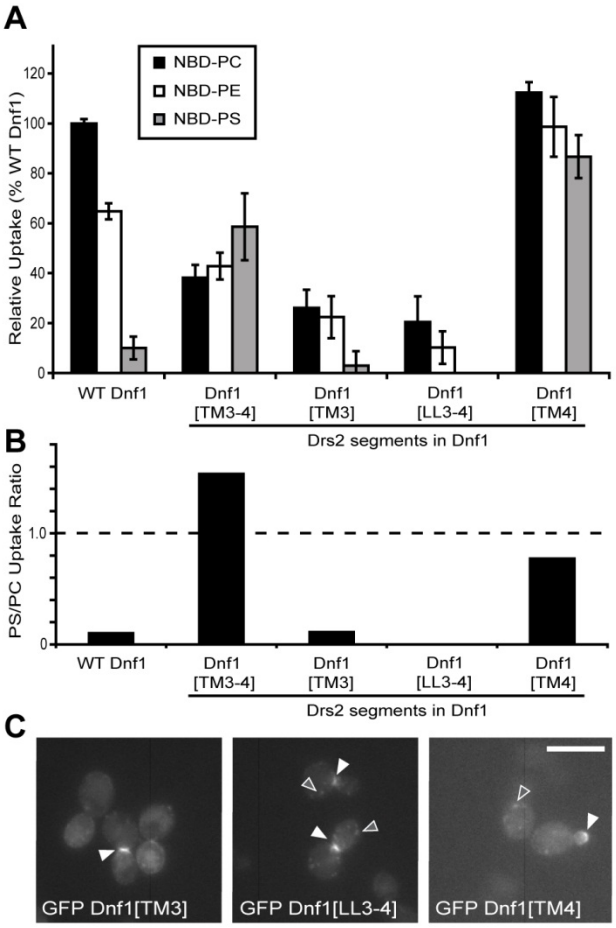

Figure 2-3 Drs2 TM3-4 confers PS preference to Dnf1, while TM4 confers a PS activity without affecting the recognition of PC or PE. (A) NBD-PL uptake shows TM4 from Drs2 is sufficient to confer a PS activity to Dnf1, while TM3 and LL3-4 are important for NBD-PC and NBD-PE selection (mean ± SEM). (B) The ratio of PS to PC uptake from panel (A) was plotted to provide a measure of substrate preference that is independent of expression level. (C) Localization of GFP tagged Dnf1[TM3], Dnf1[LL3-4] and Dnf1[TM4] chimeras in *S. cerevisiae* indicate these chimeras localize and traffic similarly to WT Dnf1. The scale bar is 10µm.

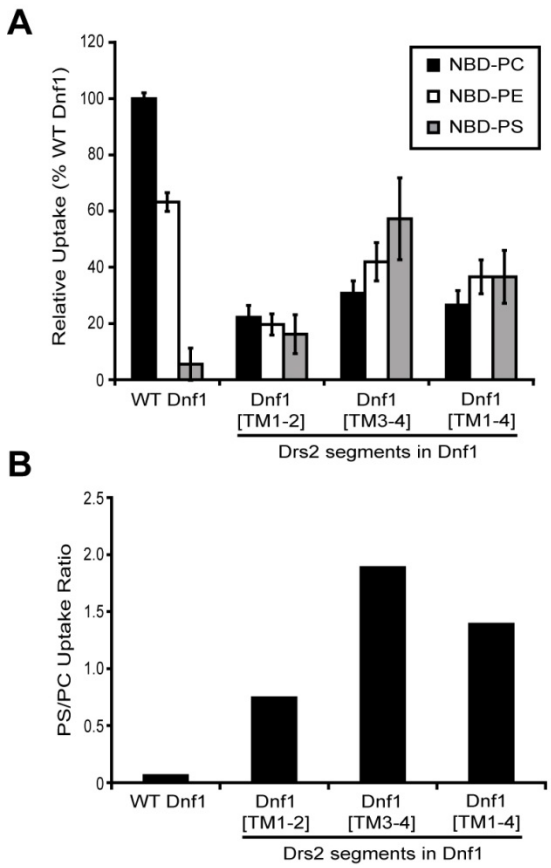

Figure 2-4. Activity and specificity of Dnf1[TM1-4]. (A) NBD-PC and NBD-PE uptake by Dnf1[TM1-4] is similar to Dnf1[TM3-4], but NBD-PS activity is slightly reduced PS. (B) The specificity of Dnf1[TM1-4] for PS is also slightly reduced relative to Dnf1[TM3-4], suggesting TM3-4 has the greatest impact on PS specificity.

TM4 contains three sequence blocks that differ between Dnf1 and Drs2 (Figure 2-5A), so we exchanged each Drs2 TM4 block independently into Dnf1 to determine their contribution to the PS activity of Dnf1[TM4]. Of these three chimeras, only Dnf1[YIS→FVT] displayed an increased activity for PS (Figure 2-5B) and a substrate preference equivalent to Dnf1[TM4] (Figure 2-5C). Therefore, we exchanged each residue individually (Y618F, I619V and S620T) and in pairwise combinations. The Dnf1 Y618F point mutation had the greatest influence on net PS activity although Dnf1 I619V and Dnf1 S620T also showed slightly enhanced PS transport relative to WT Dnf1 (Figure 2-5B).

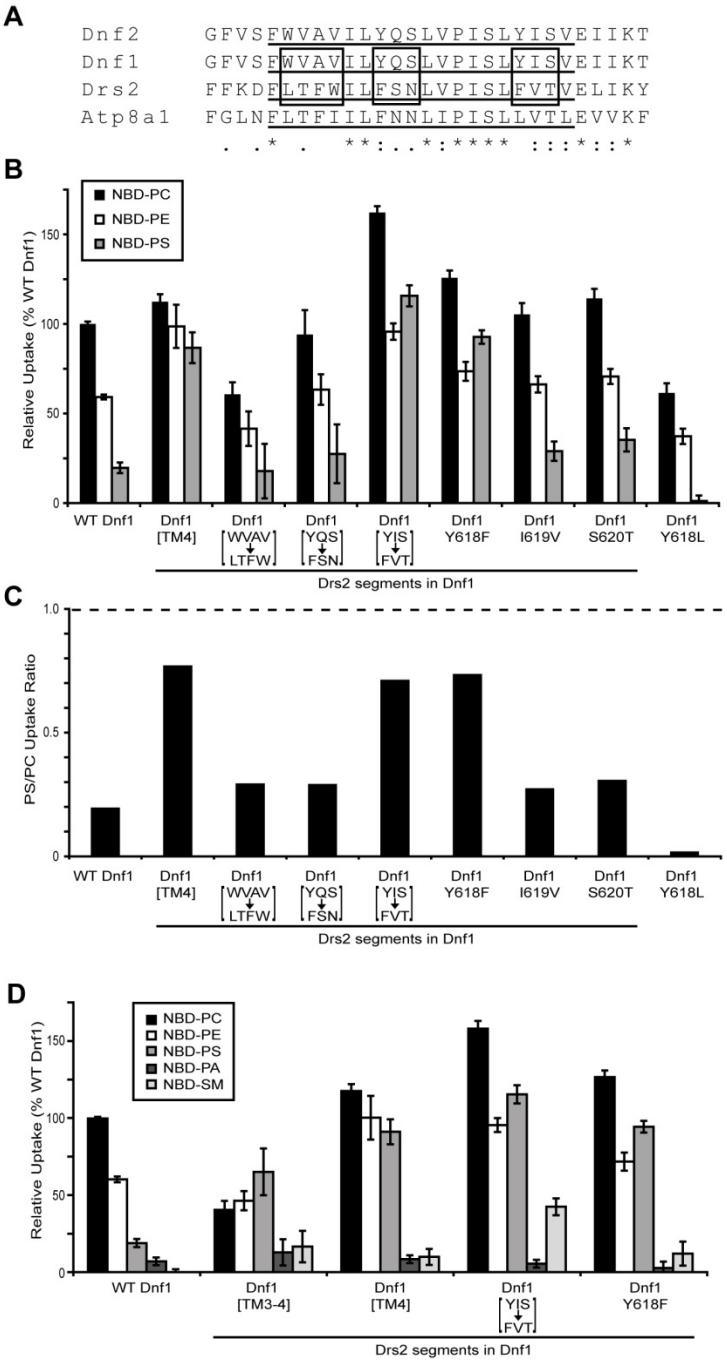

Figure 2-5. A single amino acid change, Y618F, specifically confers PS uptake activity to Dnf1. (A) Primary sequence alignment of TM4 from Dnf1, Dnf2, Drs2, and Atp8a1. Underlined sequences are the predicted TM4; boxes are regions differing between Dnf1 and Drs2. (B) NBD-PL uptake by Dnf1[Drs2] chimeras. Dnf1[YIS→FVT] and Dnf1 Y618F both transport PS (mean ± SEM). (C) PS/PC uptake ratio representing the relative preference of each chimera for either PC or PS independent of expression. (D) NBD-lipid uptake suggests Dnf1[TM3-4], Dnf1[TM4], and Dnf1 Y618F retain specificity for the phospholipid headgroup and glycerol backbone. Dnf1[YIS→FVT] is less selective than other PS transporting chimeras based on its activity for NBD-SM. Each reported value (B-D) is the average of at least three independent samples from at least three independent experiments (mean ± SEM).

Dnf1[YIS→FVT] had a greater net PS activity compared to any of the individual point mutations but this chimera had no increased preference for PS (Figure 2-5C). Dnf1 Y618F displayed specificity for PS comparable to Dnf1[TM4] and Dnf1[YIS→FVT] (Figure 2-5C) without the general increase in activity of Dnf1[YIS→FVT]. Y618, I619 and S620 were changed to Drs2 residues in pairs, with no additional specificity for PS being conferred, indicating Y618F is the key substitution enabling PS translocation (Figure 2-6A and 2-6B). The closest mammalian homolog of Drs2, Atp8a1, has a leucine in the TM4 position analogous to Y618 in Dnf1 and F511 in Drs2 (Figure 2-5A), so we generated a Y618L substitution in Dnf1 to determine if this could also allow PS uptake (Figure 2-5B). However, the Y618L substitution did not confer a PS activity and instead reduced Dnf1 activity against all three substrates.

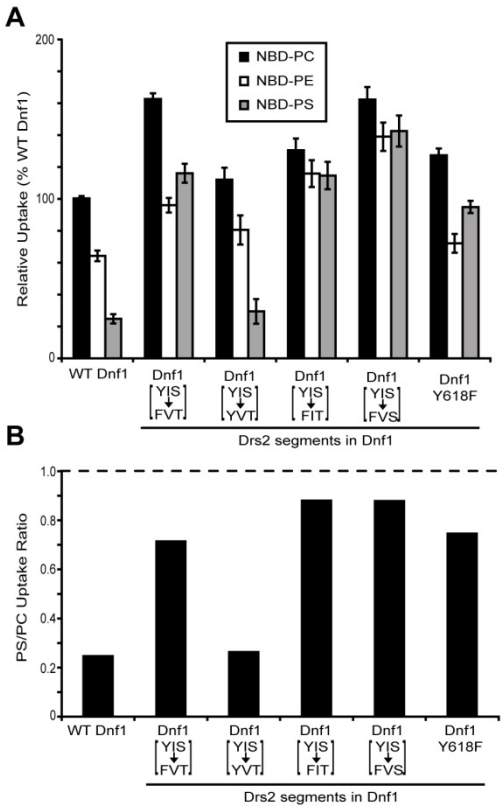

Figure 2-6. The enhanced uptake for all three substrates noted for Dnf1[YIS→FVT] was also observed for Dnf1[YI→FV] (A) Exchanging Y618F, I619V, and S620T in pairs reveals the enhanced activity seen in Dnf1[YIS→FVT] is dependent on both Y618F and I619V. (B) Each pairwise combination of changes containing Y618F results in a specificity for PS comparable to the Y618F point mutation.

The increased activity for PS by several of the chimeras could result from the specific acquisition of a new substrate, or a complete loss of specificity such that any NBD-PL would be translocated. Therefore, we tested if the chimeras could catalyze the uptake of NBD-phosphatidic acid (NBD-PA) or NBD-sphingomyelin (NBD-SM). WT Dnf1 cannot translocate NBD-SM or NBD-PA, and Dnf1[TM3-4], Dnf1[TM4], and Dnf1 Y618F retained comparable specificity (Figure 2-5C). Surprisingly, not only did Dnf1[YIS→FVT] display an increased activity for PC, PE, and PS (Figure 2-5B), it also conferred a modest increase in NBD-SM uptake (Figure 2-5D). However, Dnf1[YIS→FVT] was not capable of NBD-PA transport (Figure 2-5D), indicating it had not completely lost phospholipid selectivity nor did this chimera selectively recognize the NBD moiety. The expression level of WT Dnf1, Dnf1[YIS→FVT] and Dnf1 Y618F were similar and unlikely to account for the increased uptake observed in Dnf1[YIS→FVT] (Figure 2-7). To rule out the possibility that the mutations in Dnf1 somehow altered the localization or plasma membrane activity of Drs2, we localized GFP-Drs2 in strains harboring various Dnf1 chimeras (Figure 2-8A) and measured Dnf1 chimera NBD-PL uptake in a *dnf1,2Δdrs2Δ* strain (Figure 2-8B). In no case was the enhanced NBD-PS uptake observed attributable to Drs2.

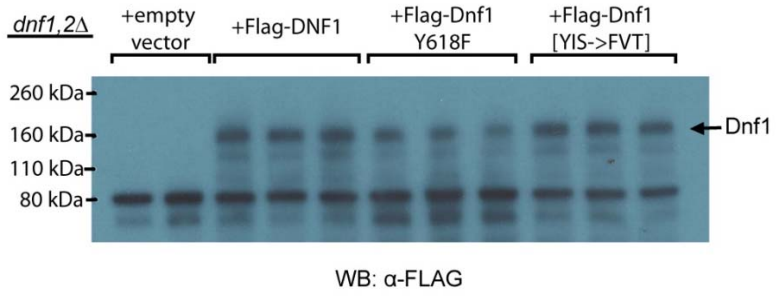

Figure 2-7. Expression levels of Flag-Dnf1, Flag-Dnf1[YIS→FVT] and Flag-Dnf1 Y618F are similar.

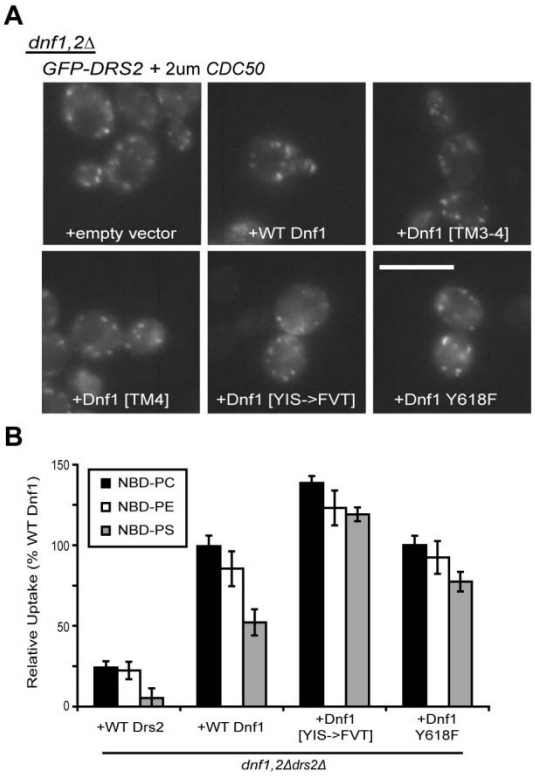

Figure 2-8. The PS uptake observed in Dnf1[Drs2] chimeras is not attributable to Drs2 (A) Localization of N-terminal GFP fused Drs2 does not change in the presence Dnf1[Drs2] chimeras in *S. cerevisiae*. The scale bar is 10µm. (B) NBD-PL uptake observed by Dnf1[Drs2] chimeras in a *dnf1,2Δdrs2Δ* strain demonstrated the uptake activity was independent of Drs2.

The reciprocal Drs2 F511Y substitution disrupts PS asymmetry

Because the Y618F substitution allowed PS recognition by Dnf1 without disrupting PE or PC flippase activity, we predicted that the reciprocal F511Y exchange in Drs2 would perturb its PS flippase activity without affecting recognition of PE. To assess Drs2 recognition of endogenous, unmodified phospholipid, we tested the influence of the Drs2 F511Y substitution on PS and PE asymmetry of the plasma membrane. Disruption of Drs2 causes a loss of membrane asymmetry and exposure of PS and PE on the extracellular leaflet of the plasma membrane (S. Chen, et al., 2006). Loss of membrane asymmetry can be measured by hypersensitivity to pore-forming toxins that bind selectively to PS (papuamide B, PapB) (Parsons et al., 2006) or PE (duramycin) (Navarro et al., 1985) exposed on the outer leaflet of the plasma

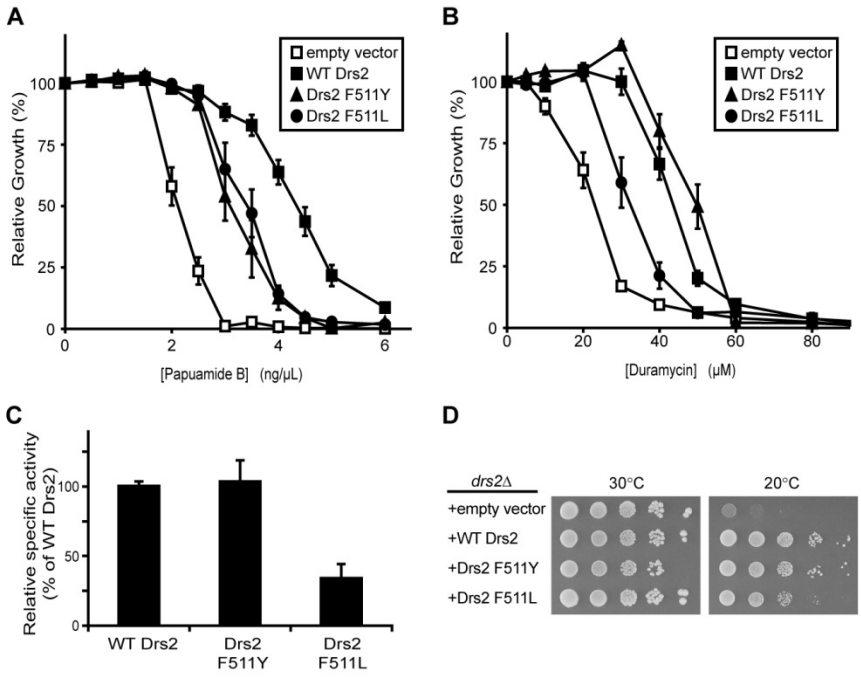

Figure 2-9. Drs2 F511Y specifically perturbs plasma membrane PS asymmetry. (A) Growth of a *drs2Δ* strain expressing an empty vector, WT Drs2, Drs2 F511Y, or Drs2 F511L in the presence of papuamide B demonstrates a partial loss of PS asymmetry with Drs2 F511Y and Drs2 F511L (mean ± SEM). (B) Growth of a *drs2Δ* strain expressing the same constructs in the presence of duramycin indicates plasma membrane PE asymmetry is maintained by WT Drs2 and Drs2 F511Y but is perturbed with Drs2 F511L (mean ± SEM). (C) Drs2 F511Y retains an ATPase specific activity comparable to WT Drs2 while Drs2 F511L has a reduced ATPase activity (mean ± SD). (D) Drs2 F511Y fully complements cold-sensitive growth defect of a *drs2Δ* strain but Drs2 F511L only partially complements.

membrane. As predicted, Drs2 F511Y caused a partial loss of PS asymmetry, as indicated by the intermediate sensitivity to PapB relative to the wild-type and *drs2Δ* strains (Figure 4A). In contrast, Drs2 F511Y conferred wild-type resistance to duramycin and therefore a normal asymmetric distribution of PE (Figure 2-9B). Thus, Drs2 F511Y is specifically defective in establishing PS asymmetry. We also generated a strain expressing the Drs2 F511L variant and found these cells displayed a partial loss of asymmetry for both PE and PS (Figure 2-9A and 2-9B). Even though Dnf1 Y618F can translocate NBD-PS across the plasma membrane, it was unable to suppress the PapB sensitivity of a *drs2Δ* strain (Figure 2-10). We assume that the highly polarized localization may not allow Dnf1 to correct a membrane asymmetry defect

across the entire plasma membrane of *drs2Δ* cells. Each form of Drs2 (WT, F511Y and F511L) was purified and assayed for ATPase activity as previously described (Zhou & Graham, 2009). While Drs2 F511Y retained wild-type activity, Drs2 F511L had a specific activity that was 35% that of wild-type Drs2 (Figure 2-9C). These data imply that the F511Y substitution causes a change in Drs2 substrate specificity without altering the activity, while F511L reduces the overall activity.

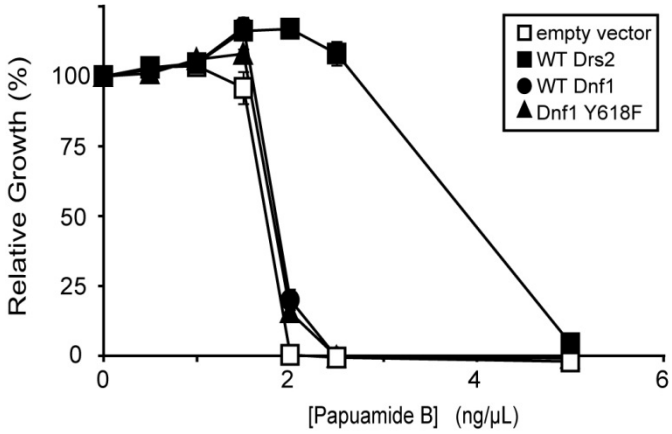

Figure 2-10. Dnf1 Y618F is unable to suppress the PapB hypersensitivity of the drs2Δ strain.

Under certain conditions, such as low temperature, *DRS2* is essential for growth because of its function in supporting protein trafficking from the *trans*-Golgi network. The *drs2-F511Y* allele fully complemented the cold-sensitive growth defect of *drs2Δ* (Figure 2-9D), indicating that Drs2 F511Y must localize properly and that the loss of PS asymmetry is not a secondary consequence of a protein trafficking defect or an inactive enzyme. The *drs2-F511L* allele was only able to partially complement the cold-sensitive growth defect of *drs2Δ* (Figure 2-9D), consistent with it being a hypomorphic allele. Strains carrying deletions of *DRS2* and all three *DNF* genes (*dnf1,2,3Δdrs2Δ*) are inviable and while *drs2-F511Y* was able to complement this growth defect, *drs2-F511L* was unable to do so (Figure 2-11B).

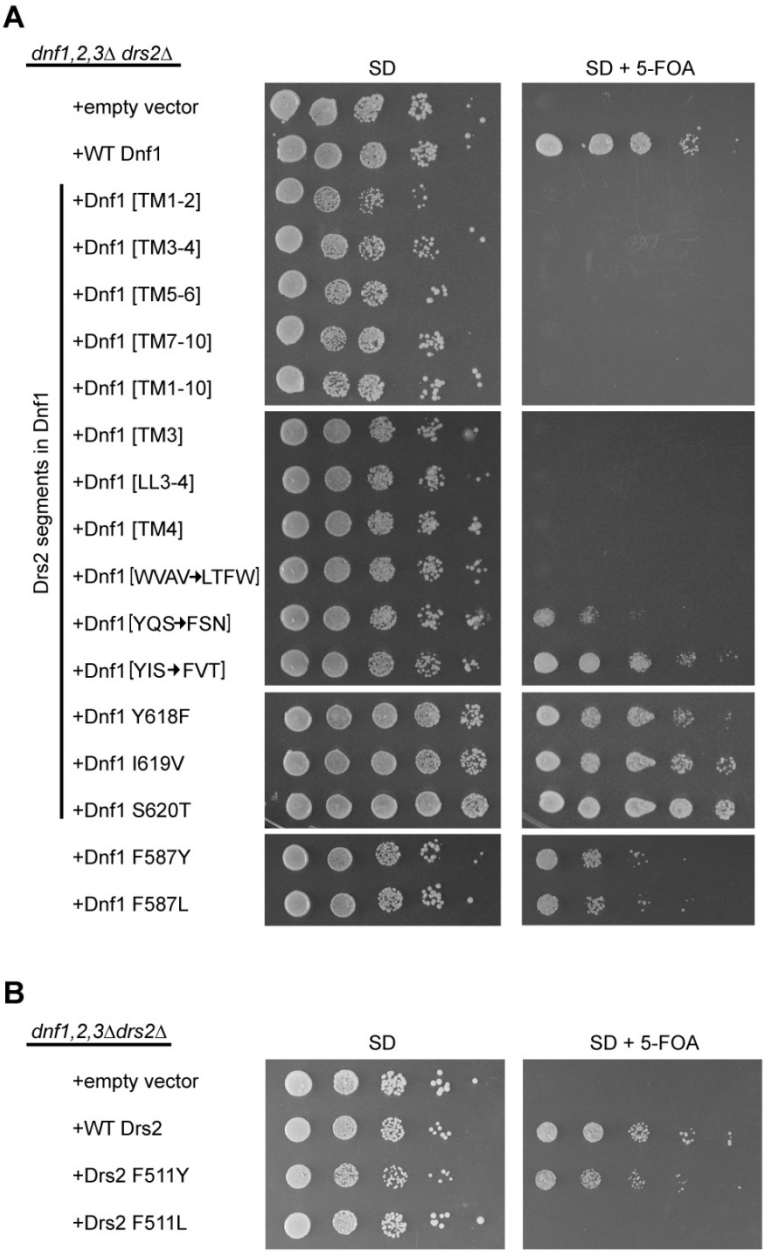

Figure 2-11. Complementation of *dnf1,2,3Δdrs2Δ* by *DNF1[DRS2]* chimeric genes. (A) Serial dilutions of strains harboring *DNF1[DRS2*] chimeric genes were plated on synthetic medium (left) or synthetic medium containing 5-FOA (right), which is lethal to cells expressing *URA3*. Growth on 5-FOA indicates the Dnf1[Drs2] chimera is capable of complementing the growth defect of the *dnf1,2,3Δdrs2Δ* strain in the absence of the covering *URA3-DRS2* plasmid. (A) Serial dilutions of strains harboring *DRS2[DNF1*] chimeric genes

The rate of NBD-PL uptake by Dnf1 Y618F is comparable to WT Dnf1

To better define the substrate preferences and transport properties of the Dnf1 [Drs2] chimeras, we examined the kinetics of NBD-PC and NBD-PS uptake. As expected, Dnf1[TM3-4] displayed a reduced rate of NBD-PC uptake compared to WT Dnf1, while Dnf1[YIS→FVT] had an increased rate of NBD-PC uptake. Dnf1[TM4] and Dnf1 Y618F showed a similar rate of NBD-PC uptake relative to WT Dnf1 (Figure 2-12A). Thus, acquisition of the ability to translocate PS did not alter the activity toward PC.

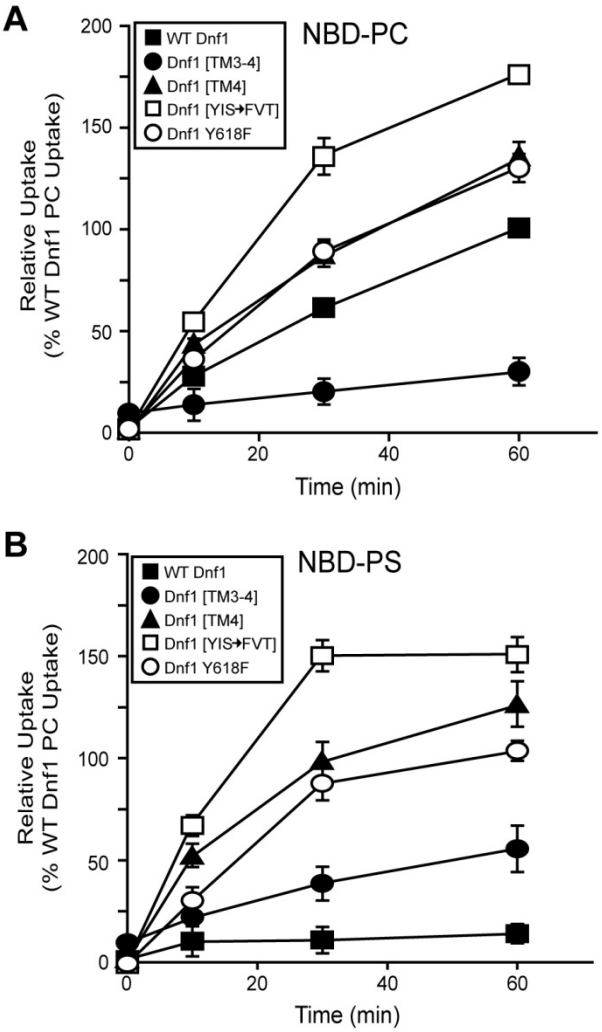

Figure 2-12. The rate of NBD-PC and NBD-PS uptake mediated by Dnf1 Y618F is comparable, suggesting a similar transport mechanism. (A) NBD-PC uptake at 0, 10, 30 and 60min where 100% corresponds to WT Dnf1 NBD-PC uptake at 1 hour (mean ± SEM). (B) NBD-PS uptake where 100% corresponds to WT Dnf1 NBD-PC uptake at 1 hour (mean ± SEM).

Each Dnf1[Drs2] chimera tested displayed a significant increase in NBD-PS uptake activity relative to Dnf1 (Figure 2-12B). Dnf1[TM3-4] had the lowest rate of NBD-PS uptake (Figure 2-12B) and Dnf1[YIS→FVT] showed the highest rate of NBD-PS uptake compared to the other Dnf1[Drs2] chimeras examined. Importantly, the rate of NBD-PS uptake by Dnf1[TM4] and Dnf1 Y618F was comparable to the rate of NBD-PC uptake by these chimeras (and WT Dnf1), suggesting a similar transport mechanism for PC and PS (Figure 2-12B).

PC recognition by Dnf1

To identify residues involved in phospholipid selection by Dnf1, we searched for residues specifically involved in recognition of PC. Based on the role of TM3 and LL3-4 in PC/PE selection (Figure 2-3A) we generated random mutations in sequences encoding TM3-4 of Dnf1 and transformed this collection of *DNF1* mutant alleles into a *dnf1,2,3Δdrs2Δ* pRS416-*DRS2* strain. These mutants were initially screened for resistance to edelfosine, a toxic PC analog (Hanson, et al., 2003), and then counter-screened for the ability to support growth of the *dnf1,2,3Δdrs2Δ* strain by selection on 5-fluoroorotic acid (5FOA, which selects for loss of *URA3* encoded on pRS416-*DRS2*). This screen should select for a functional Dnf1 with a reduced ability to flip PC. In two independent clones carrying point mutations, Phe587 (within LL3-4) was mutated to either a Tyr or Leu residue (Fig 2-13A). Dnf1 F587L and F587Y supported growth of *dnf1,2,3Δdrs2Δ* cells, although not as well as WT Dnf1 or Dnf1 Y618F (Figure 2-13B, SD +5FOA). However, strains expressing Dnf1 F587L and F587Y were able to grow at a concentration of edelfosine that killed strains expressing WT Dnf1 or Dnf1 Y618F (Fig 2-13B, SD + edelfosine). When assayed for NBD-PL uptake in a *dnf1,2Δ* strain, both Dnf1 F587Y and F587L showed a statistically significant reduction in PC uptake ($p<0.05$) with no change in PE uptake ($p>0.20$)

relative to WT Dnf1 (Figure 2-13C). The normal PE activity of these Dnf1 mutants suggests they are properly expressed and localized to the plasma membrane. We conclude that F587 is specifically involved in PC selection by Dnf1.

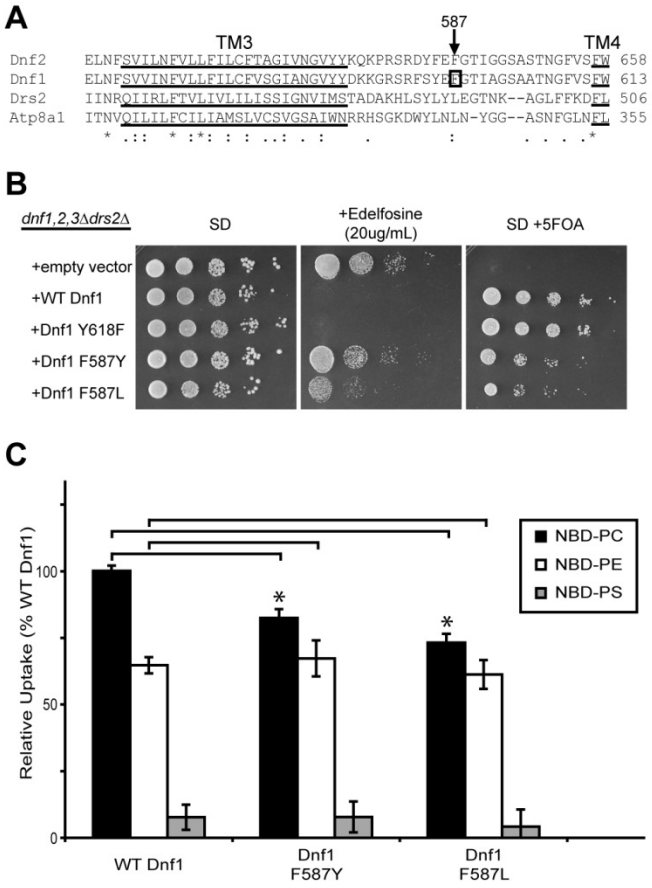

Figure 2-13. F587 substitutions specifically perturb PC uptake activity by Dnf1. (A) Primary sequence alignment of TM3-LL3-4 from Dnf1, Dnf2, Drs2, and Atp8a1. Underlined sequences are the predicted TM3 and TM4; box indicate F587 in Dnf1. (B) Growth of *dnf1,2,3Δdrs2Δ* expressing the Dnf1 constructs indicated on synthetic defined (SD) media, SD plus edelfosine, SD plus 5FOA. (C) NBD-PL uptake indicates a defect in PC uptake by Dnf1 F587Y and Dnf1 F587L ($p<0.05$) and no defect in PE uptake ($p>0.20$) (mean ± SEM).

Function of Dnf1[Drs2] chimeras *in vivo*

DNF1,2,3 and *DRS2* form an essential gene family and strains harboring mutations in all four of these genes are inviable (Hua, et al., 2002). We examined the ability of Dnf1[Drs2] chimeras to support growth of a *dnf1,2,3Δdrs2Δ* strain using the plasmid shuffling assay

described above. In each case, the chimeras with pairs of full TM segments exchanged (Dnf1[TM1-2], Dnf1[TM3-4], Dnf1[TM5-6], Dnf1[TM7-10], and Dnf1[TM1-10]) failed to support growth of a *dnf1,2,3Δdrs2Δ* strain (Figure 2-11A). Dnf1[TM3] Dnf1[LL3-4], Dnf1[TM4] and Dnf1[WVAV-LTFW] also failed to support growth of a *dnf1,2,3Δdrs2Δ* strain (Figure 2-11A). Of this group, the inability of Dnf1[TM4] to support viability was most surprising because it retained a fully functional flippase activity (Figure 2-3A). Dnf1[YQS→FSN] only partially supported growth (Figure 2-11A), even though its uptake activity was only slightly reduced relative to WT Dnf1 (Figure 2-5B). In contrast, Dnf1[YIS→FVT] and each of the point mutants (Dnf1 Y618F, Dnf1 I619V, and Dnf1 S620T) fully supported growth of a *dnf1,2,3Δdrs2Δ* strain (Figure 2-11A). Seemingly, neither an increased uptake activity (as seen in Dnf1[YIS→FVT]) nor an altered substrate specificity appears detrimental to the ability of these chimeras to support growth of a *dnf1,2,3Δdrs2Δ* strain. These data imply that flippase activity is important for *in vivo* function, but in the case of Dnf1[TM4], the Drs2 sequences are unable to support some other critical function of Dnf1 (compare Figure 2-5B and Figure 2-11A). However, it is important to note that the essential function of the P4-ATPases is exerted within the Golgi and endosomal system, not the plasma membrane where activity was measured (K. Liu, Hua, Nepute, & Graham, 2007).

Lem3 is required for Dnf1[Drs2] chimera ER export

WT Dnf1 interacts with the Cdc50 family protein Lem3, and this interaction is required for their mutual export from the ER (Saito, et al., 2004). Cdc50 family proteins may contribute to substrate recognition and transport by P4-ATPases (López-Marqués, et al., 2010; Puts & Holthuis, 2009) and it was possible that the Dnf1[Drs2] chimeras gained the ability to interact with Cdc50, thereby conferring specificity for PS. Therefore, we expressed the GFP-tagged chimeras in a *lem3*Δ strain and tested if overexpression of *CDC50* could support their transport

to the plasma membrane. GFP-Dnf1 and all of the chimeras tested were retained in the ER of the *lem3Δ* cells, even when CDC50 was overexpressed (Figure 2-14A). In contrast, *LEM3* overexpression rescued the polarized plasma membrane localization pattern for each chimera. To test the possibility that Cdc50 was responsible for the changes in substrate selection we assayed the uptake activity of several Dnf1 chimeras in the absence of Cdc50 or Lem3 (Figure 2-14B). In each case, the Dnf1 chimeras strictly required Lem3, not Cdc50, for activity at the plasma membrane. Thus, there was no change in the Lem3 requirement for proper ER export, localization, or flippase activity of the Dnf1 chimeras tested.

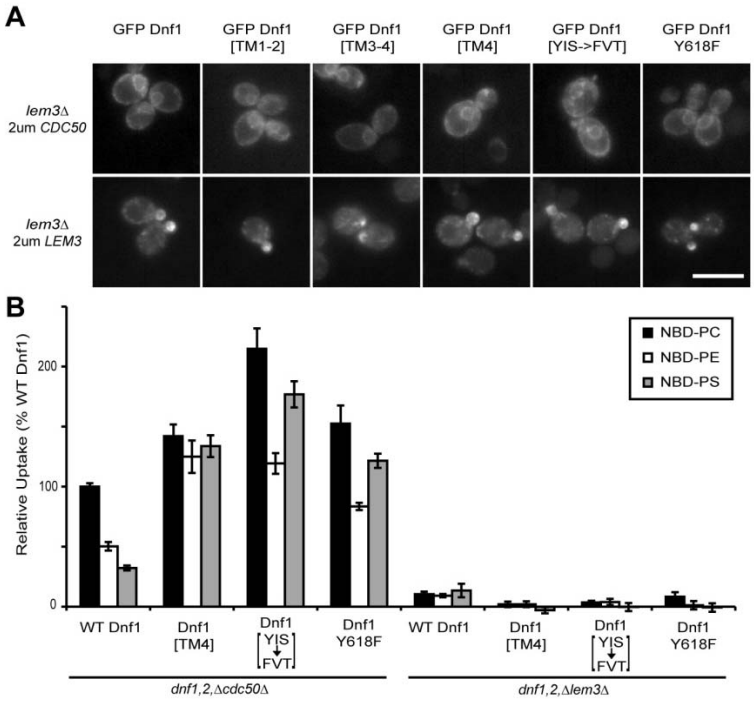

Figure 2-14. GFP tagged Dnf1[Drs2] chimeras retain a Lem3 requirement for ER export and flippase activity. (A) GFP tagged chimeras were expressed in *lem3Δ* cells (SCY119) overexpressing *CDC50* or *LEM3*. Each Dnf1[Drs2] chimera tested exhibited a characteristic ER localization pattern in *lem3Δ* cells overexpressing *CDC50*. In contrast, overexpression of *LEM3* in a *lem3Δ* strain rescues each Dnf1[Drs2] chimera polarized localization pattern. In each column, the fluorescence intensity of each image is scaled equivalently to show relative expression levels of each chimera. The scale bar is 10µm. (B) NBD-PL uptake by Dnf1[Drs2] chimeras expressed in *dnf1,2Δcdc50Δ* or *dnf1,2Δlem3Δ* strains.

Potential P4-ATPase substrate transport pathway

Based upon the functional data we have presented, a single amino acid substitution (Y618F) in TM4 of Dnf1, representing the loss of a single hydroxyl group, allows this protein to recognize and translocate NBD-PS. To better understand how such a subtle sequence change could lead to a dramatic change in the substrate preference, we generated a structural model of Dnf1 based upon the crystal structure of the Na^+/K^+ ATPase (Figure 2-15A) (PDB 2ZXE) (Shinoda, et al., 2009). We used the SWISS-MODEL workspace (Arnold, Bordoli, Kopp, & Schwede, 2006; Kiefer, Arnold, Künzli, Bordoli, & Schwede, 2009) for the initial modeling and relaxed the model in Rosetta (Simons, Kooperberg, Huang, & Baker, 1997; Yarov-Yarovoy, Schonbrun, & Baker, 2006) to obtain the final structural model (Figure 2-15C). The complete conservation of the helix-breaking Pro from the PEGL motif in cation transporting ATPases (PISL in P4-ATPases), provides a concrete anchoring point for the modeling of TM segment 4, particularly for Y618 in the proline plus 4 position (PISLY) (Figure 2-16A). The glutamate residue from the PEGL motif in TM4 of cation transporting ATPases has a critical role in binding substrate and is oriented towards the K^+ binding sites formed by residues in TM 4,5,6,8 (Figure 2-15B). In contrast, the proline plus 4 residue in each available P-type ATPase crystal structure is rotated 180° around TM4 and is oriented in a triangular cleft between TM segments 1, 3 and 4 (Gourdon, et al., 2011; Obara et al., 2005; Pedersen, et al., 2007; Shinoda, et al., 2009), in the opposite direction from the canonical cation binding sites (Figure 2-16B and 2-16C). The orientation of Dnf1 Tyr618 in the modeled structure is equivalently positioned at the apex of this triangular cleft (Figure 2-15D, 2-15F and 2-16C). Tyr618 is also near the membrane interface on the cytosolic side, suggesting this residue comprises (part of) the exit site for the phospholipid substrate. LL3-4 is much longer in the P4-ATPases than in other P-type ATPase subfamilies, and is therefore not threaded onto an experimentally determined structure. This loop likely forms the base of the

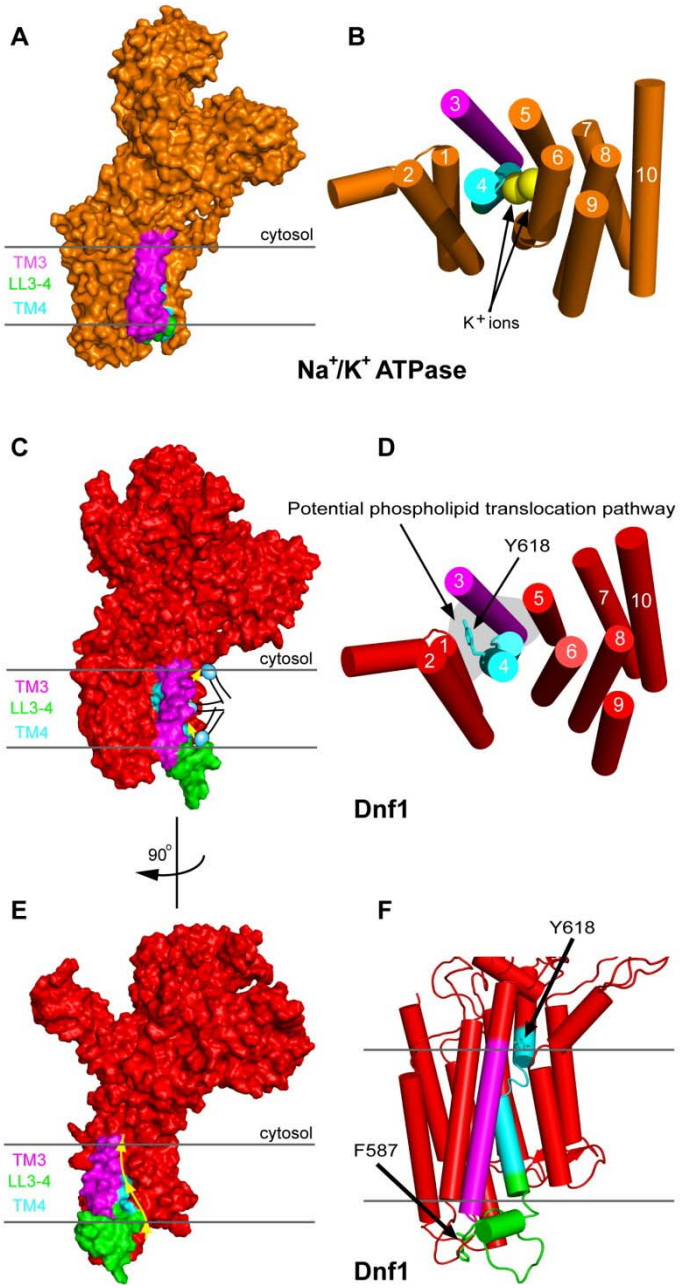

Figure 2-15. Model of the Dnf1 structure showing the orientation of Y618 and a proposed pathway for phospholipid translocation. (A) Na^+/K^+ ATPase crystal structure in the E2($2K^+$)-P_i conformation (PDB 2ZXE (Shinoda, et al., 2009)). Dark gray lines represent the membrane boundaries. (B) View of the Na^+/K^+ ATPase TM domain from the cytosolic side. (C) Structural model of Dnf1 highlighting segments involved in phospholipid selection and the groove between TM1, TM3 and TM4 forming a potential pathway for phospholipid flip. (D) View of the Dnf1 TM domain from cytosolic side of bilayer. Tyr618 is oriented on the opposite side of TM4 relative to the cation binding pocket of ion-transporting P-type ATPases. (E) Dnf1 model rotated 90° compared to (C). The yellow arrow represents the potential phospholipid transport pathway at the protein lipid interface between TM1,TM3 and TM4. (F) Triangular cleft formed from TM1, TM3, LL3-4 and TM4. Arrows indicate F587 and Y618 of Dnf1, residues involved in PC and PS selection, respectively.

triangular cleft as modeled, but the orientation of F587, a residue important for PC selection, is unclear. However, the residues important for phospholipid substrate selection in TM3, LL3-4 and the proline plus 4 position of TM4 are very unlikely to lie within the canonical substrate-binding pocket defined in cation transporters. Therefore, we propose a novel transport pathway for P4-ATPase flippases where the phospholipid headgroup is translocated along a groove between TM1, TM3 and TM4 while the fatty acyl chains reorient within the lipid environment of the membrane (Figure 2-15C-E).

DISCUSSION

Cation transporting P-type ATPases utilize a spatially restrictive ion-binding pocket in the center of the transmembrane domain. In this work, we have identified residues that contribute to phospholipid substrate specificity in *S. cerevisiae* P4-ATPases that lie outside of the canonical binding pocket. Based on the orientation of a key tyrosine residue in TM4 and the involvement of TM3 and LL3-4 residues in substrate selection, we suggest a pathway for phospholipid translocation along the protein-lipid interface that would accommodate transport of this large substrate.

We generated a series of chimeras between Dnf1 and Drs2, two P4-ATPases that differ in substrate specificity, to map amino acid residues involved in substrate selection. We sought to identify Drs2 sequences required for PS recognition by construction of chimeras that convert Dnf1 from a PC/PE flippase to a PS flippase. We have partially succeeded in this endeavor as Dnf1[TM3-4] gained the ability to flip NBD-PS and shows a preference for NBD-PS over NBD-PC. While we have significantly altered the substrate specificity of Dnf1 through incorporation of these Drs2 sequences, it appears that we have not fully recapitulated the substrate specificity of

Drs2 because Drs2 appears to have negligible activity towards NBD-PC (Natarajan, et al., 2004; Zhou & Graham, 2009). Substitution of Dnf1 TM3-4 with analogous Drs2 sequences significantly attenuates uptake of NBD-PC and NBD-PE, even though the protein localizes normally to the plasma membrane. The striking increase in PC and PE activity of the Dnf1[TM4] chimera relative to Dnf1[TM3 - 4] also implies that TM3 and LL3-4 from Dnf1 contain sequences that recognize these substrates much better than the analogous Drs2 segments. In fact, we have identified substitutions of a single residue (Phe587) within LL3-4 that reduce PC recognition without affecting recognition of PE. These are original observations as TM3-LL3-4 residues have not been implicated in substrate recognition by other P-type ATPases. LL3-4 is much larger in the P4-ATPases relative to the cation transporters and no structural information on this loop is available, but it is likely to sit at the membrane surface where phospholipid substrate would initially be selected for translocation.

The most surprising observation of this work is that the substitution of a single tyrosine residue for phenylalanine in TM4 (Y618F) conferred an NBD-PS transport activity to Dnf1 without altering the ability of this protein to flip NBD-PC or NB-PE. TM4 is also important for substrate interaction by cation transporting P-type ATPases and contains a highly conserved, helix-breaking Pro followed by a glutamate residue critical for cation binding by SERCA (Glu309) and the Na^+/K^+ ATPase (Glu334) (Figure 2-16A). The PEGLX motif in the cation transporters is replaced by PISLY (Dnf1) and PISLF (Drs2) in these P4-ATPases. Conservation of Pro implies that the P4-ATPases maintain the same break in the TM4 helix observed in the heavy metal (P1), cation (P2) and proton (P3) transporter crystal structures and that structural features of this TM segment would be similar. The critical Tyr/Phe identified in this study lies only 4 residues from the conserved proline, and in each P-type ATPase crystal structure, the residue analogous to Dnf1 Tyr618 is oriented on the opposite face of TM4 relative to the cation binding site (Figure 2-

15, 2-16). This Tyr/Phe residue in the Dnf1 structural model juts into the apex of a triangular cleft formed by TM segments 1, 3, 4 and LL3-4 that lies at the protein/lipid interface (Figure 2-15F, 2-16C).

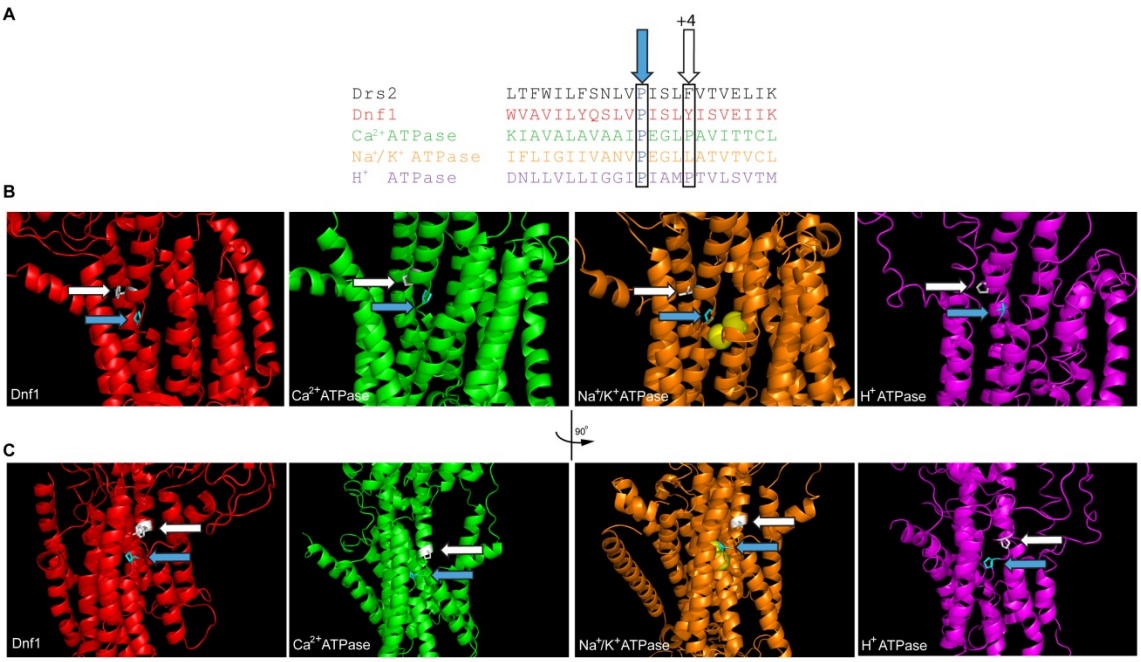

Figure 2-16. **.** Structural conservation of the P-type ATPase TM domain. (A) Sequence alignment of TM4 of P4-ATPases Dnf1 and Drs2 with crystalized P-type ATPases. (B, C) Comparison of the conserved proline (blue arrow), and "proline plus 4" position (white arrow) between each crystal structure and the structural model of Dnf1. The crystal structures used in this image are: SERCA PBD 2AGV, Na^+/K^+ ATPase PBD 2ZXE, H^+ ATPase PBD 3B8C.

We propose that the cleft bordered by TM3, LL3-4 and Y618 in TM4 provides a pathway for the flip of a phospholipid headgroup from the extracellular to the cytosolic leaflet. Alternatively, the groove between TM3, 4, and 5 could also provide a route for substrate, but unfortunately none of the chimeras we have created bearing TM5-10 from Drs2 were functional. Thus, the influence of TM5-10 on substrate selection is not yet known and cannot be ruled out as potentially contributing to phospholipid transport. By providing a substrate pathway at the protein/lipid interface, the acyl chains can simply re-orient within the lipid environment and do not have to be accommodated in a proteinaceous binding pocket. This

could explain why phospholipids with acyl tags such as spin-labels (Zachowski, et al., 1989) or the NBD moiety (Tang, et al., 1996) are transported by P4-ATPases. If these tagged phospholipids were transported using a tight binding pocket similar to the mechanism of cation transporting P-type ATPases, the bulky tag would likely prevent transport. A transport mechanism that allows the acyl chains to remain in the lipid environment significantly alleviates the giant substrate problem.

The position of the substrate-selective Tyr/Phe residue near the cytosolic side of TM4 in the membrane domain was also surprising. We assumed that residues conferring substrate specificity would define a binding site near the extracellular leaflet where substrate would load into the pump. The role of LL3-4 in PC selection, particularly Phe587, fit this expectation. The proximity of Tyr618 to the cytosolic leaflet suggests this residue forms part of the exit pathway for the phospholipid headgroup. Dnf1 can weakly recognize PS and likely retains other residues involved in loading PS into the pump, but perhaps Y618 prevents PS exit into the cytosolic leaflet. Conversely, Drs2 F511Y was specifically deficient in recognizing PS. Therefore, the Y618 hydroxyl group may either generate a steric clash with the PS carboxyl group, thereby preventing PS transport, or the hydroxyl alters the packing of TM segments in this region in a manner that specifically restricts PS transport. Interestingly, substitution of the proline plus 4 Tyr/Phe for Leu, the Atp8a1 residue, reduces the activity of Dnf1 or Drs2 without a noticeable change of substrate specificity. Perhaps the Leu is incompatible with the surrounding yeast residues that form this restriction point. However, the phospholipid is likely selected at multiple points during its transport across the membrane because 1) we identified at least two residues (on opposing membrane faces) which specifically affect substrate specificity and 2) substitution of TM3, LL3-4 and TM4 with Drs2 sequences was required to confer the greatest preference for PS.

Assuming that P4-ATPase TM segments undergo conformational changes during the catalytic cycle comparable to the Ca^{2+} ATPase, the remarkable pumping motions of TM segments 1-4 could provide the physical motion needed to flip a phospholipid substrate (Toyoshima & Nomura, 2002). Dnf1 is modeled in the E2 conformation and phospholipid substrate is thought to be pumped during the E2~P → E1 transition. During this power stroke, TM1 starts in the 90˚ bent conformation with residues in the TM1 kink modeled in close proximity to Tyr618 in TM4. As the pump relaxes back to the E1 conformation, TM1 straightens and slides down in the membrane (towards the exofacial leaflet) while TM4 moves upward. These movements place Tyr618 in proximity to the cytosolic end of the TM1 helix in the E1 conformation, such that a phospholipid headgroup docked near Tyr618 would then have access to a large opening between TM1 and TM2, perhaps representing an exit site.

Cdc50 family members have been suggested to provide the substrate specificity of their P4-ATPase counterpart by loading it with phospholipid (Puts & Holthuis, 2009). Even though we have altered the phospholipid specificity of Dnf1 by introduction of Drs2 sequences, the chimeras retain a Lem3 requirement. In no case was Cdc50 necessary or sufficient to facilitate the ER export, localization and activity of the chimeras (Figure 2-14). Our data suggest that, like *Arabidopsis thaliana* P4-ATPases (López-Marqués, et al., 2010), *S. cerevisiae* P4-ATPases do not rely on a Cdc50 family member to determine the substrate specificity of the heterodimer complex (Figure 2-5B and 2-14).

These studies provide the first glimpse into the mechanism of substrate recognition and translocation by phospholipid flippases, a distinct clade in the P-type ATPase phylogeny. The residues reported here are not likely to encompass all residues involved in phospholipid selection and more studies will be required to fully solve the giant substrate problem. It remains to be determined whether the TM4 "proline plus 4" position is universally used by all members

of this family for substrate recognition in a manner similar to the "proline plus 1" position of the cation transporters. In addition, tests for the validity of structural model will be required to support or refute the proposed substrate pathway along the TM1,3-4 protein/lipid interfacial region we propose herein. Regardless of the precise orientation of Tyr618 in Dnf1, models of substrate translocation by the P4-ATPases will need to accommodate the observation that the presence or absence of a hydroxyl group at this position substantially impacts substrate selectivity.

MATERIALS AND METHODS

Reagents

All lipids were purchased from Avanti Polar Lipids, Inc. (Alabaster, AL). 5-fluoroorotic acid (5-FOA) was purchased from Zymo Research (Irvine, CA). Edelfosine was purchased from Tocris Biosciences (Bristol, United Kingdom). Papuamide B was a gift from Raymond Andersen (University of British Columbia). Duramycin was purchased from Sigma Aldrich (St. Louis, MO).

Strains and culture

Strains used in this study are listed in Table A1. Yeast were grown in standard rich medium (YPD) or synthetic minimal glucose medium (SD) (Sherman, 2002) and transformations were performed using the lithium acetate method (R.D. Gietz & Woods, 2006). For complementation tests, 50,000 cells were spotted with 10-fold serial dilutions onto synthetic media or synthetic media containing 5-FOA. Plates were grown for 3 days before imaging.

Escherichia coli strain DH5α was used for plasmid amplification and construction. Dnf1[Drs2] chimeras were generated by either site-directed mutagenesis (for point mutations) or gene splicing overlap extension (Yon & Fried, 1989) (for >4 amino acid changes). Dnf1[Drs2]

chimeras were generated by gap repair through homologous recombination of a gapped yeast expression vector and PCR product, followed by recovery of the plasmid from yeast. All plasmids used in this study are listed in Table A2 and primers are listed in Table A3.

Edelfosine screen

In order to generate random mutations targeted to TM3-4 of Dnf1, we used pRS313-DNF1 as template with primers Dnf1(forw)@1500 and Dnf1(rev)@2297 using PCR conditions described previously (Cadwell & Joyce, 1992). We co-transformed ZHY704 with the PCR products and pRS313-DNF1 gapped with restriction enzymes MfeI and NruI to allow for gap repair through homologous recombination. Transformations were plated onto synthetic dropout plates and allowed to grow for 3 days, after which colonies were picked into 96 well plates and spotted onto synthetic dropout plates containing 20μg/mL edelfosine or 5-FOA. We sequenced *DNF1* in strains which grew on both edelfosine and 5-FOA.

Viability assay

For papuamide B and duramycin treatments, mid-log phase yeast were seeded in 96 well plates at 0.1 OD_{600}/mL with or without drug. Plates were incubated at 30°C for 20 hours and the OD_{600}/mL was measured with a Multimode Plate Reader Synergy HT (Bio-Tek, Winooski, VT). Relative growth was compared to mock-treated yeast in the assay.

Fluorescence microscopy

Images were collected with an Axioplan microscope (Carl Zeiss, Thornwood, NY) with a CCD camera and processed with MetaMorph 4.5 software (Molecular Devices, Sunnyvale, CA). To observe GFP-tagged proteins, cells were grown to mid-logarithmic phase, pelleted, and resuspended in imaging buffer (10mM Tris-HCl, pH 7.4, 2% glucose (wt/vol)). An aliquot of cells was distributed onto slides, and visualized using a GFP filter set.

NBD-lipid uptake

Lipid uptake was performed essentially as described previously (Hanson & Nichols, 2001). Briefly, overnight cultures were diluted to 0.15 OD/mL and allowed to grow to early-mid log phase. 500 µl of cells were harvested, resuspended in ice-cold SD media containing 2 µg/ml NBD-lipid (~2.5µM), and incubated on ice for 60 min. Cells were washed twice with SA media (SD media + 2% sorbitol (wt/vol), + 20mM NaN_3) + 4% BSA (wt/vol), once with SA media, and resuspended in SA media prior to analysis by flow cytometry.

Flow cytometry

Flow cytometry was performed with a BD LSRII-3 laser (BD Biosciences) using BD FACSDiva v6.1.3. NBD-lipid uptake was measured with the FITC filter set (530/30 bandpass with a 525 longpass). Prior to analysis, propidium iodide was added to the cells at a final concentration of 5µM. At least ten thousand events were analyzed using forward/side scatter to identify single cells and propidium iodide fluorescence was used to exclude dead cells.

Data analysis

Within each experiment, at least 3 independently isolated transformants harboring the same construct were assayed. The mean of these values from at least 3 separate experiments were reported as ± SEM. For each experiment, the chimera-independent background uptake for each NBD-PL was measured by the average fluorescence of the *dnf1,2Δ* strain (PFY3275F) transformed with an empty vector and subtracted from the uptake of WT Dnf1 or the Dnf1[Drs2] chimeras. In order to compare results from independent experiments, the NBD-PC uptake by WT Dnf1 after 1 hour was normalized to 100%. Each value is reported relative to WT Dnf1 PC uptake at one hour. A student's T-test was used to determine significance where indicated.

Modeling

A model of Dnf1 was generated based on the crystal structure of the Na^+/K^+ ATPase (Protein Data Bank accession code 2ZXE). We used the SWISS-MODEL workspace (Arnold, et al., 2006; Kiefer, et al., 2009) to generate the initial model based on sequence alignment of Dnf1 and the Na^+/K^+ ATPase (Figure S9). The initial structural model was relaxed in Rosetta-Membrane (Simons, et al., 1997; Yarov-Yarovoy, et al., 2006) to obtain the final structural model. Images were generated with PyMOL (v1.3r1 edu) (Schrodinger, 2010) and the pdb file is available from the Vanderbilt University Center for Structural Biology or upon request from Todd R. Graham.

Cloning

GFP-Dnf1 was an N-terminal fusion generated by standard cloning of DNF1 into the KpnI site in pRS416-GFP. KpnI sites were added to the 5' and 3' ends of DNF1 by amplifying pRS313-DNF1 with Dnf1 primers (Dnf1(forw)+KpnI and Dnf1(rev)+KpnI) to amplify a 4.7kb PCR fragment. The GFP-Dnf1 chimeras were generated by replacing the WT Dnf1 sequence through standard cloning using SphI and BseRI restriction sites from the pRS313 expression vectors (1).

Plasmid shuffling assay

A *dnf1,2,3Δdrs2Δ* strain harboring *WT DRS2* on a *URA3* plasmid was transformed with a second plasmid containing the *DNF1[DRS2]* chimera. When grown in the presence of 5-fluoroorotic acid (5FOA), any strain that is unable to lose the *URA3-DRS2* plasmid will die. Strains containing a Dnf1[Drs2] chimera capable of supporting growth of the *dnf1,2,3Δdrs2Δ* strain will be able to lose the DRS2-URA3 plasmid and grow in the presence of 5FOA.

Cell extracts and western blotting

Yeast containing N-terminal 3xFLAG tagged Dnf1 were grown in YPD to mid-log phase and harvested in SDS/urea sample buffer (40 mM Tris–HCl (pH 6.8), 8M urea, 0.1mM ethylenediaminetetraacetic acid, 1% 2-mercaptoethanol, 5% SDS and 0.25% bromophenol blue). 0.2OD cell lysate was separated by SDS-PAGE, transferred to PVDF membrane, and blotted with anti-FLAG M2 antibody (Sigma-Aldrich).

ACKNOWLEDGEMENTS

We thank Jonathan Sheehan from the Vanderbilt University Center for Structural Biology for assistance with refining the structural model and valuable discussion. We acknowledge Patrick Williamson at Amherst College for originally articulating the “giant substrate problem”. These studies were supported by NIH grant GM62367 to T.R.G. and the Cellular and Molecular Microbiology Training Program T32AI007611-11, which supported R.D.B.. The VMC Flow Cytometry Shared Resource is supported by the Vanderbilt Ingram Cancer Center (P30 CA68485) and the Vanderbilt Digestive Disease Research Center (DK058404).

CHAPTER III

A TWO GATE MECHANISM FOR PHOSPHOLIPID SELECTION AND TRANSPORT BY P4-ATPASES*

ABSTRACT

Most P-type ATPases pump specific cations or heavy metals across a membrane to form ion gradients. However, the type IV P-type ATPases (P4-ATPases) evolved the ability to transport specific phospholipid substrates rather than cations and function to establish plasma membrane asymmetry in eukaryotic cells. The mechanism for how a P-type ATPase, or any other transporter, can recognize and flip a phospholipid substrate is unclear. Here, through a combination of genetic screening and directed mutagenesis with the P4-ATPases Dnf1 and Drs2 from budding yeast, we identify more than a dozen residues that determine headgroup specificity for phospholipid transport. These residues cluster at two interfacial regions flanking transmembrane segments 1-4 and lie outside of the canonical substrate binding site operating in cation pumps. Our data imply the presence of two substrate-selecting gates acting sequentially on opposite sides of the membrane: an entry gate where phospholipid is initially selected from the extracellular leaflet and an exit gate at the cytosolic leaflet. The entry and exit gates act cooperatively but imperfectly, with neither being able to completely restrict phosphatidylserine selection when the opposing gate is tuned to permit it. This work describes a unique transport mechanism for a P-type ATPase and provides insight into how integral membrane proteins can recognize and transport phospholipid substrate across a lipid bilayer.

* This chapter has been published as Baldridge and Graham (2013) Two-gate mechanism for phospholipid selection and transport by type IV P-type ATPases. *Proc Natl Acad Sci U S A* 110: E358-E367.

INTRODUCTION

All living cells are encapsulated by a plasma membrane that separates the inside of the cell from the external environment. In eukaryotic cells, the plasma membrane is a conglomerate of protein and lipid with its lipid component composed of glycerophospholipids, sphingolipids, and sterols. The amphipathic nature of these lipids causes spontaneous formation of a bilayer structure with a hydrophobic core that prevents passage of charged or bulky polar molecules, ions and many toxins into and out of the cell. This barrier function of the bilayer allows the formation of concentration gradients across the membrane, including the component phospholipid molecules themselves. Phosphatidylserine (PS), phosphatidylethanolamine (PE) and phosphatidylinositol (PI) are enriched in the cytosolic face of the plasma membrane whereas the glycosphingolipids are exposed on the exofacial side. The polar headgroups of the phospholipids prevent spontaneous flip-flop to maintain this asymmetric structure. However, establishing membrane asymmetry requires an energetic input with ATP-dependent transporters to facilitate movement of phospholipids up the concentration gradient. The uneven distribution of phospholipids between the two membrane faces generates unique properties on each face and controlled disruption is critical in physiological processes such as blood coagulation, apoptosis, cytokinesis and host-viral interactions. (Sebastian, Baldridge, Xu, & Graham, 2012)

Establishing membrane asymmetry requires vectorial transport of the component lipids; the proteins capable of catalyzing this transport are ABC transporters and type IV P-type ATPases (P4-ATPases). ABC transporters “flop” lipids from the cytosolic to exofacial leaflet opposing the P4-ATPases which “flip” phospholipids from exofacial to cytosolic side of the membrane. The glycerophospholipid specificity of the P4-ATPases restricts PE and PS to the cytoplasmic leaflet establishing and maintaining the characteristic plasma membrane

asymmetry. The first ABC transporter identified was a P-glycoprotein capable of transporting a remarkable range of substrates out of the cell (Juliano & Ling, 1976). However, most ABC transporters have a much narrower range of substrate specificities with some capable of lipid transport. ABCA1, ABCA2, ABCB4, ABCG1 are all capable of transporting both phosphatidylcholine (PC) and cholesterol, ABCG5/G8 is specific for sterols and MsbA transports the bulky lipid A components across the *E. coli* membrane (Dean & Annilo, 2005). X-ray crystal structures have been solved for several members of the ABC transporter family highlighting some of the extreme conformational changes within their catalytic cycle (Locher, Lee, & Rees, 2002; Ward, Reyes, Yu, Roth, & Chang, 2007). Even with the extensive biochemical and structural understanding of many ABC transporters, a lack of understanding for how these proteins recognize and transport lipid substrates remains an overriding theme.

P-type ATPases also have an amazing, albeit more compact, range of substrate specificities. Many transport only a specific set of ions or heavy metals (P1, P2 and P3), while others transport a subset of phospholipids (P4). These proteins have a transmembrane (TM) domain typically composed of 10 TM segments, along with cytosolic actuator (A), phosphorylation (P) and nucleotide-binding (N) domains. X-ray crystal structures with bound substrate have been solved for ion-transporting P-type ATPases (P1-P3) and they use a highly conserved ion binding pocket within the center of the TM domain (Gourdon, et al., 2011; Morth, et al., 2007; Pedersen, et al., 2007; Toyoshima, et al., 2000). Accessibility of this canonical ion binding site is classically described within the E1-E2 states of the Post-Albers cycle (Post, et al., 1972); binding site access alternates between the cytosolic side (E1), temporary occlusion (E1P/E2P), or access to the exofacial side of the membrane (E2) (Toyoshima, et al., 2004). Ion transporting P-type ATPases use a collection of charged or polar residues in conserved positions within TM segments 4, 5, 6, 8 and 9 to coordinate the ions (Morth, et al., 2011). In the P4-

ATPases, the corresponding residues are bulky or hydrophobic amino acids that render this site useless for coordinating ions. The canonical binding site is also spatially restrictive, accommodating only ions of the appropriate charge and size. It is difficult to imagine how this canonical binding site may have evolved the capacity to bind a bulky amphipathic phospholipid, giving rise to the P4-ATPase "giant substrate problem" for how phospholipid is transported (Baldridge & Graham, 2012; Puts & Holthuis, 2009).

Two opposing models have been proposed for how P4-ATPases could transport substrate; the first model using the canonical substrate binding site and the second using a novel pathway formed at the protein/lipid interface. Support for the first model was based on an observation that mutation of a conserved lysine residue in the P4-ATPase Atp8a2, which is predicted to be near the canonical binding site within TM5, reduced the apparent affinity of this pump for substrate (Coleman, et al., 2012) . In support of the novel transport pathway, we mapped residues involved in substrate selection by the yeast P4-ATPases Dnf1, a PC and PE flippase, and Drs2, a PS flippase, to TM3-4 (Baldridge & Graham, 2012). Within TM4, we identified a single amino acid involved in substrate selection four residues from a proline that is completely conserved in all P-type ATPases. The TM4 "proline +4" position controls PS selection by these P4-ATPases; the presence of a Tyr restricts PS flip while a Phe allows PS flip. We also identified a second residue within the exofacial loop between TM3 and TM4 which specifically affected the recognition of PC by Dnf1. The orientation of Tyr618 in the Dnf1 homology model and the analogous residues in each available P-type ATPase x-ray crystal structure suggest this residue faces away from the canonical ion binding pocket and permits a distinctive transport pathway (Gourdon, et al., 2011; Morth, et al., 2007; Pedersen, et al., 2007; Toyoshima, et al., 2000). Among the integral membrane proteins capable of transporting phospholipid, P4-ATPases are the only set of proteins with any residues involved in substrate selection identified.

However, with only two to three residues implicated in substrate recognition, distinguishing between the non-canonical and canonical transport pathway models is premature (Thøgersen & Nissen, 2012).

Here, we present an extensive screen for residues in TM1-6 that define phospholipid specificity in Dnf1 and Drs2. We have identified mutations in TM1-4 that cause a gain of PS flip by Dnf1, or a loss of PS flip by Drs2. Other mutations reduce PC recognition by Dnf1 without perturbing PE flip. These residues form two clusters (or gates) in TM1-4, one on the exofacial membrane face, where substrate is initially selected, and the second near the cytosolic membrane face, where substrate is released. The positioning of residues involved in phospholipid selection within TM1-2 and 3-4 are incompatible with the canonical substrate binding site. These results support a non-canonical phospholipid transport pathway along a groove between TM segments 1, 3 and 4 and imply a two-gate mechanism for the phospholipid selection by P4-ATPases.

RESULTS

TM1-2 residues defining substrate specificity

We sought to address the mechanism through which P4-ATPases select and transport phospholipid by identifying additional residues in TM1-6 responsible for determining phospholipid specificity. We previously generated a series of chimeras by exchanging segments of Drs2, a PS flippase, into Dnf1, which preferentially flips PC and PE (mutations exchanging residues between Dnf1 and Drs2 are indicated by brackets, e.g. Dnf1[Drs2]). To assay flippase activity, the Dnf1[Drs2] chimeras were expressed in a *dnf1,2Δ* strain and relative uptake of 7-nitro-2-1,3-benzoxadiazol-4-yl phospholipid (NBD-PL) across the plasma membrane was

recorded by flow cytometry. A swap of TM1-2 from Drs2 to Dnf1 resulted in a Dnf1 chimera (Dnf1[TM1-2]) with a low NBD-PC and NBD-PE uptake activity, and a minor increase in NBD-PS activity relative to WT Dnf1 (Figure 3-1A) (Baldridge & Graham, 2012). This Dnf1[TM1,2] chimera localizes normally to the plasma membrane, thus the low overall activity is not caused by misfolding and retention in the ER (Baldridge & Graham, 2012). However, the low activity made interpretation of the substrate specificity difficult; therefore, smaller substitutions were generated. Exchanging TM1 resulted in a chimera (Dnf1[TM1]) that had an intermediate NBD-PC and NBD-PE activity compared to WT Dnf1 and Dnf1[TM1-2], but displayed an increase in PS uptake activity (Figure 3-1A). The activity of the Dnf1[TM2] was also very low compared to WT Dnf1, but had no PS uptake (Figure 3-1A). These data implied TM1-2 harbored resides important for substrate selection.

An alignment of TM1-2 sequences from P4-ATPases preferring PS (Drs2 and Atp8a1)(Ding, et al., 2000; Natarajan, et al., 2004; Zhou & Graham, 2009) and those preferring PC (Dnf1 and Dnf2)(Pomorski, et al., 2003) identified a region of interest (ROI) near the exofacial leaflet where conservation strongly correlated with substrate preference (Figure 3-1B and 3-1C). Replacing the ROI in Dnf1 with the corresponding sequence in Drs2 yielded a chimera (Dnf1[ROI], Figure 3-1D) with a low activity and substrate specificity similar to Dnf1[TM1-2] and Dnf1[TM1] (Figure 3-1A). Exchanging pairs of residues in the ROI illuminated key residues for substrate selection (Figure 3-1D). Substitution of G230Q and A231Q allowed Dnf1[GA→QQ] to translocate PS as efficiently as PE, without disturbing PC or PE uptake. The IF→HV and PG→RY substitutions reduced uptake of PC and PE, and altered the specificity as these substrates were transported almost equally well. The FQ→VP and LS→TT substitutions modestly reduced activity without significantly altering substrate specificity. A measure of substrate specificity independent of total activity or transporter numbers at the plasma membrane (Baldridge &

Graham, 2012) was determined by graphing the ratio of PE to PC uptake, and PS to PC uptake for each chimera.

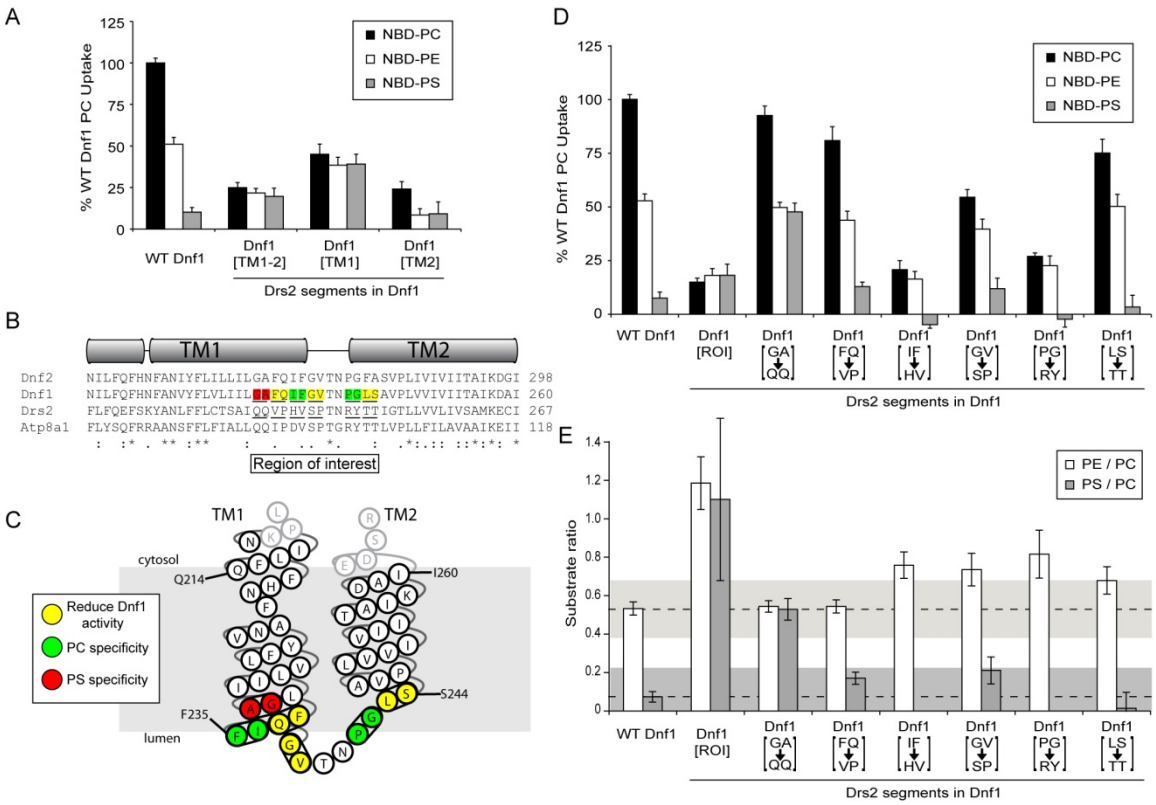

Figure 3-1. Transmembrane segments 1 and 2 (TM1-2) contribute to phospholipid selection. (A) NBD-PL uptake by wild-type (WT) Dnf1 and Dnf1[Drs2] chimeras. TM1 and 2 contain residues involved in phospholipid selection. (B) Primary sequence alignment of TM1-2 from Dnf1, Dnf2, Drs2 and Atp8a1. Predicted transmembrane helices are shown above the sequence alignment. Underlined residues are pairs exchanged from Drs2 into Dnf1. The colors indicate positions where mutations caused a change in specificity (red for changes altering PS recognition and green for PC recognition) or ≥20% reduction in activity (yellow) based on (D) and (E). (C) Topology diagram of Dnf1 TM1-2 indicating residues implicated in substrate preference based on (E). (D) NBD-PL uptake by Dnf1[Drs2] region of interest (ROI) chimeras identifying Drs2 residues involved in PS selection (QQ) and Dnf1 residues involved in PC selection (IF and PG). (E) PE/PC and PS/PC uptake ratios provide a measure of substrate preference of Dnf1 and chimeras, independent of the overall activity or the number of transporters at the plasma membrane. The gray zones indicate a confidence interval and values outside this interval define a change of specificity. For all experiments, values are the mean (± SEM). Ratios below 0 are not shown.

We defined a change in substrate specificity as a change in the PE/PC ratio or PS/PC ratio of 15% or greater without error bars (± SEM) overlapping with this zone of confidence (gray areas, Figure 3-1E). Each value falling outside of the gray zone was determined to be statistically different from WT Dnf1 by a student's T-test ($p<0.05$). Residues color coded red and green in Figure 3-1B and 3-1C indicate the substitutions at these positions cause a significant change in specificity and yellow if activity is significantly reduced without a change in specificity. These data indicate residues at the base of TM1 and 2, far removed from the canonical binding site, are critical determinants of substrate specificity.

TM3-4 residues defining substrate specificity

Dnf1 recognizes NBD-PC and -PE with short acyl chains (C6) and an NBD group in the *sn*2 position (Pomorski, et al., 2003), lyso-PC lacking the *sn*2 acyl chain (W.R. Riekhof et al., 2007) and the toxic lyso-PC analog edelfosine (Hanson, et al., 2003). Toxicity of edelfosine to yeast requires uptake by Dnf1 or Dnf2. To identify additional residues in Dnf1 involved in recognizing the phospho-choline headgroup, we randomly mutagenized Dnf1 and selected for functional variants with reduced ability to take up edelfosine. Initially, mutagenesis was targeted to the TM3-4 region because prior chimera studies indicated residues important for PC selection were present in this region (Baldridge & Graham, 2012). The mutagenized *dnf1* alleles were transformed into a *dnf1,2,3Δdrs2Δ* pRS416-*DRS2* strain and screened for mutants resistant to the edelfosine (Figure 3-2A and 3-2B). Next, functional alleles were selected by counter-screening on 5-fluoroorotic acid (5-FOA, which selects for loss of *URA3* encoded on pRS416-*DRS2*). Of the mutants resistant to both edelfosine and 5-FOA, we selected 1/3 of the clones with the strongest resistance to edelfosine for sequencing and recovered 25 point mutations within TM3-4 (Figure 3-2C, for a summary see Figure 3-2D).

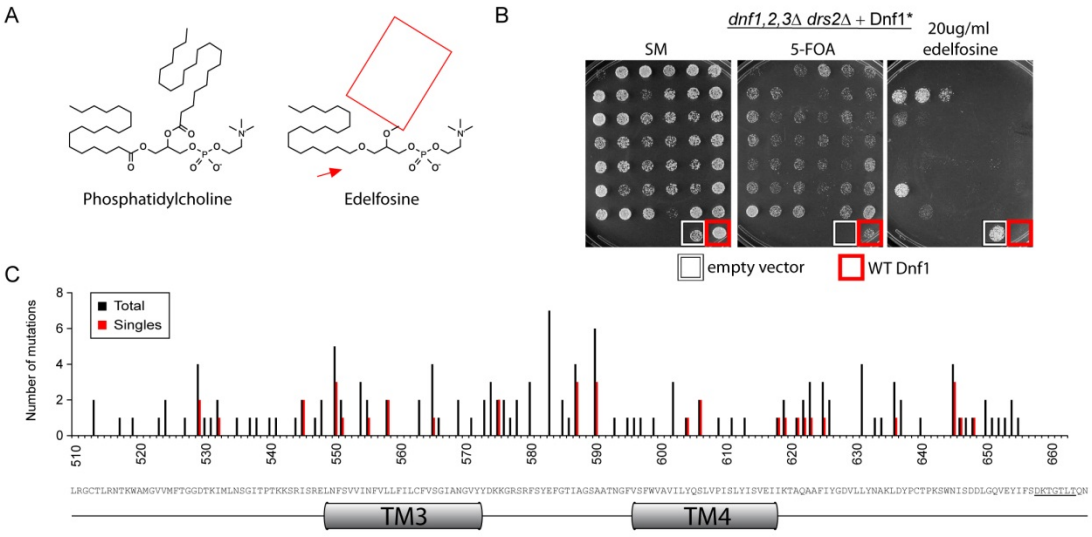

D

	Total	5-FOA Resistant	Edelfosine Resistant	Edelfosine and 5-FOA Resistant	# of mutants sequenced
TM3-4	656	326	255	244	82
	100%	49.7%	38.9%	37.2%	12.5%

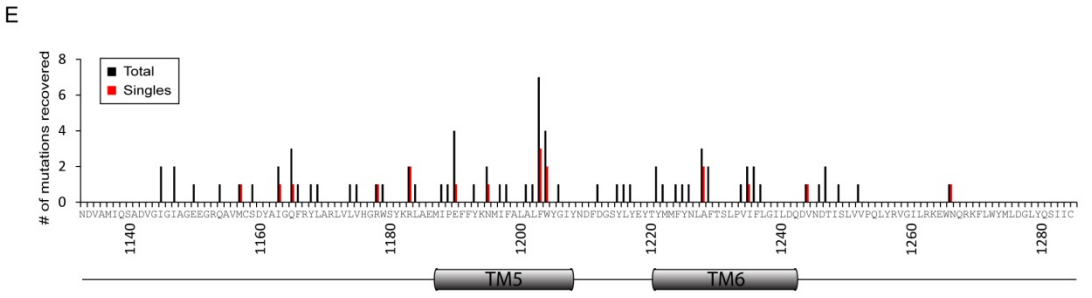

F

	Total	5-FOA Resistant	Edelfosine Resistant	Edelfosine and 5-FOA Resistant	# of mutants sequenced
TM5-6	427	213	141	141	51
	100%	49.9%	33.0%	33.0%	11.9%

Figure 3-2. Summary of the Dnf1 mutagenesis edelfosine-resistance screen.
(A) Chemical structures of phosphatidylcholine and edelfosine. Red box and arrow indicate differences between compounds. (B) Examples of plates used in the screening procedure to identify functional Dnf1 mutants capable of edelfosine resistance. (C) Position of residues identified in TM3-4 region. Red bar are point mutations, black are mutations present in combination with other mutations. (D) Summary of mutants identified after mutagenesis of the TM3-4 region. (E) Positioning of residues identified in TM5-6 region. Red bar are point mutations, black are mutations present in with other mutations. (F) Summary of mutants identified after mutagenesis of the TM5-6 region.

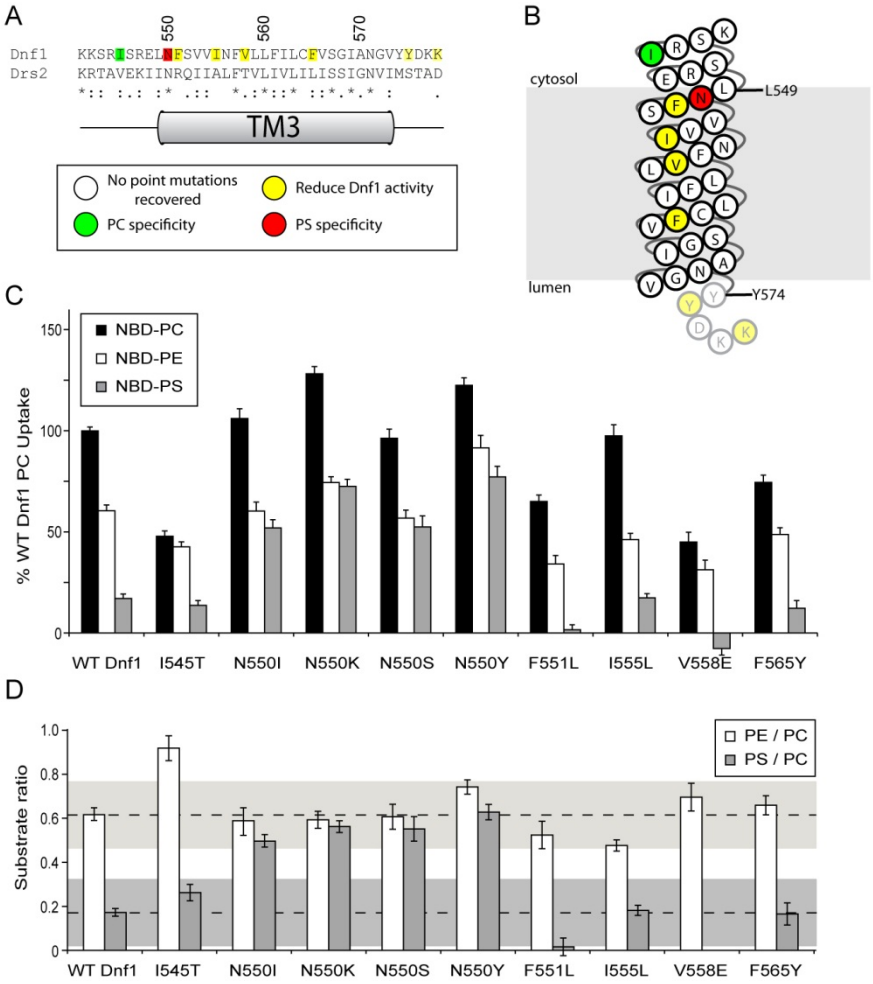

Figure 3-3. TM3 mutations conferring edelfosine resistance alter Dnf1 substrate specificity. (A) Primary sequence alignment of TM1-2 from Dnf1 and Drs2. Transmembrane sequences are indicated below the sequence alignment. (B) Topology diagram of Dnf1 TM3 indicating residues implicated in substrate preference based on (D). (C) NBD-PL uptake by edelfosine-resistant Dnf1 mutants. Substitutions at I545 decrease PC recognition and at Asn550 increase PS uptake by Dnf1. (D) PC/PE and PS/PC uptake ratios describe two residues involved in substrate specificity (Ile545, Asn550). For all experiments, values are the mean (± SEM). Ratios below 0 are not shown.

The *dnf1* alleles with point mutations were transferred into a *dnf1,2Δ* strain and the cells assayed for NBD-PL uptake activity. For the point mutations present in TM3, most caused a general reduction in activity (F551L, I555L, V558E, F565L, Figure 3-3C) without altering substrate

specificity (Figure 3-3D). Importantly, these residues should line one face of the TM3 helix. Dnf1 I545T caused a greater reduction in PC uptake activity than for PE (Figure 3-3C), which was apparent in the PE/PC uptake ratio (Figure 3-3D). Therefore, this position has a strong effect on PC selection by Dnf1. The second position of interest is Asn550, which was recovered from the screen as alleles encoding four different amino acid substitutions. Unexpectedly, in each case the substitutions for Asn550 allowed a substantial increase in NBD-PS transport by Dnf1 with minor changes in NBD-PC or NBD-PE transport (Figure 3-3C). The Asn550 residue is predicted to be in close proximity to Tyr618 near the cytoplasmic face of the membrane, and mutation of Tyr618 also increases PS activity of Dnf1 (Baldridge & Graham, 2012). However, in the case of Tyr618, acquisition of NBD-PS transport seems to require a specific substitution to Phe (Y618F), whereas multiple substitutions at Asn550 (Ile, Lys, Ser or Tyr) allow NBD-PS transport.

For the point mutations recovered in the lumenal loop between TM3 and 4 (LL3-4), we identified two residues important for activity (Y575 and Phe583) and at least two residues impacting specificity. In addition to Phe587 we previously reported, we repeatedly recovered mutations in a second position (Ile590) some of which altered the specificity of Dnf1 (Figure 3-4C and 3-4D). K578E was the only mutation in this region that enhanced NBD-PS transport, although the change in specificity indicated by the PS/PC ratio did not extend above our zone of confidence. Within TM4, we have previously reported the proline+4 position as critical in phospholipid selection by Dnf1 (Tyr618) and Drs2 (Phe511). In this screen, we recovered a single Dnf1 mutation in this position (Y618C), which caused an overall reduction in NBD-PL uptake activity, but no significant change in specificity. Two mutations in TM4 caused a change in phospholipid specificity. Dnf1 V621A acquired a minor NBD-PS activity, while Dnf1 E622V showed substantial increases in both the PE/PC and PS/PC ratios as a result of a reduced PC activity and enhanced PS activity (Figure 3-4C and 3-4D). Val621A and Glu622 are approximately

a full turn of the helix above Tyr618, which along with N550 and/or I545 in TM3 may represent a cluster of vicinal residues controlling exit of substrate to the cytosolic leaflet.

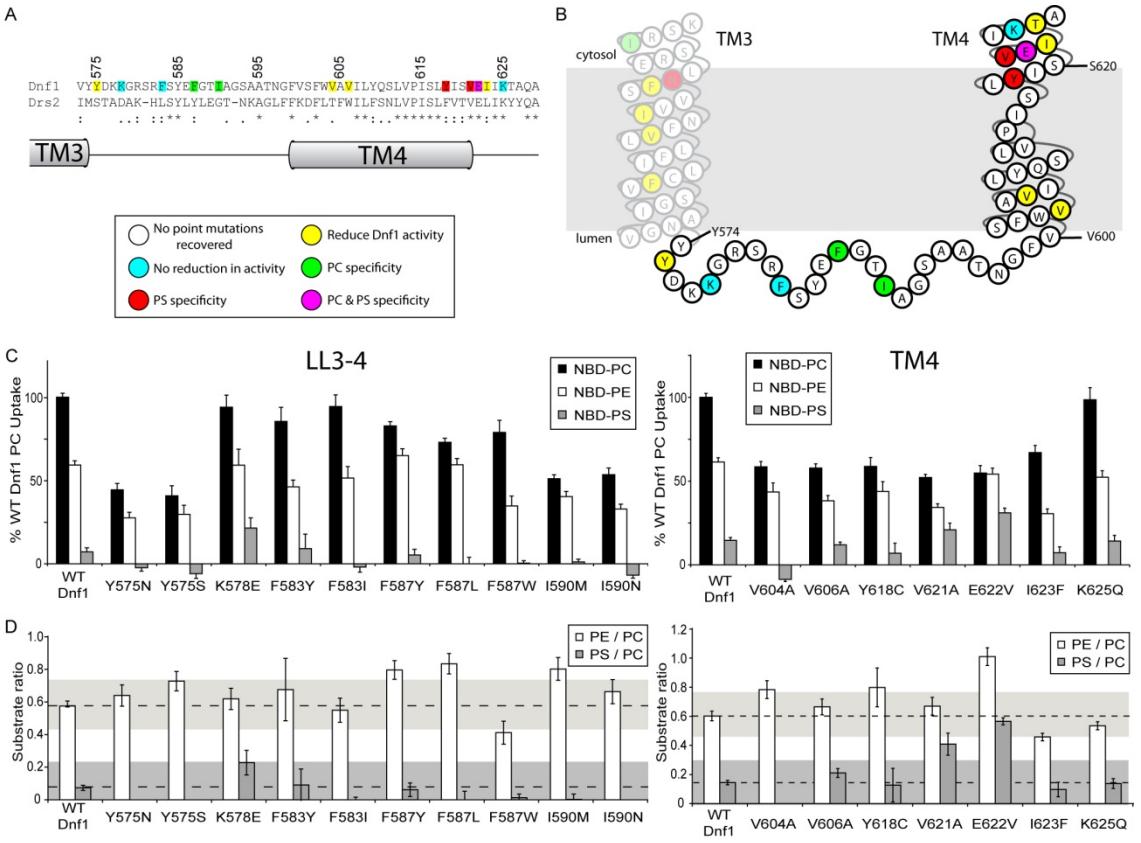

Figure 3-4. LL3-4 and TM4 mutations conferring edelfosine resistance alter Dnf1 substrate specificity. (A) Primary sequence alignment of LL3-4, TM4 from Dnf1 and Drs2 with position of transmembrane helices. (B) Topology diagram of Dnf1 TM3-4 indicating residues implicated in substrate preference based on (D). (C) NBD-PL uptake by edelfosine-resistant Dnf1 mutants with mutations in LL3-4 (left) and TM4 (right). (D) PC/PE and PS/PC uptake ratios implicate four residues involved in substrate specificity (Phe587, Ile590, Val621, Glu622). For all experiments, values are the mean (± SEM). Ratios below 0 are not shown.

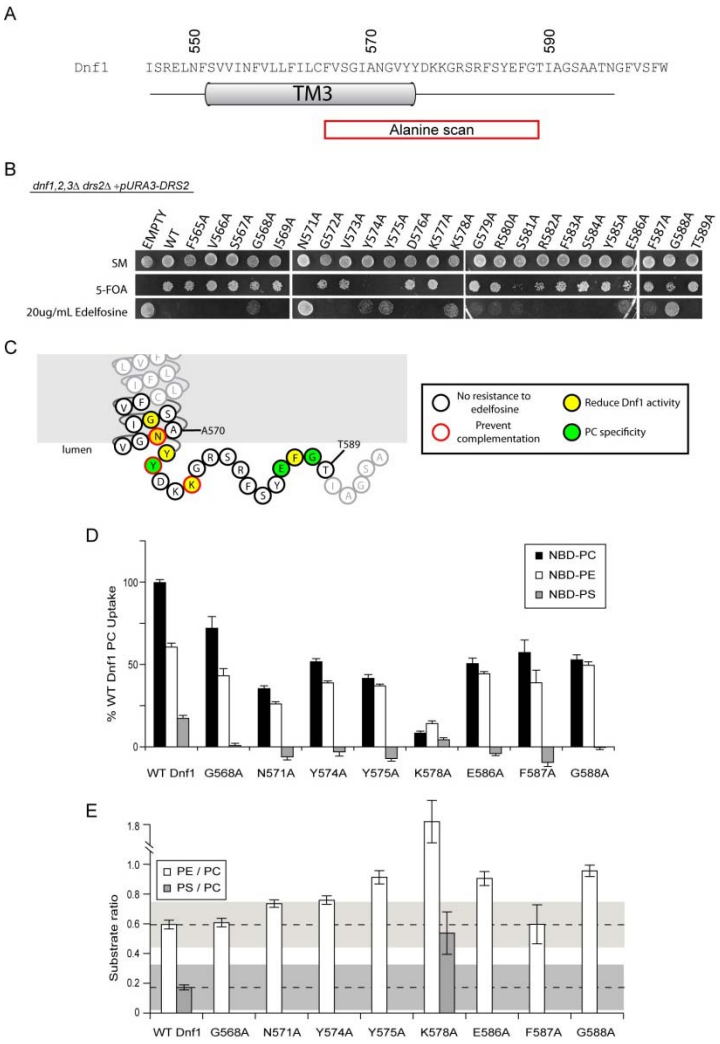

Figure 3-5. Alanine scanning mutagenesis highlights additional residues involved in Dnf1 function and substrate specificity.(A) Depiction of the residues scanned with alanine. (B) A *dnf1,2,3Δdrs2Δ +URA3-DRS2* strain expressing Dnf1 alanine scan mutants were plated on synthetic media (top), SM containing 5-FOA (middle), or SM containing 20µg/mL edelfosine. 5-FOA is toxic to yeast expressing *URA3* so growth on 5-FOA indicates the Dnf1 allele is capable of complementing the growth defect of the *dnf1,2,3Δdrs2Δ* strain in the absence of the covering *URA3-DRS2* plasmid. Edelfosine is toxic to WT yeast and the uptake is mediated by Dnf1, growth suggests a potential defect in PC uptake by Dnf1. (C) Summary of alanine scanning mutagenesis. The colors indicate if there was a change in PC specificity (green) or reduction in activity (yellow) based on (E) or lack the ability to complement a *dnf1,2,3Δdrs2Δ* growth defect (red circle). (D) NBD-PL uptake by Dnf1 alanine scanning point mutants which were slightly resistant to edelfosine. Each of these mutants displayed a reduction in Dnf1 activity. (E) PE/PC and PS/PC uptake ratios depict the substrate preference based on (D). Substitution for Y575A, E586A and G588A resulted in changes of the PC/PE preference. For all experiments, values are the mean of at least three independently-isolated transformants from at least three independent experiments (± SEM).Ratios below 0 are not shown.

To assess the saturation of the directed evolution screen on TM3-4 and identify any periodicity for residues impacting function, we also performed an alanine scan across a portion of TM3 and LL3-4 (Figure 3-5A). Within the scanned region (24 residues) three mutations (N571A, Y575A and K578A) prevented complementation of a *dnf1,2,3Δdrs2Δ* strain, and two weakly complemented (Y574A and S581A). These inactivating mutations were found at a periodicity that might suggest a critical face of an α-helix at the beginning of LL3-4. Several of the alanine mutations conferred variable degrees of resistance to edelfosine (Figure 3-5B). As expected, each allele that did not complement also conferred edelfosine resistance, consistent with a loss of function. Several other alanine scan mutants showed weak resistance to edelfosine and would not have been selected through the screen. However, one mutation (G588A) caused strong resistance to both edelfosine and 5-FOA. The G588A and several other mutants with weaker resistance to edelfosine were assayed for NBD-PL uptake activity (Figure 3-5D). Most displayed a general reduction in activity (G568A, N571A, Y574A, K578A, F587A), but Y575A, E586A, and G588A actually altered the phospholipid specificity of Dnf1 by reducing PC uptake to a greater extent than PE (Figure 3-5D and 3-5E). These LL3-4 residues, along with the substrate-defining exofacial residues in TM1-2, represent a selective gate for substrate entry.

TM5-6 residues modulate Dnf1 activity

Transmembrane segments 5-6 form a portion of the canonical transport pathway used by the ion-specific P-type ATPases. However, Dnf1[TM5-6] chimeras previously characterized were retained within the ER and likely misfolded (Baldridge & Graham, 2012). To further address the potential role(s) of TM5-6 in transport specificity, we applied the same directed evolution edelfosine resistance screen with mutagenesis targeted to TM5-6 (Figure 3-6A and 3-6B). Most clones with mutations in TM5-6 reduced activity, but did not alter the specificity (n>20) of Dnf1 whether alleles with point mutations (Figure 3-6C-H) or multiple mutations (Figure 3-7C and 3-

7D) were assayed. However, one TM5-6 mutant, I1235F, displayed an increase in overall activity, and an increase in the PS/PC ratio indicating change of specificity (Figure 3-6E and 3-6F).

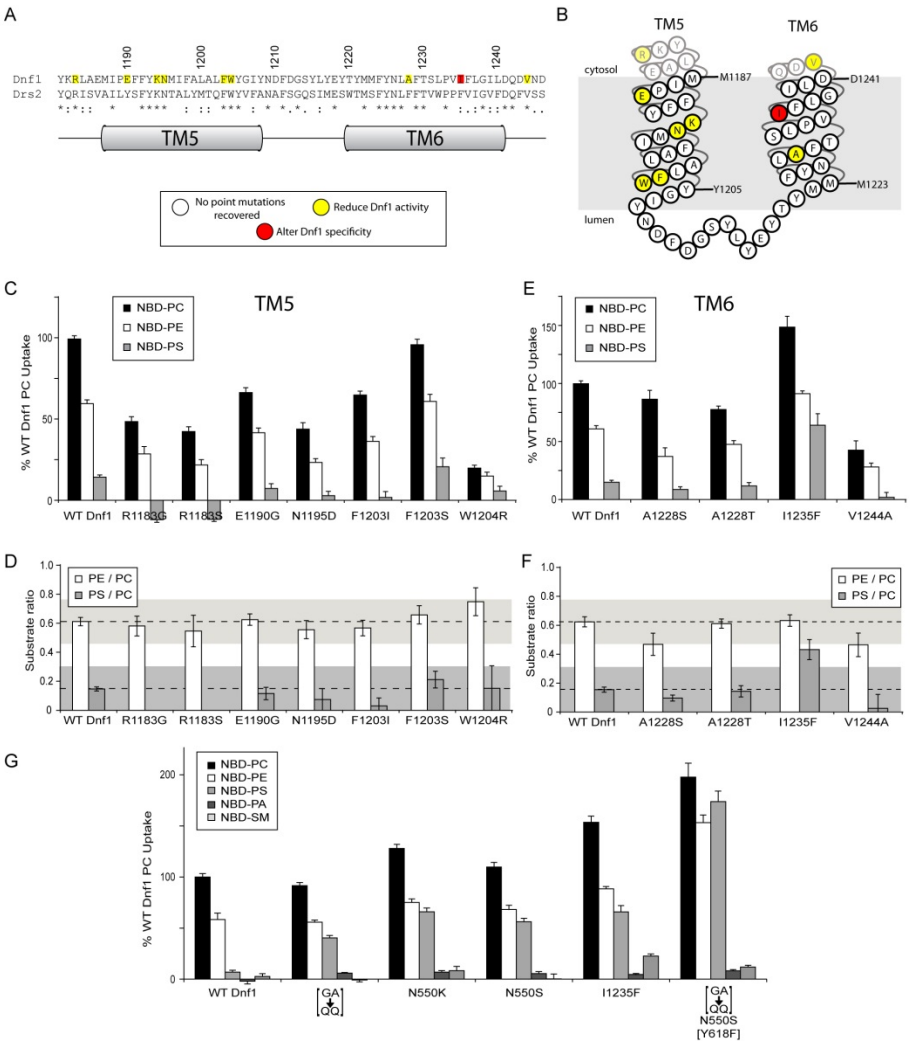

Figure 3-6. Substrate preference of TM5-6 edelfosine-resistant Dnf1 mutants.
(A) Primary sequence alignment of TM5-6 from Dnf1 and Drs2 with position of transmembrane helices. (B) Topology diagram of Dnf1 TM1-2 indicating residues implicated in substrate preference based on (D), (F). (C) NBD-PL uptake by Dnf1 TM5 point mutants recovered from edelfosine resistance screen targeted to TM5-6. These mutations reduced activity but did not change specificity (D) PE/PC and PS/PC uptake ratios provide the substrate preference based on (C). (E) NBD-PL uptake by Dnf1 TM6 point mutants recovered from edelfosine resistance screen targeted to TM5-6. (F) PE/PC and PS/PC uptake ratios depict the substrate preference based on (E). A single mutation (I1235F) affected the specificity of Dnf1 by enhancing PS uptake. (G) Dnf1[GA→QQ], Dnf1 N550K, Dnf1 N550S and Dnf1[GA→QQ],N550S,[Y618F] enhance PS uptake while maintaining specificity for the phospholipid headgroup and glycerol backbone. However, the Dnf1 I1235F mutation perturbs recognition of the glycerol backbone as indicated by increased uptake of the non-substrate sphingolipid, sphingomyelin. For all experiments, values are the mean (± SEM). Ratios below 0 are not shown.

We assayed Dnf1[GA→QQ], several Dnf1 Asn550* alleles and Dnf1 I1235F to determine if the gain-of-function activity was specific for PS or also included the non-substrate NBD-lipids, phosphatidic acid (PA) and sphingomyelin (SM). For Dnf1[GA→QQ], Dnf1 N550K and Dnf1 N550S, we observed no significant uptake activity for NBD-PA or NBD-SM, demonstrating the specific acquisition of NBD-PS as a substrate (Figure 3-8A). Dnf1 I1235F had no activity for NBD-PA but did display a significant increase in NBD-SM uptake activity relative to WT Dnf1 (Figure 3-6G). We also combined the three TM1-4 PS gain-of-function mutations into a single allele (Dnf1[GA→QQ],N550S,[Y618F]) and observed enhanced overall activity, a substantial increase in NBD-PS activity and minor increases in NBD-PA or NBD-SM. Thus, Dnf1 I1235F showed a partial loss of specificity for glycerophospholipid that was not simply a consequence of increased overall activity.

Previously with Atp8a2, a TM5 lysine (Lys873) was targeted and mutated altering the apparent affinity for substrate. This lysine was suggested to be critical for substrate interaction and proposed to be in the canonical binding pocket (Coleman, et al., 2012) . This lysine residue is highly conserved among P4-ATPases and so we generated substitutions at this position in the context of Dnf1 (Lys1194). In each case, we observed a reduction in activity with no change in specificity (Figure 3-7).

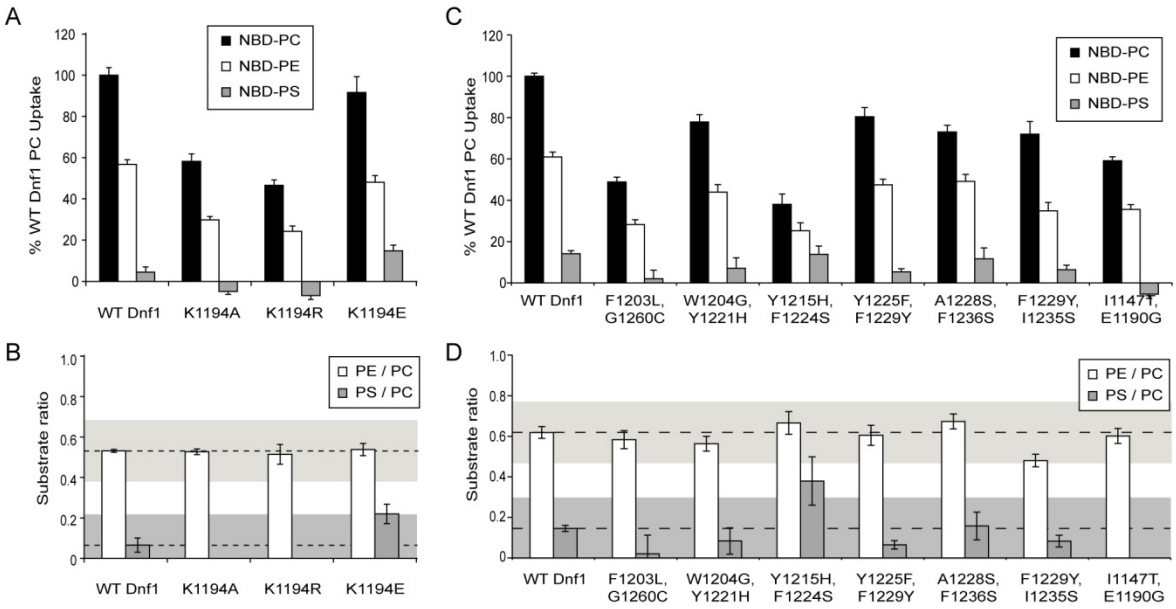

Figure 3-7. Mutation of conserved TM5 lysine and Dnf1 alleles with multiple TM5-6 mutations reduce activity without changing specificity. (A) NBD-PL Uptake of Dnf1 substitutions for the conserved lysine (Lys1194) cause a reduction in activity. It was surprising that the Dnf1 K1194R and Dnf1 K1194A present greater reductions in NBD-PL uptake than the charge reversal substitution K1194E. This may be an indication that packing in the TM5-6 region is important for overall activity of these P4-ATPases. (B) PE/PC and PS/PC uptake ratios depict the substrate preference based on (A). Substitutions at Lys1194 result in no change in substrate specificity. (C) NBD-PL uptake by Dnf1 with multiple mutations in TM5-6 recovered from edelfosine resistance screen targeted to TM5-6. (D) PE/PC and PS/PC uptake ratios depict the substrate preference based on (C).

The cytosolic and exofacial gates cooperate to restrict PS flip by Dnf1

We identified clusters of residues on both the exofacial side (entry gate) and cytosolic side (exit gate) of the membrane that contribute to phospholipid selection. Therefore, we sought to define the relationship between these gates to better understand the mechanism for phospholipid transport. Dnf1 variants harboring combinations of GA→QQ, N550S, and Y618F mutations were assayed for NBD-PL uptake activity to determine if tuning each position to allow NBD-PS flip would increase PS uptake. As shown in Figure 3-6G and 3-5A, the triple mutant displays greatly enhanced PS uptake (25-fold greater that WT Dnf1 and at least 2-fold more than each single mutant). The greatest increase in PS uptake occurred when we combined the

exofacial substitution (GA→QQ) with a cytosolic one (N550S or Y618F). Interestingly, when we combined the N550S with the Y618F mutation, there was no significant increase in the PS uptake relative to Y618F, indicating that the mutations in the cytosolic gate were not additive. These data imply that the exofacial entry gate and cytosolic exit gate act sequentially, but each imperfectly, to select substrate for transport.

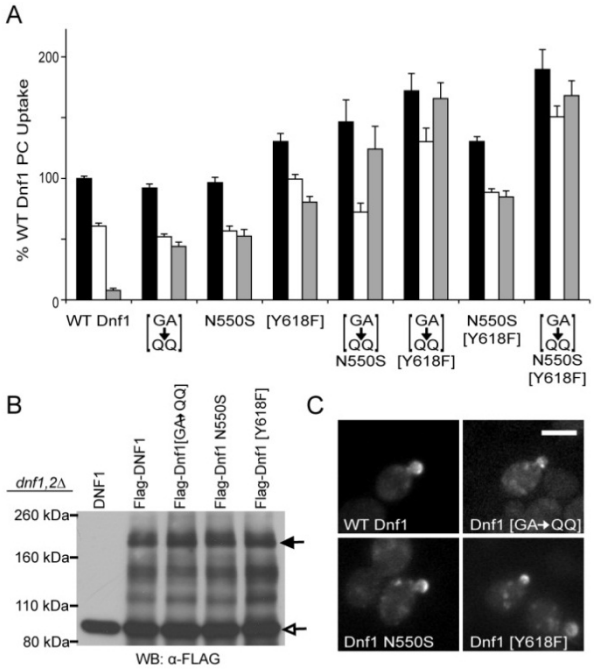

Figure 3-8. Specificity determinants on both sides of the membrane cooperate to transport phospholipid. (A) Combination of the [GA→QQ] substitution (exofacial) with either N550S or [Y618F] (cytosolic) results in additive increases in PS uptake activity relative to either substitution alone. Combining the two cytosolic residues (exit gate) N550S and [Y618F] results in a minor increase in PS uptake, suggesting they alter the same site. For all experiments, values are the mean (± SEM). (B) Expression levels of Flag- WT Dnf1, Dnf1[GA→QQ], Dnf1 N550S and Dnf1[Y618F] are similar. Closed arrow indicate Flag-Dnf1 protein, open arrow indicates a background band in *S. cerevisiae* whole cell extracts. (C) GFP-tagged WT Dnf1, Dnf1[GA→QQ], Dnf1 N550S and Dnf1[Y618F] display similar localization patterns, polarizing to the budding daughter cell.

Next, we tested the expression of each of the strong NBD-PS selective Dnf1 variants. In each case, the expression level was similar to WT Dnf1, and unlikely to account for the differences in substrate specificity or activity (Figure 3-8B). The localization of GFP-labeled versions of Dnf1, Dnf1 [GA→QQ], Dnf1 N550S and Dnf1 [Y618F] were similar and again, unlikely

to account for the difference in substrate specificity at the plasma membrane (Figure 3-8C). Examination of NBD-PC and NBD-PS by thin-layer chromatography after incubation with cells confirmed no significant degradation (Figure 3-9) as previously reported (Kean, et al., 1993). In addition, these NBD-PS selective variants of Dnf1 maintained the Lem3 β-subunit requirement (Figure 3-10).

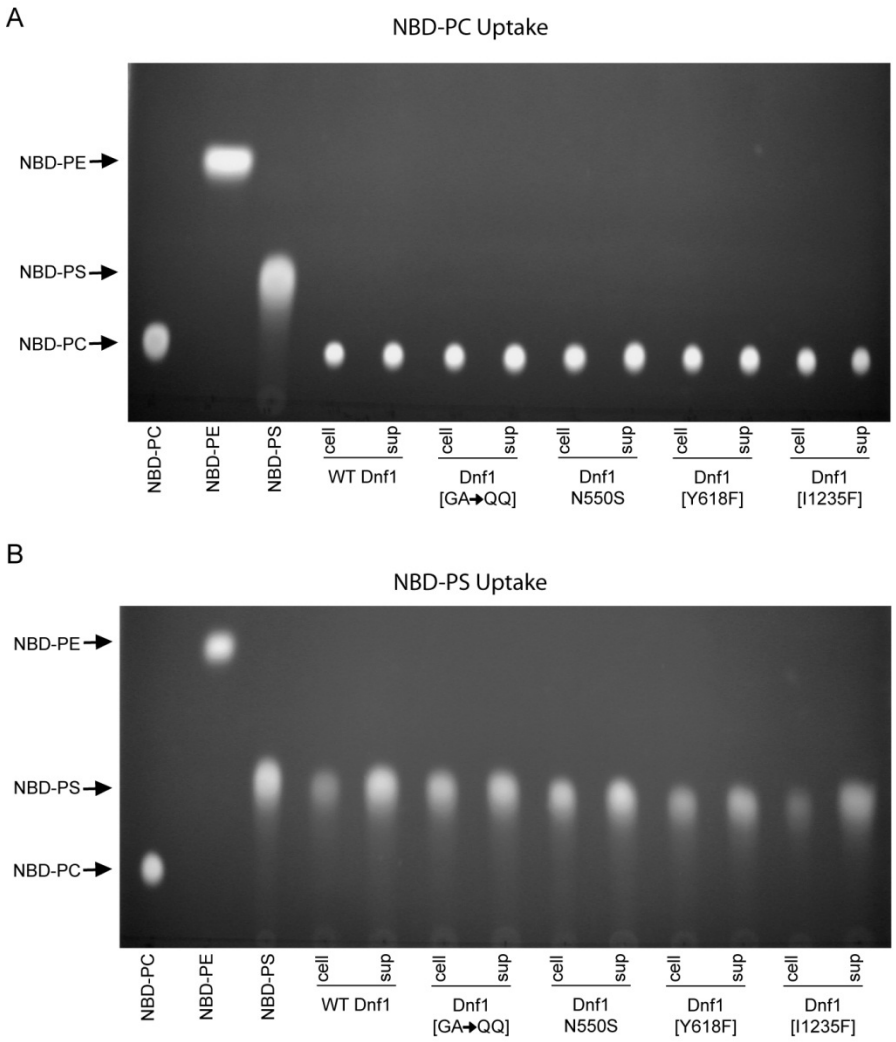

Figure 3-9. **NBD-PC and NBD-PS are not modified prior to uptake into *dnf1,2Δ* yeast.**
Mid-log yeast were incubated with NBD-PL at ~2µM for 60 min on ice to allow uptake into the yeast cells. The cells were pelleted, and the cell pellet and supernatant were each extracted with methanol:chloroform (2:1) to isolate the lipid component. Lipids were separated by thin layer chromatography and the mobility of extracted (A) NBD-PC and (B) NBD-PS were compared to NBD-PL standards. In the conditions used for the uptake assays, we observed no modification of the NBD-PL.

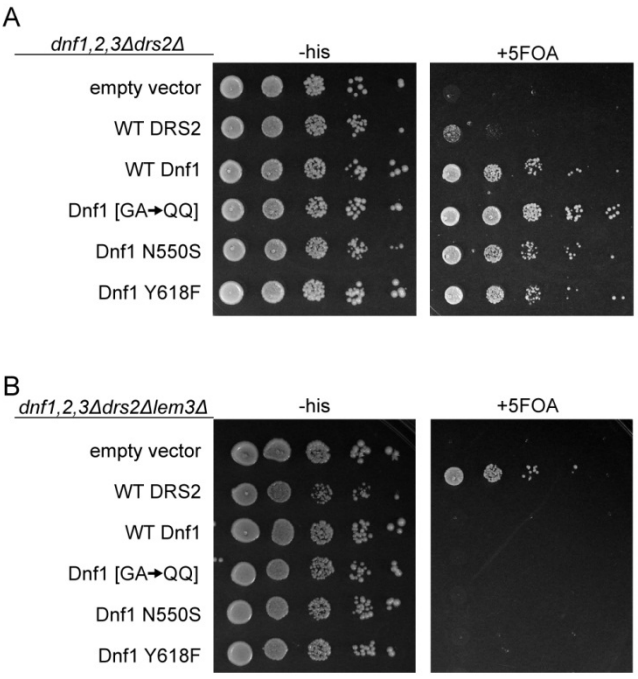

Figure 3-10. Key Dnf1 constructs allowing PS flip still require the β subunit, Lem3.
(A) Serial dilutions of *dnf1,2,3Δdrs2Δ +URA3-DRS2* strain expressing Dnf1 alleles were plated on synthetic medium (left) or synthetic medium containing 5-FOA (right), which is toxic to yeast expressing *URA3*. Growth on 5-FOA indicates the Dnf1 allele is capable of complementing the growth defect of the *dnf1,2,3Δdrs2Δ* strain in the absence of the covering *URA3-DRS2* plasmid. (B) Same as (A) except parental strain is *dnf1,2,3Δdrs2Δlem3Δ +URA3-DRS2*. Growth in this case indicates a Dnf1 allele is functional without *LEM3*.

Drs2 uses a similar two-gate mechanism for PS selection and transport

The presence of an Asn550 in TM3 of Dnf1 seems to prevent NBD-PS transport as several different mutations in this position cause enhanced NBD-PS uptake. Surprisingly, this Asn is conserved among yeast and mammalian P4-ATPases, including Drs2 (Asn445). We wondered what consequence the N445S mutation might have on Drs2 activity, by itself and in combination with F511Y (the proline + 4 mutation that abrogates PS recognition). Each single mutant and the double mutant complemented the cold sensitive growth defect of a *drs2Δ* strain (Figure 3-11A).

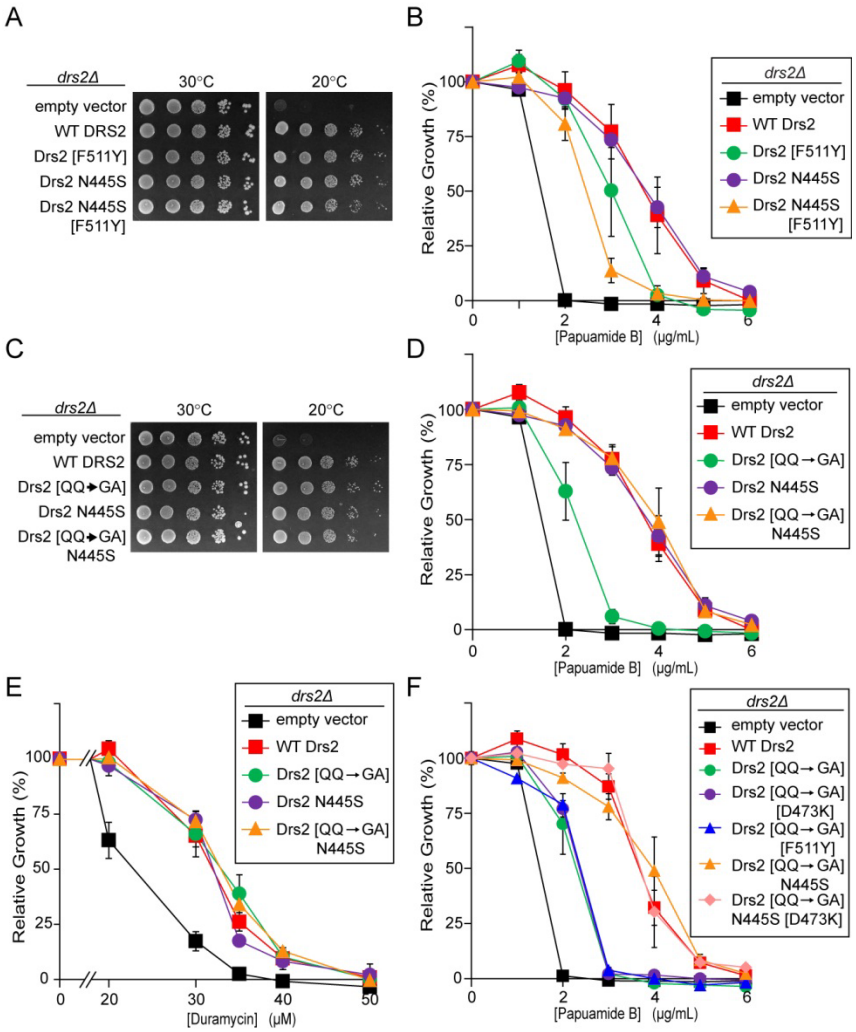

Figure 3-11. Control of Drs2 PS recognition by both cytosolic and exofacial residues
(A) *DRS2* alleles harboring cytosolic cluster (exit gate) mutations complement the cold sensitivity of a *drs2Δ* strain. (B) Influence of exit gate mutations on PS asymmetry measured by sensitivity to papuamide B. Relative to WT Drs2, Drs2[F511Y] displays a defect in PS asymmetry. Drs2 N445S maintains WT resistance to PapB while Drs2 N445S,[F511Y] slightly exacerbates the Drs2[F511Y] defect. (C) *DRS2* alleles harboring combination entry and exit gate mutations complement the cold sensitivity of a *drs2Δ* strain. (D) Relative to WT Drs2, Drs2[QQ→GA] display a major loss of PS asymmetry which can be restored by mutation of a cytosolic cluster residue (Drs2[QQ→GA],N445S) to permit increased PS recognition. (E) Influence of cytosolic cluster mutations on PE asymmetry measured by sensitivity to duramycin. Relative to WT Drs2 and *drs2Δ*, each mutant maintains normal PE asymmetry. Therefore, Drs2[QQ→GA] exhibits a specific defect in PS transport. (F) Combining the QQ→GA substitution with either D473K or F511Y does not disrupt PS asymmetry further or restore PS asymmetry. However, the exit gate mutation N445S can restore PS asymmetry to Drs2[QQ→GA] and Drs2[QQ→GA],[D473K]. Compare Drs2[QQ→GA],N445S to Drs2[QQ→GA] and Drs2[QQ→GA],[D473K],N445S to Drs2[QQ→GA],[D473K]. For all experiments, values are mean (± SEM).

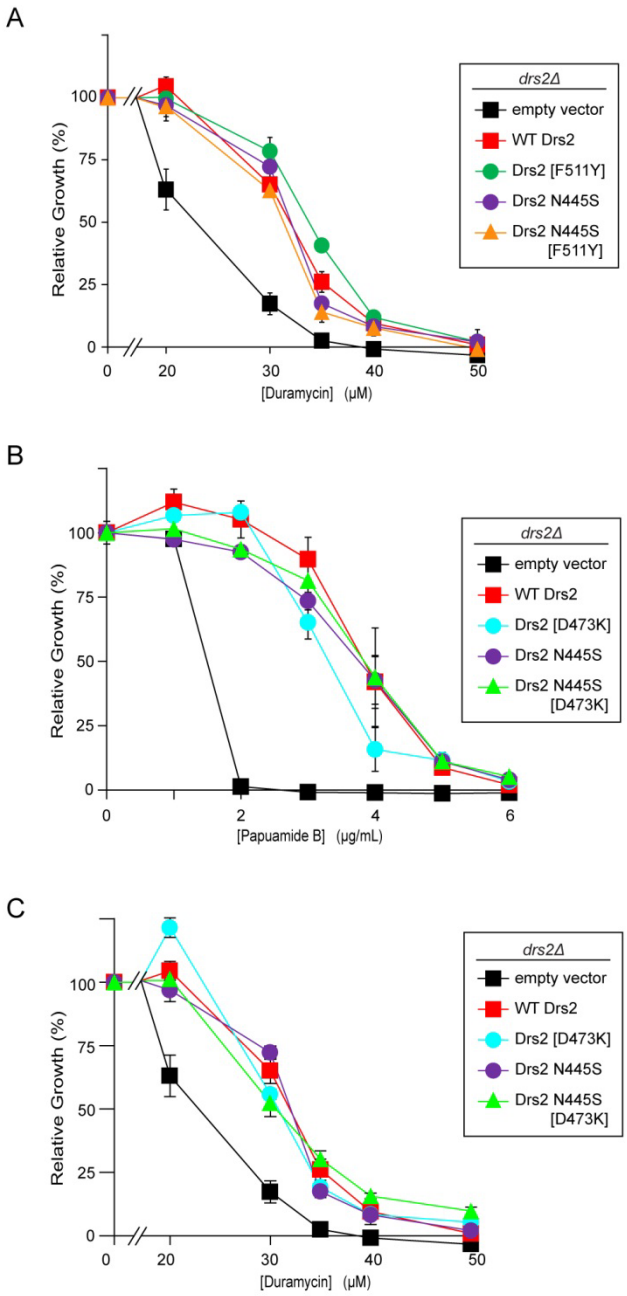

Figure 3-12. Drs2 entry and exit gate substitutions act similarly to reciprocal substitutions in Dnf1. (A) Drs2 exit gate substitutions maintain normal PE asymmetry. (B) The Drs2 entry gate substitution, D473K, is unable to maintain PS asymmetry as well and WT Drs2 or Drs2 N445S. Combining the entry and exit gate substitutions Drs2[D473K],N445S restores the PS asymmetry similarly to WT Drs2. The D473K substitution has a minor effect on PS specificity compared to the QQ→GA substitution, similar to the result with Dnf1 K578E (see Figure 3). (C) Drs2[D473K], Drs2 N445S and Drs2[D473K],F511Y maintain PE asymmetry similar to WT Drs2.

Deletion of *DRS2* also causes disruption of the plasma membrane asymmetry for PS and PE which can be monitored by sensitivity to pore-forming toxins that specifically interact with PS (Papuamide B, PapB) or PE (Duramycin) exposed on the outer leaflet (Navarro, et al., 1985; Parsons, et al., 2006). The single and double mutants were also tested for PapB sensitivity to measure the influence of the mutations on PS asymmetry. As previously reported, Drs2 [F511Y] displayed a PapB sensitivity intermediate between the empty vector (*drs2Δ*) control and cells containing WT Drs2 (Figure 3-11B)(Baldridge & Graham, 2012). The Drs2 N445S single mutant provided wild-type resistance to PapB and the double mutant (Drs2 N445S,[F511Y]) was slightly more sensitive to PapB than F511Y. Thus, N445S could not restore PS recognition to the F511Y exit gate mutant. To determine the influence of these mutations on PE asymmetry, we monitored resistance to duramycin, a toxin that specifically permeabilizes cells exposing PE. As previously reported, Drs2[F511Y] displayed no PE asymmetry loss relative to WT Drs2. And the same was true for Drs2 N445S and N445S,[F511Y] (Figure 3-12A).

The TM1 GA→QQ substitution in Dnf1 conferred gain-of-function NBD-PS recognition and so we tested if the reciprocal Drs2[QQ→GA] mutation would cause a loss of PS recognition. This entry gate mutant was functional *in vivo* as it complemented the *drs2Δ* cold sensitive growth defect (Figure 3-11C), but Drs2[QQ→GA] cells displayed a substantial loss of PS asymmetry (Figure 3-11D). Remarkably, the N445S mutation completely suppressed QQ→GA such that the Drs2[QQ→GA],N445S double mutant displayed wild-type resistance to PapB (Figure 3-11D). Importantly, each of these Drs2 mutants were capable of maintaining PE asymmetry similarly to WT Drs2 (Figure 3-11E), indicating the QQ→GA entry gate substitution specifically perturbs endogenous PS recognition by Drs2.

An LL3-4 entry gate mutation in Dnf1 (K578E) provided a marginal increase in NBD-PS uptake and the analogous Drs2 residue also carries a negative charge (Asp473). Therefore, we

tested the Drs2[D473K] substitution and consistently found a partial loss of PS asymmetry for this mutant. Again, N445S completely suppressed the loss of PS asymmetry caused by [D473K](Figure 3-12B). We then combined the two entry gate mutations (Drs2[QQ→GA][D473K]) and found they were not additive, the double mutant displayed the same PapB sensitivity as the QQ→GA mutant. Even in this context ([QQ→GA][D473K]), N445S could restore PS asymmetry to the triple mutant (Figure 3-11E). We would not expect the F511Y exit gate mutation to have this suppressive capacity as it causes loss of asymmetry; F511Y neither suppressed nor exacerbated the QQ→GA influence on PS asymmetry (Figure 3-11E). In sum, these data indicate the same relationship between entry gate and exit gate mutations in Drs2 and Dnf1. In each case, the exit gate Asn mutations in TM3 can allow PS transport even when entry gate residues are present that normally restrict PS transport.

DISCUSSION

A number of different proteins are thought to mediate the translocation of lipid across a membrane bilayer. However, very little is known about how these transporters recognize and flip their specific substrates. This issue is particularly interesting for P-type ATPases, for which the mechanism of ion recognition and transport is known in exquisite detail for P2-ATPases, but whether P4-ATPases use this canonical pathway or a non-canonical mechanism for phospholipid transport is a subject of debate.

Using an unbiased screening procedure, we identified two clusters of residues involved in phospholipid selection by P4-ATPases (Figure 3-13A). One cluster is located on the exofacial side of the membrane where phospholipid is initially selected and we propose this cluster forms an “entry gate” (Figure 3-13). The residues composing the entry gate are present on TM1, LL1-2,

TM2 and LL3-4, none of which correspond to residues in the canonical ion-binding site of the P2-ATPases. Within the entry gate, we have identified residues specifically involved in the PC preference of Dnf1 (Ile234, Phe235, Pro240, Gly241, Tyr575, Glu586, Phe587, Gly588, Ile590) and suppression of PS recognition (Gly230, Ala231, K578) (Figure 3-13A). Swapping the Gln237, Gln238 from TM1 in Drs2 for the analogous Gly230, Ala231 residues in Dnf1 (or Dnf1 Lys578 for Drs2 Asp473) conferred PS transport to Dnf1 and abrogated PS transport by Drs2 (Figure 3-11E and 3-12B). This is the first description of residues within TM1-2 and LL3-4 responsible for substrate selection by any P-type ATPase.

The second cluster of residues is located in TM3 and TM4 near the cytosolic side of the membrane and we propose this cluster forms an "exit gate" for the phospholipid (Figure 3-13). Within the exit gate, we identified residues responsible for PC preference (Ile545, Glu622) and suppression of PS transport by Dnf1 (Tyr618, Asn550, Val621, Glu622). Val621 and Glu622 are predicted to lie one turn of the helix above Tyr618 in TM4, all of which are in the vicinity of Asn550 in TM3. A specific Tyr→Phe mutation seems to be required at position 618 to confer NBD-PS activity to Dnf1, but surprisingly, several different substitutions at position 550 allow PS transport. A number of mutations were recovered in TM3 between the two gates, and it is probably significant that these mutations only reduce Dnf1 activity and line one face of the helix (Figure 3-13A), bookended by Asn571 (which is essential) and Asn550 (a specificity determinant).

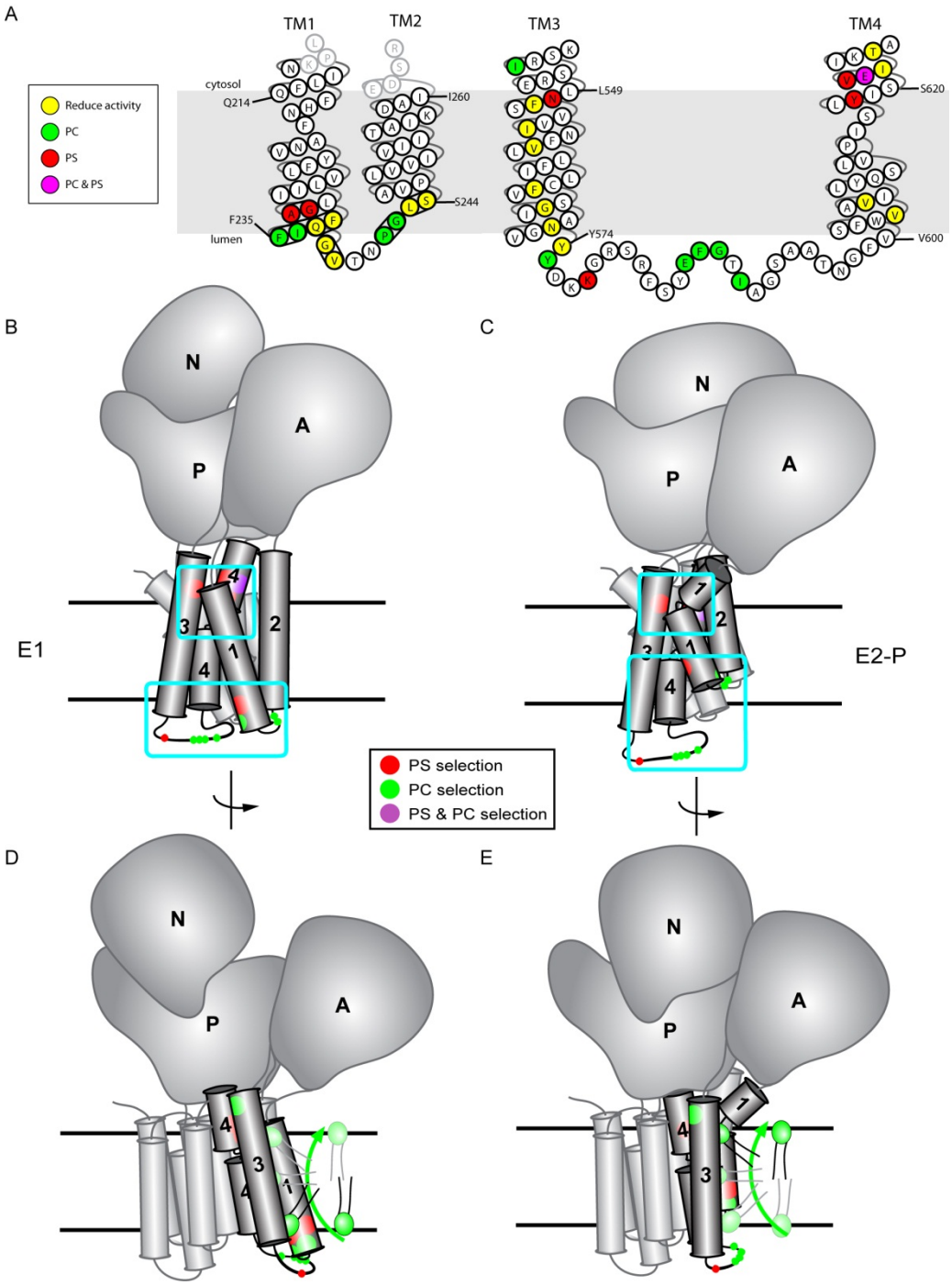

Figure 3-13 Residues affecting the phospholipid specificity of P4-ATPases cluster into two gates. (A) Topological diagram of Dnf1 TM1-2, 3-4 indicating positions of residues where mutations lead to: increased PS recognition (red), reduced PC recognition (green) or reduction of overall activity (yellow). These residues cluster around a phospholipid entry gate (exofacial membrane face) and an exit gate (cytosolic membrane face). (B) Dnf1 modeled on the E1 conformational state of SERCA1 (Toyoshima, et al., 2004) indicating relative positioning of residues involved in substrate specificity. The residues cluster into two gates where phospholipid is selected on each side of the membrane. Light blue boxes indicate the entry and exit gates; black lines denote the membrane boundaries; A, actuator domain; N, nucleotide-binding domain; P, phosphorylation

domain. (C) Dnf1 modeled on the E2-P conformational state of SERCA1 (Toyoshima, et al., 2004)highlighting the conformational changes in TM1-4 during the pumping cycle driven by transfer of phosphate from ATP to the P domain. (D and E) Proposed mechanism for phospholipid transport by P4-ATPases. Phospholipid is initially selected at the entry gate, perhaps when the pump is in the E1 conformation. Upon transfer of phosphate from ATP to the P domain to induce the E2 conformation, TM1-2 shift up dramatically in the membrane, feasibly providing the physical force the flip the phospholipid headgroup across the lipid bilayer and feed the substrate into the exit gate. Substrate would be released from the exit gate to the cytosolic leaflet in the E2 → E1 transition.

The recovery of many mutations that reduce PC transport without significantly altering PE transport is not surprising because the edelfosine screen was designed to identify residues involved in PC selection. An interesting conundrum is why the Asn550, V621A and K578E mutations allowing PS recognition were identified in edelfosine resistance screen. It is possible that strains expressing these mutants could be resistant to edelfosine because of the gain-of-function for PS transport created competition *in vivo* between endogenous PS and edelfosine for Dnf1. Regardless of the basis for edelfosine resistance, this screen illuminated additional residues involved in allowing PS recognition in Dnf1 and Drs2.

Whereas each of these TM3 and TM4 exit gate residues lie outside of the canonical binding site, we did recover a single mutation in TM6, I1235F, which enhances PS transport and corresponds to a canonical site residue (Asp800 in SERCA). There are several reasons we think the I1235F mutation is altering the function of the exit gate in a non-canonical pathway rather than perturbing binding of phospholipid substrate in the canonical site. The first is that I1235F increased overall activity of Dnf1 for all substrates and caused a partial loss of specificity for glycerophospholipid, unlike the other point mutations in TM1-4 that enhanced PS uptake with no significant increase in SM uptake including Dnf1[GA→QQ],N550S,[Y618F], which has an overall higher uptake activity but no increase in NBD-SM uptake. I1235 in TM6 is modeled very close to the TM4 exit gate residues and the enhanced SM uptake caused by I1235F is similar to

that previously observed with Dnf1[YIS→FVT], a triple mutation in the TM4 exit gate region (Baldridge & Graham, 2012). It is possible that altering the packing of the TM helices in this region perturbs recognition of the glycerol backbone of the substrate.

The second reason we believe our data support the non-canonical pathway has to do with the frequency of specificity-altering mutations recovered in the edelfosine screen. Within TM3-4, we assayed 26 point mutants (Figure 3-3 and 3-4) derived from random mutagenesis. Of these 26 mutants assayed, 10 exhibited a change of specificity (~40% of the mutants). Within TM5-6, we assayed 25 mutants in total (18 point mutations (Figure 3-6 and 3-7), 7 multiple mutations (Figure 3-7C)). Of these mutants assayed, only I1235F displayed a change in specificity (4%). This sample size should have identified at least 9-10 clones with altered specificity if the rate was similar to TM3-4 mutants (~40%). Our data indicate that TM5-6 residues are important for activity, because many of the mutations reduce activity without altering patterns of substrate recognition (Figure 3-6 and 3-7). In general, it seems most likely that the TM5-6 mutations that reduce activity are due to a defect in transducing the mechanics of phospholipid transport between the ATP-consuming cytosolic domains and substrate-selecting gates in TM1-4.

Finally, we note that a crystal structure of the Ca^{2+}-ATPase in the E2 conformation contains a PE molecule specifically bound in a cleft between TM1-4, in the region we describe as the exit gate (Figure 3-14) (PDB: 2AGV) (Obara, et al., 2005). For the Ca^{2+}-ATPase, PE likely enters and exits this binding site from the cytosolic leaflet as the pump transitions from E1→E2→E1 conformations. We suggest that this phospholipid binding site is conserved in the P4-ATPases as part of the exit gate, but the flippases evolved the ability to load this site with phospholipid selected from the exofacial leaflet using entry gate residues and expel the substrate to the cytosolic leaflet in the E2→E1 transition.

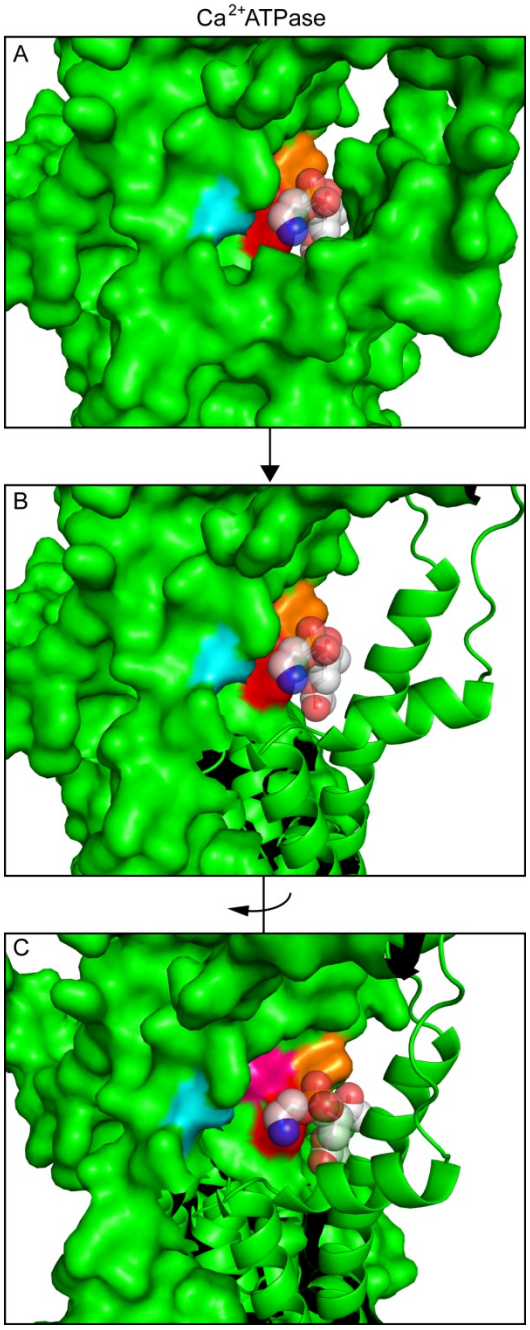

Figure 3-14. Phospholipid interaction with Ca^{2+} ATPase in E2 conformation.
(A-C) Ca^{2+} ATPase crystal structure with PE molecule co-crystallized. The equivalent residues contributing to phospholipid specificity in Dnf1 and Drs2 have been colored coded for reference. Color-coded residues on Ca^{2+} ATPase structure: Cyan-Asp254 (equivalent to Dnf1 Asn550, Drs2 Asn445), Red-Pro312 (Dnf1 Tyr618, Drs2 Phe511), Pink- Ile315 (Dnf1 Val621, Drs2 Val514) and Orange-Thr316 (Dnf1 Glu622, Drs2 Glu515). (PDB:2AGV)

The two gates appear to act in tandem to sequentially select substrate for transport. For mutations that enhance PS transport in Dnf1, we find that combining two exit gate mutations do not have an additive effect on transport. However, combining entry gate and exit gate mutations does have an additive effect. We interpret this observation to mean that phospholipid is imperfectly selected at each gate. Thus, an entry gate mutation in Dnf1 can allow PS transport even when the exit gate is tuned for PC and vice versa, but maximal PS transport requires residues at each gate that select for PS. The mechanistic coupling of the two gates seems to be conserved for Drs2. For example, the entry gate QQ→GA mutation causes a specific loss of PS asymmetry that can be restored by the N445S exit gate mutation. For Dnf1, N550S also allows PS transport when GA is present at the base of TM1.

Using the canonical ion-binding site for phospholipid transport seems unlikely given the positioning of residues within the entry and exit gates along TM1- 4. Based on the general location and cooperation of the substrate specificity determinants we have identified, we propose a two-gate mechanism for phospholipid flip. In our preferred model, phospholipid is initially selected at the entry gate in the E1-P state (Figure 3-13B and 3-13D). As the pump transitions from E1-P→E2-P, TM1-2 shifts up into the membrane, carrying the phospholipid near the exofacial side of the membrane and the exit gate (Figure 3-13C and 3-13E). The phospholipid is again selected at the exit gate prior to (or concurrently with) dephosphorylation (E2-P→E2) and release of substrate to the cytosolic leaflet (E2→E1). Substrate is required for dephosphorylation of the P4-ATPase (Coleman, et al., 2012; Ding, et al., 2000; Paterson et al., 2006); probably because the phospholipid must bind at the exit gate to induce movement of the actuator domain to dephosphorylate the pump.

These studies provide important new mechanistic insight into how integral membrane proteins recognize and select phospholipid substrate within a membrane environment. It

remains to be seen whether a similar two-gate selection mechanism is used by other lipid transporters (such as the ABC transporter family) or if this represents a unique mechanism for the P4-ATPases.

MATERIALS AND METHODS

Strains and culture

Escherichia coli strain DH5α was used for molecular cloning. Each plasmid used in this study is listed in Table A5. Strains used in this study are listed in Table A4. Yeast were grown in standard rich medium (YPD) or synthetic minimal glucose medium (SD). Yeast were transformed using the lithium acetate method (R.D. Gietz & Woods, 2006). To test complementation, 50,000 cells were spotted with 10-fold serial dilutions onto SD or SD + 5-FOA. Plates were grown at 20°C or 30°C for 3-4 days before imaging.

Edelfosine resistance screen

To generate random mutations we used procedures described previously (Baldridge & Graham, 2012). We co-transformed ZHY704 with mutagenized PCR products and pRS313-DNF1 gapped with restriction enzymes MfeI and NruI (or for TM5-6 we used pRS313-dnf1 w/SfoI site gapped with SfoI) to allow for gap repair through homologous recombination. The transformations were plated onto synthetic dropout plates, grown for 3 days and colonies were picked into 96 well plates and spotted onto synthetic dropout plates containing 20µg/mL edelfosine or 5-FOA. We sequenced *dnf1** in strains which grew strongly on both edelfosine and 5-FOA.

Viability assay

To test for Papuamide B and duramycin sensitivity, mid-log phase yeast were seeded in 96 well plates at 0.1 OD_{600}/mL +/- drug. Plates were incubated at 30°C for 20 hours and the OD_{600}/mL was measured with a Multimode Plate Reader Synergy HT (Bio-Tek, Winooski, VT). Relative growth was based upon mock-treated cells in the assay.

Fluorescence microscopy

Images were collected with an Axioplan microscope (Carl Zeiss, Thornwood, NY) using a Hamamatsu CCD camera and MetaMorph software. To observe GFP-tagged proteins, cells were grown to mid-log phase, pelleted, and resuspended in 10mM Tris-HCl, pH 7.4, 2% glucose (wt/vol). An aliquot of cells was spread onto slides, and visualized using a GFP filter set.

Cell extracts and western blotting

Yeast expressing N-terminal 3xFLAG tagged Dnf1 were grown in YPD to mid-log phase and harvested in SDS/urea sample buffer (40 mM Tris–HCl (pH 6.8), 8M urea, 0.1mM ethylenediaminetetraacetic acid, 1% 2-mercaptoethanol, 5% SDS and 0.25% bromophenol blue). Cell lysate from 0.2OD was separated by SDS-PAGE, transferred to PVDF membrane, and blotted with anti-FLAG M2 antibody (Sigma-Aldrich).

NBD-lipid uptake

Lipid uptake was performed essentially as described previously (Baldridge & Graham, 2012). Briefly, overnight cultures were subcultured to 0.15 OD/mL and allowed to grow to early-mid log phase. 500 µl of cells were harvested, resuspended in ice-cold SD media containing 2 µg/ml NBD-lipid (~2.5µM), and incubated on ice for 30 min. Cells were washed twice with SA media (SD media + 2% sorbitol (wt/vol), + 20mM NaN_3) + 4% BSA (wt/vol), once with SA media, and resuspended in SA media prior to analysis by flow cytometry.

Flow cytometry

Flow cytometry was performed with a BD LSRII-3 laser (BD Biosciences) using BD FACSDiva v6.1.3. NBD-lipid uptake was measured with the FITC filter set (530/30 bandpass with a 525 longpass). Immediately prior to analysis, propidium iodide was added at a final concentration of 5μM. At least ten thousand events were analyzed using forward/side scatter to identify single cells and propidium iodide fluorescence to exclude dead cells.

Data analysis

Within each NBD-PL uptake experiment, at least three independently isolated transformants harboring the same construct were assayed as previously described (Baldridge & Graham, 2012). The mean of these values from at least three separate experiments were reported as ± SEM. Uptake of NBD-PL for a *dnf1,2Δ* strain with an empty vector was subtracted and NBD-PC uptake by WT Dnf1 was used to normalize the data. Each value is reported relative to WT Dnf1 PC uptake at 30 min. Substrate preference ratios were determined by the dividing NBD-PE or NBD-PS uptake values by the NBD-PC uptake value for each independent replicate ($n \geq 9$). The mean of each substrate preference ratio is reported ± SEM. All Dnf1 alleles showing substrate preference ratio falling outside of the 15% confidence interval with no overlap of the error bars are significantly different ($p<0.05$) from WT Dnf1 determined by student's T-test. For drug-sensitivity assays, at least two independently-isolated transformants were assayed in two separate experiments and reported as mean ± SEM.

Reagents

Papuamide B was a gift from Raymond Andersen (University of British Columbia). Duramycin was purchased from Sigma Aldrich (St. Louis, MO), edelfosine from Tocris Biosciences

(Bristol, United Kingdom), 5-fluoroorotic acid (5-FOA) from Zymo Research (Irvine, CA) and all lipids from Avanti Polar Lipids, Inc. (Alabaster, AL).

Cloning and mutagenesis

Dnf1[Drs2] chimeras were generated by either overlap extension(for point mutations (6) or gene splicing overlap extension (for >4 amino acid changes) (7). PCR products from the overlap extension were cloned into SphI-MfeI sites in pRS313-Dnf1. Drs2 mutations were generated by overlap extension and cloned into AgeI-NcoI sites in pRS313-Drs2. To generate random mutations targeted to TM3-4 of Dnf1, we used pRS313-DNF1 as template with primers Dnf1(forw)@1500 (5'-TACTATTAATAACGTTCTGCTTCGTGG) and Dnf1(rev)@1987 (5'-ATTCCACTTGACCTAAATCGTCAG) using PCR conditions described previously (8). For mutations targeted to TM5-6 of Dnf1, we used Dnf1(forw)@3400 (5'-GACGTCGCCATGATTCAATC)and Dnf1(rev)@3853 (5'-AACAGATAATAGACTGATATAATCCGTCCA).

To prepare a linearized plasmid for recombination in the TM5-6 region, we first used overlap extension PCR to generate a 4.2kb fragment containing a SfoI site within the TM5-6 region (A3603G, T3604C, T3605C). We cloned this PCR product into the MfeI and BseRI restriction sites of pRS313-DNF1 to created pRS313-Dnf1(w/SfoI site). The pRS416-GFP-Dnf1 alleles were generated by replacing the WT Dnf1 sequence through standard cloning using SphI and BseRI restriction sites from the pRS313-Dnf1 mutant plasmids. N-terminally 3x-Flag tagged Dnf1 alleles were generated by standard cloning replacing the WT Dnf1 sequence between the SphI-MfeI (1.7kb) restriction sites in the pRS313-Flag3-Dnf1 plasmid sites with the SphI-Mfe fragment from a pRS313-Dnf1 mutant allele.

Lipid extraction and TLC analysis

Lipids were extracted using a modified Bligh and Dyer method (9). 1 OD mid-log phase yeast incubated with 2µM NBD-PL for 60 min were resuspended in 0.5mL SD media or the supernatant containing NBD-PL un-incorporated were mixed with 2mL methanol:chloroform (2:1). The mixture was centrifuged at 5000 x g to clear cellular debris. The supernatant was transferred to a tube containing 1.5mL 20mM citric acid and 0.5mL chloroform. The mixture was centrifuged at 5000 x g for 5 min, the aqueous phase was removed and the organic phase was evaporated under a nitrogen stream. Lipids were resuspended in methanol:chloroform (2:1) and spotted on silica gel 60F plates from EMD Chemicals (Billerica, MA). Lipids were separated by thin layer chromatography using chloroform:methanol:acetic acid:water (50:37.5:3.5:2) as the mobile phase. Mobility of the extracted lipids were compared to NBD-PL standards for (A) NBD-PC and (B) NBD-PS.

ACKNOWLEDGEMENTS

These studies were supported by NIH grant GM62367 to T.R.G. and the Cellular and Molecular Microbiology Training Program T32AI007611-11, which supported R.D.B.. The VMC Flow Cytometry Shared Resource is supported by the Vanderbilt Ingram Cancer Center (P30 CA68485) and the Vanderbilt Digestive Disease Research Center (DK058404).

CHAPTER IV

A ROLE FOR PHOSPHATIDYLSERINE FLIP IN VESICLE-MEDIATED PROTEIN TRANSPORT

INTRODUCTION

A defining feature of eukaryotes is membrane-enclosed organelles that serve a multitude of functions. Defined compartments present a challenge for coordinating separate steps in biochemical pathways carried out in distinct compartments, such as such as lipid synthesis, glycosylation and other post-translational modifications. One common mechanism for exchange of material between organelles of the secretory and endocytic pathways is the formation of transport vesicles that carry cargo in either the anterograde or retrograde direction. Formation of vesicles generally requires cargo to be selected by adaptor proteins and locally concentrated to interact with coat proteins. Local generation of curvature to bud the vesicle can be provided by small GTPases, coats, or other mechanisms (Graham & Kozlov, 2010). Many of these processes originate from the trans-Golgi network (TGN) including two classes of secretory vesicles containing different cargos but each destined for the plasma membrane (PM). Formation of anterograde vesicles carrying proteins from the TGN to early endosomes requires Arf, AP-1 and clathrin. Targeting vesicles to the late endosome (LE) involves Arf, GGA and clathrin and direct transport to the vacuole uses Arf and AP-3. It appears that there are two retrograde pathways from the endosome back to the TGN, one mediated by AP-1/clathrin and the second requiring the sorting nexin Snx4 and F-box protein Rcy1. Traffic can also return to the TGN from the late endosome which is facilitated by the retromer complex (Muthusamy, Natarajan, et al., 2009).

P4-ATPases are essential for viability and one of the founding members of this family, Drs2, was identified in yeast (Hua, et al., 2002; Tang, et al., 1996). Drs2 is important for many trafficking events from the trans-Golgi-network (TGN) including formation of dense-class secretory vesicles and bidirectional trafficking between the TGN and early endosome in both the AP-1/clathrin and Snx4/Rcy1 pathways. Both retrograde pathways require Drs2. Interestingly, Dnf1 cannot support these pathways in the absence of Drs2, while Drs2 and Dnf1 seem to act redundantly in other anterograde pathways departing the TGN mediated by the clathrin adaptors AP-3 or GGA proteins. Drs2 and its mammalian counterparts Atp8a1/Atp8a2 are "flippases" which uses the energy from ATP hydrolysis to catalyze "flip" of phosphatidylserine (PS) and phosphatidylethanolamine (PE) within the Golgi-endosomal system (although PS seems to be the preferred substrate). Although they are closely related to Drs2, Dnf1 and Dnf2 differ in their substrate specificity and localization. The preferred substrate of yeast P4-ATPases Dnf1 and Dnf2 is phosphatidylcholine (PC) and PE. We have recently described a series of residues involved in the substrate specificity of P4-ATPases that implicated a novel transport mechanism for a P-type ATPase using two gates to select phospholipid on opposing membrane faces (Chapters II and III)(Baldridge & Graham, 2012, 2013).

Drs2 is essential for cold-resistant growth in *S. cerevisiae* and its activity is regulated by PI4P, Gea2, Arl1 and OSH4/KES1 (Muthusamy et al., 2009; Natarajan et al., 2009; Tsai, Hsu, Liu, Chen, & Lee, 2013). However, yeast remain viable in the complete absence of PS caused by deletion of the PS synthase gene (*CHO1*) and in the absence of PS, *DRS2* is still required for growth at 20°C (K. Atkinson, Fogel, & Henry, 1980; Natarajan, et al., 2004). As such, PS is not an essential substrate for Drs2, and a definitive role for PS is unclear in the trafficking pathways. Several links between PS and vesicular traffic exist. The mammalian protein EVT-2 is partially recruited through its PS-specific PH domain to recycling endosomes where it potentially

functions as a cargo adaptor (based on a physical interaction with the cargo protein GP73) for recycling endosome→TGN traffic (Uchida et al., 2011). PS depletion in a CHO cell line impairs retrograde traffic of the cargo protein TGN38 (Lee et al., 2012). In yeast, partial depletion of PS in the absence of complex sphingolipids creates a defect in the retrograde trafficking pathway (EE→TGN) (Tani & Kuge, 2012). We have previously hypothesized that P4-ATPases contribute to membrane trafficking through a combination of specific lipid exposure and curvature generated through the unidirectional flip of phospholipid (Graham, 2004). However, no direct evidence exists for a role of specific lipid translocation in vesicular traffic.

Here, we describe Dnf1 variants that are capable of flipping endogenous, unlabeled PS. These new substitutions correspond to the analogous residues in the PS flippases Atp8a1/Atp8a2 and help define a part of phospholipid substrate binding sites. Surprisingly, Dnf1 variants that are able to flip PS and restore the PS asymmetry to a *drs2Δ* mutant are also able to effectively replace DRS2 function in protein transport. In particular, Dnf1 variants that flip endogenous PS at the appropriate locations support specific anterograde and retrograde pathways between the TGN and early endosomes. Drs2 variants deficient in endogenous PS flip, while retaining the ability to flip PE, cannot support these trafficking routes.

RESULTS

Dnf1 N550S flips endogenous PS

Deletion of *DRS2* disrupts plasma membrane asymmetry for PS and PE. Phospholipid membrane asymmetry can be monitored by sensitivity to pore-forming toxins that specifically interact with either PE (duramycin) or PS (Papuamide B, PapB). We previously reported WT Dnf1 and Dnf1[Y618F] were unable to restore the phospholipid asymmetry of a *drs2Δ* strain even though Dnf1[Y618F] was capable of NBD-PS transport. Importantly, the reciprocal change in

Drs2 specifically reduced the ability of this pump to flip endogenous PS, validating the use of NBD-PL as a substrate substitute (Baldridge & Graham, 2012). We tested the other Dnf1 constructs reported to transport NBD-PS (Dnf1[GA→QQ] and Dnf1 N550S) for the ability to restore PS asymmetry (Baldridge & Graham, 2013). Like Dnf1 [Y618F], Dnf1[GA→QQ] was unable to restore the PS asymmetry of the *drs2Δ* strain (Figure 4-1A). Incredibly, Dnf1 N550S was unique among the Dnf1 constructs reported to recognize NBD-PS in its ability to restore the PS asymmetry of a *drs2Δ* strain (Figure 4-1A). Even when overexpressed, neither WT Dnf1 nor Dnf1 [Y618F] were able to restore the PS asymmetry defect of *drs2Δ* as well as Dnf1 N550S (Figure 4-1C). This suggested that Dnf1[Y618F] was unable to transport endogenous PS, although it was capable of NBD-PS transport.

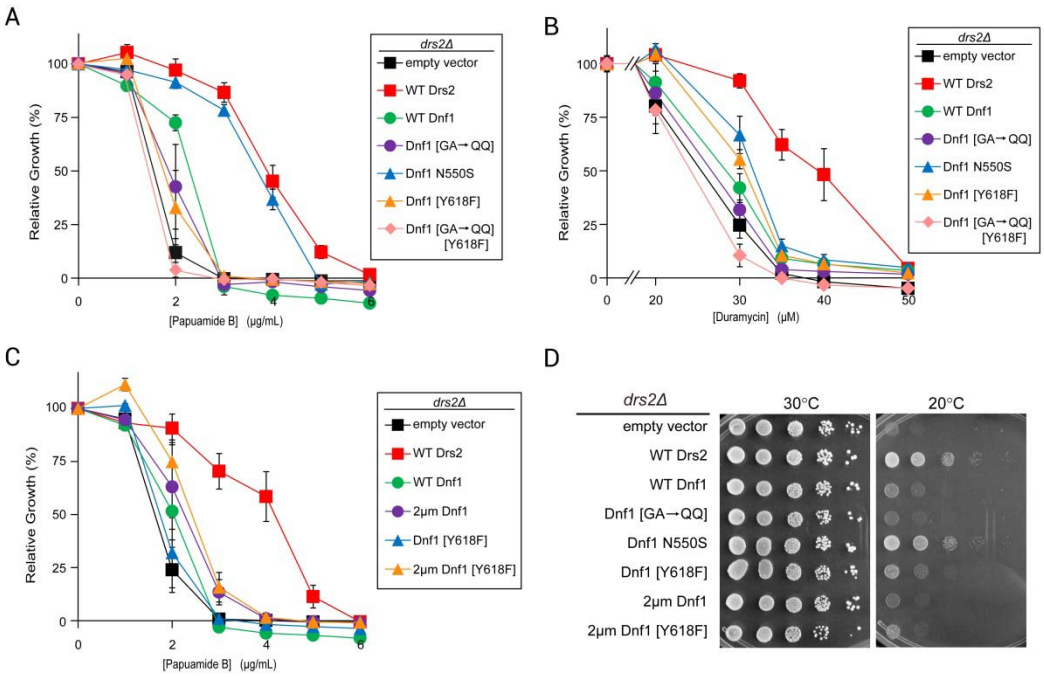

Figure 4-1. Dnf1 N550S suppresses *drs2Δ* PS asymmetry and cold-sensitive growth. Dnf1 N550S is uniquely capable of restoring plasma membrane in *drs2Δ* better than WT Dnf1 for PS asymmetry (A), but not PE asymmetry (B). Overexpressing WT Dnf1 a Dnf1 Y618F provide minor suppression of the PS asymmetry defect. Dnf1 N550S suppresses cold-sensitive growth better than WT Dnf1 and other Dnf1 NBD-PS transporting alleles.

Because Drs2 is required for growth at 20°C, we also tested the ability of the Dnf1 NBD-PS transporting alleles to suppress the cold-sensitive growth defect. Again, only Dnf1 N550S was capable of suppressing the cold sensitivity (Figure 4-1D). The localization patterns and expression levels of these variants were similar, so unlikely to account for the observed phenotypic differences (Baldridge & Graham, 2013). We wondered if the ability to flip endogenous PS *in vivo* allowed Dnf1 N550S to suppress the cold sensitivity of *drs2Δ*.

Dnf1 suppressors of Drs2 function

Previously, we used an extensive screen targeting TM3-4 in Dnf1 and identified several residues within this region involved in NBD-PS selection (Baldridge & Graham, 2013). The observation that Dnf1-N550S was uniquely capable of recognizing endogenous PS and suppressing *drs2Δ* cold-sensitive growth, suggested that a screen for dnf1 alleles that suppress *drs2Δ* cold-sensitive growth might identify additional changes allowing Dnf1 to flip endogenous PS. Mutagenesis was targeted to TM1-2 and about 500 *dnf1* mutants (out of 5000 transformants) were recovered that supported growth of a *dnf1,2,3Δdrs2Δ* strain at 20°C. We selected 20% of the largest colonies, picked these into liquid culture and grew the strains at 20°C. We recovered 25 strains which grew similarly to a *dnf1,2,3Δdrs2Δ* harboring WT Drs2 at 20°C. From these strains we sequenced the Dnf1 constructs, recovering 19 Dnf1 alleles with a single amino acid substitution. There were four positions at which we recovered multiple alleles encoding the same amino acid substitution: F213S, A244V, T254A, D258E. Except for A244V, these *dnf1* suppressor alleles each arose independently as the codons recovered were different.

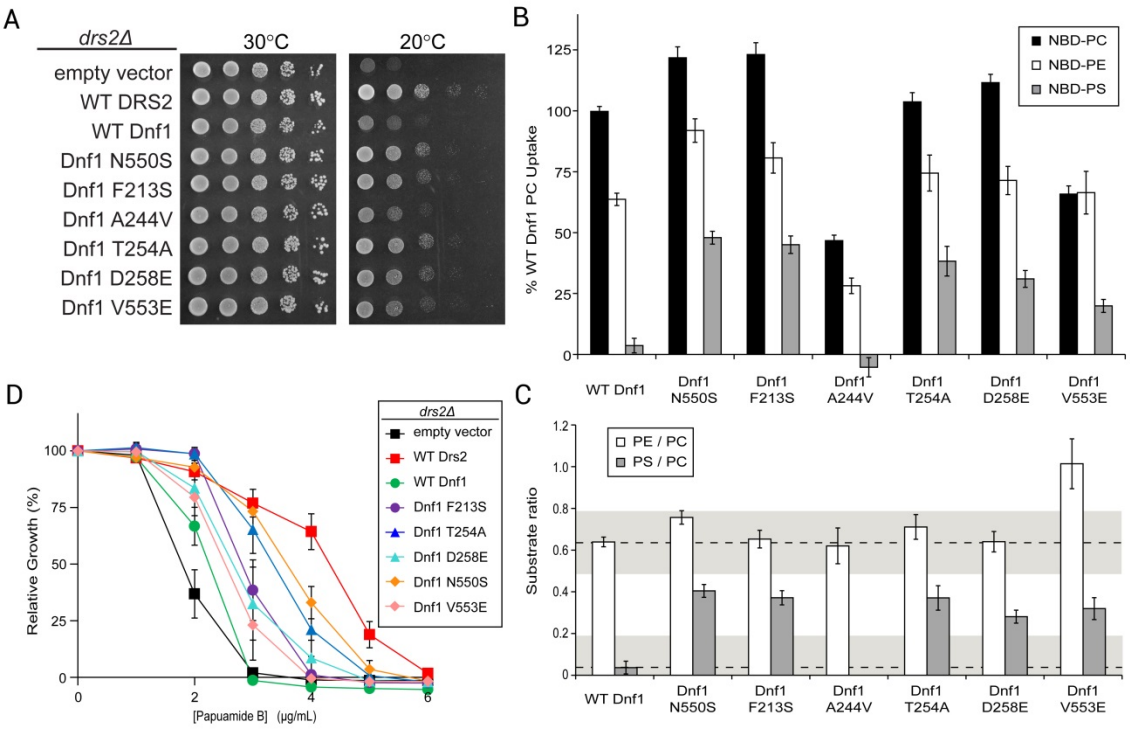

Figure 4-2. Dnf1 suppressors of *drs2Δ* cold-sensitive growth transport PS. (A) Dnf1 suppressors of *drs2Δ* recovered from the screen. (B) Each of the new variant confer NBD-PS uptake and changes in substrate specificity (C). (D) Dnf1 suppressors of cold-sensitive growth also restore PS asymmetry in a *drs2Δ*.

We next transformed these *dnf1* alleles into a *drs2Δ* strain to determine if the suppression was plasmid-linked or extragenic (Figure 4-2A). In fact, suppression of cold sensitivity was not plasmid-linked for Dnf1 A244V. Each of the other alleles did suppress the cold-sensitivity of a *drs2Δ* strain although to varying degrees. We then assayed the NBD-PL uptake activity for each of the new *dnf1* alleles in a *dnf1,2Δ* background. With the exception of the Dnf1 A244V, we observed an increase in the NBD-PS uptake for each Dnf1 mutant. Because Dnf1 N550S was capable of (1) flipping NBD-PS (Baldridge & Graham, 2013), (2) suppressing the *drs2Δ* cold-sensitivity (Figure 4-1D) and (3) flipping endogenous PS (Figure 4-1A), while Dnf1[Y618F] could only flip NBD-PS; we suspected the new Dnf1 cold-sensitive suppressor variants would also flip endogenous PS. In fact, we recovered a range of PapB resistance with

the strongest being the original N550S, closely followed by T254A (Figure 4-2D). Dnf1 F213S and D258E provided greater PapB resistance than WT Dnf1, but not as strong as T254A. Finally, V553E seemed unable to restore PS asymmetry better than WT Dnf1.

Recognition of mono vs. di-acylated phospholipid.

Each of these *dnf1* mutants were competent for NBD-PS uptake, but displayed varying resistance to PapB. We speculated that Dnf1 N550S and Dnf1 T254A were capable of recognizing endogenous, unlabeled PS while Dnf1 Y618F and Dnf1[GA→QQ] were not. To test this possibility we made use of GFP-Lact-C2 a probe that binds specifically to PS (Fairn, Hermansson, Somerharju, & Grinstein, 2011). *CHO1* (*PSS1*) encodes the phosphatidylserine synthase in *S. cerevisiae* and *cho1Δ* mutants completely lack PS (K. Atkinson, et al., 1980; K. D. Atkinson et al., 1980). In *cho1Δ*, the GFP-Lact-C2 is primarily cytosolic; when this strain is supplemented with lyso-PS the GFP-Lact-C2 returns to PM localization as this substrate is flipped to the cytosolic leaflet (Fairn, et al., 2011).

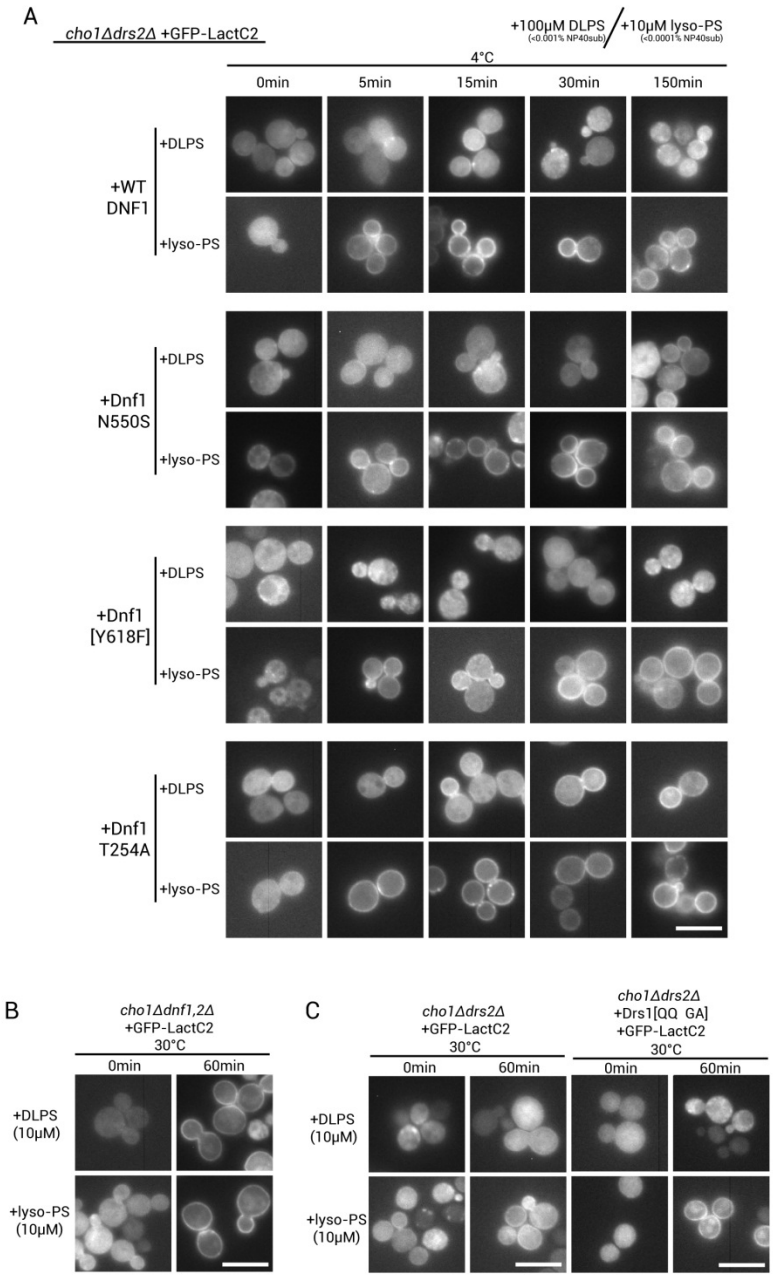

Figure 4-3. Dnf1 suppressors of *drs2Δ* flip di-acyl PS but WT Dnf1 does not. (A) In *cho1Δdrs2Δ* cells Dnf1 N550S and Dnf1 T254A can flip di-acyl PS to recruit GFP-LactC2 to the plasma membrane but WT Dnf1 and Dnf1[Y618F] cannot. (B, C) Drs2 mediates transport of DLPS in the endosomal system to recruit GFP-LactC2 but the PS-deficient Drs2[QQ→GA] cannot.

Using a *cho1Δdrs2Δ* strain, lyso-PS was rapidly flipped across the plasma membrane at 4°C (Figure 4-3A). This flip is partially mediated by Dnf1 and Dnf2 even though Dnf1 recognizes NBD-PS poorly. The low temperature is sufficient to block endocytosis and reduce the activity of

the floppases (Kean, et al., 1993). After 30 minutes of incubation with a *cho1Δ dnf1,2Δ* strain, lyso-PS crossed the membrane enough to recruit the GFP-Lact-C2, but it is at least 6 fold slower than with Dnf1 and Dnf2 present (Figure 4-4). This is consistent with a previous report suggesting yeast cells have another undefined transporter at the plasma membrane capable of taking up NBD-PS or lyso-PS (Stevens, et al., 2008). We tested whether WT Dnf1, Dnf1 N550S, Dnf1[Y618F] or Dnf1 T254A were capable of transporting dually-acylated PS (dilauryl-phosphatidylserine, DLPS). Consistent with the ability to restore plasma membrane PS asymmetry, DLPS was flipped into the cell by Dnf1 N550S and Dnf1 T254A but not by WT Dnf1 and Dnf1[Y618F] (Figure 4-3A). This suggested Dnf1 N550S and T254A were able to restore plasma membrane asymmetry in *drs2Δ* because they could facilitate transport of the dually-acylated PS, but WT Dnf1 and Dnf1[Y618F] could not. In the presence of each Dnf1 variant the lyso-PS was quickly taken up across the plasma membrane.

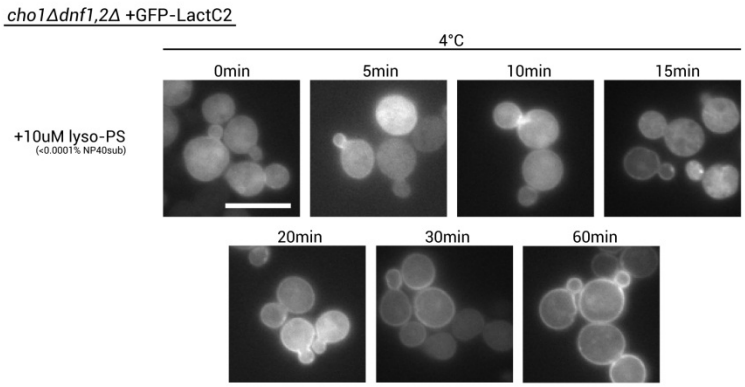

Figure 4-4. Dnf1,2 facilitate rapid uptake of lysoPS monitored by GFP-LactC2, but are not required.

We next performed similar experiments at 30°C, a condition which permits endocytosis, allowing the lyso-PS or DLPS to enter the lumenal leaflet of the Golgi-endosomal system. In a *cho1Δdnf1,2Δ*, after 1 hour at 30°C, both the lyso-PS and DLPS can recruit GFP-Lact-C2 to the plasma membrane (Figure 4-3B). We suspected this may be due to the lipid being flipped once it

reached Drs2 in the Golgi or endosome. To test this possibility, we looked at GFP-Lact-C2 localization in a *cho1Δdrs2Δ* supplemented with either lysoPS or DLPS at 30°C. In the absence of Drs2, or in the presence of Drs2[QQ→GA] (strongly deficient for PS recognition), we observed no recruitment of GFP-Lact-C2 to the PM (Figure 4-3C). Thus it appears the ability to restore PM asymmetry in a *drs2Δ* strain is consistent with the ability to flip dually-acylated phosphatidylserine at the level of the TGN-endosomal system.

PS flip is important for anterograde traffic

Drs2 plays a wide range of roles in vesicular-mediated protein trafficking. These roles partially overlap with Dnf1, so we sought to determine if the ability to flip endogenous PS and suppress the cold sensitivity is linked to trafficking phenotypes.

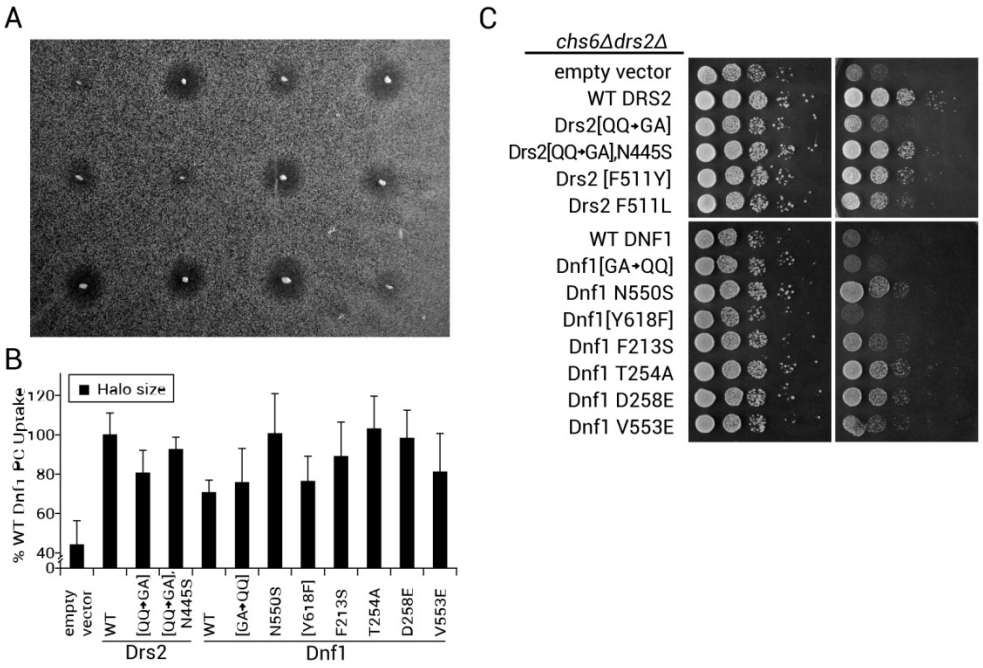

Figure 4-5. Dnf1 suppressors of *drs2Δ* cold-sensitivity suppress anterograde trafficking defects. (A) Halo formation of a matα supersensitive strain in response to *drs2Δ* cells expressing Dnf1 and Drs2 variants. All spots are *drs2Δ* Matα (ZHY615M2D). From left to right (Row 1:empty vector, WT DRS2, Drs2[QQ→GA], Drs2[QQ→GA],N445S. Row 2: WT Dnf1, Dnf1[GA→QQ], Dnf1 N550S, Dnf1[Y618F]. Row 3: Dnf1 F213S, Dnf1 T254A, Dnf1 D258E, Dnf1 V553E). (B) Mean halo size compared to cells expressing WT Drs2. (C) Growth on YPD (left) or YPD + 100µg/mL calcofluor white.

Drs2 is a facilitator and cargo for the AP-1 pathway for TGN→EE and EE→TGN trafficking. This pathway can be queried using a cargo protein, Chs3 (Valdivia, et al., 2002). Chs3 deposits chitin at the cell wall (Shaw, et al., 1991) and is retained intracellularly, trafficking within the Golgi-endosomal system in the AP-1 pathway throughout most of the cell cycle. Its trafficking to the PM during bud emergence is mediated by exomer (including Chs6) in a cell cycle dependent process (Ziman, Chuang, Tsung, Hamamoto, & Schekman, 1998). In a *chs6Δ* strain, Chs3 is retained intracellularly, and is unable to deposit chitin in the cell wall so it is resistant to calcofluor white (CW). A double knockout strain *chs6Δdrs2Δ* restores sensitivity to CW, because the AP-1 pathway is disrupted, causing Chs3 to move to PM constitutively (K. Liu, et al., 2008). As previously reported, *chs6Δdrs2Δ* expressing WT Drs2 is resistant to CW (Figure 4-5C)(K. Liu, et al., 2008). If the Dnf1/Drs2 mutants also cause CW resistance, they are restoring trafficking within the AP-1 pathway. Interestingly, Drs2[QQ→GA] was unable to restore CW resistance, indicating the AP-1 trafficking route is not supported (Figure 4-5C). In the presence of Drs2[QQ→GA], N445S a variant capable of PS transport, we observed CW resistance indicating AP-1 trafficking was restored in this mutant. Drs2[F511Y] and Drs2 F511L have partial defects in ability to flip PS, and likewise display slightly increased sensitivity to CW, suggesting they do not support AP-1 trafficking as well as WT Drs2. As previously reported, *cho1Δ* is hypersensitive to CW (Rockwell, Wolfger, Kuchler, & Thorner, 2009). This is consistent with PS being important to support the AP-1 pathway. WT Dnf1, Dnf1[GA→QQ], and Dnf1[Y618F] were incapable of supporting AP-1 trafficking. By contrast, Dnf1 N550S and Dnf1 T254A both provided increased resistance to CW suggesting they replaced Drs2 function in the AP-1 pathway. Dnf1 D258E also increased resistance to CW, and to a lesser extent Dnf1 F213S and Dnf1 V553E. Resistance to CW roughly aligned with the ability to restore PapB resistance and therefore PS asymmetry (compare Figure 4-2D to 4-5C). With Dnf1, like with Drs2, the ability to flip endogenous PS

correlates with support of AP-1 trafficking. The ability to suppress the anterograde trafficking defects (Figure 4-5) correlated with Dnf1 suppression of *drs2Δ* cold-sensitivity (Figures 1C and 2A) and with the ability to flip endogenous PS (Figures 4-1A and 4-2D).

PS flip is required for retrograde traffic

AP-1 functions in both anterograde TGN→EE and retrograde pathways EE→TGN. The calcofluor white resistance suggests AP-1 transport is supported by alleles capable of endogenous PS flip. Drs2 is involved in a second retrograde pathway, to test the influence of PS flip we monitored GFP-Snc1 recycling (K. Liu, et al., 2008). GFP-Snc1 cycles between TGN→PM→EE→TGN. In normal cells, the slow step is endocytosis and the steady-state localization is on the plasma membrane. In a *drs2Δ* strain, the slow step becomes intracellular, most likely EE→TGN but also potentially TGN→PM (Hua, et al., 2002; Sakane, Yamamoto, & Tanaka, 2006). Drs2[QQ→GA],N445S is a variant that able to flip PS and similarly to WT Drs2 restored GFP-Snc1 plasma membrane localization, while Drs2 mutants deficient in PS recognition (Drs2[QQ→GA], Drs2 F511Y, and Drs2F511L) failed to support this pathway (Figure 4-6A and 4-6B). These results suggested PS flip by Drs2 was important for GFP-Snc1 recycling. WT Dnf1, Dnf1[GA→QQ] and Dnf1[Y618F] partially suppressed the GFP-Snc1 trafficking defects of a *drs2Δ*, perhaps due to increased lyso-PS flip (Figure 4-6C and 4-6D). However, the Dnf1 alleles capable of PS flip were able to fully restore GFP-Snc1 localization to the plasma membrane.

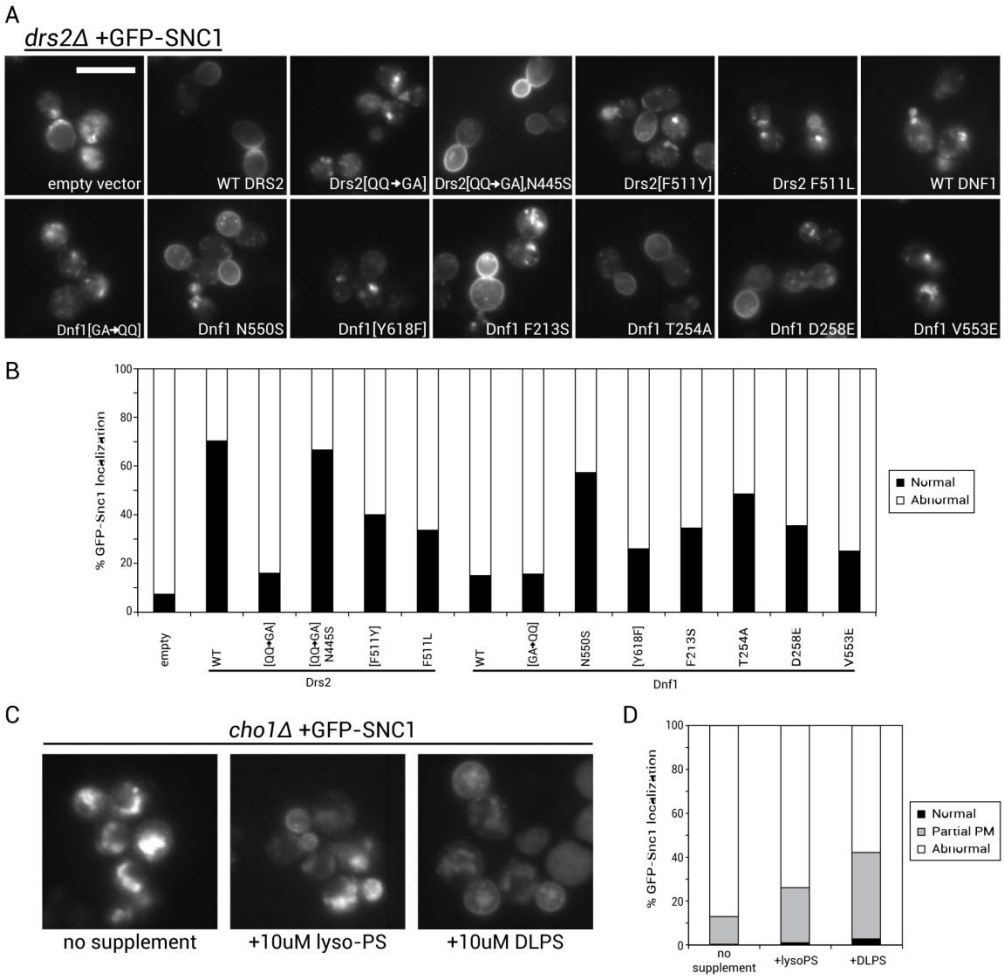

Figure 4-6. PS flip supports retrograde trafficking through the early endosomal system. (A) The ability to flip endogenous PS correlated with the ability to restore GFP-Snc1 localization to the PM (B) Cells counts of GFP-Snc1 localization in a *drs2Δ* expressing the indicated Dnf1/Drs2 variants (n=300+). (C, D) PS is important for retrograde traffic because the absence of cellular PS, GFP-Snc1 localization is perturbed. Supplementation with lysoPS or DLPS partially restore Snc1 localization.

The strong correlation between Drs2 and Dnf1 PS flip and support of the recycling pathway led us to test GFP-Snc1 localization in *cho1Δ* cells. PS is clearly an important component as the *cho1Δ* has defect in GFP-Snc1 localization (Figure 4-6C). PS is important in the recycling pathway because supplementation with lysoPS or DLPS at 30°C for 1 hour partially restores GFP-Snc1 localization (Figure 4-6C and 4-6D). PS is not essential for TGN→PM GFP-Snc1 transport because a *cho1Δ* strain expressing an endocytosis-defective Snc1 (GFP-Snc1-PM) demonstrates

PM localization (Figure 4-7). The importance of both cellular PS (Figure 4-6C and 4-6D), and contribution of Drs2 and Dnf1 variants to restoring GFP-Snc1 localization suggests PS flip at the early endosome is important to support this pathway.

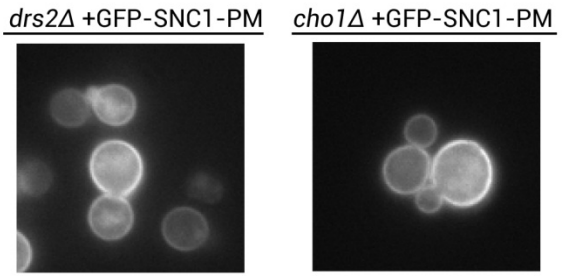

Figure 4-7. Neither Drs2 nor PS are required for transport of GFP-Snc1-PM to the plasma membrane.

To test whether it was sufficient to have PS on the intracellular leaflet of the plasma membrane, or if active PS flip at the Golgi-endosomal system was required, we mutated the endocytosis signal in Dnf1 (K. Liu, et al., 2007). The Dnf1 endocytic defective alleles tested were incapable of suppressing the cold sensitivity of a *drs2Δ* (Figure 4-8A). As previously reported, an endocytic defective Dnf1 was not able to complement *dnf1,2,3Δdrs2Δ* (Figure 4-8B)(K. Liu, et al., 2007). Neither the Dnf1 N550S PF→AI nor Dnf1[Y618F],PF→AI were able to support growth in this background (Figure 4-8B). We tested the ability of the endocytic defective mutant (Dnf1 PF→AI) to restore plasma membrane asymmetry of *drs2Δ*. Surprisingly, this mutant was no better than WT Dnf1 at restoring asymmetry (Figure 4-8C). Perhaps even more surprisingly, the endocytic-defective Dnf1 N550S,PF→AI was only partially able to restore PM asymmetry with *drs2Δ*. In *drs2Δ* cells, GFP-Snc1 trafficking was not suppressed by Dnf1(PF→AI) or Dnf1[Y618F](PF→AI) (Figure 4-8D). Phosphatidylserine flip at the plasma membrane was not sufficient, because Dnf1 N550S (PF→AI) was unable to restore GFP-Snc1 localization to the plasma membrane. These data surprisingly suggest that Dnf1 N550S is not nearly as efficient at

establishing plasma membrane asymmetry when it is trapped at the plasma membrane. The endocytic competent form is much better at establishing PS asymmetry and supporting protein trafficking steps.

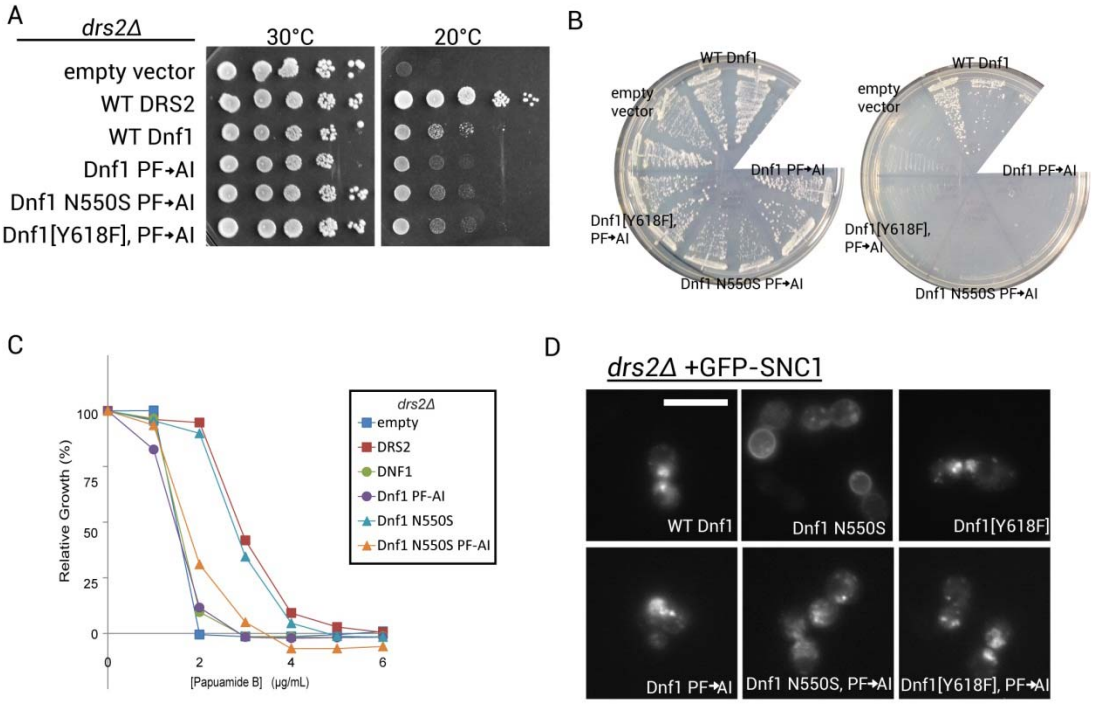

Figure 4-8. Endocytic-defective Dnf1 N550S, PF→AI does not restore Drs2-dependent functions as well as Dnf1 N550S. (A) Endocytic-defective Dnf1variants do not suppress *drs2Δ* cold-sensitivity effectively. (B) Endocytic-defective Dnf1variants do not complement *dnf1,2,3Δdrs2Δ* growth. (C) Dnf1 N550S, PF→AI is only partially capable of restoring PS asymmetry of *drs2Δ*. (D) Dnf1 N550S,PF→AI does not restore GFP-Snc1 recycling *drs2Δ*..

Recycling of GFP-Snc1 from EE→TGN requires several components including Arf1, Drs2, Cdc50, Gcs1 and Rcy1. We tested whether we could bypass the components in the second EE→TGN transport pathway. Like the *drs2Δ*, a *rcy1Δ* strain is cold-sensitive (Lafourcade, Galan, & Peter, 2003). A second copy of Drs2 (in addition to the genomic copy Drs2) was not sufficient to suppress the *rcy1Δ* cold sensitivity (Figure 4-9). A second copy of WT Dnf1 (or each of the

Dnf1 suppressor mutants) was not able to suppress the *rcy1Δ* cold sensitivity. This suggests these proteins are not able to bypass the *RCY1* requirement at cold temperatures.

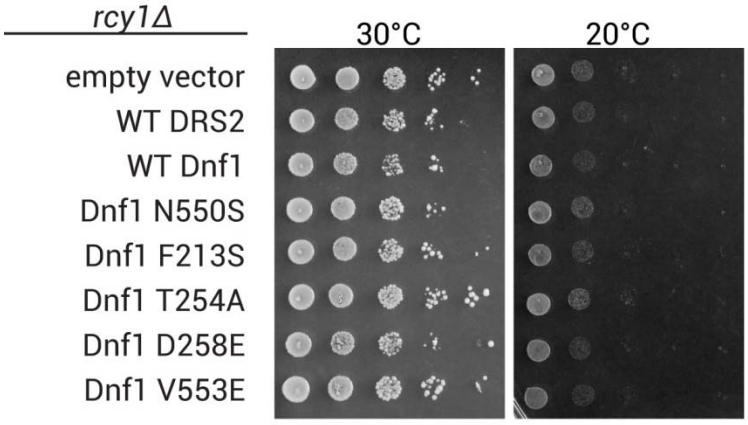

Figure 4-9. Dnf1 suppressors of *drs2Δ* do not bypass the requirement for *RCY1*.

DISCUSSION

One interesting question preceding this work is why Dnf1 alleles capable of flipping NDB-PS were not able to restore PS asymmetry in *drs2Δ* cells (Baldridge & Graham, 2012). The fact that some Dnf1 mutants which are fully capable of NBD-PS flip, but seemingly unable to flip endogenous PS, suggests these variants either had altered localization, abundance, or substrate specificity to gain the ability to restore the *drs2Δ* PS asymmetry. The localization and abundance were similar between each of the Dnf1 mutants previously reported to flip NBD-PS (Baldridge & Graham, 2013). We set up an alternate way to qualitatively monitor unlabeled-PS flip across the membrane by P4-ATPases (Figure 4-3). Using this method, we provide an explanation as to why Dnf1[Y618F] is unable to restore the *drs2Δ* PS asymmetry; it does not recognize dually-acylated PS very well. In fact, WT Dnf1 also appears to flip lyso-PL much better than di-acyl phospholipid. While WT Dnf1 does not flip endogenous PS very well, it seems to have a minor activity to NBD-

PS that can be increased in certain cases (Baldridge & Graham, 2012; Pomorski, et al., 2003). The Dnf1Y618F and Dnf1[GA→QQ] are certainly important in substrate recognition because reciprocal changes in Drs2 altered its ability to recognize endogenous PS, not just NBD-PL. The NBD-PL may be capable of mimicking a lyso-PL, a natural substrate for Dnf1, as well as the dually-acylated PL substrate of Drs2. However, like *drs2Δ*, a *dnf1,2Δ* strain is also sensitive to PapB (S. Chen, et al., 2006). This could be because of an increased exposure of lyso-PS on the extracellular leaflet of the *dnf1,2Δ* bilayer. Lyso-PS accounts for about 10% of PS in *S. cerevisiae* which would likely be enough for PapB to permeabilize the cell (Fairn, et al., 2011).

A second question is why do yeast maintain two P4-ATPases that appear to function only as lyso-phospholipid transporters? Is this an apparent role for scavenging phospholipid from the environment? Could they be functioning to flip phospholipids that have been damaged by phospholipases in the extracellular environment? Yeast produce lyso-PL when using phospholipids as an acyl donor in triglyceride synthesis (Oelkers et al., 2000), and this species can be flopped by Pdr5 and Yor1 to the extracellular leaflet (Decottignies et al., 1998). Dnf1,2 may be required to retain the lyso-PL species on the cytosolic leaflet, where they are available to repair enzymes for acylation by Ale1 (Jain et al., 2007; Wayne R. Riekhof, Wu, Jones, & Voelker, 2007). The ecological positioning of true wild-type yeast is in and around plants and animals, scavenging nutrients from the environment. The ability to scavenge nearly whole lipids (lyso-PL) would be a strong selective advantage saving considerable energy from synthesis in the Kennedy pathway (Voelker, 2000). Additionally, it is becoming increasingly apparent that lyso-PL species are involved in signaling events. Recent work has implicated accumulation of long-chain lyso-PS species in a mammalian neurodegenerative condition, PHARC (Blankman, Long, Trauger, Siuzdak, & Cravatt, 2013). Lyso-PC serves as a signaling lipid in plants enhancing responsiveness

for a Na^+ activated H^+ channel (Viehweger, Dordschbal, & Roos, 2002) and activating the plasma membrane proton pump, AHA2 (Palmgren & Christensen, 1994).

Our results suggest that PS is important for trafficking within the Golgi-endosomal system. For Dnf1, the ability to flip PS allows more effective replacement of Drs2. It seems that the restriction of PS to the cytosolic leaflet is not enough; the active flip is important (Figure 4-8). The Dnf1 alleles capable of endogenous PS flip *in vivo* were able to restore AP-1 trafficking. Consistently, a Drs2 variant strongly defective in PS flip, Drs2[QQ→GA] was defective in AP-1 trafficking. In the absence of Drs2, AP-1 coat components assemble on the membrane surface, but vesicles do not form efficiently (K. Liu, et al., 2008). Consistent with a role for PS, *cho1Δ* is hypersensitive to CW, probably due to defective AP-1 trafficking (Rockwell, et al., 2009). This affords the possibility that Drs2 drives vesicle budding by flipping phospholipid and inducing curvature through the bilayer-couple hypothesis. It remains a possibility that the Dnf1 variants capable of endogenous PS flip are better at inducing curvature because dually-acylated phospholipid and lyso-phospholipid have differing ability to drive curvature.

Retrograde pathways are also affected by the ability of Drs2 or Dnf1 to flip PS. The localization of GFP-Snc1 is altered in the complete absence of PS (Figure 5D and 5E). We were able to demonstrate that GFP-Snc1 trafficking required PS, specifically PS flip within the Golgi-endosomal system (Figure 4-6 and 4-8). Supplementing *cho1Δ* with lyso-PS restored PS levels to WT levels within 1 hour (Fairn, et al., 2011) and partially restored GFP-Snc1 traffic (Figure 4-6D and 4-6E). Similarly to GFP-Snc1, in *cho1Δ*, Cdc42 localization is disrupted and supplementation with lyso-PS partially restored its localization to the bud tip. In this case, Cdc42 polarization was restored to about 50% of cells, similar to what we observed with GFP-Snc1 localization (Figure 4-6) (Fairn, et al., 2011). PS is also involved in formation of endocytic patches at the plasma membrane yeast (Sun & Drubin).One possible explanation for the Dnf1 suppression observed in

CW resistance and GFP-Snc1 trafficking is an altered rate of endocytosis. This seemed unlikely because an increased rate of endocytosis would be needed to remove Chs3 from the PM, and a decreased rate would be required to maintain GFP-Snc1 PM localization. In addition, the functioning of Drs2 variants with substrate specificity changes (Drs2[QQ→GA] and Drs2[QQ→GA],N445S) is more consistent with the gain of PS as a substrate being the driving force.

It is noteworthy that in one of the crystal structures of the Ca^{2+} ATPase the analogous residues to Dnf1 Thr254 and Asp258 are coordinating the phospholipid headgroup (along with the proline +4 position) (Figure 4-10) (Obara, et al., 2005). This provides a rational basis for how the P4-ATPases evolved to recognize their phospholipid substrates and suggests they are using a conserved phospholipid binding site with other P-type ATPases. Additional studies will be needed to specifically address whether or not the mammalian proteins are using the same two-gate mechanism as the yeast P4-ATPases. Conservation of critical residues (Baldridge & Graham, 2013), and the identification new of residues conferring PS specificity (likely within the same exit gate) suggest this is likely.

This work demonstrates a specific role for P4-ATPases in vesicular mediated protein transport. Using a new set of Dnf1 variants, we have demonstrated active PS flip at specific locations facilitates membrane traffic. This provides important mechanistic insight for how P4-ATPases function and facilitate membrane trafficking events. Whether or not the primary function of the PS flip is recruitment of a specific protein, or primarily to generate curvature is an open question. It remains to be seen if active translocation of specific phospholipids at distinct locations is specific to these pathways, or is a more general feature of budding events.

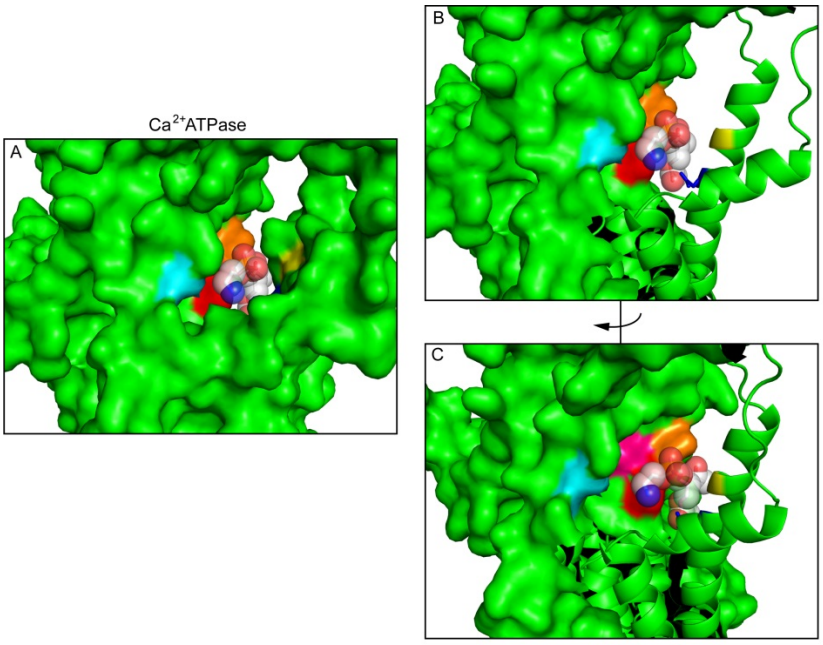

Figure 4-10. Updated phospholipid interaction with Ca^{2+} ATPase in E2 conformation. (A-C) Ca^{2+} ATPase crystal structure with PE molecule co-crystallized. The equivalent residues contributing to phospholipid specificity in Dnf1 and Drs2 have been colored coded for reference. Color-coded residues on Ca^{2+} ATPase structure: Cyan-Asp254 (equivalent to Dnf1 Asn550, Drs2 Asn445), Red-Pro312 (Dnf1 Tyr618, Drs2 Phe511), Pink- Ile315 (Dnf1 Val621, Drs2 Val514) and Orange-Thr316 (Dnf1 Glu622, Drs2 Glu515), Blue- Asn101 (Dnf1 Thr254, Drs2 Ser261), Yellow Gly105 (Dnf1 Asp258, Drs2 Glu265). (PDB:2AGV)

MATERIALS AND METHODS

Cold resistance screen

To generate random mutations we used previously reported procedures. We co-transformed a *dnf1,2,3Δdrs2Δ strain* (ZHY704) with mutagenized PCR products and pRS313-DNF1 gapped with restriction enzymes AflII and MluI to allow for gap repair through homologous recombination. The transformations were plated onto synthetic dropout plates with 5-fluoroorotic acid, grown for 4 days at 20°C and colonies were picked into 96 well plates. We compared growth of the strains expressing dnf1 mutants strains to those expressing WT DNF1 or WT DRS2 and sequenced dnf1* from the strains which grew strongly at 20°C.

Strains and culture

Escherichia coli strain DH5α was used for molecular cloning. All plasmids and strains used in this study are listed in Tables A6 and A7. Yeast were cultured with glucose in standard rich medium (YPD) or synthetic minimal medium (SD) at indicated temperatures. Yeast transformation used the lithium acetate method (R. D. Gietz & Schiestl, 2007).

Viability assay

To test for drug sensitivity, mid-log phase yeast were distributed into 96 well plates at 0.1 OD_{600}/mL. Plates were incubated at 30°C for 20 hours and the OD_{600}/mL was measured using a Multimode Plate Reader Synergy HT (Bio-Tek, Winooski, VT). Relative growth was determined by growth mock-treated cells in the assay.

α-factor secretion assay

Plates containing mat A supersensitive strains were prepared as described previously (Hopkins, Sato, Nakano, & Graham, 2000). Mat α strains to be tested were selected with a toothpick and spotted onto the surface of the plates containing the mat A supersensitive strain.

Pulse-chase labeling and immunoprecipitation of cargo proteins

This procedure was performed as described previously (Graham, 2001). We subcultured overnight cultures to 0.15 OD_{600}/mL and allowed to grow to mid-log phase. The cells were pelleted and resuspended at 5 OD_{600}/mL. We labeled with 25µCi/OD_{600} cells with EXPRESS^{35}S (Perkin-Elmer) at 20°C for 10min. The chase was performed with 1mM methionine, 0.1mM cysteine for the indicated times. To stop the reaction, we added ¼ volume of 50% TCA. The reactions were incubated on ice for 15 min, then centrifuged at top speed for 10min. The supernatant was aspirated, the pelleted was resuspended in 2 volumes of ice-cold acetone, and re-centrifuged for 10min. The acetone wash was repeated, and the pellets were dried to

completion in a Speed-Vac. We resuspended the pellets in 100µL SDS/urea buffer (50mM Tris Cl, pH7.5, 1mM EDTA, 1% SDS, 6M urea). and incubated at room temp for 15 minutes. We added ~70% volume of glass beads, vortexed for 1 min, heated to 85°C for 4 minutes, and vortexed for 15 sec. We added 900µL of detergent IP buffer (50mM Tris Cl, pH7.5, 0.1mM EDTA, 150mM NaCl, 0.5% Tween-20). The reactions were pelleted at top speed for 15 minutes, and ~850µL of supernatant was transferred to a new tube.

To immunoprecipitate protein from these samples, we added 75uL protein A-Sepharose CL-4B and 1-2uL antibody per OD_{600} cells. The reactions were incubated overnight with end-over-end rotation at 4°C. The samples were centrifuged at 3,000 x g for 5 min, the pellets were resuspended in detergent/urea buffer (100mM Tris Cl, pH7.5, 200mM NaCl, 0.5% Tween-20, 2M urea) and re-pelleted. The supernatants were cleared with a second batch of protein A-Sepharose and kept for a second immunoprecipitation. The pellets were resuspended a second time in detergent/urea buffer, re-pelleted, resuspended in detergent IP buffer, re-pelleted, and dried in a Speed Vac. The dried protein A-Sepharose was resuspended in Laemmli sample buffer with fresh 5% β-mercaptoethanol (vol/vol).

Serial dilutions

50,000 cells were spotted with 10-fold serial dilutions onto YPD plates, YPD + 100 µg/mL calcofluor white, SD, or SD +5FOA. Plates were grown at 20°C or 30°C for 3-5 days before imaging.

Lipid uptake

Lipid uptake was performed essentially as described previously (Hanson & Nichols, 2001). Briefly, overnight cultures were subcultured to 0.15 OD_{600}/mL and allowed to grow to early-mid log phase. 500 µl of cells were harvested, resuspended in ice-cold SD media containing

2 µg/ml NBD-lipid (~2.5µM), and incubated on ice for 30 min. Cells were washed twice with SA media (SD media + 2% sorbitol (wt/vol), + 20mM NaN_3) + 4% BSA (wt/vol), once with SA media, and resuspended in SA media prior to analysis by flow cytometry.

To facilitate lyso-PS (similar to (Fairn, et al., 2011)) and dilauryl-PS uptake, overnight cultures of *cho1Δ* yeast were subcultured to 0.15 OD_{600}/mL and allowed to grow to mid log phase (0.5 – 0.8 OD600/mL). 1500 µl of cells were pelleted, resuspended in SD media containing the indicated final concentration of lyso-PS or DLPS (added from a 10mg/mL stock in 0.1% NP-40 substitute), and incubated in 30°C shaker (or on ice) for 1 hour. To end the phospholipid uptake, we added SA media +4% BSA (w/v) at a 1:1 ratio with the reaction. The cells were pelleted and resuspended once in SA media + 4% BSA (w/v), followed SA media (no BSA), and finally, pelleted and resuspended in imaging buffer.

Flow cytometry

We used a BD LSRII-3 laser (BD Biosciences) using BD FACSDiva v6.1.3. NBD-lipid uptake was measured with the FITC filter set (530/30 bandpass with a 525 longpass). Immediately prior to analysis, propidium iodide was added at a final concentration of 5µM. At least ten thousand events were analyzed using forward/side scatter to identify single cells and propidium iodide fluorescence to exclude dead cells.

Calcofluor white staining

Overnight cultures were subcultured to 0.15 OD_{600}/mL and allowed to grow to mid-log phase. 1000 µl of cells were pelleted, resuspended in water, re-pelleted and resuspended in 100 µl of a 0.05% calcofluor white solution (wt/vol) (BD Biosciences) for 10 minutes. The cells were washed (pelleted and resuspended) twice with water and finally in imaging buffer (10mM Tris-HCl, pH 7.4, 2% glucose (wt/vol)).

Fluorescence microscopy

Images were collected with an Axioplan microscope (Carl Zeiss, Thornwood, NY) using a Hamamatsu CCD camera and MetaMorph software. To observe GFP-tagged proteins, cells were grown to mid-log phase, pelleted, and resuspended in imaging buffer (10mM Tris-HCl, pH 7.4, 2% glucose (wt/vol)). An aliquot of cells was spread onto slides, and visualized using a GFP filter set.

Data analysis

Within each NBD-PL uptake experiment, at least three independently isolated transformants harboring the same construct were assayed. The mean of these values from at least three separate experiments were reported as ± SEM. Uptake of NBD-PL for a *dnf1,2Δ* strain with an empty vector was subtracted and NBD-PC uptake by WT Dnf1 was used to normalize the data to 100%. Each value is reported relative to NDB-PC uptake by WT Dnf1 at 30 min. Substrate preference ratios were determined by the dividing NBD-PE or NBD-PS uptake values by the NBD-PC uptake value for each independent replicate (n≥9). The mean of each substrate preference ratio is reported ± SEM. For drug-sensitivity assays, at least two independently-isolated transformants were assayed in two separate experiments and reported as mean ± SEM.

ACKNOWLEDGEMENTS

We thank Scott Emr, Greg Fairn, Sergio Grinstein and Nava Segev for plasmids used in this work.

CHAPTER V

PROBING THE MECHANISM FOR HOW P4-ATPASES WITH A PROLINE +4 LEUCINE RECOGNIZE SUBSTRATE

INTRODUCTION

In chapter 2, we described an important role for the P+4 position in yeast P4-ATPase substrate specificity. Among each of the yeast and mammalian P4-ATPases, most of the Drs2/Dnf1 homologs have a Tyr in this position while the closest homologs to Drs2 (Atp8a1 and Atp8a2) actually have a leucine in this position (Figure 5-1). Purified Atp8a1/a2 shows a preference for PS and has a much higher ATPase activity *in vitro* than does Drs2 or Dnf1 (Coleman, et al., 2009; Ding, et al., 2000; Zhou & Graham, 2009). Strangely, a leucine at the P+4 position causes a reduction in overall activity for both Dnf1 and Drs2. We hypothesized that the P+4 leucine acts in concert with surrounding residues to allow activity of Atp8a1/a2, and these residues are not present in the yeast P4-ATPases.

Here, we report the identification of amino acid substitutions within Dnf1 and Drs2, which allow function in the presence of a P+4 leucine. These alleles restore growth, cold-resistance, and flippase activity to yeast deficient in multiple P4-ATPases.

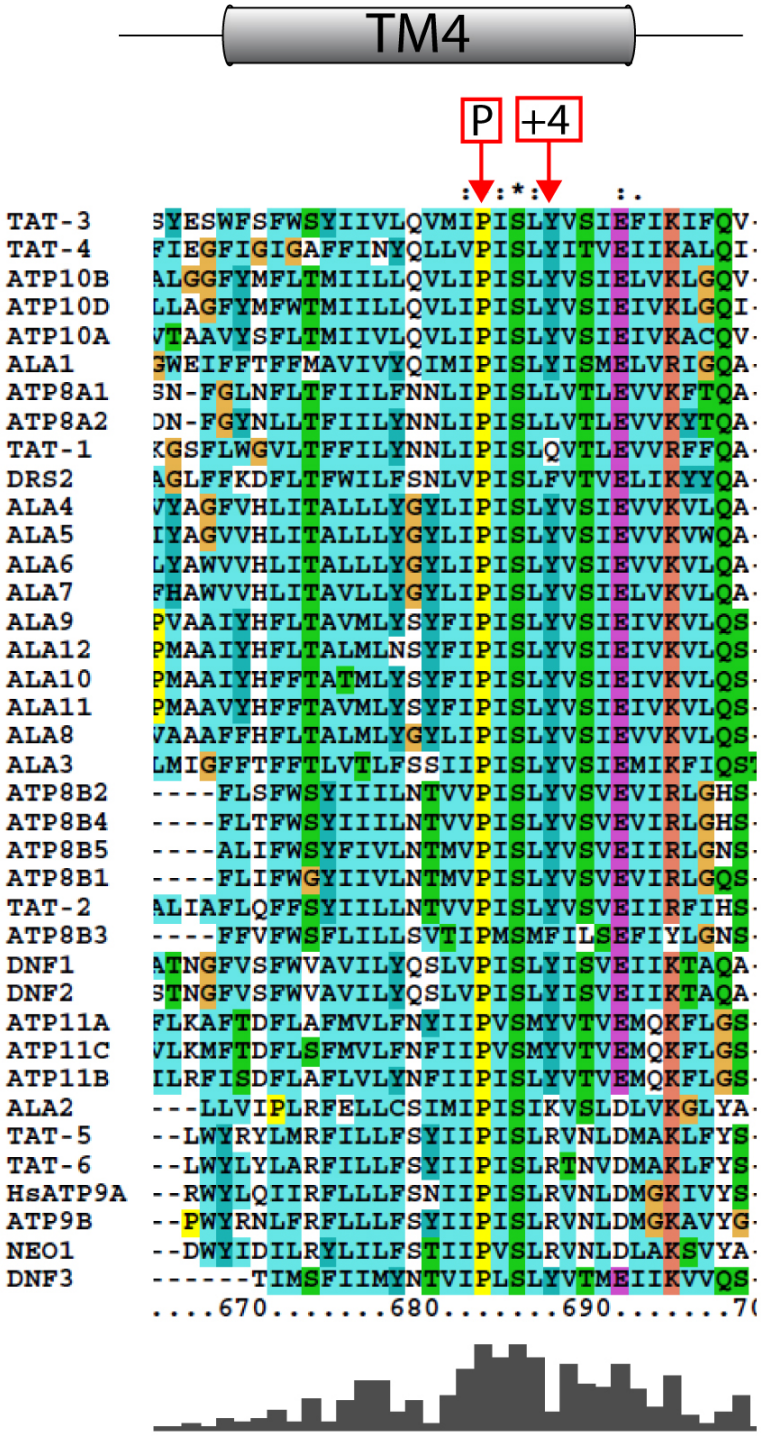

Figure 5-1. Alignment of P4-ATPases from *S. cerevisiae*, *C. elegans*, *A. thaliana*, and mammals.

RESULTS AND DISCUSSION

To test how a P4-ATPase might use a P+4 leucine for substrate recognition, we designed a screen to identify additional intragenic mutations that would restore function to drs2-F511L or Dnf1-Y618L. As a proof of principle, we combined the Drs2 N445S and F511L mutations and tested if this combination would restore activity relative to Drs2 F511L. The Drs2 N445S,F511L variant did partially restore activity measured by PapB and duramycin sensitivity assays (Figure 5-2A and 5-2B). It also allowed this construct to complement the cold sensitivity of *drs2Δ* and growth defect of *dnf1,2,3Δdrs2Δ* (Figure 5-2C and 5-2D). This suggested it was possible to restore activity while maintaining the P+4 leucine.

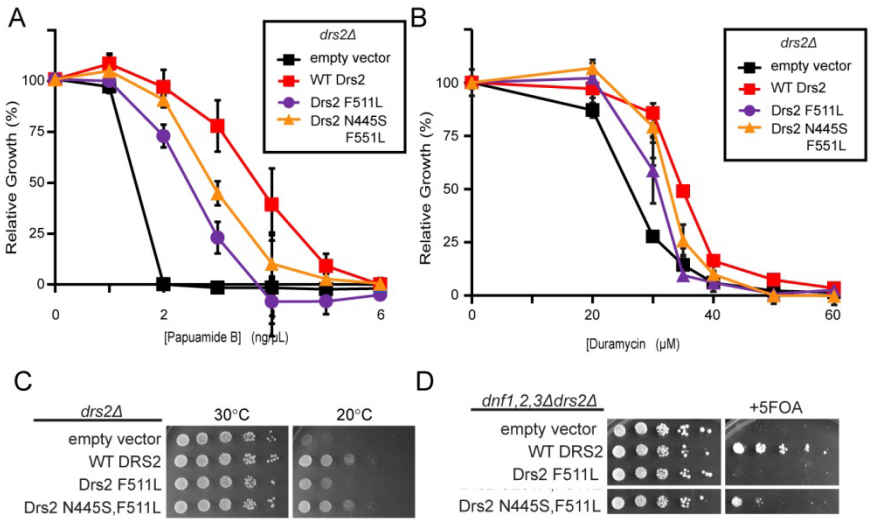

Figure 5-2. Drs2 N445S,F511L partially restores function compared to Drs2 F511L. (A)Drs2 N445S, F511L restores PS membrane asymmetry and PE asymmetry (B). (C) N445S improves cold-resistant growth of a *drs2Δ* compared to Drs2 F511L. (D) Drs2 N445S,F511L faciliatates growth of *dnf1,2,3Δdrs2Δ*.

Therefore, we screened for additional mutations that could restore function to Drs2 F511L. We targeted mutagenesis to TM3-4 using error prone PCR and co-transformed a Drs2 TM3-4 gapped plasmid with the PCR products. To select against non-functional *drs2* alleles, we

plated the transformations at 20°C. After 3 days of growth, we observed over 5000+ colonies and collected the cells that facilitated *drs2Δ* cold-resistant growth into synthetic media +15% gylcerol. These cells were frozen in aliquots at -80°C for later use. We next tested the potency of a PS-specific drug, Papuamide A (PapA) for a concentration in solid media which would selectively kill *drs2Δ* but not those expressing WT Drs2 (Figure 5-3).

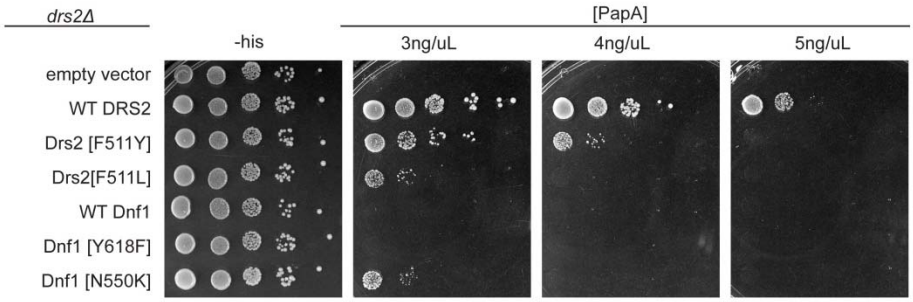

Figure 5-3. Papuamide A is toxic to yeast exposing PS on the plasma membrane.

WT Drs2 provided resistance to at least 5µg/mL PapA. We plated ~5,000 cells from the frozen aliquots onto SD + 5µg/mL PapA and selected the colonies which grew (~80 colonies). After re-testing the cold-resistance and PapA resistance we were left with about 60 mutants and sequenced *drs2* from most of these mutants. Amazingly, every mutant we recovered had a reversion of the P+4 position to Phe (n=47). We had anticipated that at minimum, we would recover a substitution at the Asn445 position that would restore cold-sensitivity and membrane asymmetry. This was not the case, and in retrospect, the Drs2 N445S, F511L only partially restored membrane asymmetry. Half of the clones had a second mutation within TM3-4 in addition to the reversion of L511F (23/47) (Figure 5-4). These results suggest that other than the reversion, a single substitution within TM3-4 cannot restore full PS translocase activity in the presence of a P+4 leucine.

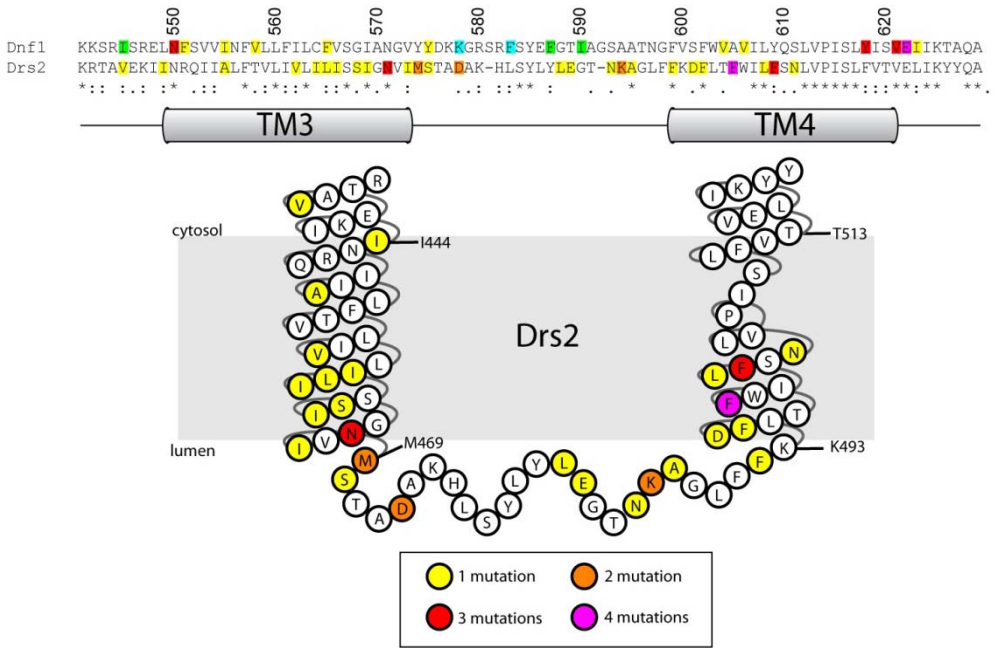

Figure 5-4. Summary of the frequency of mutations recovered with the L511F reversion mutation from the Drs2 PapA evolution screen.

In the screen for Dnf1 suppressors of *drs2Δ* cold-sensitive growth (chapter 4), we identified several mutations in TM1-2 of Dnf1 that correspond to the analogous residues in Atp8a1 (Figure 5-5). These residues confer the ability to flip NBD-PS and endogenous PS (Figure 4-2) and support trafficking functions of Drs2. We thought these may represent residues used by Atp8a1/a2 to function in the context of a P+4 leucine. To test this, we generated combinations of Dnf1 Y618L with the suppressors corresponding to Atp8a1 residues. Dnf1 Y618L does not suppress the cold sensitivity of *drs2Δ* nor does it support growth of *dnf1,2,*3Δdrs2Δ.In the context of the Atp8a1/a2 residues, the double mutants (Dnf1 F213S,Y618L, Dnf1 T254A,Y618L, Dnf1 D258E,Y618L) were able to restore cold-resistance to *drs2Δ*, and support growth of *dnf1,2,3Δdrs2Δ* (Figure 5-6), Indicating at least partial function had been restored.

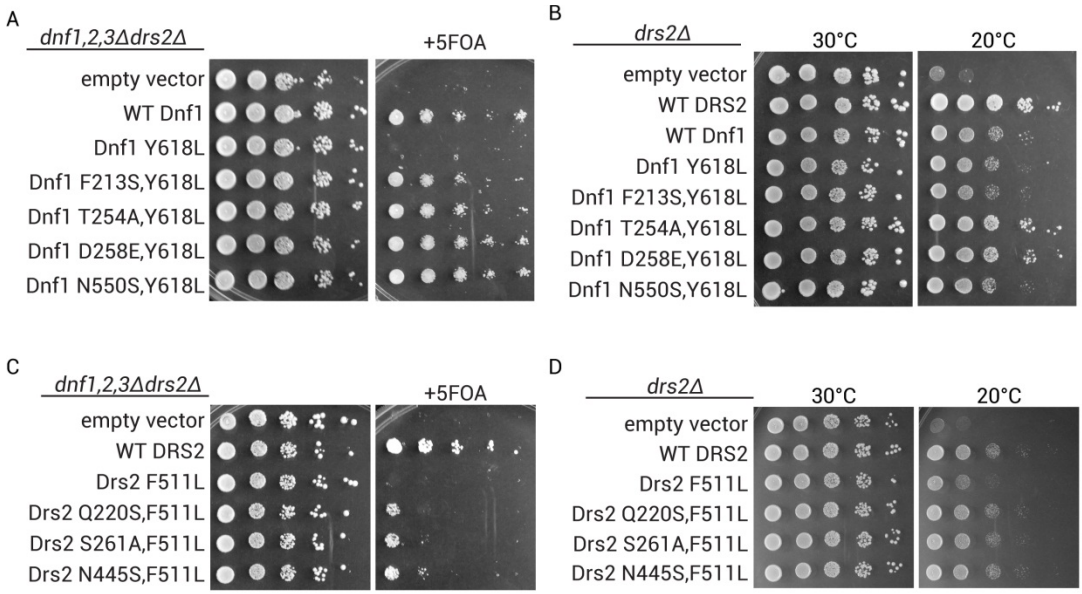

Figure 5-5. Combinations of Atp8a1 residues with the P+4 leucine restore function in Dnf1 Y618L and Drs2 F511L.

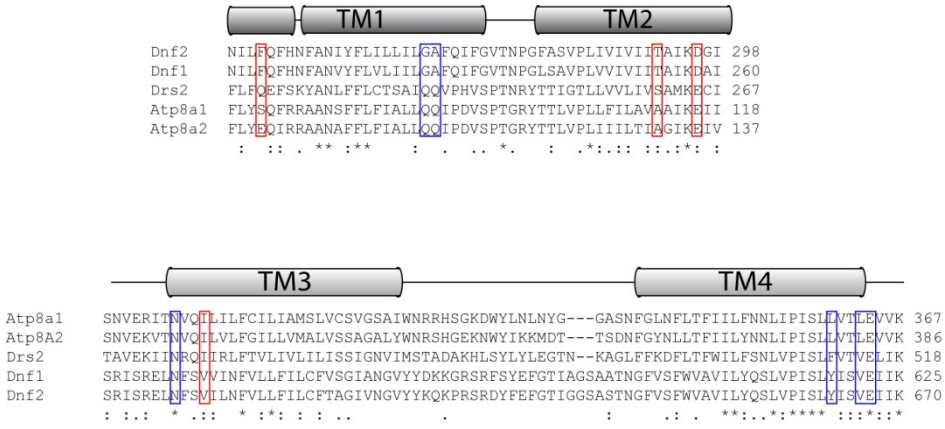

Figure 5-6. Alignment of critical residues involved in PS selection by P4-ATPases. Blue boxes indicate residues reported in chapters 2 and 3. Red boxes indicate new residues characterized and discussed in chapter 4.

We tested these same substitutions in Drs2 with the P+4 leucine (Drs2 F511L). Like Dnf1 Y618L, Drs2 F511L does not restore cold-resistance in *drs2Δ* and does not support growth of *dnf1,2,3Δdrs2Δ* (Baldridge & Graham, 2012). When we combined the P+4 leucine with the equivalent Atp8a1/a2 residues, Drs2 was again functional. This result suggests that Atp8a1/a2 are using the P+4 leucine in combination with residues on TM1-2 to maintain functional exit gate activity. So far we have not tested the ability to transport labeled, or unlabeled substrate *in vivo*. These results support the notion that yeast and mammalian P4-ATPases are using a conserved substrate binding site for transport.

CHAPTER VI

TESTING THE BIOCHEMICAL PROPERTIES OF DNF1

INTRODUCTION

The initial identification of the enzyme responsible for a sodium, potassium and magnesium dependent ATPase activity and the later classification of the Na^+/K^+ ATPase as the founding member of the P-type ATPase family occurred over 50 years ago. Since that time, detailed mechanics for the entry/exit of substrate and ATP were described within the Post-Albers cycle. A groundbreaking discovery occurred when the Toyoshima lab solved the x-ray crystal structure of the sarcoplasmic/endoplasmic reticulum calcium ATPase (SERCA), a member of the P-type ATPase family. This first high resolution structure actually had two Ca^{2+} ions co-crystallized and was closely followed by several more structures in different states of the catalytic cycle. These structures confirmed the use of an ion-binding site previously identified using targeted mutagenesis and crosslinking studies (Clarke, Loo, Inesi, & MacLennan, 1989; Rice, Green, & MacLennan, 1997). This ion-binding site is buried within the center of the transmembrane domain, and the structures helped to identify the mechanism of gating access to this site.

The canonical ion-binding site is formed by transmembrane (TM) segment 4,5,6 and 8 with basic passage to this site originally described through the Post-Albers mechanism. As the catalytic cycle of the Ca^{2+} ATPase begins, the ion-binding sites are open to the cytosolic side of the membrane. After the ions enter, the interaction of ATP with the nucleotide-binding (N) domain induces the closure of the cytosolic pathway into the canonical site. The γ-PO_4 is

transferred to the conserved aspartic acid residue within the DKTGTL motif in the phosphorylation domain stimulating opening of the lumenal pathway into the canonical ion-binding site. The Ca^{2+} exits and is replaced by protons that balance the negatively charged residues in the canonical site. The phosphate is hydrolyzed from the protein, triggering occlusion of the binding site before the pump resets, and opens the pathway to the cytosol, releasing the protons, and allowing new Ca^{2+} to enter. Whether the P4-ATPases are using the same conformational changes to drive phospholipid transport is unknown.

Here we describe preliminary work designed to address the mechanism through which P4-ATPases select and transport phospholipid substrate. Using recently described residues involved in substrate selection (Baldridge & Graham, 2012, 2013), we aim to use low resolution structural biological techniques to address the approximate orientation of these critical residues to one another and to test the structural model presented in chapter 2. Of particular importance is the orientation of N550, Y618, T254, D258 and F213 side chains relative to each other. We also describe the purification of Dnf1 and a preliminary set of experiments demonstrating the *in vitro* ATPase activity of Dnf1. This preliminary work has created a foundation for future studies to probe the orientation of critical residues in the structural model, test *in vitro* flippase activity and test the proposed two-gate mechanism for selection and transport.

RESULTS AND DISCUSSION

Probing the orientation of residues critical for substrate specificity

To test the orientation of key residues involved in phospholipid selection (Figure 3-13 and 4-10), we wanted to use a crosslinking approach, coupled with protease cleavage and detection with gel shifts (Figure 6-1). It was important that when we induce crosslinking, Dnf1 is in a native membrane to help retain its normal conformational states. To obtain protein for crosslinking and cleavage, we enriched for membranes containing Dnf1 by collecting the $P_{130,000}$

fraction from cell lysates. Initially, we generated an N-terminal hemagglutinin-tagged Dnf1 (HA-Dnf1). To identify the orientations of critical residues, we introduced a series of cysteines at a variety of positions to test for crosslinking under oxidizing conditions (green, blue, cyan and yellow residues in Figure 6-2). The majority of these Cys residues supported Dnf1 function as indicated by complementation of *dnf1,2,3Δdrs2Δ* (Figure 6-3), many even showed partial activity in the NBD-PL uptake assay even if they did not complement growth (data not shown). I originally tried to use the chemical compound hydroxylamine to cleave Dnf1 within LL3-4. Hydroxylamine cleaves after the sequence Asn-Gly, but even after changing dozens of parameters I was never able to obtain strong cleavage and the HA antibody produced several background bands even within the $P_{130,000}$ fraction, which made detection of the cleavage product difficult (data not shown).

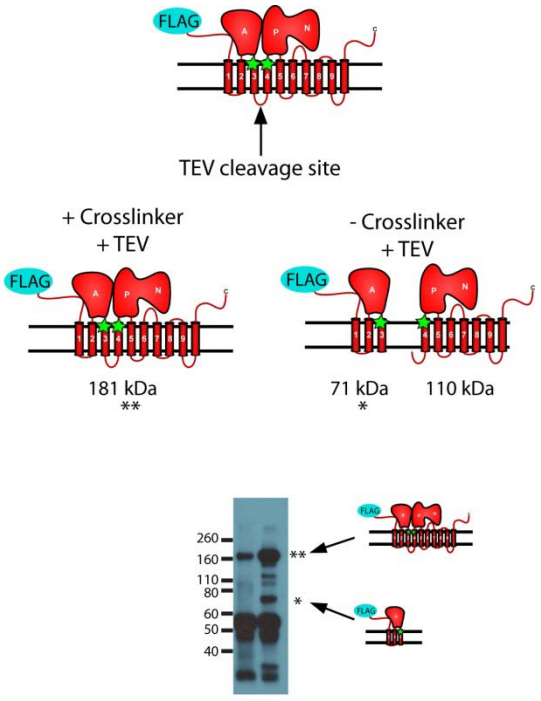

Figure 6-1. Schematic for crosslinking , protease cleavage, and detection with mobility shift.

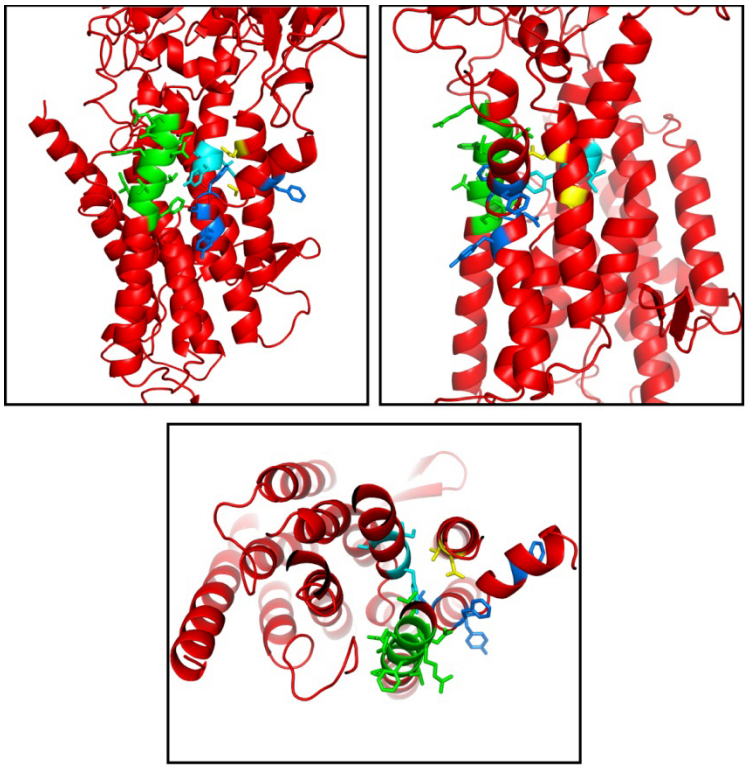

Figure 6-2. Positioning of introduced cysteines on the structural model of Dnf1. Blue residues indicate TM1 (Phe218, Asn220, Tyr222), yellow mark TM2 (Thr254, Asp258), green label TM3 (Leu547-Phe557), and cyan denotes TM4 (Tyr618, Ile619, Ser620).

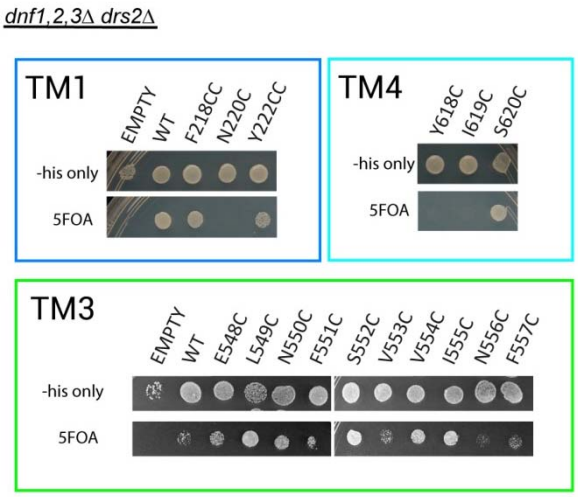

Figure 6-3. Most of the introduced cysteines support growth of *dnf1,2,3Δdrs2Δ*.

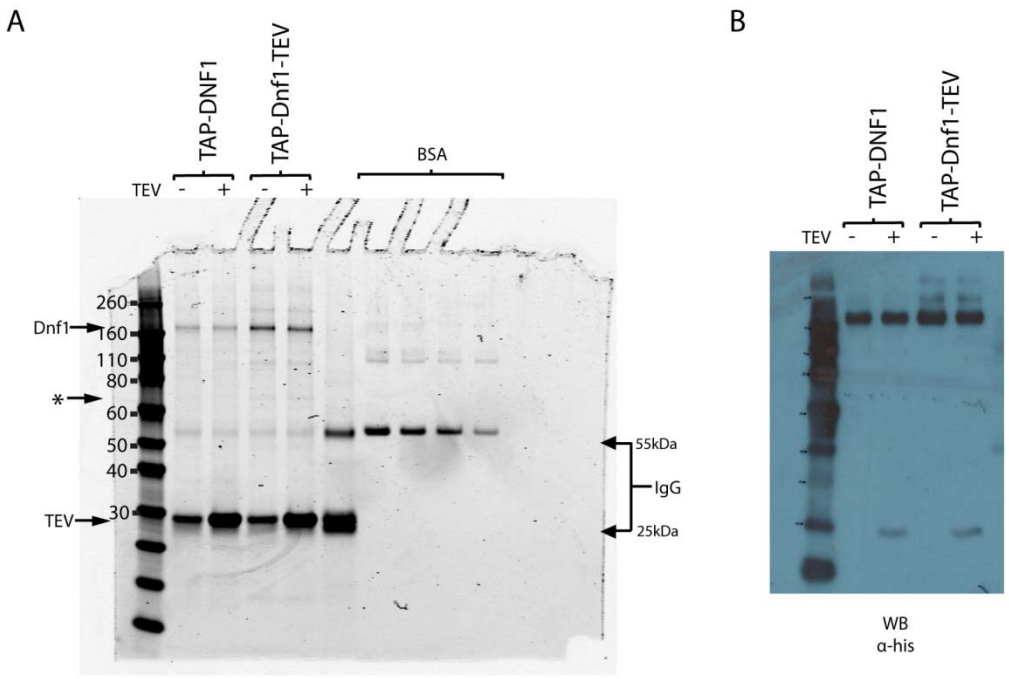

Figure 6-4. TAP-Drs2-TEV was purified to near homogeneity, but digestion with TEV was inefficient.

We tested a TAP-tagged version of Dnf1 with a TEV site introduced within LL3-4 to see if we could improve the cleavage with higher purity or improve detection speed and quantitation using Coomassie staining. We were able to purify this TAP-Dnf1-TEV to near homogeneity but were not able to convincingly detect the cleavage products by coomassie and western blotting (Figure 6-4). We were able to detect better cleavage with the single step purified Dnf1, but this could only be visualized by western blotting because the single step purified material was very heterogeneous.

To improve the detection of the cleavage, I re-engineered the constructs. This time, we used *dnf1,2Δ* cells overexpressing N-terminal GPD_{prom}-3xFLAG-Dnf1-TEV and the Dnf1 β-subunit, Lem3 (GPD_{prom}-myc-Lem3). With the enriched membrane fraction ($P_{130,000}$) of Dnf1 we induced crosslinking with either $CuPh_3$, O-PDM, or BMOE. In the absence of introduced cysteines and induction of the crosslink, we were able to detect the proteolyzed N-terminal fragment near its

predicted size. This was important because it indicated there were no crosslinks forming between another pair of cysteines linking the 71kDa and 110kDa fragments (Figure 6-1) which could have made this assay much more difficult or unusable. Obtaining good TEV cleavage for Dnf1 took some optimization, and we obtained the best results when the samples were solubilized in 10mM Tris pH7.5, 1% $C_{12}E_9$ and pulled down with α-FLAG m2 sepharose and washed twice with 40mM Tris, pH7.5, 150mM NaCl 0.1% $C_{12}E_9$ before resuspending and digesting (on the sepharose) with 50mM Tris, pH8.0, 0.5mM EDTA, 0.1 units TEV/OD, incubating at 30° for 4 hours with end-over-end rotation. At best, we were attaining <50% cleavage but with the detection method, this was sufficient to easily detect the 71kDa proteolyzed fragment (Figure 6-5).

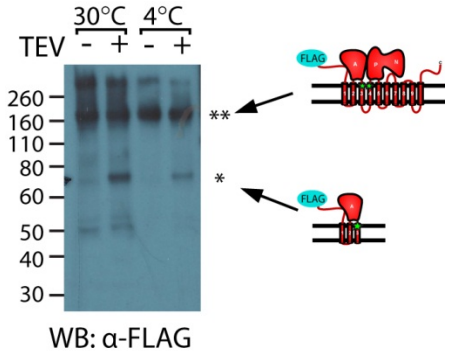

Figure 6-5. With a partially purified Flag3-Dnf1-TEV, TEV digestion improved significantly.

Purification and measurement of ATPase activity with Dnf1

We wanted to test the specific activity of TAP2-DNF1 *in vitro*, so we followed the basic protocol described by our lab (Zhou & Graham, 2009). I recovered about 6 µg of Dnf1 after a two-step purification (either Ni-NTA + IgG or Ni-NTA + flotation). The specific activity I observed for Dnf1 was 0.13 µmol/min/mg (n=2) (Figure 6-6). This is lower than the published value for

Drs2 (~0.4 µmol/min/mg), but upon repeating this procedure the actual specific activity of Dnf1 may be different than that reported here.

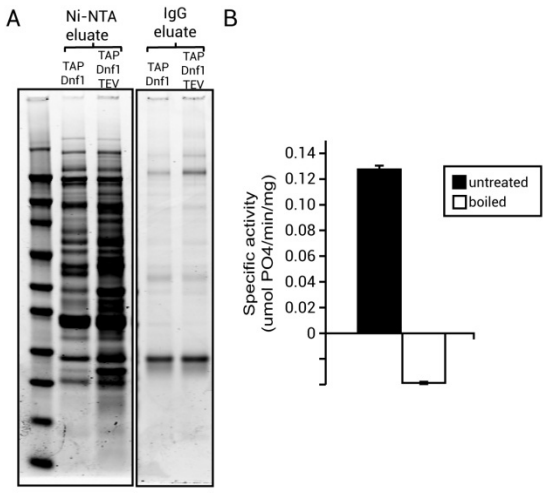

Figure 6-6. TAP Dnf1 was purified to near homogeneity and maintained ATPase activity *in vitro*.

At this point, we have introduced cysteines at many of the critical positions within TM1,3 and 4 and verified function by either complementation or activity. The preliminary work with crosslinking approaches has been productive, but this step requires optimization for the different crosslinking reagents. We can also obtain relatively good TEV cleavage and detect mobility shifts with SDS-PAGE and western blotting. We have purified Dnf1 to near homogeneity toward a goal of testing for substrate stimulation of the ATPase activity and reconstitution the flippase activity *in vitro*. Compared to purified Drs2, we would have significant advantage with purified Dnf1 enzyme because we have identified a significantly greater number of residues involved in substrate selection. In summary, the materials for testing the orientation of TM1-4 and *in vitro* characterization of Dnf1 are ready to go.

MATERIALS AND METHODS

Cloning

TM1,2,3 cysteines were prepared using the Quickchange protocol in pGEM-Dnf1 (SphI-MfeI fragment). The resulting plasmids were sequenced to verify the mutation. We digested pRS313-dnf1(w/AflII and MluI sites) and the mutagenized pGEM cysteine plasmids with SphI and MfeI, gel purified the fragments of interest (9347bp and 1735bp, respectively), and ligated the fragments and transformed into *E.coli*. Correct incorporation of the cysteine was verified by digesting with AflII which was in the original SphI-MfeI fragment but not upon replacement with the cysteine fragment.

For TM4 cysteines, we used the Quickchange protocol with pGEM-Dnf1 (SphI-2569). We sequenced to verify the mutation and digested the plasmids with EcoRI. We gel purified the mutagenized fragment (2378 bp), and the 10590bp fragment from pRS313-Dnf1 digested with MfeI and NruI (removes 492bp including TM4). We co-transformed a *dnf1,2Δ* strain the mutagenized fragment and gapped plasmid and selected colonies from –his dropout plates. The plasmids were recovered from yeast as previously described, and sequenced to verify correct recombination and validate the appropriate sequences.

Purification

For TAP-Dnf1 purification, we used the procedures described previously for Drs2 (Zhou & Graham, 2009). To enrich Dnf1 membranes, we used the general procedure described previously with the following modifications (Graham, Seeger, Payne, MacKay, & Emr, 1994). We prepared spheroplasts by collecting 500 OD_{600} cells in mid-log phase, washed with ice-cold 10mM NaN_3, resuspended at 10 OD/mL in softening buffer (100mM Tris, pH9.4, 10mM NaN_3, β-mercaptoethanol) and incubated on ice for 10min. The cells were re-pelleted and resuspended

at 50 OD/mL in spheroplasting buffer (10mM Tris, pH 7.5, 10mM NaN_3, 1M sorbitol) + 1mg zymolyase 20T/OD_{600} cells. The reactions were incubated at 30°C for 30 min, pelleted, washed in spheroplasting buffer 25 OD/mL, pelleted, and resuspended in ice-cold lysis buffer (10mM TEA, pH7.5, 1mM EDTA, 100mM sorbitol, protease inhibitors).The cells were lysed with 15 strokes of a tight Dounce homogenizer before centrifuging at 13,000 x g to clear the large membranes. We then centrifuged the supernatant $S_{13,000}$ at 130,000 x g and collected the pellet consisting of the smaller membranes within the cell containing Dnf1 (vesicles, Golgi, endosomes). We removed the supernatant, and resuspended the pellet in 100mM Tris, pH 7.5 at 200 ODeq/mL and stored at -80°C until further use.

CHAPTER VII

DISCUSSION

Identification of residues selecting phospholipid suggests a novel transport pathway

Historically, a major issue in the P-type ATPase field has been if the P4-ATPases were sufficient to flip phospholipid. Prior to demonstration of the flippase activity, a significant amount of genetic support existed, but each of these observations could be explained as a secondary transport mechanism (see Chapter 1). In the absence of direct biochemical evidence for a flippase activity it was impossible to distinguish a primary versus secondary transport mechanism for the influence of P4-ATPases on phospholipid transport. In spite of the genetic evidence for phospholipid flip, the difficulty of reconciling how P4-ATPases could use the same canonical substrate-binding site (presumably) as ion transporters prevented complete acceptance of a direct role for P4-ATPases in establishing membrane asymmetry (Graham, 2004; Palmgren & Nissen, 2011; Poulsen, López-Marqués, & Palmgren, 2008). The independent purification and reconstitution of a yeast and mammalian P4-ATPase supported the previous work and confirmed this family as phospholipid flippases (Coleman, et al., 2009; Zhou & Graham, 2009). After demonstration of the *in vitro* flippase activity, one of the primary unanswered questions was: how do the P4-ATPases flip phospholipid?

Towards this goal, I started out to identify residues involved in phospholipid selection. I took the approach of generating chimeras between Drs2 and Dnf1, flippases preferring PS and PC, respectively. Dnf1 was chosen as the acceptor because it is expressed on the plasma membrane and the assay for activity can be performed with whole yeast cells whereas Drs2 is

present intracellularly. We initially searched for regions of high conservation between P4-ATPases with similar substrate specificity (PS flippases Dnf2, Atp8a1 andAtp8a2 and PC flippases Dnf1 and Dnf1). Next, we searched for regions that also had low conservation between PS and PC flippases. This analysis illuminated a region within TM1-2, which we termed the region of interest (ROI) (Figure 3-1B). After swapping pairs of residue through this region, I identified a potential change in specificity with several chimeras in the Dnf1 ROI. When I was first assembling Chapter 2, however, it was not clear if the differences we were observing with ROI swaps were significant.

I decided to move on, from the difficult judgment calls of TM1-2 and examine the rest of the TM domain. When I swapped the next pair of transmembrane segments, I immediately observed a NBD-PS activity with two different TM3-4 swaps (one of which has been published in Chapter 2) (Figure 2-1B). The Dnf1[TM3-4] chimera actually showed a preference for NBD-PS over NBD-PC (or NBD-PE). This substrate preference is similar to what is known for Drs2. I continued to swap the transmembrane segments from Drs2 into Dnf1, but found the Dnf1[TM5-6], Dnf1[TM7-10], and even the Dnf1[TM1-10] chimeras were retained in the ER (Figure 2-1C), and thus could not support a PM uptake activity (Figure 2-1B). I focused on TM3-4 and generated progressively smaller chimeras between Dnf1 and Drs2 and identified a single residue within TM4 which controlled the ability of Dnf1 to flip NBD-PS (Figure 2-5B). This residue is 4 amino acids away from a proline, which is completely conserved in all P-type ATPases, so it was called the proline +4 position (P+4)(Figure 2-16A). In WT Dnf1, the presence of a Tyr restricts the ability to flip NBD-PS while substitution for the Drs2 residue Phe allows NBD-PS flip. The closest mammalian homologs to Drs2 (Atp8a1/Atp8a2, also PS flippases) have a leucine in the P+4 position. The Y618F change was specific for allowing NBD-PS flip, because if I introduced a leucine substitution or others at this position (Cys, Gln, Asn, Arg) it reduced the overall activity

and did not increase the NBD-PS activity (Y618L in Figure 2-5B and data not shown). I tested the activity of the key chimeras in the absence of Drs2, Cdc50 or Lem3. In each case, Lem3 was still required and Cdc50 was neither required, nor sufficient for the altered activity of the Dnf1 variants. Thus, I had changed the specificity of Dnf1 without affecting the requirement for Lem3.

An important test for the role of the P+4 position came with the reciprocal change to Dnf1 Y618F in Drs2. Drs2[F511Y] specifically lost the ability to flip endogenous PS without affecting its ability to flip endogenous PE (Figure 2-9). Similarly to Dnf1 with a leucine in the P+4 position, Drs2 F511L displayed an overall reduction in flippase activity measured by PM asymmetry. I was able to purify Drs2, Drs2[F511Y] and Drs2 F511L and observed a reduction in ATPase activity of Drs2 F511L while Drs2[F511Y] retained normal ATPase activity. Many P-type ATPases show a stimulation of their ATPase activities in response to substrate (Graf & Penniston, 1981; A. K. Mandal, Cheung, & Argüello, 2002; D. Mandal, Woolf, & Rao, 2000; Skou, 1957; Vara & Serrano, 1982). This reduction in activity may have been caused by the inability of Drs2 F511L to be stimulated by substrate which likely co-purifies with Drs2.

Using a mapping procedure based on Dnf1/Drs2 chimeras, our results implicated TM3-4 as a critical determinant of substrate specificity. Specifically, the P+4 position was able to control the ability of Dnf1 and Drs2 to select PS. Using a structural model of Dnf1, based upon the Na^+/K^+ ATPase structure (PDB:2ZXE), the P+4 position is oriented directly away from the canonical ion-binding site used by most P-type ATPases (Figure 2-15). When we looked at the orientation of this residue in each of the available P-type ATPase crystal structures, it is always oriented in this direction, directly away from the canonical ion-binding site. This is not likely to be a coincidence because the completely conserved proline creates a general feature of each structure, it breaks the TM4 helix and opens space on the other side of TM4 for main-chain

carbonyl ion coordination. Thus our results suggested a non-canonical mechanism for phospholipid transport by P4-ATPases (Chapter 2)(Baldridge & Graham, 2012).

Potential support for a P4-ATPase canonical mechanism was published in *PNAS* in back-to-back issues with our work. The Molday and Andersen groups purified Atp8a2 and demonstrated *in vitro* autophosphorylation and stimulation of dephosphorylation by substrate. Their support for a canonical mechanism was based on a reduction in PS-stimulated activity when they made substitutions in a conserved transmembrane lysine. This was interpreted as a reduction in affinity for substrate, but the likelihood is it just reduced the capability of the pump to proceed through the reaction cycle. Nonetheless, my previous work could be consistent with a canonical mechanism if the orientation of the P+4 was unique to the P4-ATPases.

To test for the possibility of a canonical or non-canonical mechanism, I set up a screening procedure to identify additional residues involved in substrate selection within TM3-4. This screen was based upon finding functional Dnf1 variants resistant to the toxic PC analog, edelfosine (Chapter 2 and 3). I was able to identify a large number of residues within TM3-4 that were involved in both PC and PS selection by Dnf1. I also tested a range of the PS selective residues in Drs2, and verified the involvement in endogenous PS selection. To address the possibility of a canonical mechanism, I subjected TM5-6 to the same screening tactics as with TM3-4. Targeting mutagenesis to TM5-6, I screened through over half of the number of mutant alleles as for TM3-4 but was unable to identify any residues involved in substrate selection. I concluded that TM5-6 were unlikely to be directly involved in substrate selection and thus, the flippases are not likely to use a canonical transport mechanism. I continued to search for support for a canonical or non-canonical transport mechanism by identifying residues involved in substrate selection. I came back to the original region-of-interest where this story began. With the benefit of confirmed PS-transporting Dnf1 variants and an alternate method for

analyzing the results I was able to affirm additional changes in specificity caused by substitutions within TM1-2. The use of TM1-2 for substrate selection was unique from ion-transporting P-type ATPases and in definite support of a non-canonical transport mechanism.

A curious result came from this work. Dnf1[Y618F] could flip NBD-PS very well, but was unable to restore plasma membrane PS asymmetry in *drs2Δ* (Figure 2-3 and 2-10). It is possible that the localization of Dnf1 and Dnf1[Y618F] was insufficient to restore membrane asymmetry. Dnf1 populates the Golgi-endosomal system but is also located at the plasma membrane where it is highly polarized to the bud tip or bud neck (Figure 2-1C) (Baldridge & Graham, 2012, 2013; Hua, et al., 2002; Saito, et al., 2004). It is possible that this highly polarized localization is insufficient to restore PM asymmetry. However, using a newer collection of Dnf1 variants, I discovered that one of our NBD-PS transporting Dnf1 variants also transported endogenous PS (Chapter 4). Dnf1 N550S was able to restore PS asymmetry within the plasma membrane of *drs2Δ* cells (Figure 4-1). The localization and expression patterns were similar for this Dnf1 N550S compared to WT Dnf1 and Dnf1[Y618F], so it seemed the localization was not the reason for the inability of Dnf1[Y618F] to restore PS asymmetry. I also noticed that *DNF1-N550S* suppressed the cold-sensitivity of a *drs2Δ* strain. I thought that if we could generate additional Dnf1 alleles capable of suppressing the cold-sensitivity of the *drs2Δ* strain, they may also flip endogenous PS. I targeted mutagenesis to TM1-2, TM3-4 and TM5-6 individually. I did not recover any alleles from TM5-6 that were able to suppress *drs2Δ* cold-sensitivity. Within TM3-4, I only recovered a single new allele in multiple clones, DNF1-V553E, which suppressed *drs2Δ* cold-sensitivity. This interesting because this residue is approximately 1 turn of a helix from Asn550, the impetus for this screen. Within TM1-2, I recovered four substitutions from multiple clones. Three out of four (F213S, T254A, D258E but not A244V) present as different codons for the same amino acid substitution, clearly having arisen independently in the screening

procedure. When I re-introduced these clones into a *drs2Δ* strain, Dnf1 F213S, Dnf1 T254A and Dnf1 D258E each suppressed the cold-sensitivity (Dnf1 A244V did not)(Figure 4-2). Interestingly, these alleles each restored PS asymmetry of a *drs2Δ* strain better than WT Dnf1 but to differing degrees (Figure 4-2). The ability to suppress cold-sensitivity of *drs2Δ* was linked to the flip of endogenous PS.

Phosphatidylserine is important for Drs2 function

One of the best characterized functions of P4-ATPases is their contribution to vesicular-mediated protein trafficking within yeast. However, even though contributions have been reported, a specific role in trafficking is unclear. I tested if the ability to flip PS was important to support Drs2 trafficking functions. Both Dnf1 and Drs2 likely facilitate Snc1 recycling through the Rcy1/Gcs1 pathway (Hua, et al., 2002). Drs2 is a primary contributor because in *drs2Δ*, GFP-Snc1 is trapped within the early endosomal system (Sakane, et al., 2006). A *dnf1Δ* mutant does not strongly mislocalize GFP-Snc1, nor does a *dnf2,3Δ mutant*. However, *dnf1,2Δ* or *dnf1,3Δ* mutants do have a noticeable effect (Hua, et al., 2002). I tested the ability of Drs2 variants deficient in PS flip to support this pathway in a *drs2Δ* strain. Using the different Drs2 alleles, I observed a strong defect with Drs2 mutants having reduced PS activity. When I tested Dnf1 and the Dnf1 alleles with ability to flip PS only Dnf1 variants capable of flipping endogenous PS were able to support Snc1 recycling in a *drs2Δ* strain. Consistent with these results, when PS is removed from the cell in a *cho1Δ* strain, GFP-Snc1 is mislocalized (Figure 4-6). GFP Snc1 localization could be partially restored by supplementation with lyso-PS or DLPS.

Drs2 is distinct from Dnf1 in its ability to support AP-1/clathrin trafficking between the TGN and EE (K. Liu, et al., 2008). I monitored this trafficking event by resistance to CW, which stains chitin deposited around nascent budding sites by Chs3 (Shaw, et al., 1991). In a strain with

disrupted exomer (*chs6Δ*), Chs3 is not trafficked to the cell surface and is retained intracellularly by AP-1 trafficking (Valdivia, et al., 2002; Ziman, et al., 1998). A double knockout strain *chs6Δdrs2Δ* restored sensitivity to CW, because the AP-1 pathway is disrupted, causing Chs3 to move to the PM constitutively (K. Liu, et al., 2008). In each case, the ability to flip endogenous PS with both Dnf1 and Drs2 variants correlated with the ability to restore AP-1 between the TGN and EE (Figure 4-5).

A second unique pathway supported by Drs2 is formation of dense-class secretory vesicles. There does not appear to be a strong kinetic block in secretion of known cargos, although invertase shows a very minor effect which is difficult to detect (Hua, et al., 2002). Until recently, the only experimentally verified way to determine a contribution to dense-class secretory vesicle formation was by using electron microscopy and an epistasis experiment with mutants blocking fusion of the dense-class vesicles. In *sla2Δ* cells, dense-class vesicles accumulate because fusion with the plasma membrane is blocked. However, the dense class vesicles do not accumulate in a *drs2Δsla2Δ* double mutant because they fail to form. Recently, Tsai et al. reported that Drs2 and Arl1 are required for transport of Gas1-RFP to the plasma membrane. In a *drs2Δ* strain this protein was trapped intracellularly (Tsai, et al., 2013). The implication was that Gas1 represented a cargo that actually required the dense-class secretory vesicles. However, I was unable to reproduce this result. In my hands, Gas1 localized to the plasma membrane even in the absence of Drs2. Therefore, I may need to use the epistasis experiment to test the contribution of PS flip to secretion. So far, it seems that the ability to support endogenous PS flip also confers the ability to support Drs2-dependent functions in the anterograde and retrograde pathways.

P4-ATPases use a novel two-gate mechanism

Through the screening procedures described in chapters 2, 3 and 4, we have identified a wide range of residues in two clusters (gates) that are involved in phospholipid selection (Figure 3-13). Having identified residues in both gates that allowed Dnf1 (and Drs2) to flip PS allowed us to test the relationship between the two gates. We found that the gates function in the same transport route so they are likely functioning sequentially. Importantly, the gates seem to act imperfectly at least with the changes we have identified. Restricting PS selection at either the entry or exit gate for PS can be restored by altering the opposing gate to increase PS transport.

An important question for the P4-ATPases is how the E1-E2 cycle is coupled to substrate translocation. The mammalian homologs of Drs2, Atp8a1 and Atp8a2 have both been purified and demonstrate substrate stimulation of ATPase activity. For Drs2, our lab was unable to observe substrate stimulation to the extent observed with Atp8a1 or Atp8a2 (Coleman, et al., 2009; Ding, et al., 2000; Zhou & Graham, 2009). A useful test would be to use a phosphorylation/de-phosphorylation assay described with several P-type ATPases in response to substrate (Bramkamp & Altendorf, 2005; Skou, 1957).

Atp8a1/Atp8a2 have also been shown to autophosphorylate when ATP is added in the absence of substrate, and are then stimulated to dephosphorylate upon substrate addition (Coleman, et al., 2012; Ding, et al., 2000). This dephosphorylation was interpreted as substrate being required to trigger the E2-P → E2 transition. However, the work with Atp8a2 suggested that substrate is actually important for inducing E1-P → E2-P and also perhaps E2-P → E2 transitions. Coleman et al. (2012) made use of a mutation that blocks hydrolysis of the aspartyl-phosphate with Atp8a2 (E198Q) to examine the requirement of substrate for transition between E1-P and E2-P states. In the presence of substrate, Atp8a2 accumulates exclusively in E2-P. In the absence of substrate, the transition from E1-P → E2-P is slower with 75% accumulating in

E2-P. This result is consistent with substrate interacting in the E1-P →E2-P transition, but does not represent an absolute requirement. According to these results, it is formally possible that the substrate is actually functioning both in the E1-P → E2-P transition and to trigger the final dephosphorylation. I propose the E1-P →E2-P step requires phospholipid binding at the entry gate, whereas the E2-P →E2 transition requires phospholipid at the exit gate for dephosphorylation. Testing the flippase activity with Atp8a2 E198Q, Coleman et al. actually saw a reversal in the net transport of NBD-PS. Instead of ~5% NBD-PS flipped to the outer leaflet of liposomes (as with WT Atp8a2), they observed a ~1% transport into the inner leaflet of the liposome (Coleman, et al., 2012). I interpret this to mean that when de-phosphorylation is prevented, the pump may transition from E2-P to E1-P readily (opposite from the normal reaction cycle) moving phospholipid from outer leaflet to inner leaflet between exit and entry gate. In a fully functional pump, the directionality is assured from hydrolysis of the phosphoryl-aspartate (and the net energetic input of ATP hydrolysis).

Consistent with this interpretation, in one of the Ca^{2+} ATPase crystal structures, a phospholipid headgroup actually co-crystallized in the "exit site" within the E2 conformation (stabilized by BHQ (2,5-di-tert-butyl-1,4-dihydroxybenzene) and TG (thapsigargin)). This phospholipid was modeled as PE but it could be a different phospholipid (i.e. PC or PS) with variations in the positioning of the differentiating functional groups (Obara, et al., 2005). The Ca^{2+} ATPase and Na^{+}/K^{+} ATPase each have functional links to phospholipid in their reaction cycle. Both the Ca^{2+} and Na^{+}/K^{+} ATPases require phospholipid for proper function seemingly beyond the membrane anchoring properties (Obara, et al., 2005; Ottolenghi, 1975, 1979). There is some evidence for lipids that form a fairly stable ring around the hydrophobic portion of the transmembrane domain of integral membrane proteins (Belrhali et al., 1999; Jost, Griffith, Capaldi, & Vanderkooi, 1973). These "boundary lipids" are essential components to the

properties of the proteins that are interacting with the membrane domain similar to the way a soluble protein is hydrated in an aqueous solution. In many cases, a specific lipid requirement is not important, the boundary lipids in part help to maintain a seal around the protein, even when dramatic conformational changes occur. However, the Na^+/K^+ ATPase is remarkably specific in its preference for long, unsaturated acyl chains on PS suggesting some boundary lipids serve a specific role (Haviv et al., 2007).

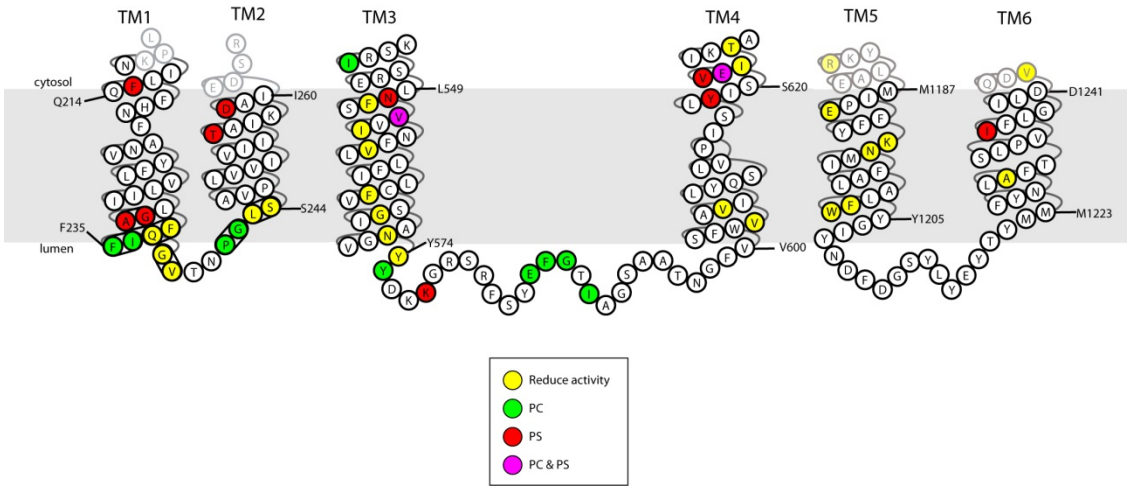

Figure 7-1. Summary of residues involved in substrate selection and transport by P4-ATPases.

Through the use of P4-ATPase chimeras and screening procedures, we have identified 20+ residues in Dnf1 and Drs2 that contribute to phospholipid specificity (Figure 7-1). With unbiased screening procedures, we identified residues determining P4-ATPase specificity as each of the analogous residues coordinating the phospholipid in the E2 Ca^{2+} ATPase structure (Figure 4-10). This seems unlikely to be a coincidence and I think these observations suggest how the P4-ATPases may have evolved from a cation transporter. In the case of the Ca^{2+} ATPase, the phospholipid is likely a boundary lipid that enters and exits the binding site from the cytosolic leaflet. We speculate that P4-ATPases have evolved with the same phospholipid

binding site observed in the Ca^{2+} ATPase, but in the case of the flippases, the phospholipid is loaded from the lumenal leaflet using a new binding site I refer to as the entry gate. With the acquisition of a new substrate that provided a selective advantage to the cell, the selective pressure to maintain the original cation binding site would have been diminished and so this site was eventually lost.

Transport along the TM1-4 groove

The primary barrier to phospholipid flip across a lipid bilayer is the passage of the bulky charged headgroup through the hydrophobic core. Consistent with this notion, diacylglycerol (DAG) a glycerolipid without a charged headgroup is able to spontaneously flip-flop across the membrane with a $t_{1/2}$ of less than one second (Allan, Thomas, & Michell, 1978; Bai & Pagano, 1997; Pagano & Longmuir, 1985). With increasing acyl chain length causing a thickening of the hydrophobic core, the rate of spontaneous flip/flop decreases (Sapay, Bennett, & Tieleman, 2009). Adding a bulky or charged headgroup as in PC, PE and PS slows the rate of spontaneous flip-flip to a $t_{1/2}$ ranging from hours to days (Kornberg & McConnell, 1971; J. Liu & Conboy, 2005). The plasma membrane of eukaryotic cells has a characteristic asymmetry, but "early" membranes of primordial cells would have likely had a symmetric organization. Most lipids are synthesized on the lumenal leaflet of the ER, and a protein dependent but energy independent flip/flop activity helps stabilize the ER membrane as new phospholipids are synthesized (Daleke, 2003). There is evidence that even a single transmembrane segment can facilitate this rapid and spontaneous process. With the antimicrobial peptide Magainin-2, a rapid flip-flop was catalyzed but these membranes seemed to open a water-filled pore, permeable to both ions and lipids (Matsuzaki, Murase, Fujii, & Miyajima, 1996). A more recent report demonstrated this process could happen without formation of a pore. The passage of small ions was not tested, but at least

a “potential” pore was not large enough to allow dithionite passage (Langer, Sah, Veser, Gütlich, & Langosch, 2013). This does not necessarily mean that a single TM-spanning α-helix (or a ring formed by several helices) actually facilitates the flip/flop in a biologically meaningful way. These are model systems with an incredibly high concentration of peptide at ~1 mol% compared to lipid. Interestingly though, this spontaneous flip-flop is sequence dependent and enhanced by charged residues flanking the TM domain.

A key question remaining is how can P4-ATPases transport a phospholipid headgroup across the bilayer? This is an energetically unfavorable process, but so is ion transport and protein translocation, which are also essential for survival. Estimates for the activation energy required to flip a PC molecule across a model POPC bilayer are around 200 kJ/mol depending on the acyl chains (J. Liu & Conboy, 2005). This is significantly greater than the energy gained from hydrolysis of a single ATP (~31 kJ/mol). By shielding the hydrophilic headgroup from the hydrophobic core of a membrane bilayer the activation energy must become manageable. There are at least 3 possibilities for how the TM1-4 groove could support phospholipid translocation. These four helices may open a pore similar to the anti-microbial peptides, they may just destabilize the protein-lipid interface, or create a hydrophilic pathway for the headgroup to be shielded from the membrane core.

Formation of a pore is unlikely because the yeast plasma membrane maintains a proton gradient during the phospholipid transport process. In fact, the proton gradient appears to facilitate NBD-PL uptake across the plasma membrane (Stevens & Nichols, 2007). Additionally, with the *in vitro* assay system, the proteoliposomes are impermeable to dithionite even when transporting phospholipid. General bilayer destabilization also seems unlikely because the flipping process is quite specific and seems to be coupled to ATP hydrolysis. Providing an amenable route from the lumenal to cytosolic leaflet seems to be a plausible explanation for

transport. Consistent with this idea, the properties of the groove between TM1-4 for Dnf1 are quite different from the ion transporting P-type ATPases. The groove for Dnf1 has a greater number of aromatic residues (6/14) compared to the Ca^{2+} (3/18), Na^{+}/K^{+} (2/17), Cu^{2+} (2/20), H^{+} (0/15) ATPases (Figure 7-2A, cyan residues). Additionally, these aromatic residues seem to be clustered near the center of the membrane core; unlike any of the other protein-lipid interface grooves (Figure 7-2B and 7-2C, cyan residues). Many times aromatic residues are found near the aqueous interface within transmembrane segments, and are less frequent within the hydrophobic core of the bilayer itself (Landolt-Marticorena, Williams, Deber, & Reithmeier, 1993). Dnf1 also has two hydrophilic non-aromatic residues along this groove (2/14), further altering the character compared to many of the ion transporters (Ca^{2+} (3/18), Na^{+}/K^{+} (2/17), Cu^{2+} (0/20), H^{+} (0/15) ATPases). The properties of this groove may make it more amenable to moving a phospholipid headgroup.

Assuming the motions observed in the Ca^{2+} ATPase are maintained in the P4-ATPases, by coupling the motion of TM1-2 with phospholipid headgroup interaction, the lipid headgroup could be clamped and shifted up into the membrane within the E1-P to E2-P transition (Figure 1-4 and 3-13). The hydrophilic properties could be shielded by quadrupole moments generated from the stacking of the benzene rings within the aromatic residues. The aromatic rings could be forming a network through stacking, or be rotated 90° acting as paddles, shuffling the lipid through the core. Another possibility is the space created by moving the large rings may open up space for a phospholipid and the quadrupole moments of the benzyl rings could hydrogen bond with the phospholipid headgroup, or water molecules hydrating it. Regardless of the specifics used to transport the substrate, P4-ATPases have evolved to lower the free energy requirements of this process to less than that of an ATP, and are even capable of robust transport at 4°C.

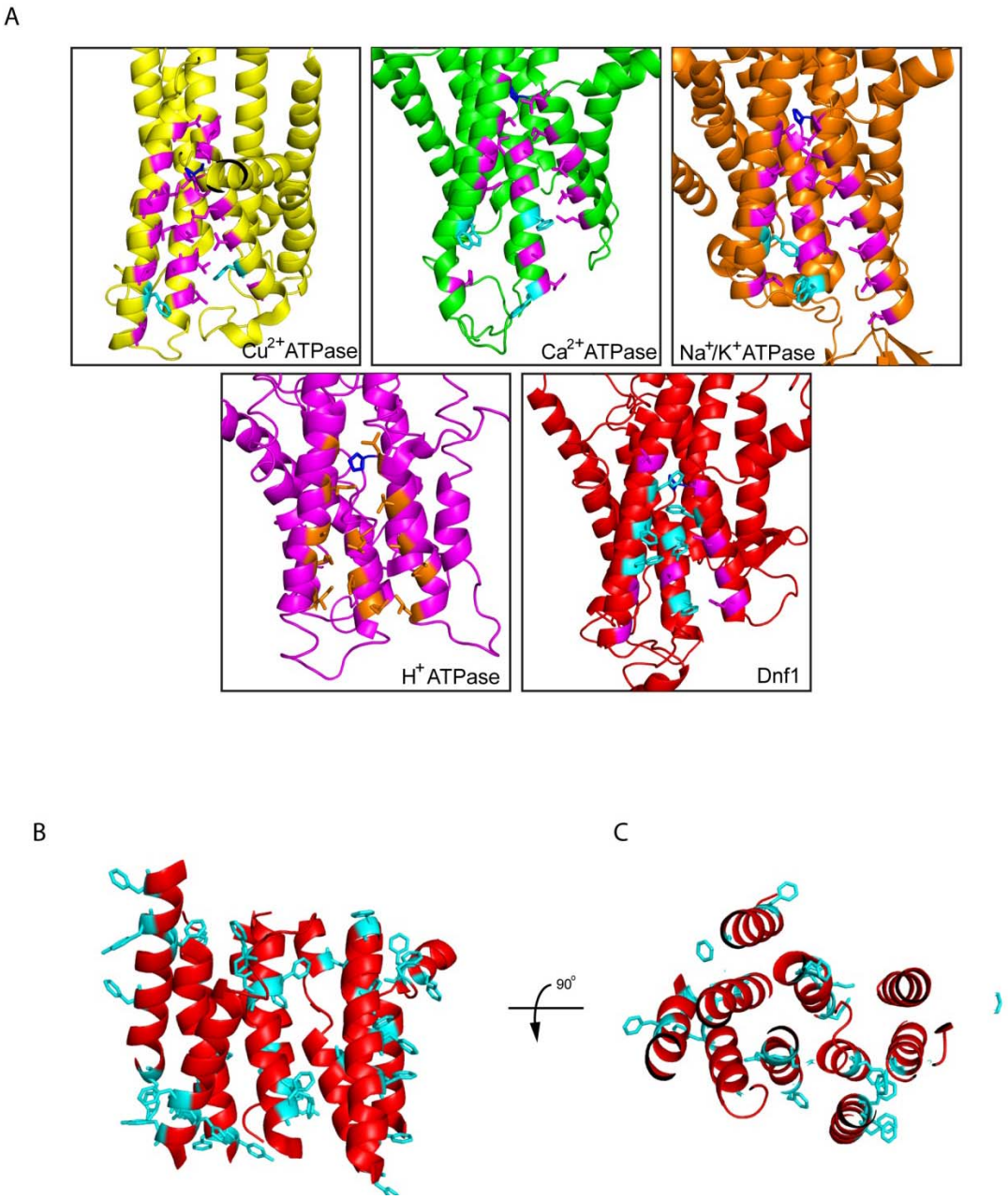

Figure 7-2. Proposed phospholipid transport pathway has a greater number of aromatic residues compared to the ion transporters. (A) Orange/purple residues highlight the propose phospholipid transport pathway. Aromatic residues (Phe, Tyr, Trp) are colored cyan. (B, C) Throughout most of the TM domain of Dnf1, the aromatic are not present in the bilayer core. In the proposed phospholipid transport pathway there is a distinct cluster of aromatic residues within the hydrophobic core.

One caveat for the transport process is the P4-ATPase β-subunits from the Cdc50 family. Based on mutants that stall Drs2 at different places in the reaction cycle, Cdc50 seems to preferentially interact with the E2-P state of Drs2 (but not E1-P). It is possible that this β-subunit plays a role in assuring directionality of the transport process or recognizing a general feature of substrate, but at E2-P the lipid would likely have been selected and perhaps even flipped across the membrane. The Palmgren lab reported the Arabidopsis P4-ATPase specificity and localization does not depend on the β-subunit (López-Marqués, et al., 2010). Our work also partially addresses this question because we were able to change the specificity of Dnf1 without changing the β-subunit, Lem3. But the question still remains, what **is** the function of the β-subunit? Does it perform a function beyond that of a chaperone? Is it an integral part of the transport process? Does it associate with the parts of the P4-ATPase involved in selecting substrate? Regardless, it seems that the β-subunit does not define the specificity of the P4-ATPase complex. To determine the actual contribution to the flippase activity will likely require the purification and reconstitution of both a stoichiometric complex and the complete depletion of the β-subunit.

The proline +4 position

The difference of a single hydroxyl (Tyr vs Phe) at the P+4 position is able to dictate PS transport by Dnf1 and Drs2. How Tyr618 cooperates with other residues (potentially Asn550, Thr254, Asp258 or others) to selectively gate against PS is potentially similar to a mechanism proposed to govern phospholipid passage into the beta-barrel of the lipopolysaccharide (LPS) acyl transferase, PagP. PagP transfers a palmitoyl group from a glycerophospholipid to LPS resulting in palmitoylated lipid A. To specifically select a glycerophospholipid with a palmitoyl group, PagP needs to “measure” the acyl chain length; this is accomplished by moving the lipid

into the center of its beta-barrel. A gate forms between a Tyr residue phenolic hydroxyl and neighboring beta strand by hydrogen bonding to an amide hydrogen. The hydrogen bonding prevents phospholipid acyl chain access to the beta barrel interior. When the Tyr was changed to Phe, the passage of phospholipid increased 2-3 fold. Dnf1 may use the combination of the proline +4 position Tyr hydrogen bonding to another side chain or main chain to specifically restrict PS. The cytosolic PS gate for Drs2 is normally opened but it can be restricted by F511Y. Combining Drs2 N445S,[F511Y] cannot restore PS asymmetry relative to Drs2[F511Y] and actually exacerbates the defect (Figure 3-6E). Drs2 N445S[F511Y] also causes a defect in the PE asymmetry relative to Drs2[F511Y] suggesting this may be due to impaired function caused by excessive changes in the cytosolic exit gate.

The closest mammalian homologs of Drs2, Atp8a1 and Atpa82 have a leucine at the P+4 position. As we reported, a leucine at the P+4 position causes a reduction in activity for both Dnf1 and Drs2. To address this conundrum, we designed a screen to give a clue as to how Atp8a1/2 were able to use a P+4 leucine. We started with Drs2 F511L, mutagenized TM3-4 and selected for Drs2 alleles that could provide resistance to 5µg/mL Papuamide A (PapA). We thought that we would recover a substitution similar to the Dnf1 N550S, which in Dnf1, any substitution seemed to increase PS activity. In this case, the Drs2 N445 mutations were not recovered. Drs2 N445S,F511L does increase resistance to PapB (Figure 5-2), but is unable to increase it to the point where it would have been recovered in the screening procedure (5µg/mL PapA). It was very surprising when we sequenced through ~50 clones, and in each case found a reversion of the F511L back to Phe. Along with the reversion (L511F) we recovered a series of additional mutations, which did not disrupt PS flip by Drs2 (monitored by PapA resistance) and the positions of these substitutions are summarized in Figure 5-4. Based on the frequency of reversion in this PapA resistance screen, it became apparent that other than the reversion, there

is not a single substitution within TM3-4 that can restore PS activity back to WT levels in the presence of a P+4 leucine.

Our recent screen to identify Dnf1 mutants capable of suppressing *drs2Δ* cold-sensitivity has actually provided significant insight into how the P+4 leucine may be used by Atp8a1/2. We identified several Dnf1 mutations that suppressed *drs2Δ* cold-sensitivity. The changes that were identified in Dnf1 were actually substituted for the equivalent Atp8a1 residues at those positions. When we assayed the activity, these variants provided increased NBD-PS and endogenous PS flip (Figure 4-2). When we introduced these substitutions in the context of Dnf1 Y618L or Drs2 F511L (P+4 leucine), these substitutions allowed complementation of the *dnf1,2,3Δdrs2Δ* growth defect (Figure 5-5). In the combinations tested (Dnf1 T254A,Y618L and Dnf1 D258E,Y618L), the NBD-PL uptake activity was restored compared to the Dnf1 Y618L single mutant (data not shown). It appears that with Drs2 containing F511L, the best suppression can actually be produced by substitutions in TM1-2 for residues that are present in Atp8a1/a2 (Figure 5-5). It is worth noting that we have not yet tested the ability to flip PS and restore PapB resistance in a *drs2Δ* strain. In accordance with the improved growth of the double mutants, we expect to see an increased PapB resistance indicating at least partial restoration of PS asymmetry, (similarly to Drs2 N445S, F511L). These data imply a specific coupling between the P + 4 residue and residues within TM 1-2 (Figure 7-3). This observation supports our original suggestion that the P+4 residue is oriented away from the canonical binding site, towards a new substrate binding site formed from TMs 1 – 4.

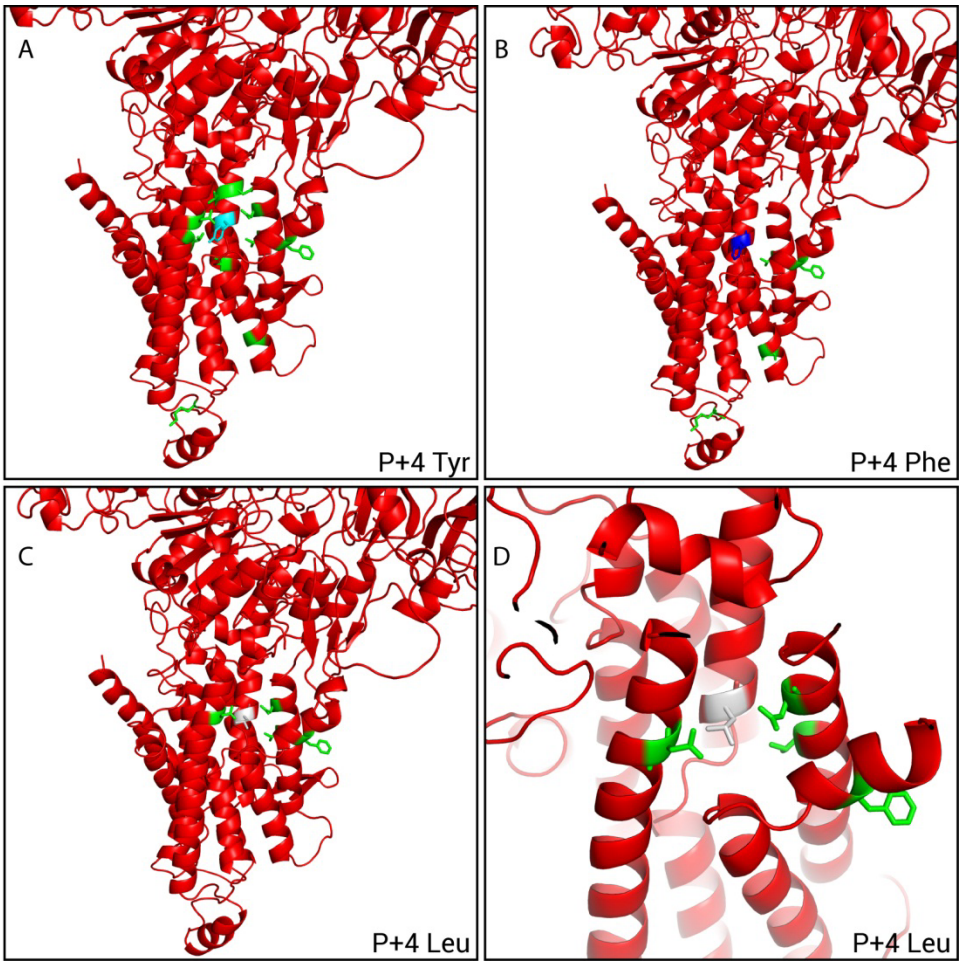

Figure 7-3. Coupling of residues in the P4-ATPase exit gate. (A) in the presence of a P+4 Tyr (cyan), Dnf1 can gain the ability to flip PS with a substitution at the green residues. (B) As in Drs2 with a P+4 Phe the indicated green positions can affect PS transport. (C) With a P+4 Leu (As with Atp8a1) substitution for a Atp8a1 residue at the indicated green positions are critical for PS flip and overall activity.

During the mapping procedure tracking the PS activity, we observed an increased NBD-SM activity by Dnf1[YIS→FVT]. The PS activity mapped exclusively to the first position Y618F substitution and this mutation did not increase NBD-SM uptake. We observed an increased overall activity with Dnf1[YIS→FVS], Dnf1[YIS→FIT], or Dnf1[YIS→FVT] relative to Dnf1[Y618F] (Figure 2-5 and 2-6). However, we did not determine if the enhanced NBD-SM activity mapped to the I619V or S620T substitutions. With the screening procedure designed to identify

additional residues in substrate selection, we recovered a mutation in TM6 (I1235F), which also caused an increased SM activity (along with PS) (Figure 3-6). It w interesting to see if this residue is actually oriented near the Ile619 and S620 residues or near the canonical ion-binding site. A potential reason for the alterations of specificity toward the non-substrate sphingomyelin could be explained by alterations in the packing of TM segments within this region. The packing on the backside of this helix could be affecting the spacing within the phospholipid exit site. This is not unprecedented because the yeast Ca^{2+}/Mn^{2+} ATPase, PMR1, can alter selection of substrate based upon packing of the transmembrane segments relative to one another without affecting residues specifically identified in substrate coordination (D. Mandal, Rulli, & Rao, 2003).

Given the wide range of residues involved in determining substrate specificity for Dnf1 and Drs2 (Tyr, Phe, Aln, Gln, Asp, Glu, Thr, Ser, Lys, His, Ile, Leu, Val, Ala, Gly), we favor a model where the spatial organization of a set of residues defines the specificity of the P4-ATPases. The *in vitro* studies of Dnf1 could help test the two-gate mechanism for phospholipid selection in transport. According to the two-gate model, phospholipid may be positioned within the exit gate region in E2-P, and this position could be trapped with vanadate. If we were able to capture phospholipid within this gate in the presence of vanadate, we could make use of substitutions to change the specificity and detect changes of lipids able to interact. It seems likely we could also change phospholipid binding within the exit gate by altering the entry gate. If we could restrict the ability of phospholipid to enter through the entry gate, we may see an effect on the final binding in the presence of vanadate. It is also possible that the exit gate may be able to "load" without the lipid passing through the entry gate and we may not be able to affect the specificity in this manner. Regardless, the information derived through these analyses would provide useful information for the mechanism of phospholipid binding.

Conclusion

The work presented in this dissertation has radically propelled the P-type ATPase, membrane transporter and membrane trafficking fields forward. The initial goal of identifying residues within a substrate selection site for the P4-ATPases blossomed from a functional study of Dnf1 to a novel transport mechanism for P4-ATPases in general. The variety of tools we generated allowed us to investigate a biological role for flip of specific phospholipids within the membrane trafficking pathways. Future work will be needed to determine if the role of PS flip is critical for generation of curvature, specific lipid interactions of adaptors/coats, or both. The two gate model for phospholipid selection and transport will dramatically benefit from structural information. This insight could come from crosslinking approaches, EPR, or ideally x-ray crystal structures with substrate in each gate.

APPENDIX A

YEAST STRAINS, PLASMIDS AND PRIMERS

Table A1. Yeast strains used in chapter 2

Strain	Genotype	Plasmid	Source
BY4741	MATa *his3Δ1 leu2Δ0 ura3Δ0 met15Δ0*		Invitrogen
BY4742	MATα *his3Δ1 leu2Δ0 ura3Δ0 lys2Δ0*		Invitrogen
PFY3275F	MATa *his3Δ1 leu2Δ0 ura3Δ0 met15Δ0 dnf1Δ dnf2Δ*		(Hua, et al., 2002)
SCY119	*MATα his3Δ1 leu2Δ0 ura3Δ0 met15Δ0 lem3Δ*		This study
ZHY615M2D	MATα *his3Δ1 leu2Δ0 ura3Δ0 lys2Δ0 drs2Δ*		(Hua, et al., 2002)
ZHY709	MATa *his3Δ1 leu2Δ0 ura3Δ0 met15Δ0 dnf1Δ dnf2Δ drs2Δ::LEU2*		(Hua, et al., 2002)
ZHY704	MATα *his3Δ1 leu2Δ0 ura3Δ0 lys2Δ0 dnf1Δ dnf2Δ dnf3Δ drs2Δ::LEU2 pRS416-DRS2*	pRS416-DRS2	(Hua, et al., 2002)
XZY0035	BY4742 *CDC50::KanMX4-GPD atp2 Δ::URA3*		This study
RBY201	ZHY704	pRS313	This study
RBY204	ZHY704	pRS313-DNF1	This study
RBY240	ZHY704	pRS313-Dnf1[TM1-2]	This study
RBY255	ZHY704	pRS313-Dnf1[TM3-4]	This study
RBY2100	ZHY704	pRS313-Dnf1[TM5-6]	This study
RBY2121	ZHY704	pRS313-Dnf1[TM7-10]	This study
RBY2130	ZHY704	pRS313-Dnf1[TM1-10]	This study
RBY264	ZHY704	pRS313-Dnf1[TM3]	This study
RBY267	ZHY704	pRS313-Dnf1[LL3-4]	This study
RBY261	ZHY704	pRS313-Dnf1[TM4]	This study
RBY282	ZHY704	pRS313-Dnf1[WVAV→LTFW]	This study
RBY285	ZHY704	pRS313-Dnf1[YQS→FSN]	This study
RBY288	ZHY704	pRS313-Dnf1[YIS→FVT]	This study
RBY2177	ZHY704	pRS313-Dnf1 Y618F	This study
RBY2180	ZHY704	pRS313-Dnf1 I619V	This study
RBY2183	ZHY704	pRS313-Dnf1 S620T	This study
RBY2308	ZHY704	pRS313-Dnf1 F587Y	This study
RBY2311	ZHY704	pRS313-Dnf1 F587L	This study
RBY2200	ZHY704	pRS313-DRS2	This study
RBY2203	ZHY704	pRS313-Drs2 F511Y	This study
RBY2209	ZHY704	pRS313-Drs2 F511L	This study
RBY2810	SCY119	pRS416-GFP-DNF1 +pRS425-CDC50	This study
RBY2812	SCY119	pRS416-GFP-DNF1 +pRS425-LEM3	This study
RBY2814	SCY119	pRS416-GFP-Dnf1[TM1-2] +pRS425-CDC50	This study
RBY2816	SCY119	pRS416-GFP-Dnf1[TM1-2] +pRS425-LEM3	This study
RBY2818	SCY119	pRS416-GFP-Dnf1[TM3-4] +pRS425-CDC50	This study
RBY2820	SCY119	pRS416-GFP-Dnf1[TM3-4] +pRS425-LEM3	This study
RBY2826	SCY119	pRS416-GFP-Dnf1[TM4] +pRS425-CDC50	This study
RBY2828	SCY119	pRS416-GFP-Dnf1[TM4] +pRS425-LEM3	This study
RBY2838	SCY119	pRS416-GFP-Dnf1[YIS→FVT] +pRS425-CDC50	This study
RBY2840	SCY119	pRS416-GFP-Dnf1[YIS→FVT] +pRS425-LEM3	This study
RBY2842	SCY119	pRS416-GFP-Dnf1 Y618F +pRS425-CDC50	This study
RBY2844	SCY119	pRS416-GFP-Dnf1 Y618F +pRS425-LEM3	This study
RBY3210	XZY0035	pRS313-GPD-TAP2-Drs2	This study
RBY3213	XZY0035	pRS313-GPD-TAP2-Drs2 F511Y	This study
RBY3216	XZY0035	pRS313-GPD-TAP2-Drs2 F511L	This study
RBY3506	ZHY615M2D	pRS313-DNF1	This study
RBY3527	ZHY615M2D	pRS313-Dnf1 Y618F	This study
RBY3901	ZHY615M2D	pRS313	This study
RBY3904	ZHY615M2D	pRS313-DRS2	This study
RBY3907	ZHY615M2D	pRS313-Drs2 F511Y	This study
RBY3913	ZHY615M2D	pRS313-Drs2 F511L	This study
RBY4503	ZHY709	pRS313	This study
RBY4506	ZHY709	pRS313-DRS2	This study

Table A1. Cont.

Strain	Genotype	Plasmid	Source
RBY4509	ZHY709	pRS313-DNF1	This study
RBY4518	ZHY709	pRS313-Dnf1[YIS→FVT]	This study
RBY4521	ZHY709	pRS313-Dnf1 Y618F	This study
RBY501	PFY3275F	pRS416-GFP-DNF1 + pRS425-LEM3	This study
RBY537	PFY3275F	pRS416-GFP-Dnf1[TM1-2] +pRS425-LEM3	This study
RBY565	PFY3275F	pRS416-GFP-Dnf1[TM3-4] +pRS425-LEM3	This study
RBY571	PFY3275F	pRS416-GFP-Dnf1[TM5-6] +pRS425-LEM3	This study
RBY574	PFY3275F	pRS416-GFP-Dnf1[TM7-10] +pRS425-LEM3	This study
RBY577	PFY3275F	pRS416-GFP-Dnf1[TM1-10] +pRS425-LEM3	This study
RBY559	PFY3275F	pRS416-GFP-Dnf1[TM3] +pRS425-LEM3	This study
RBY562	PFY3275F	pRS416-GFP-Dnf1[LL3-4] +pRS425-LEM3	This study
RBY556	PFY3275F	pRS416-GFP-Dnf1[TM4] +pRS425-LEM3	This study
RBY601	PFY3275F	pRS313	This study
RBY604	PFY3275F	pRS313-DNF1	This study
RBY640	PFY3275F	pRS313-Dnf1[TM1-2]	This study
RBY667	PFY3275F	pRS313-Dnf1[TM3-4]	This study
RBY6100	PFY3275F	pRS313-Dnf1[TM5-6]	This study
RBY6121	PFY3275F	pRS313-Dnf1[TM7-10]	This study
RBY6130	PFY3275F	pRS313-Dnf1[TM1-10]	This study
RBY676	PFY3275F	pRS313-Dnf1[TM3]	This study
RBY679	PFY3275F	pRS313-Dnf1[LL3-4]	This study
RBY673	PFY3275F	pRS313-Dnf1[TM4]	This study
RBY682	PFY3275F	pRS313-Dnf1[WVAV→LTFW]	This study
RBY685	PFY3275F	pRS313-Dnf1[YQS→FSN]	This study
RBY688	PFY3275F	pRS313-Dnf1[YIS→FVT]	This study
RBY6151	PFY3275F	pRS313-Dnf1 Y618F	This study
RBY6154	PFY3275F	pRS313-Dnf1 I619V	This study
RBY6157	PFY3275F	pRS313-Dnf1 S620T	This study
RBY6160	PFY3275F	pRS313-Dnf1 Y618L	This study
RBY6200	PFY3275F	pRS313-Dnf1 F587Y	This study
RBY6203	PFY3275F	pRS313-Dnf1 F587L	This study
RBY658	PFY3275F	pRS313-Dnf1[TM1-4]	This study
RBY6172	PFY3275F	pRS313-Dnf1[YIS→YVT]	This study
RBY6175	PFY3275F	pRS313-Dnf1[YIS→FIT]	This study
RBY6178	PFY3275F	pRS313-Dnf1[YIS→FVS]	This study
RBY6503	PFY3275F	pRS313-Flag3-DNF1	This study
RBY6506	PFY3275F	pRS313-Flag3-Dnf1 Y618F	This study
RBY6509	PFY3275F	pRS313-Flag3-Dnf1[YIS→FVT]	This study
RBY9604	PFY3275F	+pRS416-GFP-Drs2 +pRS425-Cdc50 +pRS313	This study
RBY9607	PFY3275F	+pRS416-GFP-Drs2 +pRS425-Cdc50 +pRS313-Dnf1	This study
RBY9610	PFY3275F	+pRS416-GFP-Drs2 +pRS425-Cdc50 +pRS313-Dnf1[TM3-4]	This study
RBY9613	PFY3275F	+pRS416-GFP-Drs2 +pRS425-Cdc50 +pRS313-Dnf1[TM4]	This study
RBY9616	PFY3275F	+pRS416-GFP-Drs2 +pRS425-Cdc50 +pRS313-Dnf1[YIS→FVT]	This study
RBY9619	PFY3275F	+pRS416-GFP-Drs2 +pRS425-Cdc50 +pRS313-Dnf1 Y618F	This study
RBY9701	PFY3275F *lem3Δ::natNT2*		This study
RBY9707	RBY9701	pRS313	This study
RBY9710	RBY9701	pRS313-DNF1	This study
RBY9716	RBY9701	pRS313-Dnf1[TM4]	This study
RBY9719	RBY9701	pRS313-Dnf1[YIS→FVT]	This study
RBY9722	RBY9701	pRS313-Dnf1 Y618F	This study
RBY9750	PFY3275F *cdc50Δ::natNT2*		This study
RBY9756	RBY9750	pRS313	This study
RBY9759	RBY9750	pRS313-DNF1	This study
RBY9765	RBY9750	pRS313-Dnf1[TM4]	This study
RBY9768	RBY9750	pRS313-Dnf1[YIS→FVT]	This study
RBY9771	RBY9750	pRS313-Dnf1 Y618F	This study

Table A2. Plasmids used in chapter 2

Plasmid	Notes	Source
pRS313		(Sikorski & Hieter, 1989)
pRS313-DNF1		(K. Liu, et al., 2007)
pRS313-Dnf1[TM1-2]	N210-I260 replaced with F217-I267 (from Drs2)	This study
pRS313-Dnf1[TM3-4]	I545-S620 replaced with V440-T513 (from Drs2)	This study
pRS313-Dnf1[TM5-6]	L1184-L1240 replaced with I1008-F1064 (from Drs2)	This study
pRS313-Dnf1[TM7-10]	L1271-R1393 replaced with W1095-D1220 (from Drs2)	This study
pRS313-Dnf1[TM1-10]	N210-I260, I545-S620, L1184-L1240, L1271-R1393 replaced with F217-I267, V440-T513, I1008-F1064, W1095-D1220 (from Drs2)	This study
pRS313-Dnf1[TM3]	I545-Y574 replaced with V440-M469 (from Drs2)	This study
pRS313-Dnf1[LL3-4]	Y575-F602 replaced with S470-F495 (from Drs2)	This study
pRS313-Dnf1[TM4]	W603-S620 replaced with L496-T513 (from Drs2)	This study
pRS313-Dnf1[WVAV→LTFW]	W603L, V604T, A605F, V606W	This study
pRS313-Dnf1[YQS→FSN]	Y609F, Q610S, S611N	This study
pRS313-Dnf1[YIS→FVT]	Y618F, I619V, S620T	This study
pRS313-Dnf1 Y618F	Y618F	This study
pRS313-Dnf1 I619V	I619V	This study
pRS313-Dnf1 S620T	S620T	This study
pRS313-Dnf1 Y618L	Y618L	This study
pRS313-Dnf1 F587Y	F587Y	This study
pRS313-Dnf1 F587L	F587L	This study
pRS313-Dnf1[TM1-4]	N210-I260, I545-S620 replaced with F217-I267, V440-T513 (from Drs2)	This study
pRS313-Dnf1[YIS→YVT]	I619V, S620T	This study
pRS313-Dnf1[YIS→FIT]	Y618F, S620T	This study
pRS313-Dnf1[YIS→FVS]	Y618F, I619V	This study
pRS313-DRS2		(Natarajan, et al., 2004)
pRS313-Drs2 F511Y	F511Y	This study
pRS313-Drs2 F511L	F511L	This study
pRS313-Flag3-DNF1	N-terminal 3xFlag fusion, *DNF1* promoter	This study
pRS313-Flag3-Dnf1[YIS→FVT]	Y618F, I619V, S620T	This study
pRS313-Flag3-Dnf1 Y618F	Y618F	This study
pRS416-DRS2		(Hua, et al., 2002)
pRS416-GFP-DNF1	N-terminal GFP fusion, *PRC1* promoter	This study
pRS416-GFP-Dnf1[TM1-2]	N210-I260 replaced with F217-I267 (from Drs2)	This study
pRS416-GFP-Dnf1[TM3-4]	I545-S620 replaced with V440-T513 (from Drs2)	This study
pRS416-GFP-Dnf1[TM5-6]	L1184-L1240 replaced with I1008-F1064 (from Drs2)	This study
pRS416-GFP-Dnf1[TM7-10]	L1271-R1393 replaced with W1095-D1220 (from Drs2)	This study
pRS416-GFP-Dnf1[TM1-10]	N210-I260, I545-S620, L1184-L1240, L1271-R1393 replaced with F217-I267, V440-T513, I1008-F1064, W1095-D1220 (from Drs2)	This study
pRS416-GFP-Dnf1[TM3]	I545-Y574 replaced with V440-M469 (from Drs2)	This study
pRS416-GFP-Dnf1[LL3-4]	Y575-F602 replaced with S470-F495 (from Drs2)	This study
pRS416-GFP-Dnf1[TM4]	W603-S620 replaced with L496-T513 (from Drs2)	This study
pRS416-GFP-Dnf1[YIS→FVT]	Y618F, I619V, S620T	This study
pRS416-GFP-Dnf1 Y618F	Y618F	This study
pRS425-CDC50		(S. Chen, et al., 2006)
pRS425-LEM3		This study

Table A3. Primers used in chapter 2

Primer	Sequence (5'→3')	For creation of constructs
Dnf1(rev)SOE1	AAATTCTTGGAACAAAAATTTTGGTAAGAATGTTAACGGGG	Dnf1[TM1-2]
Dnf1(forw)SOE3	GCCATGAAGGAATGTATCGAAGACTCAAGAAGAACCGTCCTAG	Dnf1[TM1-2]
Dnf1(rev)SOE6	GTTGATAATTTTCTCAACCCTGGACTTCTTGGTGGGTG	Dnf1[TM3-4], Dnf1[TM3]
Dnf1(rev)SOE8	TAGAATCCAAAATGTTAAAAATGAGACGAAACCGTTTGTC	Dnf1[TM4]
Dnf1 (forw) SOE8	ggcttattcttcaaagacTTTTGGGTTGCTGTTATTCTTTACC	Dnf1[LL3-4]
Dnf1(forw)SOE9	ATTTCTCTATTTGTCACCGTGGAGATCATCAAAACTGCACA	Dnf1[TM3-4], Dnf1[TM4]
Dnf1 (rev) SOE10	tttggcatctgcagtagaATATACACCATTTGCAATACCAGAAAC	Dnf1[LL3-4]
Dnf1 (forw) SOE10	attggtaatgttattatgTACGACAAAAAAGGCAGATCAC	Dnf1[TM3]
Dnf1 (rev) SOE11	CAAAATTGCGACAGAAATTCTCTTATAAGACCACCTACCGTGAAC	Dnf1[TM5-6
Dnf1 (forw) SOE13	TTTGTCATTGGTGTATTTGACCAGGACGTGAATGACACA	Dnf1[TM5-6]
Dnf1 (rev) SOE18	ATTAATAATCCATCCCCAGAACTTTCTTTGGTTCCATTCTTTC	Dnf1[TM7-10]
Dnf1 (forw) SOE20	TTTGCACTGGTAAGAGATTTCACATATGACAGTTTTCAAAAATTTTTC	Dnf1[TM7-10]
Dnf1(forw) WVAVmut	AACGGTTTCGTCTCATTTttaacattttggATTCTTTACCAATCTTTA	Dnf1[WVAV→LTFW]
Dnf1(rev) WVAVmut	TAAAGATTGGTAAAGAATccaaaatgttaaAAATGAGACGAAACCGTT	Dnf1[WVAV→LTFW]
Dnf1 (forw) YQSmut	TGGGTTGCTGTTATTCTTTtttcgaaTTTAGTCCCAATCTCTTTG	Dnf1[YQS→FSN]
Dnf1 (rev) YQSmut	CAAAGAGATTGGGACTAAAttcgaaaAAAGAATAACAGCAACCCA	Dnf1[YQS→FSN]
Dnf1 (forw) YISmut	CTTTAGTCCCAATCTCTTTGtttgtcaccGTGGAGATCATCAAAACTGC	Dnf1[YIS→FVT]
Dnf1 (rev) YISmut	GCAGTTTTGATGATCTCCACggtgacaaaCAAAGAGATTGGGACTAAAG	Dnf1[YIS→FVT]
Dnf1(forw)Y618F	CTTTAGTCCCAATCTCTTTGTttATTTCTGTGGAGATCATCAAAAC	Dnf1 Y618F
Dnf1(rev)Y618F	GTTTTGATGATCTCCACAGAAATaaACAAAGAGATTGGGACTAAAG	Dnf1 Y618F
Dnf1(forw)I619V	TAGTCCCAATCTCTTTGTACgtcTCTGTGGAGATCATCAAAAC	Dnf1 I619V
Dnf1(rev)I619V	GTTTTGATGATCTCCACAGAgacGTACAAAGAGATTGGGACTA	Dnf1 I619V
Dnf1(forw)S620T	GTCCCAATCTCTTTGTACATTaccGTGGAGATCATCAAAACTGC	Dnf1 S620T
Dnf1(rev)S620T	GCAGTTTTGATGATCTCCACggtAATGTACAAAGAGATTGGGAC	Dnf1 S620T
Dnf1(forw)Y618L	CTTTAGTCCCAATCTCTTTGTtgATTTCTGTGGAGATCATCAAAAC	Dnf1 Y618L
Dnf1(rev)Y618L	GTTTTGATGATCTCCACAGAAATcaACAAAGAGATTGGGACTAAAG	Dnf1 Y618L
Dnf1(forw)YIS→YVT	CTTTAGTCCCAATCTCTTTGTACgtcaccGTGGAGATCATCAAAACTGC	Dnf1[YIS→YVT]
Dnf1(rev)YIS→YVT	GCAGTTTTGATGATCTCCACggtgacGTACAAAGAGATTGGGACTAAAG	Dnf1[YIS→YVT]
Dnf1(forw)YIS→FIT	CTTTAGTCCCAATCTCTTTGtttATTaccGTGGAGATCATCAAAACTGC	Dnf1[YIS→FIT]
Dnf1(rev)YIS→FIT	GCAGTTTTGATGATCTCCACggtAATaaaCAAAGAGATTGGGACTAAAG	Dnf1[YIS→FIT]
Dnf1(forw)YIS→FVS	CTTTAGTCCCAATCTCTTTGtttgtcTCTGTGGAGATCATCAAAACTGC	Dnf1[YIS→FVS]
Dnf1(rev)YIS→FVS	GCAGTTTTGATGATCTCCACAGAgacaaaCAAAGAGATTGGGACTAAAG	Dnf1[YIS→FVS]
Dnf1(forw) +KpnI	GACGACGGTACCTCTGGAACTTTTCATGGCG	GFP-Dnf1
Dnf1(rev) +KpnI	GACGACGGTACCTATTAATTGTTCTGTTGTGTTCCGA	GFP-Dnf1
Drs2(forw)SOE1	TTAACATTCTTACCAAAATTTTTGTTCCAAGAATTTTCCAAA	Dnf1[TM1-2]
Drs2(rev)SOE3	GGTTCTTCTTGAGTCTTCGATACATTCCTTCATGGCAGAAAC	Dnf1[TM1-2]
Drs2(forw)SOE6	CCCACCAAGAAGTCCAGGGTTGAGAAAATTATCAACAGACAGATTATTC	Dnf1[TM3-4], Dnf1[TM3]
Drs2(forw)SOE8	AACGGTTTCGTCTCATTTTTAACATTTTGGATTCTATTTTCGAATC	Dnf1[TM4]
Drs2 (rev) SOE8	aataacagcaacccaaaaGTCTTTGAAGAATAAGCCAGCCTT	Dnf1[LL3-4]
Drs2(rev)SOE9	AGTTTTGATGATCTCCACGGTGACAAATAGAGAAATAGGAACTAGATTC	Dnf1[TM3-4], Dnf1[TM4]
Drs2 (forw) SOE10	attgcaaatggtgtatatTCTACTGCAGATGCCAAACATTT	Dnf1[LL3-4]
Drs2 (rev) SOE10	tctgccttttttgtcgtaCATAATAACATTACCAATTGAAGAAATTAAAA	Dnf1[TM3]
Drs2 (forw) SOE11	AGGTGGTCTTATAAGAGAATTTCTGTCGCAATTTTGTACTCTTT	Dnf1[TM5-6
Drs2 (rev) SOE13	GTCATTCACGTCCTGGTCAAATACACCAATGACAAAAGGGG	Dnf1[TM5-6]
Drs2 (forw) SOE18	TGGAACCAAAGAAAGTTCTGGGGATGGATTATTAATGGC	Dnf1[TM7-10]
Drs2 (rev) SOE20	AAAACTGTCATATGTGAAATCTCTTACCAGTGCAAAAATTGG	Dnf1[TM7-10]
Drs2 (forw) F511Y	CGAATCTAGTTCCTATTTCTCTATACGTCACCGTTGAATTAATC	Drs2[F511Y]
Drs2 (rev) F511Y	GATTAATTCAACGGTGACGTATAGAGAAATAGGAACTAGATTCG	Drs2[F511Y]
Drs2 (forw) F511L	CGAATCTAGTTCCTATTTCTCTATTgGTCACCGTTGAATTAATC	Drs2[F511L]
Drs2 (rev) F511L	GATTAATTCAACGGTGACcAATAGAGAAATAGGAACTAGATTCG	Drs2[F511L]
Dnf1(forw)@1500	TACTATTAATAACGTTCTGCTTCGTGG	
Dnf1(rev)@2297	CATCTTTGTTGTACTTCACCACTAGC	

Table A4. Yeast strains used in chapter 3

Strain	Genotype	Plasmid	Source
PFY3275F	MATa *his3Δ1 leu2Δ0 ura3Δ0 met15Δ0 dnf1Δ dnf2Δ*		(Hua, et al., 2002)
ZHY615M2D	MATα *his3Δ1 leu2Δ0 ura3Δ0 lys2Δ0 drs2Δ*		(Hua, et al., 2002)
ZHY704	MATα *his3Δ1 leu2Δ0 ura3Δ0 lys2Δ0 dnf1Δ dnf2Δ dnf3Δ drs2Δ::LEU2 pRS416-DRS2*	pRS416-DRS2	(Hua, et al., 2002)
RBY8600	MATα *his3Δ1 leu2Δ0 ura3Δ0 lys2Δ0 dnf1Δ dnf2Δ dnf3Δ drs2Δ::LEU2 lem3Δ::natNT2 pRS416-DRS2*	pRS416-DRS2	This study
RBY201	ZHY704	pRS313	(Baldridge & Graham, 2012)
RBY204	ZHY704	pRS313-DNF1	(Baldridge & Graham, 2012)
RBY3901	ZHY615M2D	pRS313	(Baldridge & Graham, 2012)
RBY3904	ZHY615M2D	pRS313-DRS2	(Baldridge & Graham, 2012)
RBY3907	ZHY615M2D	pRS313-Drs2 [F511Y]	(Baldridge & Graham, 2012)
RBY3916	ZHY615M2D	pRS313-Drs2 N445S	This study
RBY3922	ZHY615M2D	pRS313-Drs2 N445S, [F511Y]	This study
RBY3928	ZHY615M2D	pRS313-Drs2 [Q237G]	This study
RBY3931	ZHY615M2D	pRS313-Drs2 [Q238A]	This study
RBY3934	ZHY615M2D	pRS313-Drs2 [QQ→GA]	This study
RBY3937	ZHY615M2D	pRS313-Drs2 [QQ→GA], N445S	This study
RBY3940	ZHY615M2D	pRS313-Drs2 [QQ→GA], F511Y	This study
RBY3970	ZHY615M2D	pRS313-Drs2 [D473K]	This study
RBY3973	ZHY615M2D	pRS313-Drs2 [QQ→GA], [D473K]	This study
RBY3976	ZHY615M2D	pRS313-Drs2 [D473K], N445S	This study
RBY3979	ZHY615M2D	pRS313-Drs2 [D473K],[F511Y]	This study
RBY3982	ZHY615M2D	pRS313-Drs2 [QQ→GA], [D473K],N445S	This study
RBY501	PFY3275F	pRS416-GFP-DNF1 + pRS425-LEM3	(Baldridge & Graham, 2012)
RBY504	PFY3275F	pRS416-GFP-Dnf1 [GA→QQ] + pRS425-LEM3	This study
RBY580	PFY3275F	pRS416-GFP-Dnf1 N550S + pRS425-LEM3	This study
RBY581	PFY3275F	pRS416-GFP-Dnf1 [Y618F] + pRS425-LEM3	This study
RBY601	PFY3275F	pRS313	(Baldridge & Graham, 2012)
RBY604	PFY3275F	pRS313-DNF1	(3)
RBY640	PFY3275F	pRS313-Dnf1 [TM1-2]	(3)
RBY6206	PFY3275F	pRS313-Dnf1 [TM1]	This study
RBY6209	PFY3275F	pRS313-Dnf1 [TM2]	This study
RBY637	PFY3275F	pRS313-Dnf1 [ROI]	This study
RBY607	PFY3275F	pRS313-Dnf1 [GA→QQ]	This study
RBY610	PFY3275F	pRS313-Dnf1 [FQ→VP]	This study
RBY616	PFY3275F	pRS313-Dnf1 [IF→HV]	This study
RBY619	PFY3275F	pRS313-Dnf1 [GV→SP]	This study
RBY625	PFY3275F	pRS313-Dnf1 [PG→RY]	This study
RBY628	PFY3275F	pRS313-Dnf1 [LS→TT]	This study
RBY6212	PFY3275F	pRS313-Dnf1 [G230Q]	This study
RBY6215	PFY3275F	pRS313-Dnf1 [A231Q]	This study
RBY6218	PFY3275F	pRS313-Dnf1 N550K	This study
RBY6221	PFY3275F	pRS313-Dnf1 N550S	This study
RBY6224	PFY3275F	pRS313-Dnf1 [GA→QQ], N550S	This study
RBY6227	PFY3275F	pRS313-Dnf1 [GA→QQ], [Y618F]	This study
RBY6230	PFY3275F	pRS313-Dnf1 N550S, [Y618F]	This study
RBY6233	PFY3275F	pRS313-Dnf1 [GA→QQ], N550S, [Y618F]	This study
RBY6151	PFY3275F	pRS313-Dnf1 [Y618F]	(Baldridge & Graham, 2012)
RBY6200	PFY3275F	pRS313-Dnf1 F587Y	(Baldridge & Graham, 2012)
RBY6203	PFY3275F	pRS313-Dnf1 F587L	(Baldridge & Graham, 2012)
RBY6503	PFY3275F	pRS313-Flag3-DNF1	(Baldridge & Graham, 2012)
RBY6506	PFY3275F	pRS313-Flag3-Dnf1 [Y618F]	(Baldridge & Graham, 2012)
RBY6512	PFY3275F	pRS313-Flag3-Dnf1 [GA→QQ]	This study
RBY6515	PFY3275F	pRS313-Flag3-Dnf1 N550S	This study

Table A5. Plasmids used in Chapter 3

Plasmid	Notes	Source
pRS313		(Sikorski & Hieter, 1989)
pRS313-DNF1		(K. Liu, et al., 2007)
pRS313-dnf1(w/SfoI)	Dnf1 A3603G, T3604C, T3605C substitutions to create SfoI restriction endonuclease site (SfoI site at position 3600-3605)	This study
pRS313-Dnf1[TM1-2]	Dnf1 N210-I260 replaced with F217-I267 (from Drs2)	(Baldridge & Graham, 2012)
pRS313-Dnf1[TM1]	Dnf1 N210-Q233 replaced with F217-P240 (from Drs2)	This study
pRS313-Dnf1[TM2]	Dnf1 S243-I260 replaced with T250-I267 (from Drs2)	This study
pRS313-Dnf1[ROI]	Dnf1 G230-S243 replaced with Q237-T250 (from Drs2)	This study
pRS313-Dnf1[GA→QQ]	Dnf1 G230Q, A231Q substitutions	This study
pRS313-Dnf1[FQ→VP]	Dnf1 F232V, Q233P substitutions	This study
pRS313-Dnf1[IF→HV]	Dnf1 I234H, F235V substitutions	This study
pRS313-Dnf1[GV→SP]	Dnf1 G236S, V237P substitutions	This study
pRS313-Dnf1[PG→RY]	Dnf1 P240R, G241Y substitutions	This study
pRS313-Dnf1[LS→TT]	Dnf1 L242T, S243T substitutions	This study
pRS313-Dnf1[Y618F]		(Baldridge & Graham, 2012)
pRS313-Dnf1 Y618L		(Baldridge & Graham, 2012)
pRS313 Dnf1 G230Q		This study
pRS313 Dnf1 A231Q		This study
pRS313-Dnf1[GA→QQ], N550S		This study
pRS313-Dnf1[GA→QQ], [Y618F]		This study
pRS313-Dnf1 N550S, [Y618F]		This study
pRS313-Dnf1[GA→QQ], N550S, [Y618F]		This study
pRS313-Dnf1 I545T	3-4 mut	This study
pRS313-Dnf1 N550I	3-4 mut	This study
pRS313-Dnf1 N550K	3-4 mut	This study
pRS313-Dnf1 N550S	3-4 mut	This study
pRS313-Dnf1 N550Y	3-4 mut	This study
pRS313-Dnf1 F551L	3-4 mut	This study
pRS313-Dnf1 I555L	3-4 mut	This study
pRS313-Dnf1 V558E	3-4 mut	This study
pRS313-Dnf1 F565Y	3-4 mut	This study
pRS313-Dnf1 Y575N	3-4 mut	This study
pRS313-Dnf1 Y575S	3-4 mut	This study
pRS313-Dnf1 K578E	3-4 mut	This study
pRS313-Dnf1 F583Y	3-4 mut	This study
pRS313-Dnf1 F583I	3-4 mut	This study
pRS313-Dnf1 F587Y	3-4 mut	(Baldridge & Graham, 2012)
pRS313-Dnf1 F587L	3-4 mut	(Baldridge & Graham, 2012)
pRS313-Dnf1 F587W	3-4 mut	This study
pRS313-Dnf1 I590M	3-4 mut	This study
pRS313-Dnf1 I590N	3-4 mut	This study
pRS313-Dnf1 I590T	3-4 mut	This study
pRS313-Dnf1 V604A	3-4 mut	This study
pRS313-Dnf1 V606A	3-4 mut	This study
pRS313-Dnf1 Y618C	3-4 mut	This study
pRS313-Dnf1 V621A	3-4 mut	This study
pRS313-Dnf1 E622V	3-4 mut	This study
pRS313-Dnf1 I623F	3-4 mut	This study
pRS313-Dnf1 K625Q	3-4 mut	This study
pRS313-Dnf1 R1183G	5-6 mut	This study
pRS313-Dnf1 R1183S	5-6 mut	This study
pRS313-Dnf1 E1190G	5-6 mut	This study
pRS313-Dnf1 N1195D	5-6 mut	This study
pRS313-Dnf1 F1203I	5-6 mut	This study
pRS313-Dnf1 F1203S	5-6 mut	This study
pRS313-Dnf1 W1204R	5-6 mut	This study
pRS313-Dnf1 A1228S	5-6 mut	This study
pRS313-Dnf1 A1228T	5-6 mut	This study
pRS313-Dnf1 I1235F	5-6 mut	This study
pRS313-Dnf1 V1244A	5-6 mut	This study
pRS313-Dnf1 K1194A		This study
pRS313-Dnf1 K1194R		This study
pRS313-Dnf1 K1194E		This study
pRS313-Dnf1 F565A	Alanine scan	This study
pRS313-Dnf1 V566A	Alanine scan	This study
pRS313-Dnf1 S567A	Alanine scan	This study
pRS313-Dnf1 G568A	Alanine scan	This study
pRS313-Dnf1 I569A	Alanine scan	This study
pRS313-Dnf1 N571A	Alanine scan	This study
pRS313-Dnf1 G572A	Alanine scan	This study

pRS313-Dnf1 V573A	Alanine scan	This study
pRS313-Dnf1 Y574A	Alanine scan	This study
pRS313-Dnf1 Y575A	Alanine scan	This study
pRS313-Dnf1 D576A	Alanine scan	This study
pRS313-Dnf1 K577A	Alanine scan	This study
pRS313-Dnf1 K578A	Alanine scan	This study
pRS313-Dnf1 G579A	Alanine scan	This study
pRS313-Dnf1 R580A	Alanine scan	This study
pRS313-Dnf1 S581A	Alanine scan	This study
pRS313-Dnf1 R582A	Alanine scan	This study
pRS313-Dnf1 F583A	Alanine scan	This study
pRS313-Dnf1 S584A	Alanine scan	This study
pRS313-Dnf1 Y585A	Alanine scan	This study
pRS313-Dnf1 E586A	Alanine scan	This study
pRS313-Dnf1 F587A	Alanine scan	This study
pRS313-Dnf1 G588A	Alanine scan	This study
pRS313-Dnf1 T589A	Alanine scan	This study
pRS313-DRS2		(Natarajan, et al., 2004)
pRS313-Drs2 F511Y		(Baldridge & Graham, 2012)
pRS313-Drs2 Q237G		This study
pRS313-Drs2 Q238A		This study
pRS313-Drs2 [QQ→GA]		This study
pRS313-Drs2 N445S		This study
pRS313-Drs2 [QQ→GA], N445S		This study
pRS313-Drs2 N445S, F511Y		This study
pRS313-Drs2 [D473K]		This study
pRS313-Drs2 [QQ→GA], [D473K]		This study
pRS313-Drs2 [D473K], N445S		This study
pRS313-Drs2 [D473K],[F511Y]		This study
pRS313-Drs2 [QQ→GA], [D473K],N445S		This study
pRS313-Flag3-DNF1	N-terminal 3xFlag fusion, DNF1 promoter	(Baldridge & Graham, 2012)
pRS313-Flag3-Dnf1 [GA→QQ]		This study
pRS313-Flag3-Dnf1 N550S		This study
pRS313-Flag3-Dnf1 [Y618F]		(Baldridge & Graham, 2012)
pRS416-DRS2		(Hua, et al., 2002)
pRS416-GFP-DNF1	N-terminal GFP fusion, PRC1 promoter	(Baldridge & Graham, 2012)
pRS416-GFP-Dnf1 [GA→QQ]		This study
pRS416-GFP-Dnf1 N550S		This study
pRS416-GFP-Dnf1 [Y618F]		(Baldridge & Graham, 2012)
pRS425-LEM3		(Baldridge & Graham, 2012)

Table A6. Yeast strains used in Chapters 4,5,6

Strain	Genotype	Plasmid	Source
BY4741	MATa *his3Δ1 leu2Δ0 ura3Δ0 met15Δ0*		Invitrogen
ZHY615M2D	MATα *his3Δ1 leu2Δ0 ura3Δ0 lys2Δ0 drs2Δ*		(Hua, et al. 2002)
KLY022	MATa *his3Δ1 leu2Δ0 ura3Δ0 lys2Δ0 drs2Δ::KanMX6 chs6Δ::KanMX6*		(Liu, et al. 2008)
PFY3275F	MATa *his3Δ1 leu2Δ0 ura3Δ0 met15Δ0 dnf1Δ dnf2Δ*		(Hua, et al. 2002)
ZHY704	MATα *his3Δ1 leu2Δ0 ura3Δ0 lys2Δ0 dnf1Δ dnf2Δ dnf3Δ drs2Δ::LEU2 pRS416-DRS2*		(Hua, et al. 2002)
RBY8700	MATa *his3Δ1 leu2Δ0 ura3Δ0 met15Δ0, cho1Δ::natNT2*		This study
JWY2203	MATα *his3Δ1 leu2Δ0 ura3Δ0 lys2Δ0 cho1Δ::Kanr drs2Δ::LEU2*		(Natarajan, et al., 2004)
RBY3901	ZHY615M2D (*drs2Δ*)	pRS313	(Baldridge and Graham, 2012)
RBY3904	ZHY615M2D (*drs2Δ*)	pRS313-DRS2	(Baldridge and Graham, 2012)
RBY3934	ZHY615M2D (*drs2Δ*)	pRS313-Drs2 [QQ→GA]	(Baldridge and Graham, 2013)
RBY3946	ZHY615M2D (*drs2Δ*)	pRS313-DNF1	(Baldridge and Graham, 2012)
RBY3949	ZHY615M2D (*drs2Δ*)	pRS313-Dnf1 [GA→QQ]	This study
RBY3952	ZHY615M2D (*drs2Δ*)	pRS313-Dnf1 N550S	This study
RBY3958	ZHY615M2D (*drs2Δ*)	pRS313-Dnf1 [Y618F]	This study
RBY3961	ZHY615M2D (*drs2Δ*)	pRS313-Dnf1 [GA→QQ],[Y618F]	This study
RBY3988	ZHY615M2D (*drs2Δ*)	pRS313-Dnf1 F213S	This study
RBY3991	ZHY615M2D (*drs2Δ*)	pRS313-Dnf1 A244V	This study
RBY3994	ZHY615M2D (*drs2Δ*)	pRS313-Dnf1 T254A	This study
RBY3997	ZHY615M2D (*drs2Δ*)	pRS313-Dnf1 D258E	This study
RBY4000	ZHY615M2D (*drs2Δ*)	pRS313-Dnf1 V553E	This study
RBY4048	ZHY615M2D (*drs2Δ*)	pRS423-DNF1 + pRS425-LEM3	This study
RBY4051	ZHY615M2D (*drs2Δ*)	pRS423-Dnf1 [Y618F] + pRS425-LEM3	This study
RBY3913	ZHY615M2D (*drs2Δ*)	pRS313-Drs2 F511L	This study
RBY4030	ZHY615M2D (*drs2Δ*)	pRS313-Drs2 Q220S,F511L	This study
RBY4033	ZHY615M2D (*drs2Δ*)	pRS313-Drs2 S261A,F511L	This study
RBY3925	ZHY615M2D (*drs2Δ*)	pRS313-Drs2 N445S,F511L	This study
RBY4003	ZHY615M2D (*drs2Δ*)	pRS313-Dnf1 Y618L	This study
RBY4006	ZHY615M2D (*drs2Δ*)	pRS313-Dnf1 F213S,Y618L	This study
RBY4009	ZHY615M2D (*drs2Δ*)	pRS313-Dnf1 T254A,Y618L	This study
RBY4012	ZHY615M2D (*drs2Δ*)	pRS313-Dnf1 D258E,Y618L	This study
RBY4015	ZHY615M2D (*drs2Δ*)	pRS313-Dnf1 N550S,Y618L	This study
RBY201	ZHY704 (*dnf1,2,3Δdrs2Δ*)	pRS313	This study
RBY2200	ZHY704 (*dnf1,2,3Δdrs2Δ*)	pRS313-DRS2	This study
RBY2209	ZHY704 (*dnf1,2,3Δdrs2Δ*)	pRS313-Drs2 F511L	This study
RBY2317	ZHY704 (*dnf1,2,3Δdrs2Δ*)	pRS313-Drs2 Q220S,F511L	This study
RBY2320	ZHY704 (*dnf1,2,3Δdrs2Δ*)	pRS313-Drs2 S261A,F511L	This study
RBY2323	ZHY704 (*dnf1,2,3Δdrs2Δ*)	pRS313-Drs2 N445S,F511L	This study
RBY204	ZHY704 (*dnf1,2,3Δdrs2Δ*)	pRS313-DNF1	This study
RBY2326	ZHY704 (*dnf1,2,3Δdrs2Δ*)	pRS313-Dnf1 Y618L	This study
RBY2329	ZHY704 (*dnf1,2,3Δdrs2Δ*)	pRS313-Dnf1 F213S,Y618L	This study
RBY2332	ZHY704 (*dnf1,2,3Δdrs2Δ*)	pRS313-Dnf1 T254A,Y618L	This study
RBY2335	ZHY704 (*dnf1,2,3Δdrs2Δ*)	pRS313-Dnf1 D258E,Y618L	This study
RBY2338	ZHY704 (*dnf1,2,3Δdrs2Δ*)	pRS313-Dnf1 N550S,Y618L	This study
RBY604	PFY3275F (*dnf1,2Δ*)	pRS313-DNF1	This study
RBY6221	PFY3275F (*dnf1,2Δ*)	pRS313-Dnf1 N550S	This study
RBY6236	PFY3275F (*dnf1,2Δ*)	pRS313-Dnf1 F213S	This study
RBY6239	PFY3275F (*dnf1,2Δ*)	pRS313-Dnf1 A244V	This study
RBY6242	PFY3275F (*dnf1,2Δ*)	pRS313-Dnf1 T254A	This study
RBY6245	PFY3275F (*dnf1,2Δ*)	pRS313-Dnf1 D258E	This study
RBY6248	PFY3275F (*dnf1,2Δ*)	pRS313-Dnf1 V553E	This study
RBY4900	GWY2203 (*cho1Δdrs2Δ)*	pRS416-GFP-LactC2	This study
RBY4906	GWY2203 (*cho1Δdrs2Δ)*	pRS416-GFP-LactC2 +pRS313	This study
RBY4915	GWY2203 (*cho1Δdrs2Δ)*	pRS416-GFP-LactC2 +pRS313-DNF1	This study
RBY4918	GWY2203 (*cho1Δdrs2Δ)*	pRS416-GFP-LactC2 +pRS313-Dnf1-N550S	This study
RBY4921	GWY2203 (*cho1Δdrs2Δ)*	pRS416-GFP-LactC2 +pRS313-Dnf1-[Y618F]	This study
RBY4924	GWY2203 (*cho1Δdrs2Δ)*	pRS416-GFP-LactC2 +pRS313-Dnf1-T254A	This study
RBY4909	GWY2203 (*cho1Δdrs2Δ)*	pRS416-GFP-LactC2 +pRS313-DRS2	This study
RBY4912	GWY2203 (*cho1Δdrs2Δ)*	pRS416-GFP-LactC2 +pRS313-Drs2[QQ→GA]	This study
RBY4104	ZHY615M2D (*drs2Δ*)	pRS416 GFP SNC1 + pRS313	This study
RBY4107	ZHY615M2D (*drs2Δ*)	pRS416 GFP SNC1 + pRS313 DRS2	This study
RBY4115	ZHY615M2D (*drs2Δ*)	pRS416 GFP SNC1 + pRS313 Drs2 [QQ→GA]	This study
RBY4133	ZHY615M2D (*drs2Δ*)	pRS416 GFP SNC1 + pRS313 DNF1	This study
RBY4139	ZHY615M2D (*drs2Δ*)	pRS416 GFP SNC1 + pRS313 Dnf1 N550S	This study
RBY8401	KLY022 (*chs6Δdrs2Δ*)	pRS313	This study

Table A6. Cont.

Strain	Genotype	Plasmid	Source
RBY8404	KLY022 (*chs6Δdrs2Δ*)	pRS313 DRS2	This study
RBY8413	KLY022 (*chs6Δdrs2Δ*)	pRS313 Drs2 [QQ→GA]	This study
RBY8419	KLY022 (*chs6Δdrs2Δ*)	pRS313 DNF1	This study
RBY8425	KLY022 (*chs6Δdrs2Δ*)	pRS313 Dnf1 N550S	This study
RBY8706	RBY8700 (*cho1Δ*)	pRS416-GFP-SNC1	This study
RBY8721	RBY8700 (*cho1Δ*)	pNS571 (GFP-SNC1-PM URA3) integrating	This study
RBY4303	ZHY615M2D (*drs2Δ*)	pNS571 (GFP-SNC1-PM URA3) integrating	This study
RBY8801	rcy1Δ (matα) KO collection	pRS313	This study
RBY8804	rcy1Δ (matα) KO collection	pRS313 DRS2	This study
RBY8807	rcy1Δ (matα) KO collection	pRS313 DNF1	This study
RBY8810	rcy1Δ (matα) KO collection	pRS313 Dnf1 N550S	This study
RBY8813	rcy1Δ (matα) KO collection	pRS313 Dnf1 F213S	This study
RBY8816	rcy1Δ (matα) KO collection	pRS313 Dnf1 T254A	This study
RBY8819	rcy1Δ (matα) KO collection	pRS313 Dnf1 D258E	This study
RBY8822	rcy1Δ (matα) KO collection	pRS313 Dnf1 V553E	This study

Table A7. Plasmids used in Chapters 4,5,6

Plasmid	Notes	Source
pRS313		(Sikorski and Hieter, 1989)
pRS313-DRS2		(Natarajan, et al. 2006)
pRS313-Drs2 [QQ→GA]		(Baldridge and Graham, 2013)
pRS313-Drs2 F511L		(Baldridge and Graham, 2012)
pRS313-Drs2 Q220S,F511L		This study
pRS313-Drs2 S261A,F511L		This study
pRS313-Drs2 N445S,F511L		This study
pRS313-DNF1		(Liu, et al., 2007)
pRS313-Dnf1 [GA→QQ]		(Baldridge and Graham, 2013)
pRS313-Dnf1 N550S		(Baldridge and Graham, 2013)
pRS313-Dnf1 [Y618F]		(Baldridge and Graham, 2012)
pRS313-Dnf1 F213S		This study
pRS313-Dnf1 A244V		This study
pRS313-Dnf1 T254A		This study
pRS313-Dnf1 D258E		This study
pRS313-Dnf1 V553E		This study
pRS313-Dnf1 Y618L		(Baldridge and Graham, 2012)
pRS313-Dnf1 F213S,Y618L		This study
pRS313-Dnf1 T254A,Y618L		This study
pRS313-Dnf1 D258E,Y618L		This study
pRS313-Dnf1 N550S,Y618L		This study
pRS423-DNF1		This study
pRS423-Dnf1[Y618F]		This study
pRS425-LEM3		(Baldridge and Graham, 2012)
pRS416-GFP-LactC2		(Yeung, et al., 2012)

REFERENCES

Albers, R. W., Fahn, S., & Koval, G. J. (1963). The role of sodium ions in the activation of electrophorus electric organ adenosine triphosphatase. *Proceedings of the National Academy of Sciences, 50*(3), 474-481.

Alder-Baerens, N., Lisman, Q., Luong, L., Pomorski, T., & Holthuis, J. C. M. (2006). Loss of P4 ATPases Drs2p and Dnf3p disrupts aminophospholipid transport and asymmetry in yeast post-Golgi secretory vesicles. *Molecular Biology of the Cell, 17*, 1632-1642.

Allan, D., Thomas, P., & Michell, R. H. (1978). Rapid transbilayer diffusion of 1,2-diacylglycerol and its relevance to control of membrane curvature. [10.1038/276289a0]. *Nature, 276*(5685), 289-290.

Arnold, K., Bordoli, L., Kopp, J., & Schwede, T. (2006). The SWISS-MODEL workspace: a web-based environment for protein structure homology modelling. *Bioinformatics, 22*(2), 195-201.

Atkinson, K., Fogel, S., & Henry, S. A. (1980). Yeast mutant defective in phosphatidylserine synthesis. *Journal of Biological Chemistry, 255*(14), 6653-6661.

Atkinson, K. D., Jensen, B., Kolat, A. I., Storm, E. M., Henry, S. A., & Fogel, S. (1980). Yeast mutants auxotrophic for choline or ethanolamine. *Journal of Bacteriology, 141*(2), 558-564.

Auland, M. E., Roufogalis, B. D., Devaux, P. F., & Zachowski, A. (1994). Reconstitution of ATP-dependent aminophospholipid translocation in proteoliposomes. *Proceedings of the National Academy of Sciences of the United States of America, 91*(23), 10938-10942.

Axelsen, K. B., & Palmgren, M. G. (1998). Evolution of substrate specificities in the P-Type ATPase superfamily. *Journal of Molecular Evolution, 46*(1), 84-101.

Bai, J., & Pagano, R. E. (1997). Measurement of Spontaneous Transfer and Transbilayer Movement of BODIPY-Labeled Lipids in Lipid Vesicles†. *Biochemistry, 36*(29), 8840-8848. doi: 10.1021/bi970145r

Baldridge, R. D., & Graham, T. R. (2012). Identification of residues defining phospholipid flippase substrate specificity of type IV P-type ATPases. *Proceedings of the National Academy of Sciences of the United States of America, 109*(6), E290-E298. doi: 10.1073/pnas.1115725109

Baldridge, R. D., & Graham, T. R. (2013). Two gate mechanism for phospholipid selection and transport by type-IV P-type ATPases. *Proceedings of the National Academy of Sciences, 110*(5), E358-E367. doi: 10.1073/pnas.1216948110

Bänziger, C., Soldini, D., Schütt, C., Zipperlen, P., Hausmann, G., & Basler, K. (2006). Wntless, a Conserved Membrane Protein Dedicated to the Secretion of Wnt Proteins from Signaling Cells. *Cell, 125*(3), 509-522.

Belenkaya, T. Y., Wu, Y., Tang, X., Zhou, B., Cheng, L., Sharma, Y. V., . . . Lin, X. (2008). The Retromer Complex Influences Wnt Secretion by Recycling Wntless from Endosomes to the Trans-Golgi Network. *Developmental Cell, 14*(1), 120-131.

Belrhali, H., Nollert, P., Royant, A., Menzel, C., Rosenbusch, J. P., Landau, E. M., & Pebay-Peyroula, E. (1999). Protein, lipid and water organization in bacteriorhodopsin crystals: a molecular view of the purple membrane at 1.9 Å resolution. *Structure (London, England : 1993), 7*(8), 909-917.

Blankman, J. L., Long, J. Z., Trauger, S. A., Siuzdak, G., & Cravatt, B. F. (2013). ABHD12 controls brain lysophosphatidylserine pathways that are deregulated in a murine model of the neurodegenerative disease PHARC. *Proceedings of the National Academy of Sciences, 110*(4), 1500-1505. doi: 10.1073/pnas.1217121110

Bogan, J. S., & Kandror, K. V. (2010). Biogenesis and regulation of insulin-responsive vesicles containing GLUT4. *Current Opinion in Cell Biology, 22*(4), 506-512. doi: 10.1016/j.ceb.2010.03.012

Bramkamp, M., & Altendorf, K. (2005). Single Amino Acid Substitution in the Putative Transmembrane Helix V in KdpB of the KdpFABC Complex of Escherichia coli Uncouples ATPase Activity and Ion Transport†. *Biochemistry, 44*(23), 8260-8266. doi: 10.1021/bi050135n

Bryde, S., Hennrich, H., Verhulst, P. M., Devaux, P. F., Lenoir, G., & Holthuis, J. C. (2010). CDC50 proteins are critical components of the human class-1 P4-ATPase transport machinery. *Journal of Biological Chemistry*.

Buch-Pedersen, M. J., & Palmgren, M. G. (2003). Conserved Asp684 in Transmembrane Segment M6 of the Plant Plasma Membrane P-type Proton Pump AHA2 Is a Molecular Determinant of Proton Translocation. *Journal of Biological Chemistry, 278*(20), 17845-17851. doi: 10.1074/jbc.M212729200

Buch-Pedersen, M. J., Venema, K., Serrano, R., & Palmgren, M. G. (2000). Abolishment of Proton Pumping and Accumulation in the E 1P Conformational State of a Plant Plasma Membrane H+-ATPase by Substitution of a Conserved Aspartyl Residue in Transmembrane Segment 6. *Journal of Biological Chemistry, 275*(50), 39167-39173. doi: 10.1074/jbc.M007537200

Bull, L. N., van Eijk, M. J., Pawlikowska, L., DeYoung, J. A., Juijn, J. A., Liao, M., . . . Freimer, N. B. (1998). A gene encoding a P-type ATPase mutated in two forms of hereditary cholestasis. *Nature Genetics, 18*, 219-224.

Cadwell, R. C., & Joyce, G. F. (1992). Randomization of genes by PCR mutagenesis. *Genome Research, 2*(1), 28-33. doi: 10.1101/gr.2.1.28

Cai, S.-Y., Gautam, S., Nguyen, T., Soroka, C. J., Rahner, C., & Boyer, J. L. (2009). ATP8B1 Deficiency Disrupts the Bile Canalicular Membrane Bilayer Structure in Hepatocytes, But FXR Expression and Activity Are Maintained. *Gastroenterology, 136*(3), 1060-1069.e1064. doi: 10.1053/j.gastro.2008.10.025

Charnock, J. S., & Post, R. L. (1963). Evidence of the Mechanism of Ouabain Inhibition of Cation Activated Adenosine Triphosphatase. [10.1038/199910a0]. *Nature, 199*(4896), 910-911.

Chen, B., Jiang, Y., Zeng, S., Yan, J., Li, X., Zhang, Y., . . . Wang, X. (2010). Endocytic Sorting and Recycling Require Membrane Phosphatidylserine Asymmetry Maintained by TAT-1/CHAT-1. *PLoS Genetics, 6*(12), e1001235. doi: 10.1371/journal.pgen.1001235

Chen, C. Y., & Graham, T. R. (1998). An arf1Delta synthetic lethal screen identifies a new clathrin heavy chain conditional allele that perturbs vacuolar protein transport in Saccharomyces cerevisiae. *Genetics, 130*(2), 577-589.

Chen, C. Y., Ingram, M. F., Rosal, P. H., & Graham, T. R. (1999). Role for Drs2p, a P-Type ATPase and Potential Aminophospholipid Translocase, in Yeast Late Golgi Function. *Journal of Cell Biology, 147*(6), 1223-1236.

Chen, S., Wang, J., Muthusamy, B.-P., Liu, K., Zare, S., Andersen, R. J., & Graham, T. R. (2006). Roles for the Drs2p-Cdc50p complex in protein transport and phosphatidylserine asymmetry of the yeast plasma membrane. *Traffic, 7*, 1503-1517.

Clarke, D. M., Loo, T. W., Inesi, G., & MacLennan, D. H. (1989). Location of high affinity Ca2+-binding sites within the predicted transmembrane domain of the sarcoplasmic reticulum Ca2+-ATPase. *Nature, 339*(6224), 476-478.

Coleman, J. A., Kwok, M. C. M., & Molday, R. S. (2009). Localization, purification, and functional reconstitution of the P4-ATPase Atp8a2, a phosphatidylserine flippase in photoreceptor disc membranes. *Journal of Biological Chemistry, 284*(47), 32670-32679.

Coleman, J. A., & Molday, R. S. (2011). Critical Role of the β-Subunit CDC50A in the Stable Expression, Assembly, Subcellular Localization, and Lipid Transport Activity of the P4-ATPase ATP8A2. *Journal of Biological Chemistry, 286*(19), 17205-17216. doi: 10.1074/jbc.M111.229419

Coleman, J. A., Vestergaard, A. L., Molday, R. S., Vilsen, B., & Peter Andersen, J. (2012). Critical role of a transmembrane lysine in aminophospholipid transport by mammalian photoreceptor P4-ATPase ATP8A2. *Proceedings of the National Academy of Sciences of the United States of America, 109*(5), 1449-1454. doi: 10.1073/pnas.1108862109

Cooper, A. A., & Stevens, T. H. (1996). Vps10p cycles between the late-Golgi and prevacuolar compartments in its function as the sorting receptor for multiple yeast vacuolar hydrolases. *The Journal of Cell Biology, 133*(3), 529-541. doi: 10.1083/jcb.133.3.529

Costaguta, G., Stefan, C. J., Bensen, E. S., Emr, S. D., & Payne, G. S. (2001). Yeast Gga Coat Proteins Function with Clathrin in Golgi to Endosome Transport. *Molecular Biology of the Cell, 12*(6), 1885-1896.

Daleke, D. L. (2003). Regulation of transbilayer plasma membrane phospholipid asymmetry. [Review]. *Journal of Lipid Research, 44*(2), 233-242.

Daleke, D. L. (2007). Phospholipid Flippases. [Review]. *Journal of Biological Chemistry, 282*(2), 821-825.

Daleke, D. L., & Huestis, W. H. (1985). Incorporation and translocation of aminophospholipids in human erythrocytes. *Biochemistry, 24*(20), 5406-5416.

Daleke, D. L., & Huestis, W. H. (1989). Erythrocyte morphology reflects the transbilayer distribution of incorporated phospholipids. *Journal of Cell Biology, 108*(4), 1375-1385. doi: 10.1083/jcb.108.4.1375

Dean, M., & Annilo, T. (2005). Evolution of the ATP-binding cassette (ABC) transporter superfamily in vertebrates. *Annual Review of Genomics and Human Genetics, 6*(1), 123-142. doi: doi:10.1146/annurev.genom.6.080604.162122

Decottignies, A., Grant, A. M., Nichols, J. W., de Wet, H., McIntosh, D. B., & Goffeau, A. (1998). ATPase and Multidrug Transport Activities of the Overexpressed Yeast ABC Protein Yor1p. *Journal of Biological Chemistry, 273*(20), 12612-12622. doi: 10.1074/jbc.273.20.12612

Dhar, M. S., Sommardahl, C. S., Kirkland, T., Nelson, S., Donnell, R., Johnson, D. K., & Castellani, L. W. (2004). Mice heterozygous for Atp10c, a putative amphipath, represent a novel model of obesity and type 2 diabetes. *Journal of Nutrition, 134*(4), 799-805.

Ding, J., Wu, Z., Crider, B. P., Ma, Y., Li, X., Slaughter, C., . . . Xie, X. S. (2000). Identification and Functional Expression of Four Isoforms of ATPase II, the Putative Aminophospholipid Translocase. *Journal of Biological Chemistry, 275*(30), 23378-23386. doi: 10.1074/jbc.M910319199

Duncan, J. R., & Kornfeld, S. (1988). Intracellular movement of two mannose 6-phosphate receptors: return to the Golgi apparatus. *The Journal of Cell Biology, 106*(3), 617-628. doi: 10.1083/jcb.106.3.617

Emoto, K., Kobayashi, T., Yamaji, A., Aizawa, H., Yahara, I., Inoue, K., & Umeda, M. (1996). Redistribution of phosphatidylethanolamine at the cleavage furrow of dividing cells during cytokinesis. *Proceedings of the National Academy of Sciences of the United States of America, 93*(23), 12867-12872.

Emre Onat, O., Gulsuner, S., Bilguvar, K., Nazli Basak, A., Topaloglu, H., Tan, M., . . . Ozcelik, T. (2012). Missense mutation in the ATPase, aminophospholipid transporter protein ATP8A2 is associated with cerebellar atrophy and quadrupedal locomotion. *European Journal of Human Genetics*. doi: 10.1038/ejhg.2012.170

Fairn, G. D., Hermansson, M., Somerharju, P., & Grinstein, S. (2011). Phosphatidylserine is polarized and required for proper Cdc42 localization and for development of cell polarity. [10.1038/ncb2351]. *Nat Cell Biol, 13*(12), 1424-1430. doi: 10.1038/ncb2351

Furuta, N., Fujimura-Kamada, K., Saito, K., Yamamoto, T., & Tanaka, K. (2007). Endocytic recycling in yeast is regulated by putative phospholipid translocases and the Ypt31p/32p-Rcy1p pathway. *Molecular Biology of the Cell, 18*(1), 295-312.

Gall, W. E., Geething, N. C., Hua, Z., Ingram, M. F., Liu, K., Chen, S. I., & Graham, T. R. (2002). Drs2p dependent formation of exocytic clathrin-coated vesicles in vivo. . *Current Biology, 12*, 1623-1627. doi: 10.1016/S0960-9822(00)00771-5

Gall, W. E., Higginbotham, M. A., Chen, C.-Y., Ingram, M. F., Cyr, D. M., & Graham, T. R. (2000). The auxilin-like phosphoprotein Swa2p is required for clathrin function in yeast. *Current Biology, 10*(21), 1349-1358. doi: 10.1016/S0960-9822(00)00771-5

Ghosh, R. N., Mallet, W. G., Soe, T. T., McGraw, T. E., & Maxfield, F. R. (1998). An Endocytosed TGN38 Chimeric Protein Is Delivered to the TGN after Trafficking through the Endocytic Recycling Compartment in CHO Cells. *The Journal of Cell Biology, 142*(4), 923-936. doi: 10.1083/jcb.142.4.923

Gietz, R. D., & Schiestl, R. H. (2007). High-efficiency yeast transformation using the LiAc/SS carrier DNA/PEG method. *Nat Protoc, 2*(1), 31-34.

Gietz, R. D., & Woods, R. A. (2006). Yeast transformation by the LiAc/SS Carrier DNA/PEG method. *Methods Mol Biol, 313*, 107-120. doi: 10.1385/1-59259-958-3:107

González-Guerrero, M., Eren, E., Rawat, S., Stemmler, T. L., & Argüello, J. M. (2008). Structure of the Two Transmembrane Cu+ Transport Sites of the Cu+-ATPases. *Journal of Biological Chemistry, 283*(44), 29753-29759. doi: 10.1074/jbc.M803248200

Gourdon, P., Liu, X.-Y., Skjorringe, T., Morth, J. P., Moller, L. B., Pedersen, B. P., & Nissen, P. (2011). Crystal structure of a copper-transporting PIB-type ATPase. *Nature, 475*(7354), 59-64. doi: doi:10.1038/nature10191

Graf, E., & Penniston, J. T. (1981). CaATP: the substrate, at low ATP concentrations, of Ca2+ ATPase from human erythrocyte membranes. *Journal of Biological Chemistry, 256*(4), 1587-1592.

Graham, T. R. (2001). Metabolic labeling and immunoprecipitation of yeast proteins. *Curr Protoc Cell Biol, Chapter 7*, Unit 7 6. doi: 10.1002/0471143030.cb0706s06

Graham, T. R. (2004). Flippases and vesicle-mediated protein transport. [Review]. *Trends in Cell Biology, 14*(12), 670-677.

Graham, T. R., & Kozlov, M. M. (2010). Interplay of proteins and lipids in generating membrane curvature. *Curr Opin Cell Biol*.

Graham, T. R., Seeger, M., Payne, G. S., MacKay, V. L., & Emr, S. D. (1994). Clathrin-dependent localization of alpha 1,3 mannosyltransferase to the Golgi complex of Saccharomyces cerevisiae. *The Journal of Cell Biology, 127*(3), 667-678. doi: 10.1083/jcb.127.3.667

Hachiro, T., Yamamoto, T., Nakano, K., & Tanaka, K. (2012). Phospholipid flippases Lem3p-Dnf1p and Lem3p-Dnf2p are involved in the sorting of the tryptophan permease Tat2p in yeast. *Journal of Biological Chemistry*. doi: 10.1074/jbc.M112.416263

Hanson, P. K., Malone, L., Birchmore, J. L., & Nichols, J. W. (2003). Lem3p Is essential for the uptake and potency of alkylphosphocholine drugs, edelfosine and miltefosine. *Journal of Biological Chemistry, 278*(38), 36041-36050. doi: 10.1074/jbc.M305263200

Hanson, P. K., & Nichols, J. W. (2001). Energy-dependent flip of fluorescence-labeled phospholipids is regulated by nutrient starvation and transcription factors, PDR1 and PDR3. *Journal of Biological Chemistry, 276*(13), 9861-9867.

Harsay, E., & Bretscher, A. (1995). Parallel secretory pathways to the cell surface in yeast. *Journal of Cell Biology, 131*, 297-310.

Haviv, H., Cohen, E., Lifshitz, Y., Tal, D. M., Goldshleger, R., & Karlish, S. J. D. (2007). Stabilization of Na+,K+-ATPase Purified from Pichia pastoris Membranes by Specific Interactions with Lipids†. *Biochemistry, 46*(44), 12855-12867. doi: 10.1021/bi701248y

Hopkins, D. B., Sato, K., Nakano, A., & Graham, T. R. (2000). Introduction of Kex2 cleavage sites in fusion proteins for monitoring localization and transport in yeast secretory pathway. In S. D. E. Jeremy Thorner & N. A. John (Eds.), *Methods in Enzymology* (Vol. Volume 327, pp. 107-118): Academic Press.

Hua, Z., Fatheddin, P., & Graham, T. R. (2002). An essential subfamily of Drs2p-related P-type ATPases is required for protein trafficking between Golgi complex and endosomal/vacuolar system. *Molecular Biology of the Cell, 13*, 3162-3177.

Jain, S., Stanford, N., Bhagwat, N., Seiler, B., Costanzo, M., Boone, C., & Oelkers, P. (2007). Identification of a Novel Lysophospholipid Acyltransferase in Saccharomyces cerevisiae. *Journal of Biological Chemistry, 282*(42), 30562-30569. doi: 10.1074/jbc.M706326200

Jost, P. C., Griffith, O. H., Capaldi, R. A., & Vanderkooi, G. (1973). Evidence for Boundary Lipid in Membranes. *Proceedings of the National Academy of Sciences, 70*(2), 480-484.

Juliano, R. L., & Ling, V. (1976). A surface glycoprotein modulating drug permeability in Chinese hamster ovary cell mutants. *Biochimica et Biophysica Acta (BBA) - Biomembranes, 455*(1), 152-162. doi: 10.1016/0005-2736(76)90160-7

Kato, U., Emoto, K., Fredriksson, C., Nakamura, H., Ohta, A., Kobayashi, T., . . . Umeda, M. (2002). A novel membrane protein, Ros3p, is required for phospholipid translocation across the plasma membrane in Saccharomyces cerevisiae. *Journal of Biological Chemistry, 277*, 37855-37862.

Kato, U., Inadome, H., Yamamoto, M., Emoto, K., Kobayashi, T., & Umeda, M. (2012). Role for phospholipid flippase complex of ATP8A1 and CDC50A in cell migration. *Journal of Biological Chemistry*. doi: 10.1074/jbc.M112.402701

Kean, L. S., Fuller, R. S., & Nichols, J. W. (1993). Retrograde lipid traffic in yeast: identification of two distinct pathways for internalization of fluorescent-labeled phosphatidylcholine from the plasma membrane. *Journal of Cell Biology, 123*, 1403-1419.

Kiefer, F., Arnold, K., Künzli, M., Bordoli, L., & Schwede, T. (2009). The SWISS-MODEL Repository and associated resources. *Nucleic Acids Research*(37), D387-392.

Kornberg, R. D., & McConnell, H. M. (1971). Inside-outside transitions of phospholipids in vesicle membranes. *Biochemistry, 10*, 1111-1120.

Kuhlbrandt, W. (2004). Biology, structure and mechanism of P-type ATPases. [Review]. *Nat Rev Mol Cell Biol, 5*(4), 282-295.

Lafourcade, C., Galan, J.-M., & Peter, M. (2003). Opposite Roles of the F-Box Protein Rcy1p and the GTPase-Activating Protein Gyp2p During Recycling of Internalized Proteins in Yeast. *Genetics, 164*(2), 469-477.

Landolt-Marticorena, C., Williams, K. A., Deber, C. M., & Reithmeier, R. A. F. (1993). Non-random Distribution of Amino Acids in the Transmembrane Segments of Human Type I Single Span Membrane Proteins. *Journal of Molecular Biology, 229*(3), 602-608. doi: 10.1006/jmbi.1993.1066

Langer, M., Sah, R., Veser, A., Gütlich, M., & Langosch, D. (2013). Structural Properties of Model Phosphatidylcholine Flippases. *Chemistry and Biology, 20*(1), 63-72.

Lee, S., Uchida, Y., Emoto, K., Umeda, M., Kuge, O., Taguchi, T., & Arai, H. (2012). Impaired retrograde membrane traffic through endosomes in a mutant CHO cell defective in phosphatidylserine synthesis. *Genes to Cells, 17*(8), 728-736. doi: 10.1111/j.1365-2443.2012.01622.x

Lenoir, G., Williamson, P., Puts, C. F., & Holthuis, J. C. M. (2009). Cdc50p plays a vital role in the ATPase reaction cycle of the putative aminophospholipid transporter Drs2p. *Journal of Biological Chemistry, 284*(27), 17956-17967.

Levano, K., Punia, V., Raghunath, M., Debata, P. R., Curcio, G. M., Mogha, A., . . . Banerjee, P. (2011). Atp8a1 Deficiency is Associated with Phosphatidylserine Externalization in Hippocampus and Delayed Hippocampus-Dependent Learning. *Journal of Neurochemistry*, no-no. doi: 10.1111/j.1471-4159.2011.07543.x

Lewis, M. J., Nichols, B. J., Prescianotto-Baschong, C., Riezman, H., & Pelham, H. R. B. (2000). Specific Retrieval of the Exocytic SNARE Snc1p from Early Yeast Endosomes. *Molecular Biology of the Cell, 11*(1), 23-38.

Liu, J., & Conboy, J. C. (2005). 1,2-Diacyl-Phosphatidylcholine Flip-Flop Measured Directly by Sum-Frequency Vibrational Spectroscopy. *Biophysical Journal, 89*(4), 2522-2532.

Liu, K., Hua, Z., Nepute, J. A., & Graham, T. R. (2007). Yeast P4-ATPases Drs2p and Dnf1p are essential cargos of the NPFXD/Sla1p endocytic pathway. *Molecular Biology of the Cell, 18*, 487-500.

Liu, K., Surendhran, K., Nothwehr, S. F., & Graham, T. R. (2008). P4-ATPase requirement for AP-1/clathrin function in protein transport from the trans-Golgi network and early endosomes. *Molecular Biology of the Cell, 19*, 3526-3535.

Locher, K. P., Lee, A. T., & Rees, D. C. (2002). The E. coli BtuCD Structure: A Framework for ABC Transporter Architecture and Mechanism. *Science, 296*(5570), 1091-1098. doi: 10.1126/science.1071142

Lodish, H. F. (1988). Transport of secretory and membrane glycoproteins from the rough endoplasmic reticulum to the Golgi. A rate-limiting step in protein maturation and secretion. *Journal of Biological Chemistry, 263*(5), 2107-2110.

López-Marqués, R. L., Poulsen, L. P., Hanisch, S., Meffert, K., Buch-Pedersen, M. J., Jakobsen, M. K., . . . Palmgren, M. G. (2010). Intracellular targeting signals and lipid specificity determinants of the ALA/ALIS P4-ATPase complex reside in the catalytic ALA alpha-subunit. *Molecular Biology of the Cell, 21*(5), 791-801.

Mallard, F., Antony, C., Tenza, D., Salamero, J., Goud, B., & Johannes, L. (1998). Direct Pathway from Early/Recycling Endosomes to the Golgi Apparatus Revealed through the Study of Shiga Toxin B-fragment Transport. *The Journal of Cell Biology, 143*(4), 973-990. doi: 10.1083/jcb.143.4.973

Mandal, A. K., Cheung, W. D., & Argüello, J. M. (2002). Characterization of a Thermophilic P-type Ag+/Cu+-ATPase from the ExtremophileArchaeoglobus fulgidus. *Journal of Biological Chemistry, 277*(9), 7201-7208. doi: 10.1074/jbc.M109964200

Mandal, D., Rulli, S. J., & Rao, R. (2003). Packing Interactions between Transmembrane Helices Alter Ion Selectivity of the Yeast Golgi Ca2+/Mn2+-ATPase PMR1. *Journal of Biological Chemistry, 278*(37), 35292-35298. doi: 10.1074/jbc.M306166200

Mandal, D., Woolf, T. B., & Rao, R. (2000). Manganese Selectivity of Pmr1, the Yeast Secretory Pathway Ion Pump, Is Defined by Residue Gln783 in Transmembrane Segment 6: RESIDUE Asp778 IS ESSENTIAL FOR CATION TRANSPORT. *Journal of Biological Chemistry, 275*(31), 23933-23938. doi: 10.1074/jbc.M002619200

Marcusson, E. G., Horazdovsky, B. F., Cereghino, J. L., Gharakhanian, E., & Emr, S. D. (1994). The sorting receptor for yeast vacuolar carboxypeptidase Y is encoded by the VPS10 gene. *Cell, 77*(4), 579-586.

Marx, U., Polakowski, T., Pomorski, T., Lang, C., Nelson, H., Nelson, N., & Herrmann, A. (1999). Rapid transbilayer movement of fluorescent phospholipid analogues in the plasma membrane of endocytosis-deficient yeast cells does not require the Drs2 protein. *European Journal of Biochemistry, 263*(1), 254-264. doi: 10.1046/j.1432-1327.1999.00497.x

Matsuzaki, K., Murase, O., Fujii, N., & Miyajima, K. (1996). An Antimicrobial Peptide, Magainin 2, Induced Rapid Flip-Flop of Phospholipids Coupled with Pore Formation and Peptide Translocation†. *Biochemistry, 35*(35), 11361-11368. doi: 10.1021/bi960016v

Mercer, J., & Helenius, A. (2008). Vaccinia virus uses macropinocytosis and apoptotic mimicry to enter host cells. *Science, 320*, 531-535.

Moriyama, Y., & Nelson, N. (1988). Purification and properties of a vanadate- and N-ethylmaleimide-sensitive ATPase from chromaffin granule membranes. *Journal of Biological Chemistry, 263*(17), 8521-8527.

Morrot, G., Zachowski, A., & Devaux, P. F. (1990). Partial purification and characterization of the human erythrocyte Mg2+ -ATPase A candidate aminophospholipid translocase. *FEBS Letters, 266*(1-2), 29-32. doi: 10.1016/0014-5793(90)81498-d

Morth, J. P., Pedersen, B. P., Buch-Pedersen, M. J., Andersen, J. P., Vilsen, B., Palmgren, M. G., & Nissen, P. (2011). A structural overview of the plasma membrane Na+,K+-ATPase and

H+-ATPase ion pumps. [Review]. *Nat Rev Mol Cell Biol, 12*(1), 60-70. doi: 10.1038/nrm3031

Morth, J. P., Pedersen, B. P., Toustrup-Jensen, M. S., Sørensen, T. L., Petersen, J., Andersen, J. P., . . . Nissen, P. (2007). Crystal structure of the sodium-potassium pump. *Nature, 450*(7172), 1043-1049. doi: 10.1038/nature06419

Muthusamy, B. P., Natarajan, P., Zhou, X., & Graham, T. R. (2009). Linking phospholipid flippases to vesicle-mediated protein transport. [Review]. *Biochim Biophys Acta, 1791*(7), 612-619.

Muthusamy, B. P., Raychaudhuri, S., Natarajan, P., Abe, F., Liu, K., Prinz, W. A., & Graham, T. R. (2009). Control of protein and sterol trafficking by antagonistic activities of a type IV P-type ATPase and oxysterol binding protein homologue. *Molecular Biology of the Cell, 20*(12), 2920-2931.

Natarajan, P., Liu, K., Patil, D. V., Sciorra, V. A., Jackson, C. L., & Graham, T. R. (2009). Regulation of a Golgi flippase by phosphoinositides and an ArfGEF. *Nat Cell Biol, 11*(12), 1421-1426.

Natarajan, P., Wang, J., Hua, Z., & Graham, T. R. (2004). Drs2p-coupled aminophospholipid translocase activity in yeast Golgi membranes and relationship to *in vivo* function. *Proceedings of the National Academy of Sciences of the United States of America, 101*(29), 10614-10619. doi: 10.1073/pnas.0404146101

Navarro, J., Chabot, J., Sherrill, K., Aneja, R., Zahler, S. A., & Racker, E. (1985). Interaction of duramycin with artificial and natural membranes. *Biochemistry, 24*(17), 4645-4650. doi: 10.1021/bi00338a025

The Nobel Prize in Chemistry. (1997). *Nobelprize.org*.

Obara, K., Miyashita, N., Xu, C., Toyoshima, I., Sugita, Y., Inesi, G., & Toyoshima, C. (2005). Structural role of countertransport revealed in Ca(2+) pump crystal structure in the absence of Ca(2+). *Proceedings of the National Academy of Sciences of the United States of America, 102*(41), 14489-14496. doi: 10.1073/pnas.0506222102

Odorizzi, G., Cowles, C. R., & Emr, S. D. (1998). The AP-3 complex: a coat of many colours. *Trends in Cell Biology, 8*(7), 282-288.

Oelkers, P., Tinkelenberg, A., Erdeniz, N., Cromley, D., Billheimer, J. T., & Sturley, S. L. (2000). A Lecithin Cholesterol Acyltransferase-like Gene Mediates Diacylglycerol Esterification in

Yeast. *Journal of Biological Chemistry, 275*(21), 15609-15612. doi: 10.1074/jbc.C000144200

Ottolenghi, P. (1975). The reversible delipidation of a solubilized sodium-plus-potassium ion-dependent adenosine triphosphatase from the salt gland of the spiny dogfish. *Biochemical Journal, 151*(1), 61-66.

Ottolenghi, P. (1979). The Relipidation of Delipidated Na,K-ATPase. *European Journal of Biochemistry, 99*(1), 113-131. doi: 10.1111/j.1432-1033.1979.tb13238.x

Pagano, R. E., & Longmuir, K. J. (1985). Phosphorylation, transbilayer movement, and facilitated intracellular transport of diacylglycerol are involved in the uptake of a fluorescent analog of phosphatidic acid by cultured fibroblasts. *Journal of Biological Chemistry, 260*(3), 1909-1916.

Palmgren, M. G., & Christensen, G. (1994). Functional comparisons between plant plasma membrane H(+)-ATPase isoforms expressed in yeast. *Journal of Biological Chemistry, 269*(4), 3027-3033.

Palmgren, M. G., & Nissen, P. (2011). P-Type ATPases. *Annual Review of Biophysics, 40*(1), 243-266. doi: doi:10.1146/annurev.biophys.093008.131331

Parsons, A. B., Lopez, A., Givoni, I. E., Williams, D. E., Gray, C. A., Porter, J., . . . Boone, C. (2006). Exploring the mode-of-action of bioactive compounds by chemical-genetic profiling in yeast. *Cell, 126*(3), 611-625. doi: 10.1016/j.cell.2006.06.040

Paterson, J. K., Renkema, K., Burden, L., Halleck, M. S., Schlegel, R. A., Williamson, P., & Daleke, D. L. (2006). Lipid specific activation of the murine P4-ATPase Atp8a1 (ATPase II). *Biochemistry, 45*(16), 5367-5376. doi: DOI: 10.1021/bi052359b

Paulusma, C. C., Folmer, D. E., Ho-Mok, K. S., de Waart, D. R., Hilarius, P. M., Verhoeven, A. J., & Oude Elferink, R. P. J. (2008). ATP8B1 requires an accessory protein for endoplasmic reticulum exit and plasma membrane lipid flippase activity. *Hepatology, 47*(1), 268-278.

Paulusma, C. C., Groen, A., Kunne, C., Ho-Mok, K. S., Spijkerboer, A. L., Rudi de Waart, D., . . . Oude Elferink, R. P. J. (2006). Atp8b1 deficiency in mice reduces resistance of the canalicular membrane to hydrophobic bile salts and impairs bile salt transport. *Hepatology, 44*(1), 195-204.

Paulusma, C. C., & Oude Elferink, R. P. (2005). The type 4 subfamily of P-type ATPases, putative aminophospholipid translocases with a role in human disease. [Review]. *Biochim Biophys Acta, 1741*(1-2), 11-24.

Pedersen, B. P., Buch-Pedersen, M. J., Morth, J. P., Palmgren, M. G., & Nissen, P. (2007). Crystal structure of the plasma membrane proton pump. *Nature, 450*(7172), 1111-1114. doi: 10.1038/nature06417

Pérez-Victoria, F. J., Sánchez-Cañete, M. P., Castanys, S., & Gamarro, F. (2006). Phospholipid Translocation and Miltefosine Potency Require Both L. donovani Miltefosine Transporter and the New Protein LdRos3 in Leishmania Parasites. *Journal of Biological Chemistry, 281*(33), 23766-23775. doi: 10.1074/jbc.M605214200

Pomorski, T., Lombardi, R., Riezman, H., Devaux, P. F., van Meer, G., & Holthuis, J. C. M. (2003). Drs2p-related P-type ATPases Dnf1p and Dnf2p are required for phospholipid translocation across the yeast plasma membrane and serve a role in endocytosis. *Molecular Biology of the Cell, 14*(3), 1240-1254. doi: 10.1091/mbc.E02-08-0501

Post, R. L., Hegyvary, C., & Kume, S. (1972). Activation by Adenosine Triphosphate in the Phosphorylation Kinetics of Sodium and Potassium Ion Transport Adenosine Triphosphatase. *Journal of Biological Chemistry, 247*(20), 6530-6540.

Post, R. L., & Jolly, P. C. (1957). The linkage of sodium, potassium, and ammonium active transport across the human erythrocyte membrane. *Biochimica et Biophysica Acta, 25*(0), 118-128. doi: 10.1016/0006-3002(57)90426-2

Post, R. L., & Sen, A. K. (1965). AN ENZYMATIC MECHANISM OF ACTIVE SODIUM AND POTASSIUM TRANSPORT. *Journal of Histochemistry and Cytochemistry, 13*(2), 105-112. doi: 10.1177/13.2.105

Post, R. L., Sen, A. K., & Rosenthal, A. S. (1965). A Phosphorylated Intermediate in Adenosine Triphosphate-dependent Sodium and Potassium Transport across Kidney Membranes. *Journal of Biological Chemistry, 240*(3), 1437-1445.

Poulsen, L. R., López-Marqués, R. L., McDowell, S. C., Okkeri, J., Licht, D., Schulz, A., . . . Palmgren, M. G. (2008). The Arabidopsis P4-ATPase ALA3 localizes to the golgi and requires a beta-subunit to function in lipid translocation and secretory vesicle formation. *Plant Cell, 20*(3), 658-676.

Poulsen, L. R., López-Marqués, R. L., & Palmgren, M. G. (2008). Flippases: still more questions than answers. *Cell Mol Life Sci, 65*, 3119-3125.

Puertollano, R., Aguilar, R. C., Gorshkova, I., Crouch, R. J., & Bonifacino, J. S. (2001). Sorting of Mannose 6-Phosphate Receptors Mediated by the GGAs. *Science, 292*(5522), 1712-1716. doi: 10.1126/science.1060750

Puts, C. F., & Holthuis, J. C. (2009). Mechanism and significance of P4 ATPase-catalyzed lipid transport: lessons from a Na+/K+-pump. *Biochim Biophys Acta, 1791*(7), 603-611. doi: 10.1016/j.bbalip.2009.02.005

Radji, M., Kim, J.-M., Togan, T., Yoshikawa, H., & Shirahige, K. (2001). The cloning and characterization of the CDC50 gene family in Saccharomyces cerevisiae. *Yeast, 18*, 195-205.

Rice, W. J., Green, N. M., & MacLennan, D. H. (1997). Site-directed disulfide mapping of helices M4 and M6 in the Ca2+ binding domain of SERCA1a, the Ca2+ ATPase of fast twitch skeletal muscle sarcoplasmic reticulum. *Journal of Biological Chemistry, 272*(50), 31412-31419.

Riekhof, W. R., Wu, J., Gijón, M. A., Zarini, S., Murphy, R. C., & Voelker, D. R. (2007). Lysophosphatidylcholine metabolism in Saccharomyces cerevisiae: the role of P-type ATPases in transport and a broad specificity acyltransferase in acylation. *Journal of Biological Chemistry, 282*, 36853-36861. doi: 10.1074/jbc.M706718200

Riekhof, W. R., Wu, J., Jones, J. L., & Voelker, D. R. (2007). Identification and Characterization of the Major Lysophosphatidylethanolamine Acyltransferase in Saccharomyces cerevisiae. *Journal of Biological Chemistry, 282*(39), 28344-28352. doi: 10.1074/jbc.M705256200

Robinson, M., Poon, P. P., Schindler, C., Murray, L. E., Kama, R., Gabriely, G., . . . Gerst, J. E. (2006). The Gcs1 Arf-GAP Mediates Snc1,2 v-SNARE Retrieval to the Golgi in Yeast. *Molecular Biology of the Cell, 17*(4), 1845-1858. doi: 10.1091/mbc.E05-09-0832

Rockwell, N., Wolfger, H., Kuchler, K., & Thorner, J. (2009). ABC Transporter Pdr10 Regulates the Membrane Microenvironment of Pdr12 in <i>Saccharomyces cerevisiae</i&gt. *Journal of Membrane Biology, 229*(1), 27-52. doi: 10.1007/s00232-009-9173-5

Saito, K., Fujimura-Kamada, K., Furuta, N., Kato, U., Umeda, M., & Tanaka, K. (2004). Cdc50p, a protein required for polarized growth, associates with the Drs2p P-type ATPase implicated in phospholipid translocation in Saccharomyces cerevisiae. *Molecular Biology of the Cell, 15*, 3418-3432.

Sakane, H., Yamamoto, T., & Tanaka, K. (2006). The functional relationship between the Cdc50p-Drs2p putative aminophospholipid translocase and the Arf GAP Gcs1p in vesicle

formation in the retrieval pathway from yeast early endosomes to the TGN. *Cell Structure and Function, 31*(2), 87-108.

Sapay, N., Bennett, W. F. D., & Tieleman, D. P. (2009). Thermodynamics of flip-flop and desorption for a systematic series of phosphatidylcholine lipids. *Soft Matter, 5*(17), 3295-3302.

Schrodinger, L. (2010). *The PyMOL Molecular Graphics System, Version 1.3r1*.

Seaman, M. N. J., Michael McCaffery, J., & Emr, S. D. (1998). A Membrane Coat Complex Essential for Endosome-to-Golgi Retrograde Transport in Yeast. *The Journal of Cell Biology, 142*(3), 665-681. doi: 10.1083/jcb.142.3.665

Sebastian, T. T., Baldridge, R. D., Xu, P., & Graham, T. R. (2012). Phospholipid flippases: Building asymmetric membranes and transport vesicles. *Biochimica et Biophysica Acta (BBA) - Molecular and Cell Biology of Lipids, 1821*(8), 1068-1077. doi: 10.1016/j.bbalip.2011.12.007

Seigneuret, M., & Devaux, P. F. (1984). ATP-dependent asymmetric distribution of spin-labeled phospholipids in the erythrocyte membrane: relation to shape changes. *Proceedings of the National Academy of Sciences of the United States of America, 81*, 3751-3755.

Shaw, J. A., Mol, P. C., Bowers, B., Silverman, S. J., Valdivieso, M. H., Durán, A., & Cabib, E. (1991). The function of chitin synthases 2 and 3 in the Saccharomyces cerevisiae cell cycle. *The Journal of Cell Biology, 114*(1), 111-123. doi: 10.1083/jcb.114.1.111

Sheetz, M. P., & Singer, S. J. (1974). Biological membranes as bilayer couples. A molecular mechanism of drug- erythrocyte interactions. *Proceedings of the National Academy of Sciences of the United States of America, 71*, 4457-4461.

Sherman, F. (2002). Getting Started with Yeast. *Methods Enzymol, 350*, 3-41.

Shinoda, T., Ogawa, H., Cornelius, F., & Toyoshima, C. (2009). Crystal structure of the sodium-potassium pump at 2.4A resolution. *Nature, 459*(7245), 446-450.

Siegmund, A., Grant, A., Angeletti, C., Malone, L., Nichols, J. W., & Rudolph, H. K. (1998). Loss of Drs2p does not abolish transfer of fluorescence-labeled phospholipids across the plasma membrane of Saccharomyces cerevisiae. *Journal of Biological Chemistry, 273*(51), 34399-34405.

Siggs, O. M., Arnold, C. N., Huber, C., Pirie, E., Xia, Y., Lin, P., . . . Beutler, B. (2011). The P4-type ATPase ATP11C is essential for B lymphopoiesis in adult bone marrow. *Nature Immunology, 12*(5), 434-440. doi: 10.1038/ni.2012

Siggs, O. M., Schnabl, B., Webb, B., & Beutler, B. (2011). X-linked cholestasis in mouse due to mutations of the P4-ATPase ATP11C. *Proceedings of the National Academy of Sciences of the United States of America, 108*(19), 7890-7895. doi: 10.1073/pnas.1104631108

Sikorski, R. S., & Hieter, P. (1989). A system of shuttle vectors and yeast host strains designed for efficient manipulation of DNA in Saccharomyces cerevisiae. *Genetics, 122*(1), 19-27.

Simons, K. T., Kooperberg, C., Huang, E., & Baker, D. (1997). Assembly of protein tertiary structures from fragments with similar local sequences using simulated annealing and Bayesian scoring functions. *Journal of Molecular Biology, 268*(1), 209-225.

Skou, J. C. (1957). The influence of some cations on an adenosine triphosphatase from peripheral nerves. *Biochimica et Biophysica Acta, 23*(0), 394-401. doi: 10.1016/0006-3002(57)90343-8

Soupene, E., & Kuypers, F. A. (2006). Identification of an erythroid ATP-dependent aminophospholipid transporter. *British Journal of Haematology, 133*(4), 436-438.

Stapelbroek, J. M., Peters, T. A., van Beurden, D. H., Curfs, J. H., Joosten, A., Beynon, A. J., . . . Houwen, R. H. (2009). ATP8B1 is essential for maintaining normal hearing. *Proceedings of the National Academy of Sciences of the United States of America, 106*(24), 9709-9714

Stevens, H. C., Malone, L., & Nichols, J. W. (2008). The putative aminophospholipid translocases, DNF1 and DNF2, are not required for 7-nitrobenz-2-oxa-1,3-diazol-4-yl-phosphatidylserine flip across the plasma membrane of Saccharomyces cerevisiae. *Journal of Biological Chemistry, 283*(50), 35060-35069.

Stevens, H. C., & Nichols, J. W. (2007). The Proton Electrochemical Gradient across the Plasma Membrane of Yeast Is Necessary for Phospholipid Flip. *Journal of Biological Chemistry, 282*(24), 17563-17567.

Sun, Y., & Drubin, D. G. The functions of anionic phospholipids during clathrin-mediated endocytosis site initiation and vesicle formation. *Journal of Cell Science*. doi: 10.1242/jcs.115741

Sune, A., Bette-Bobillo, P., Bienvenue, A., Fellmann, P., & Devaux, P. F. (1987). Selective outside-inside translocation of aminophospholipids in human platelets. *Biochemistry, 26*(11), 2972-2978. doi: 10.1021/bi00385a003

Takahashi, Y., Fujimura-Kamada, K., Kondo, S., & Tanaka, K. (2011). Isolation and characterization of novel mutations in CDC50, the non-catalytic subunit of the Drs2p phospholipid flippase. *Journal of Biochemistry, 149*(4), 423-432. doi: 10.1093/jb/mvq155

Takatsu, H., Baba, K., Shima, T., Umino, H., Kato, U., Umeda, M., . . . Shin, H.-W. (2011). ATP9B, a P4-ATPase (a Putative Aminophospholipid Translocase), Localizes to the trans-Golgi Network in a CDC50 Protein-independent Manner. *Journal of Biological Chemistry, 286*(44), 38159-38167. doi: 10.1074/jbc.M111.281006

Tang, X., Halleck, M. S., Schlegel, R. A., & Williamson, P. (1996). A subfamily of P-type ATPases with aminophospholipid transporting activity. *Science, 272*(5267), 1495-1497.

Tani, M., & Kuge, O. (2012). Involvement of complex sphingolipids and phosphatidylserine in endosomal trafficking in yeast Saccharomyces cerevisiae. *Molecular Microbiology, 86*(5), 1262-1280. doi: 10.1111/mmi.12057

Thøgersen, L., & Nissen, P. (2012). Flexible P-type ATPases interacting with the membrane. *Current Opinion in Structural Biology, 22*(4), 491-499. doi: 10.1016/j.sbi.2012.05.009

Toyoshima, C. (2008). Structural aspects of ion pumping by Ca2+-ATPase of sarcoplasmic reticulum. [Review]. *Arch Biochem Biophys, 476*(1), 3-11.

Toyoshima, C., & Mizutani, T. (2004). Crystal structure of the calcium pump with a bound ATP analogue. *Nature, 430*(6999), 529-535.

Toyoshima, C., Nakasako, M., Nomura, H., & Ogawa, H. (2000). Crystal structure of the calcium pump of sarcoplasmic reticulum at 2.6 [angst] resolution. *Nature, 405*(6787), 647-655. doi: 10.1038/35015017

Toyoshima, C., & Nomura, H. (2002). Structural changes in the calcium pump accompanying the dissociation of calcium. *Nature, 418*(6898), 605-611.

Toyoshima, C., Nomura, H., & Tsuda, T. (2004). Lumenal gating mechanism revealed in calcium pump crystal structures with phosphate analogues. *Nature, 432*(7015), 361-368. doi: 10.1038/nature02981

Tsai, P.-C., Hsu, J.-W., Liu, Y.-W., Chen, K.-Y., & Lee, F.-J. S. (2013). Arl1p regulates spatial membrane organization at the trans-Golgi network through interaction with Arf-GEF Gea2p and flippase Drs2p. *Proceedings of the National Academy of Sciences*. doi: 10.1073/pnas.1221484110

Uchida, Y., Hasegawa, J., Chinnapen, D., Inoue, T., Okazaki, S., Kato, R., . . . Arai, H. (2011). Intracellular phosphatidylserine is essential for retrograde membrane traffic through endosomes. *Proceedings of the National Academy of Sciences, 108*(38), 15846-15851. doi: 10.1073/pnas.1109101108

Ujhazy, P., Ortiz, D., Misra, S., Li, S., Moseley, J., Jones, H., & Arias, I. M. (2001). Familial intrahepatic cholestasis 1: Studies of localization and function. *Hepatology, 34*(4), 768-775. doi: 10.1053/jhep.2001.27663

Valdivia, R. H., Baggott, D., Chuang, J. S., & Schekman, R. W. (2002). The Yeast Clathrin Adaptor Protein Complex 1 Is Required for the Efficient Retention of a Subset of Late Golgi Membrane Proteins. *Developmental Cell, 2*(3), 283-294.

van der Velden, L. M., Wichers, C. G., van Breevoort, A. E., Coleman, J. A., Molday, R. S., Berger, R., . . . van de Graaf, S. F. (2010). Heteromeric interactions required for abundance and subcellular localization of human CDC50 proteins and class 1 P4 ATPases. *Journal of Biological Chemistry*.

van Meer, G., Voelker, D. R., & Feigenson, G. W. (2008). Membrane lipids: where they are and how they behave. [Review]. *Nat Rev Mol Cell Biol, 9*(2), 112-124.

Vara, F., & Serrano, R. (1982). Partial purification and properties of the proton-translocating ATPase of plant plasma membranes. *Journal of Biological Chemistry, 257*(21), 12826-12830.

Verhulst, P. M., van der Velden, L. M., Oorschot, V., van Faassen, E. E., Klumperman, J., Houwen, R. H., . . . Klomp, L. W. (2010). A flippase-independent function of ATP8B1, the protein affected in familial intrahepatic cholestasis type 1, is required for apical protein expression and microvillus formation in polarized epithelial cells. *Hepatology, 51*(6), 2049-2060.

Viehweger, K., Dordschbal, B., & Roos, W. (2002). Elicitor-Activated Phospholipase A2 Generates Lysophosphatidylcholines That Mobilize the Vacuolar H+ Pool for pH Signaling via the Activation of Na+-Dependent Proton Fluxes. *The Plant Cell Online, 14*(7), 1509-1525. doi: 10.1105/tpc.002329

Voelker, D. R. (2000). Interorganelle transport of aminoglycerophospholipids. *Biochimica et Biophysica Acta (BBA) - Molecular and Cell Biology of Lipids, 1486*(1), 97-107. doi: 10.1016/S1388-1981(00)00051-2

Wang, L., Beserra, C., & Garbers, D. L. (2004). A novel aminophospholipid transporter exclusively expressed in spermatozoa is required for membrane lipid asymmetry and normal fertilization. *Developmental Biology, 267*(1), 203-215.

Ward, A., Reyes, C. L., Yu, J., Roth, C. B., & Chang, G. (2007). Flexibility in the ABC transporter MsbA: Alternating access with a twist. *Proceedings of the National Academy of Sciences of the United States of America, 104*(48), 19005-19010. doi: 10.1073/pnas.0709388104

Xie, X. S., Stone, D. K., & Racker, E. (1989). Purification of a vanadate-sensitive ATPase from clathrin-coated vesicles of bovine brain. *Journal of Biological Chemistry, 264*(3), 1710-1714.

Xu, P., Okkeri, J., Hanisch, S., Hu, R. Y., Xu, Q., Pomorski, T. G., & Ding, X. Y. (2009). Identification of a novel mouse P4-ATPase family member highly expressed during spermatogenesis. *Journal of Cell Science, 122*, 2866-2876.

Xu, Q., Yang, G.-Y., Liu, N., Xu, P., Chen, Y.-L., Zhou, Z., . . . Ding, X. (2012). P4-ATPase ATP8A2 acts in synergy with CDC50A to enhance neurite outgrowth. *FEBS Letters, 586*(13), 1803-1812.

Yabas, M., Teh, C. E., Frankenreiter, S., Lal, D., Roots, C. M., Whittle, B., . . . Enders, A. (2011). ATP11C is critical for the internalization of phosphatidylserine and differentiation of B lymphocytes. *Nature Immunology, 12*(5), 441-449. doi: 10.1038/ni.2011

Yarov-Yarovoy, V., Schonbrun, J., & Baker, D. (2006). Multipass membrane protein structure prediction using Rosetta. *Proteins, 62*(4), 1010-1025.

Yon, J., & Fried, M. (1989). Precise gene fusion by PCR. *Nucleic Acids Research, 17*(12), 4895.

Zachowski, A., Henry, J. P., & Devaux, P. F. (1989). Control of transmembrane lipid asymmetry in chromaffin granules by an ATP-dependent protein. *Nature, 340*(6228), 75-76.

Zhou, X., & Graham, T. R. (2009). Reconstitution of phospholipid translocase activity with purified Drs2p, a type-IV P-type ATPase from budding yeast. *Proceedings of the National Academy of Sciences of the United States of America, 106*(39), 16586-16591. doi: 10.1073/pnas.0904293106

Zhu, X., Libby, R. T., de Vries, W. N., Smith, R. S., Wright, D. L., Bronson, R. T., . . . John, S. W. M. (2012). Mutations in a P-Type ATPase Gene Cause Axonal Degeneration. *PLoS Genetics, 8*(8), e1002853. doi: 10.1371/journal.pgen.1002853

Ziman, M., Chuang, J. S., Tsung, M., Hamamoto, S., & Schekman, R. (1998). Chs6p-dependent Anterograde Transport of Chs3p from the Chitosome to the Plasma Membrane in Saccharomyces cerevisiae. *Molecular Biology of the Cell, 9*(6), 1565-1576.

Zwaal, R. F. A., & Schroit, A. J. (1997). Pathophysiologic Implications of Membrane Phospholipid Asymmetry in Blood Cells. *Blood, 89*, 1121-1132.